UNIVERSITY OF CALIFORNIA

Santa Barbara

Investigation of conditions relevant to the use of reclaimed water for managed aquifer recharge in two aquifer systems in the Western United States

A dissertation submitted in partial satisfaction of the

requirements for the degree Doctor of Philosophy in Earth Science

by

Sarah Paschal Gerenday

Committee in charge:

Professor Jordan F. Clark, Chair

Professor David Valentine

Professor Debra Perrone

September 2022

This dissertation of Sarah Paschal Gerenday is approved.

David Valentine

Debra Perrone

Jordan F. Clark, Committee Chair

September 2022

Investigation of conditions relevant to the use of reclaimed water for managed aquifer recharge in two aquifer systems in the Western United States

by

Sarah Paschal Gerenday

ACKNOWLEDGEMENTS

I would like to thank everyone who helped make this dissertation possible. Firstly, to my advisor, Jordan Clark, you opened my eyes to the world of managed aquifer recharge and helped me work through tough problems when I was stuck. To Menso de Jong, thank you for all your help in the lab and for being around for great conversations about groundwater, work, and life. To Professor Debra Perrone, thank you for motivating me and helping me find the best approach to the most interesting questions. I would also like to express my gratitude to Dr. George Kourakos and Mr. David Parkhurst for their guidance on implementing the innovative modeling programs that they developed. Further appreciation is given to the LOTT Clean Water Alliance for funding the first portion of this research and to the people at HDR Engineering, Inc. for the field and logistical work that made it possible. Thanks to Peter Green for keeping my ancient laptop chugging along throughout the whole process and for always being ready with a smile and accounts of your latest adventures. Finally, I must offer my heartfelt gratitude to all of my family and friends for inspiring me, supporting me, and keeping me sane. I truly could not have done it without you.

VITA OF SARAH PASCHAL GERENDAY

August 2022

EDUCATION

Bachelor of Science in Earth Science, Rice University, May 2017 (magna cum laude)

Doctor of Philosophy in Earth Science, University of California, Santa Barbara, September 2022 (expected)

PROFESSIONAL EMPLOYMENT

2018-21: Teaching Assistant, Department of Earth Science, University of California, Santa Barbara

Summer 2019: Guest Hydrologist, Wolf Trap National Park for the Performing Arts

Summer 2017: Intern, Terracon

Summer 2015: Science Undergraduate Laboratory Intern, Applied Geoscience and Environmental Management, Argonne National Laboratory

PUBLICATIONS

Gerenday, S. P., J. F. Clark, J. Hansen, I. Fischer, and J. Koreny. 2020. Sulfur Hexafluoride and Potassium Bromide as Groundwater Tracers for Managed Aquifer Recharge. *Groundwater* 58, no. 5: 777–87, https://doi.org/10.1111/gwat.12983.

Gerenday, S. P., D. Perrone, J. F. Clark, and N. Ulibarri. (In review). Recycled water aquifer recharge may be viable for Central Valley Groundwater Sustainability Agencies. *California Agriculture*.

AWARDS

Alumni Graduate Award for Research Excellence, Department of Earth Science, University of California, Santa Barbara, 2020, 2021

G.K. Gilbert Award for presentation of original research, Department of Earth Science, University of California, Santa Barbara, 2020

Chancellor's Fellowship, University of California, Santa Barbara 2017-2022

FIELDS OF STUDY

Groundwater geochemistry and aqueous transport with Professor Jordan F. Clark

Site suitability for managed aquifer recharge using reclaimed water with Professor Debra Perrone

ABSTRACT

Investigation of conditions relevant to the use of reclaimed water for managed aquifer recharge in two aquifer systems in the Western United States

by

Sarah Paschal Gerenday

Managed aquifer recharge (MAR) is an increasingly popular strategy for maintaining a sustainable water supply. Reclaimed water (sometimes referred to as recycled water) can be used as a supply of recharge water, providing environmental benefits, while natural processes improve the quality of this water. Planning and implementing such projects requires understanding of the flow patterns and geochemistry of the target aquifers in addition to health and logistical constraints. This dissertation contains three studies of conditions for various phases of reclaimed water MAR projects in two different hydrogeologic and legal settings.

Chapter 2 is a suitability analysis of land for reclaimed water MAR in the California's Central Valley in the context of the Sustainable Groundwater Management Act, which requires Groundwater Sustainability Agencies (GSA) to develop Groundwater Sustainability Plans (GSP). Land is scored in terms of the suitability of its soil and proximity to potential sources of reclaimed water. Inherently unsuitable land is excluded based on land cover and mandatory buffers for domestic wells. Backwards particle tracking is used to identify areas where recharged water would not meet minimum residence time criteria specified in California's water code, and these areas are also excluded. Land deemed suitable for reclaimed water MAR is compared to the land needed by GSAs in critically overdrafted

basins to fulfil the recharge goals laid out in their GSPs. Potential recycled water availability is determined based on the discharge volumes of local water recycling and wastewater treatment plants. Under existing conditions, only 2 out of 29 GSAs have enough potentially suitable land to meet their recharge goals using sufficiently high-quality reclaimed water as a source, and none have enough high quality water, though the numbers increase if existing treatment plants can be upgraded.

Chapter 3 details a tracer study and monitoring project conducted at the LOTT Clean Water Alliance's Hawks Prairie Reclaimed Water Ponds and Recharge Basins site in Thurston County, Washington. The study employs sulfur hexafluoride (SF_6) and bromide (Br^-) as added tracers to identify flow paths and determine residence times for reclaimed water recharged from the basins. As a low-solubility gas, the SF_6 exhibits an exsolution – dissolution behavior according to Henry's law in the presence of air trapped within the soil and aquifer media, resulting in its retardation relative to the Br^-. This retardation is used to calculate an air to water ratio of 10^{-3} to 10^{-2} along the flow paths of the recharge water. It is also demonstrated that the water follows several non-linear preferential pathways and that water can travel between the two uppermost aquifers in certain locations.

Chapter 4 examines the broader geochemistry of groundwater in the upper and intermediate aquifer units of Thurston County, Washington, where the Hawks Prairie MAR site from chapter 3 is located. Groundwater is determined to be composed of concentrated meteoric water with additional solutes from mineral weathering. More evolved waters contain lower levels of oxygen with higher iron, manganese, and phosphorus contents. Groundwater may also be contaminated by seawater intrusion or septic effluent, resulting in elevated concentrations of chloride and, in the case of septic contamination, nitrate. This

demonstrates the importance of familiarity with the local inputs that control groundwater quality in order to ensure compatibility with MAR.

Together, these studies demonstrate the major phases and considerations of reclaimed water MAR projects. To be successful, projects must consider appropriate siting, transport conditions and geochemistry. With sufficient planning and attention to these details, reclaimed water MAR can be a valuable tool for ensuring water sustainability.

DISCLOSURE OF PERSONAL CONTRIBUTION

Chapters 2 and 3 of this dissertation have been published/ submitted for publication as multi-author journal articles. Citations and quantification of my personal contribution to each are detailed below.

Paper 1 (Chapter 2): Gerenday, S. P., D. Perrone, J. F. Clark, and N. Ulibarri. (In review). Recycled water aquifer recharge may be viable for Central Valley Groundwater Sustainability Agencies. *California Agriculture*.

Paper 2 (Chapter 3): Gerenday, S. P., J. F. Clark, J. Hansen, I. Fischer, and J. Koreny. 2020. Sulfur Hexafluoride and Potassium Bromide as Groundwater Tracers for Managed Aquifer Recharge. *Groundwater* 58, no. 5: 777–87, https://doi.org/10.1111/gwat.12983.

Personal contributions

	Data acquisition	Analysis and interpretation	Manuscript drafting	Revision of drafts
Chapter 2 (Paper 1)	50%	75%	95%	80%
Chapter 3 (Paper 2)	40%	90%	100%	80%
Chapter 4 (unpublished)	100%	95%	100%	95%

TABLE OF CONTENTS

TABLE OF TABLES

TABLE OF FIGURES

Chapter 1 Introduction

Groundwater is a vital resource in the western United States (Dieter et al., 2018). Water managers face a variety of challenges relating to its quantity and quality. One management strategy is to employ managed aquifer recharge (MAR), which is the deliberate replenishment of groundwater, often via surface infiltration in engineered basins (Dillon et al., 2009). MAR can offset environmental and supply issues associated with declining groundwater levels and is an efficient, environmentally friendly way of storing water (Bouwer et al., 2008). The process of infiltration and subsurface travel can result in natural improvements to the quality of the infiltrated water, making MAR a useful step in the treatment of reclaimed or recycled water (Drewes, 2009). In order to achieve a safe, sustainable, and high quality water supply, sites must be selected with attention to the physical and chemical properties of the local soils and underlying aquifers, along with proximity to potable water sources and a supply of recharge water (Sallwey et al., 2018). This may entail GIS analyses, modeling, and tracer studies.

The typical progression of a reclaimed water MAR project begins with identifying a water management need that could be addressed by groundwater recharge and identifying a source of recharge water (Figure 1.1). If the management need is primarily related to preventing groundwater depletion, then these two components may be distinct processes. On the other hand, if reclaimed water is available but requires additional treatment that could be provided by infiltration through the vadose zone, then identifying the management need and recharge water source may occur simultaneously. Once the goal is identified, a site must be selected for the MAR project. This may include GIS-based suitability mapping and model development. Then hydrogeology and geochemistry must be characterized to confirm that the

prospective site is suitable for reclaimed water MAR. Data gathered during this stage may be used to produce updated models and influence the planning of pilot MAR operations. During the pilot phase of a reclaimed water MAR project, a tracer study is typically conducted to characterize transport from the basins. Additional hydrologic and geochemical monitoring must also occur. Information gathered during this stage informs the development of full scale operations, sometimes via further model development.

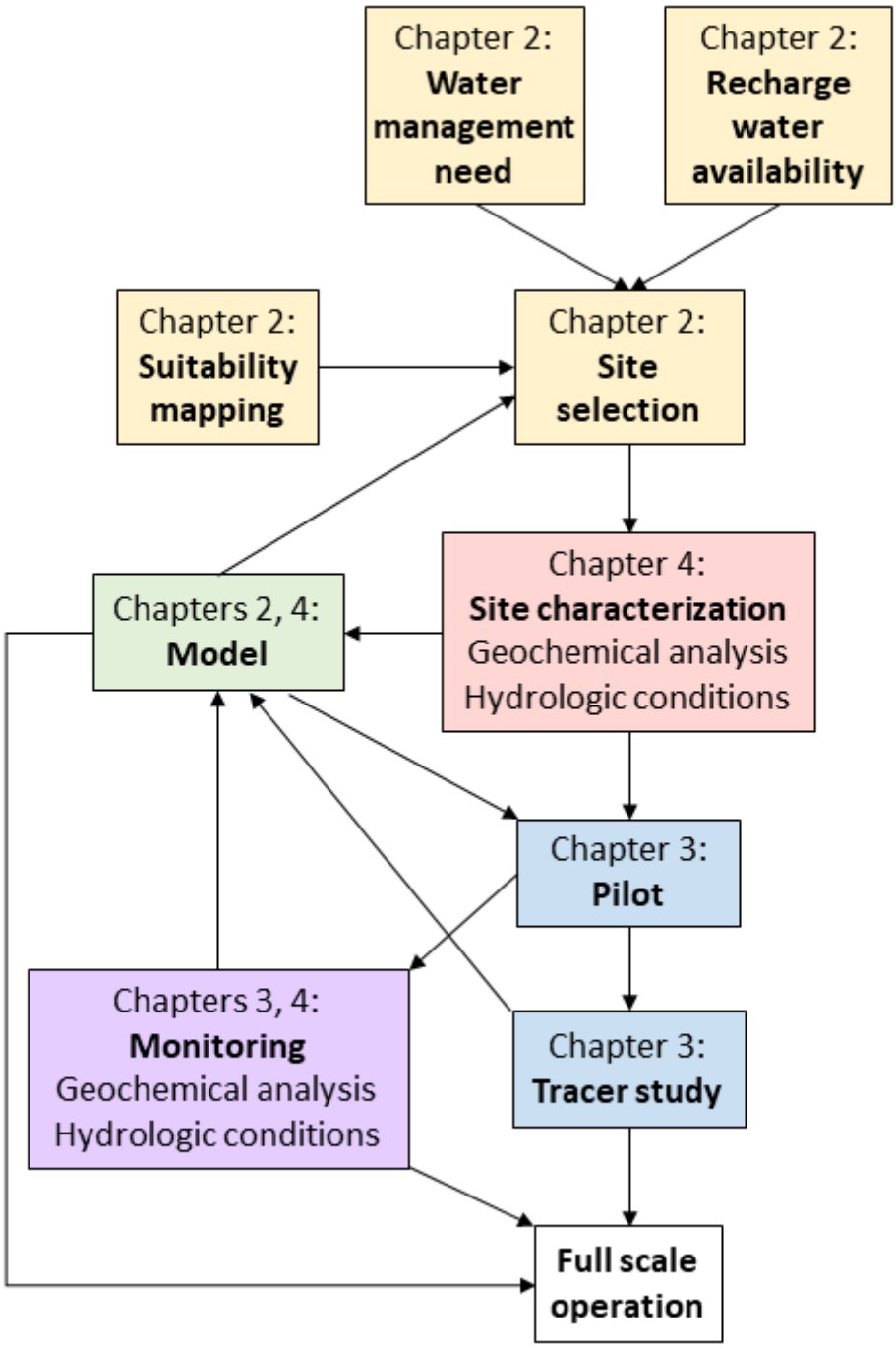

Figure 1.1: Basic progression of a reclaimed water MAR project and layout of dissertation

This dissertation will address various stages of this process for two different aquifer systems. Chapter 2 addresses recharge potential in California's Central Valley, where MAR is a desired strategy for achieving the goals of the Sustainable Groundwater Management Act (SGMA). Land in the Valley is evaluated in terms of its potential for reclaimed, or as it is referred to in California, recycled water MAR. The resulting areas are compared to the amount of land needed for recharge and the amount of recycled water available to meet sustainability goals outlined by local agencies in Groundwater Sustainability Plans (GSP). This is a regional scale analysis that must be followed by localized studies, such as those described in chapters 3 and 4, before MAR can be initiated. Chapters 3 and 4 of this dissertation focus on the groundwater of Thurston County, Washington, USA, where the LOTT Clean Water Alliance conducts MAR using reclaimed water. Chapter 3 is an analysis of a tracer study conducted at the infiltration site, with a characterization of the tracer behaviors and aquifer properties. Chapter 4 uses water quality data collected during the tracer study, along with historical data, to identify factors contributing to the chemical properties of the water. This knowledge is important for ensuring that MAR operations provide a net benefit to local water quantity and quality.

While the two study areas may seem disconnected, both are locations with a growing interest in reclaimed water MAR (Cupps and Morris, 2005; Crook, 2004; Mukherjee and Jensen, 2020). Many groundwater management projects are currently in the exploratory or planning phase in California's Central Valley, making a regional scale suitability study timely and relevant (DWR, 2022). Meanwhile, the LOTT Clean Water Alliance has been developing recharge operations in Thurston County, Washington throughout the past decade. Conducting a tracer study and geochemical analysis was deemed necessary to inform

ongoing and future operations and to improve community buy-in (LOTT Clean Water Alliance, 2022). These two study areas show the approaches to recycled water MAR in multiple parts of the western United States at various stages of development.

Hydrogeologic settings

Central Valley, California

Chapter 2 focuses on the Central Valley (CV) of California. The CV is a structural trough 400 miles long and, on average 50 miles wide. The Valley is bounded on the east side by the Sierra Nevada Mountains. The Sierra Nevada batholith was emplaced between the late Jurassic and late Cretaceous and, after an extended period of erosion, was tilted up and to the east, forming the mountain range. The basin was flooded by the Pacific Ocean until it was gradually cut off by the formation of the Coast Range during the Cretaceous. Parts of the Valley remained inundated until the late Pliocene, approximately ~2-3 Ma. The resulting marine deposits contain saline water, which has been partially diluted from water expelled from clays during burial (Wilson et al., 1999; Bertoldi et al., 1991). The Coast Range bounds the CV on the west side, with marine beds of the Great Valley sequence, along with several faults, forming a barrier to groundwater flow (Bertoldi et al., 1991).

The aquifers of the CV are contained in post-Eocene continental deposits. The sediments are mainly fluvial and lacustrine, though some of the deposits are volcanic in origin (Bertoldi et al., 1991). The average thickness of the post-Eocene deposits is 730 m (2,400 ft.) with an average horizontal hydraulic conductivity of 1.8 m/d. Over half of the thickness of these deposits consists of discontinuous lenses of fine-grained sediments (Williamson et al., 1989). The most notable of the fine-grained units is the Corcoran Clay

Member of the Tulare Formation, which underlies much of the San Joaquin Valley. This clay originated as lacustrine deposits in a downwarping basin below the Tulare Lake bed (Page, 1986). The Corcoran Clay has historically served as a significant confining unit, though the presence of many large-diameter wells perforated above and below the clay now allow for greater connectivity between shallower and deeper beds (Bertoldi et al., 1991).

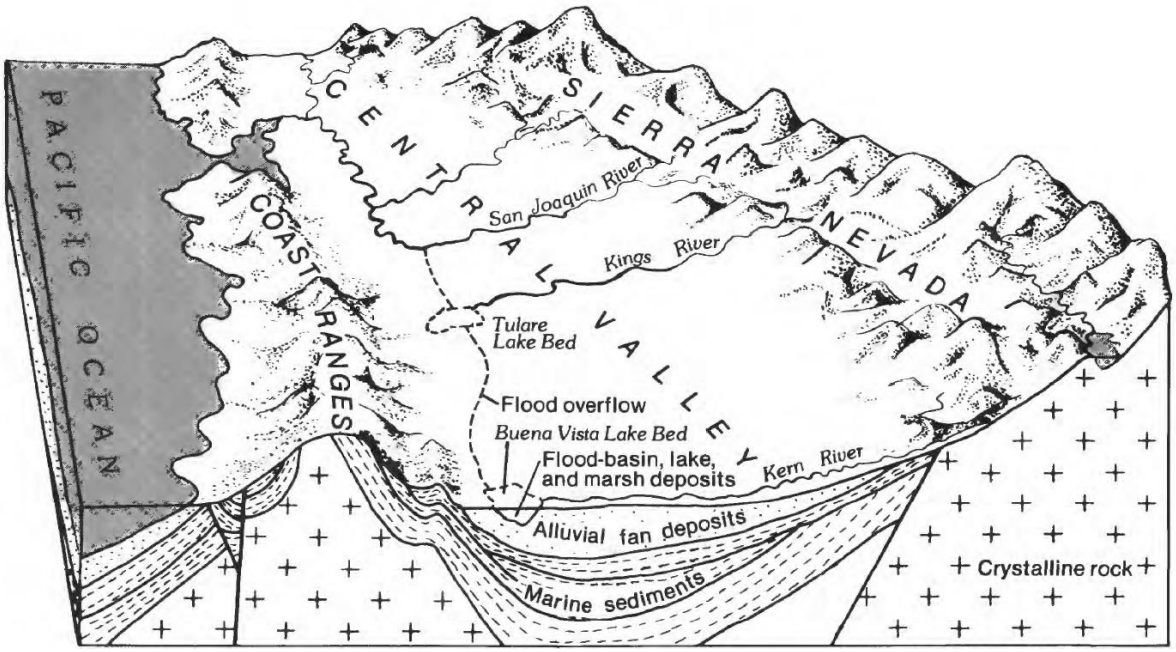

Figure 1.2: Generalized block diagram of the Central Valley. Original by Dale et al. (1964, fig.7), modified by R.W. Page (1980), cited in (Page, 1986).

The CV is commonly divided into three or four drainage basins: the Sacramento Valley, the San Joaquin Basin of the San Joaquin Valley, the Tulare Basin of the San Joaquin Valley, and sometimes the Delta (Bertoldi et al., 1991; Hatch, 2020). The CV is in the rain shadow of the Coast Range and receives little precipitation. The majority of streamflow and recharge originates as precipitation in the Sierra Nevada and Klamath Mountains (Bertoldi et al., 1991). The most significant rivers are the Sacramento and the San Joaquin. The Sacramento River has its headwaters in the Cascade Mountains, though it also has tributaries that flow from the Coast Range and Sierra Nevada. The San Joaquin River also receives

water from the Coast Range and Sierra Nevada but not from the Cascades (Hatch, 2020). Both rivers drain into the Sacramento – San Joaquin Delta. To get there, the water must flow through the Carquinez Strait, which cuts west through the Coast Range and is the only natural surface outlet from the CV. The main form of discharge from the Valley was formerly evapotranspiration, but now is pumping for irrigation (Bertoldi et al., 1991).

Prior to major human use of groundwater in the Valley, groundwater flow primarily followed topography, flowing towards the Sacramento – San Joaquin Delta or towards Tulare Lake. In the present day, water still flows towards these points, but also to major cones of depression and away from mounding caused by irrigation, canal leakage, and MAR projects (Hatch, 2020). Overpumping of groundwater in the CV has resulted in serious overdraft. By 1977, the Valley's aquifers had experienced a 70 billion m^3 (60 million acre-foot) decline in groundwater storage relative to pre-development conditions (Williamson et al., 1989). The falling water table has caused the inelastic compaction of fine-grained beds in the San Joaquin Valley starting in the 1940's, which has resulted in the area experiencing greater land subsidence than anywhere else in the world (Bertoldi et al., 1991). As recently as 2014, parts of the CV have experienced over 0.3 m/year (1ft/year) of subsidence (Borchers et al., 2014).

Thurston County, Washington

The next two chapters examine natural and human-altered groundwater systems in Thurston County Washington. This area is part of the Puget Lowland, a topographic and structural basin situated between Cascade Range and the Olympic Mountains. Regional tectonics are controlled primarily by oblique subduction of the Juan de Fuca plate along the Cascadia subduction zone. Clockwise Cenozoic rotation has resulted in north-south shortening of the forearc basin and the development of east-west trending fault zones, like

the Seattle fault zone, which cuts across the Puget Lowland approximately 60 km north of the study area (Wells, 1998; Troost and Booth, 2008). The Puget lobe of the Cordilleran glacier advanced southward across the lowland at least seven times during the last 2.4 million years, dominating the geologic record. The most recent of these advances was the Vashon Stade of the Fraser Glaciation during the Pleistocene (Drost et al., 1998; Troost and Booth, 2008) (Figure 1).

The tracer study and monitoring described in chapters 3 and 4 was conducted at the Hawks Prairie Reclaimed Water Ponds and Recharge Basins managed by the LOTT Clean Water Alliance. The Hawks Prairie site is located to the southwest of the Nisqually Reach of Puget Sound, in the north of Thurston County. Additional data collected from Thurston County glacial aquifers more broadly was also used in Chapter 4.

The shallowest of these aquifers, along with the vadose zone, consist of deposits from the Vashon Glaciation. Closest to the surface are the Alluvium Vashon Recessional Gravel Outwash and the Vashon Advance Outwash, which consist largely of sand and gravel from the Cascades and other regions to the north (Logan et al., 2003). These formations comprise the vadose zone and shallow aquifer. Frequently the two outwash formations are separated by the Vashon Till, a highly compacted, unstratified mixture of clay, silt, sand, and gravel with low permeability, which can serve as a confining unit for the shallow aquifer. Where the till is not present, as is the case in much of the Hawks Prairie site, the Advance and Recessional Outwashes act as a single hydrologic unit (Drost et al., 1998; HDR Engineering, Inc., 2018a). The shallow aquifer discharges to overlying rivers and streams and to Puget Sound, with groundwater at the Hawks Prairie site flowing southwest towards Woodland Creek (Drost et al., 1998; HDR Engineering, Inc., 2018a). Hydraulic conductivity in the advance outwash

range from 0.04 to 900 m/d and has been measured at 30 to 70 m/d in the Hawks Prairie area (Vaccaro et al., 1998; HDR Engineering, Inc., 2018a). The horizontal head gradient at the Hawks Prairie site has been calculated as 0.023 except in the southwest corner where it decreases to 0.00241 (HDR Engineering, Inc., 2018b).

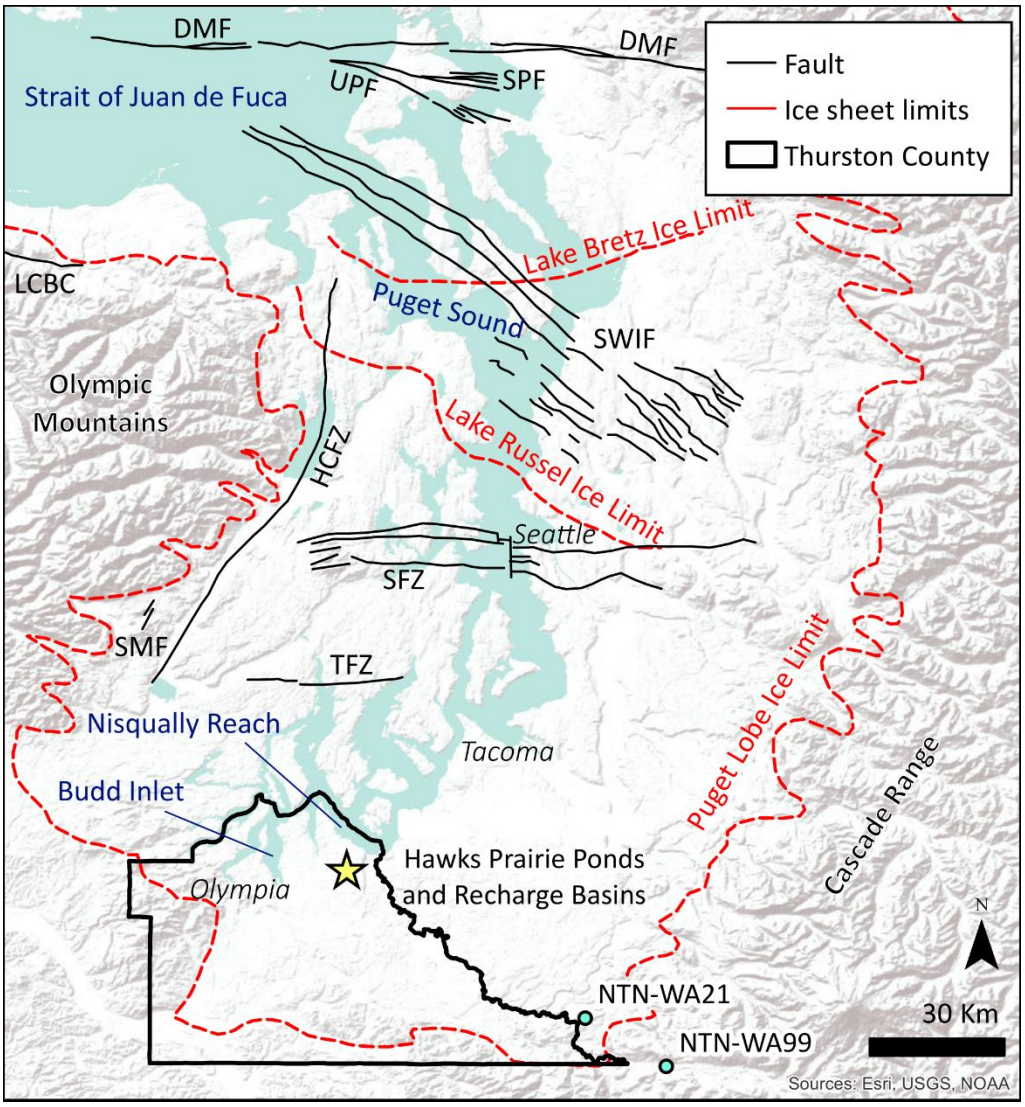

Figure 1.3: Map of the Puget Lowland with Hawks Prairie site denoted by star and National Atmospheric Deposition Project monitoring stations marked with teal dots. Thurston County outlined in black. DMF—Devils Mountain fault zone, HCFZ—Hood Canal fault zone, LCBC—Lake Creek–Boundary Creek fault, SFZ—Seattle fault zone, SMF— Saddle Mountain fault, SPF—Strawberry Point fault, SWIF—Southern Whidbey Island fault zone, TFZ— Tacoma fault zone, UPF—Utsalady Point fault. Faults and ice limits from Troost and Booth (2008).

Below the shallow aquifer is the fine-grained Kitsap formation, composed primarily of what is believed to be lacustrine clay and silt, generally 5 to 20 m thick (Drost et al., 1998). The Kitsap generally serves as a confining layer between the shallow and underlying sea level aquifers, though portions with higher sand transmit some water. The vertical head gradient across the Kitsap has been measured as -0.09 to -0.45 (HDR Engineering, Inc., 2018a). The sea level aquifer is contained in the Pre-Vashon Coarse Deposits, also known as the Salmon Springs Drift and penultimate glacial deposits. These consist of stratified sands and gravels of glacial origin, typically 5 to 15 m thick (Drost et al., 1998; HDR Engineering, Inc., 2017). The aquifer has a horizontal head gradient of 0.01 at the Hawks Prairie site with flow to the east into McAllister Creek (HDR Engineering, Inc., 2018a). The aquifer also discharges to Lake St. Claire and the Deschutes River, and also to Puget Sound (Drost et al., 1998). Hydraulic conductivities in the Salmon Springs Drift, one of the main units forming the sea level aquifer have been observed to range from 0.1 to 1600 m/d (Vaccaro et al., 1998). Sea level aquifer hydraulic conductivities at the Hawks Prairie site exhibit the smaller range of 0.6 to 12 m/d (HDR Engineering, Inc., 2018a). The shallow aquifer is tapped primarily by private residential wells, while the sea level aquifer is used mostly for municipal supply (HDR Engineering, Inc., 2017).

Regulatory settings

Regulation of water reuse and MAR at the federal level is minimal (Sanchez-Flores et al., 2016; Mukherjee and Jensen, 2020). Federal regulations are fairly general and provide more of an overarching framework than specific rules. The EPA's Guidance for Water Reuse highlights best practices for water reuse projects including MAR, but does not contain binding rules (US EPA, 2012). The National Pollutant Discharge Elimination System

(NPDES) requires a permit if recharge water is shown to reach a surface water body, but not if it remains in the aquifer until being withdrawn from a well. The Safe Drinking Water Act requires protection for drinking water sources including groundwater. It does not directly regulate MAR, but it does provide the authority for the Environmental Protection Agency's (EPA) Underground Injection Control (UIC) program (US EPA, 2021). The UIC program regulates the injection of any fluid into the ground via wells, including aquifer storage and recovery (ASR) wells used for direct groundwater recharge. Under the program, ASR wells must either be individually permitted or rule authorized. States granted primacy for a given class of wells by the EPA are in charge of authorizing those wells within their boundaries under the UIC program. The State of Washington has successfully applied for primacy regarding ASR wells, but California has not, meaning that ASR wells in California must be directly authorized by the EPA (US EPA, 2015). Indirect aquifer recharge by infiltration is not regulated by the federal government provided it does not endanger drinking water sources or affect surface water. Similarly, the federal government does not regulate how states manage their water budgets.

California

California has regulated surface water for over a century and was one of the first states to regulate water reuse; however, groundwater in California remained unregulated at the state level until the passage of the Sustainable Groundwater Management Act (SGMA) in 2014 (Table 1.1) (PPC Land Consultants, Inc., 2017; Springhorn et al., 2021). The state has recognized the importance of managing groundwater. The California Water Action Plan outlines a goal of attaining "more reliable water supplies, the restoration of important species and habitat, and a more resilient, sustainably managed water resources system". This is to be

achieved through providing essential data for groundwater management, funding partnerships for storage projects, updating California's Groundwater Plan, Bulletin 118, improving sustainable groundwater management, supporting distributed groundwater storage, increasing statewide recharge, and accelerating groundwater cleanup while preventing future contamination (CNRA et al., 2014).

SGMA acknowledges that groundwater is best managed at the local level and, to that end, authorizes the establishment of Groundwater Sustainability Agencies (GSA). Any local agency or group of agencies whose jurisdiction overlies a groundwater basin may form a GSA for that basin (SGMA, 2014). Basins and subbasins are prioritized in Bulletin 118 according to a set of factors relating to current and future water demand, groundwater dependence, and documented negative impacts to groundwater (State of California, 2015a; Springhorn et al., 2021). California contains 515 recognized groundwater basins, of which 48 were classified as medium priority and 46 as high in 2019. Out of the 46 high priority basins, 20 are considered critically overdrafted, meaning that they will face severe impacts if they continue with their present course of water management (Springhorn et al., 2021). Within the boundaries of the CV, there are 45 basins, with 14 medium priority and 21 high. Of these, 11 face critical overdraft (DWR, 2020b). SGMA requires the establishment of GSAs for basins with a priority level of medium or high, and allows voluntary establishment for basins with lower priority. Adjudicated basins, which are those subject to action by a superior or federal court are exempt; however, there are none located in the CV (DWR, 2020a, SGMA, 2014).

GSAs representing medium or high priority basins are required to submit Groundwater Sustainability Plans (GSP), and those representing very low or low priority basins may also choose to do so. In a basin with multiple GSAs, the GSAs can work together

to submit a single GSP or they may submit a set of coordinated GSPs. GSPs for basins in critical overdraft were due January 31, 2020, while the remaining medium and high priority GSPs were due January 31, 2022. The plans must achieve sustainability within 20 years of their implementation (SGMA, 2014). As of May 2022, 113 GSPs have been submitted, and eight have been approved by the Department of Water Resources (DWR). Another 34 were deemed incomplete, while the rest are still under review (DWR, n.d., b).

In order to be considered complete, GSPs must contain detailed information about the administration of the plan and agency, the basin setting, sustainable management criteria, monitoring networks, projects and management actions, and interagency agreements. The sustainable management criteria include goals, undesirable results to be avoided, minimum thresholds to determine when undesirable results are occurring, and measurable objectives to gage progress towards sustainability. The DWR is responsible for reviewing and approving GSPs and also provides financial and technical assistance for their implementation. In the event that a medium or high priority basin is not covered by GSAs or if the DWR determines a GSP to be insufficient and the basin is in long term overdraft or is experiencing surface water depletion due to groundwater extraction, the State Water Resources Control Board (SWRCB) can place a basin on probation or prepare an interim plan in what is referred to as state intervention (SGMA, 2014). As of yet, state intervention has not occurred in any basin.

One potential project or management action that can be taken to help achieve sustainability is recycled water MAR, which will be the focus of chapter 2 of this dissertation. Such projects are encouraged by SWRCB and CA Environmental Protection Agency policy, which states, "Groundwater recharge with recycled water for later extraction and use in accordance with this Policy and state and federal water quality law is to the benefit

of the people of the state of California" (SWRCB and Cal EPA, 2018). Several agencies are involved in overseeing recycled water MAR projects under SGMA. DWR approves the GSPs and provides support to the GSAs. DWR also sets statewide targets for water recycling and, along with the SWRCB, collects data and reports on recycled water use. The SWRCB has the broadest responsibilities. It is responsible for developing general policies on permitting recycled water projects and uniform recycling criteria for particular water uses. The SWRCB also handles wastewater change petitions for projects that could reduce flow to a watercourse, reviews and approves Title 22 engineering reports that demonstrate how projects comply with water recycling regulations, and reviews regional board permitting practices. The regional water boards issue permits, with the goal of streamlining the process and encouraging recycled water use. The regional boards also assess the salt and nutrient monitoring data from projects every five years following implementation (SWRCB and Cal EPA, 2018). Finally, the Department of Health oversees backflow prevention in the recycled water systems in accordance with Title 17 (State of California, 2015b).

Obtaining recycled water for recharge involves the owner of the treatment facility, as the owner has rights to the water; however, they do not necessarily have the unrestricted right to use this water (State of California, 1980; SWRCB and Cal EPA, 2018). If a recycled water project would result in reduced discharge to a stream, the reduction may not harm another legal water user, cannot unreasonably affect in-stream uses, such as fish and wildlife, and must be in the public interest. Regional water boards approve recycled water MAR projects on a site specific basis, with surface spreading projects that employ reverse osmosis and a satisfactory brine disposal method receiving high priority for review. Projects must comply with Title 17, Title 22, and SWRCB recommendations, monitor for contaminants of

emerging concern, and give robust consideration to salt and nutrient management (SWRCB and Cal EPA, 2018). Additionally, recharge projects are subject to antidegradation requirements and must complete an antidegradation analysis (SWRCB, 1968; SWRCB and Cal EPA, 2018).

The most technical requirements for recycled water MAR are found in Title 17, which addresses cross-connection control, and, more notably, Title 22, which contains the majority of requirements for recycled water use (State of California, 2015b; State of California, 2018). Recycled water MAR, or groundwater replenishment reuse projects (GRRP), as referred to in Title 22, must utilize at least disinfected tertiary treated water for surface spreading methods or advanced treated water for subsurface application. Disinfected tertiary water is recycled water that has been oxidized, filtered and disinfected, with no more than 2.2 total coliforms per 100 mL. Advanced treated water must undergo reverse osmosis and has more stringent oxidation requirements. The treatment train for either type of water must result in a 12-log reduction in viruses, and 10-log reductions of Giardia and Cryptosporidium. Since pathogens may be naturally killed or deactivated in the environment, recharged water can receive one log reduction credit for viruses for each month spent in the ground, for up to six log reduction credits. After six months underground, water infiltrated from the surface also receives credit for 10-log reductions for Giardia and Cryptosporidium. Regardless of whether underground residence time is used to achieve pathogen reduction credits, the water must spend at least two months in the ground. Also, there must be adequate response retention time, such that a detected violation of water quality requirements could be remedied before the water reaches a potable supply well. To this end, the operators must conduct downgradient monitoring between the recharge location and the nearest drinking

water wells. In addition to pathogens, water quality standards must be met for total organic carbon, nitrogen compounds, and regulated drinking water contaminants. Recognized unregulated contaminants must also be monitored. Beyond the boundaries of the recharge site, the fraction of recycled water in the groundwater, or the recycled municipal wastewater contribution (RWC), is initially limited to 20% for surface spreading projects. With evidence that water quality is being protected, the regional board may grant permission for a RWC up to 100%. No limit is set for the RWC of subsurface recharge projects (State of California, 2018).

Table 1.1: Statutes, regulations, and policy documents relevant to recycled water MAR in the State of California

Document	Relevant details
SGMA	• Requires prioritization of groundwater basins under B118, updated every 5 years • Requires the establishment of GSAs and the implementation of GSPs • Requires that sustainability goals be reached within 20 years of plan implementation • Allows for state intervention if local entities do not implement sufficient plans • Exempts adjudicated basins

Bulletin 118	• Reports on the state of groundwater in California, including
	  ○ Economic value
	  ○ Management actions
	  ○ Hydrologic conditions
	• Maps and assigns priority level to all groundwater basins in the state

WAT Div. 6 Part 2.11 Ch. 3	Sets criteria for B118 basin prioritization
WAT Div. 2 Part 2 Ch. 1	• States that wastewater treatment plant owners have right to the treated water • Requires approval for changes in use
Policy for Water Quality Control for Recycled Water	• Assigns roles to state agencies • Sets permitting requirements • Sets antidegradation requirements • Prohibits uses that would harm other legal water users or in-stream use
Title 17	Sets construction requirements for cross-connection control and backflow prevention
Title 22	• Sets treatment criteria for recycled water • Lists allowed uses for recycled water by type • Provides detailed requirements for indirect potable reuse projects

All GRRPs must include a tracer study during pilot testing in order to demonstrate underground residence times and RWC if relevant. During planning stages, however, a

model may be used to achieve log reduction credits. Greater credence is given to methods with less unaccounted for uncertainty (Table 1.2) (State of California, 2018). Chapter 4 will involve the use of models to establish residence time, and thus will assume 0.5-log reductions per month.

Table 1.2: Log reductions in viruses credited to different methods of demonstrating residence time (Title 22 table 60320.108)

Method used to estimate the retention time to the nearest downgradient drinking water well	Virus Log Reduction Credit per Month
Tracer study utilizing an added tracer.	1.0 log
Tracer study utilizing an intrinsic tracer.	0.67 log
Numerical modeling consisting of calibrated finite element or finite difference models using validated and verified computer codes used for simulating groundwater flow.	0.50 log
Analytical modeling using existing academically-accepted equations such as Darcy's Law to estimate groundwater flow conditions based on simplifying aquifer assumptions.	0.25 log

Washington

On a state level, much of Washington's authority to regulate groundwater recharge comes from RCW 90.03.370, which expands the definition of "reservoir" to "in addition to any surface reservoir, any naturally occurring underground geological formation where water is collected and stored for subsequent use as part of an underground artificial storage and recovery project" (State of Washington, 2000a). This, in turn, authorizes RCW 90.44.460, which allows the Department of Ecology (Ecology) to issue permits for ASR projects (State of Washington, 2000b). The specific code governing ASR in the State of Washington, WAC 173-157, exempts projects that use reclaimed water, though WAC 173-218, through which

the state administers the UIC program, states that ASR wells that use reclaimed water in compliance with the state's reclaimed water rule are rule authorized (State of Washington, 2003, 2008). Additionally, WAC 173-218 exempts groundwater recharge through infiltration basins, which is a common MAR method. Therefore, groundwater recharge with reclaimed water is largely its own subject in Washington law (Table 1.3).

RCW 90.46 (Reclaimed Water Use Act) is the overarching law governing reclaimed water in the state, first instituted in 1992. The law stipulates that reclaimed water may be used for surface percolation if it meets state drinking water quality standards (defined in WAC 246-290), or other standards set by the Departments of Ecology and Health, in the groundwater beneath or downgradient of the project site. It also directs the departments to develop standards for direct recharge (State of Washington, 2011, 2019). The other element of RCW 90.46 of particular significance is its establishment of reclaimed water rights (State of Washington, 2011). In general, ASR projects require that the recharger have a right to the water they use for recharge, a reservoir permit to inject the water, and a secondary permit to withdraw it (State of Washington, 2003). Under RCW 90.46, whoever treats what would have otherwise been wastewater to reclaimed water standards has the right to that water, provided that the wastewater effluent is not needed to fulfill a downstream user's allocation (Wetch, 2015). RCW 90.46 does not specifically require consideration of upstream water rights; however, the Department of Ecology cautions that since water rights are determined by seniority, not position in stream, it is possible for upstream rights to be impaired if reclaiming water causes a flow reduction that requires an upstream user to curtail their use in order to meet in-stream flow requirements (Washington State Department of Ecology, 2009).

WAC 173-219 Reclaimed Water contains the standards for reclaimed water use required by RCW 90.46. The code defines two classes of reclaimed water: class B, which is oxidized and disinfected, and class A, which in addition to being oxidized and disinfected, is also coagulated and filtered. Indirect recharge may use either class, but direct recharge may only use class A. In either case, injection or infiltration must occur no less than 200 feet from any water supply well, and the recharge water must meet groundwater quality standards in addition to any relevant UIC requirements. Additionally, compliance with drinking water maximum contaminant levels (MCL) is required in the finished water or at an alternate point of compliance. If the recharged water is to be recovered later, it must be demonstrated that extraction will not harm groundwater quality, the environment, or other water rights holders (State of Washington, 2018). The groundwater quality standards are set in WAC 173-200, which provides MCLs and describes the antidegradation policy. Antidegradation, guided by the Water Pollution Control Act and Water Resources Act of 1971, is intended to protect existing water quality, in addition to current and future beneficial uses, by prohibiting the degradation of outstanding water resources of quality better than the minimum required by elsewhere in the code (State of Washington, 1990). With regards to this, RCW 90.46.005 specifies that reclaimed water use is *not inconsistent* with antidegradation policies, though it does not guarantee that it *is* consistent in any particular case (State of Washington, 2011). Water quality is measured at some point of compliance which extends through the top of the saturated zone through the lowest potentially affected depth. The point of compliance is supposed to be as close to the source as technologically and hydrogeologically feasible, but an alternate point may be established at a distance not past the property boundary (State of Washington, 1990). Water quality standards and point of compliance may be modified by

Ecology on the basis of overriding consideration of public interest if all known, available, and reasonable technology has been applied to removing the contaminants of concern from the reclaimed water (Shaleen-Hansen, 2017).

Table 1.3: Relevant statutes and regulations for reclaimed water MAR in the State of Washington

Code	Relevant details
RCW 90.03.370	• Requires secondary permit to use water from reservoirs • Defines "reservoir" to include aquifers used for storage • Defines "underground artificial storage and recovery project" as a project that artificially store water in the ground for later use • Excludes projects using reclaimed water from definition of "underground artificial storage and recovery project"
RCW 90.44.460	Allows Department of Ecology to issue reservoir permits for ASR
RCW 90.46	• Allows use of reclaimed water for surface percolation if drinking water criteria are met in groundwater beneath or downgradient of site • Treatment facility operator has right to reclaimed water but cannot use it for profit • No extra permit required for recovery from underground storage if criteria from RCW 90.03.370 met (though RCW 90.03.370 itself exempts reclaimed water) • Use of reclaimed water cannot impair downstream rights without compensation or mitigation
WAC 173-157	• Sets requirements for aquifer storage and recovery permits • Identical definition for "underground artificial storage and recovery project" as RCW 90.03.370. Interchangeable with "aquifer storage and recovery" or ASR project. • Defines "artificial recharge" as controlled addition of water to aquifer for the purpose of replenishment • Exempts projects using reclaimed water
WAC 173-200	• Sets groundwater quality criteria • Requires antidegradation • Establishes point of compliance as close to source as technically, hydrogeologically, and geographically feasible and no farther than the property boundary • Allows Department of Ecology to set alternative criteria based on overriding consideration of public interest if all known, available, and reasonable technology have been applied to meet groundwater quality standards in discharge

WAC 173-219	• Defines groundwater recharge as: introduction of reclaimed water to groundwater aquifers and includes the following: • Indirect recharge: Where reclaimed water is introduced to groundwater through surface or subsurface infiltration or percolation, where the introduced water travels through an unsaturated vadose zone and the commingling with groundwater of the state is not immediate. • Direct recharge: Where reclaimed water is released directly and immediately into groundwater of the state through direct injection or other means. • Defines reclaimed water as "water derived in any part from a wastewater with a domestic wastewater component that has been adequately and reliably treated to meet the requirements of this chapter, so that it can be used for beneficial purposes. Reclaimed water is not considered a wastewater." • Requires a permit for reclaimed water use • Sets criteria for class A and B reclaimed water • Allows groundwater recharge by infiltration with class A or B and injection using the same standards as WAC 173-157 with class A only • Requires 200 ft. setback between recharge site and water supply wells • Water must meet groundwater and drinking water standards at point of compliance • If water is recovered, recovery must not negatively impact groundwater quality, environment, or other rights holders
WAC 246-290	Sets standards for drinking water

Chapter 2 Recycled water aquifer recharge may be viable for Central Valley Groundwater Sustainability Agencies

Abstract

To address groundwater overdraft, Groundwater Sustainability Agencies are considering managed aquifer recharge. One source of recharge water is recycled municipal wastewater. We employ suitability mapping and the models C2VSimFG and ICHNOS to delineate areas appropriate for managed aquifer recharge with recycled water in the Central Valley of California. Factors influencing suitability include soil properties, proximity to a recycled water source, and residence time of recharged water. Suitable land is present in many parts of the Central Valley immediately adjacent to water recycling facilities, but access to supply is an issue in most locations. Roughly half of the Groundwater Sustainability Agencies in critically overdrafted basins of the Central Valley have enough potentially suitable locations to meet their recharge goals using recycled water, but fewer are likely to have enough recycled water to do so. The methods demonstrated here can be a tool for agencies considering recharging recycled water.

Introduction

California's Central Valley (CV) is a productive agricultural region with a history of unregulated groundwater pumping and overdraft (Springhorn et al., 2021). The Sustainable Groundwater Management Act (SGMA) of 2014 seeks to address overdraft by directing the Department of Water Resources to assign priority levels to basins and requiring basins with the highest priority (i.e., critically overdrafted, medium, and high priority) to create and implement Groundwater Sustainability Plans (GSP). Out of the Valley's 45 subbasins, 11 are

considered critically overdrafted (DWR, 2020b), meaning that "continuation of present water management practices would probably result in significant adverse overdraft-related environmental, social, or economic impacts" (Springhorn et al., 2021). Within these 11 critically overdrafted subbasins, 36 Groundwater Sustainability Agencies (GSA) submitted GSPs (Figure 2.1) (Springhorn et al., 2021). These plans outline how GSAs will meet groundwater sustainability goals.

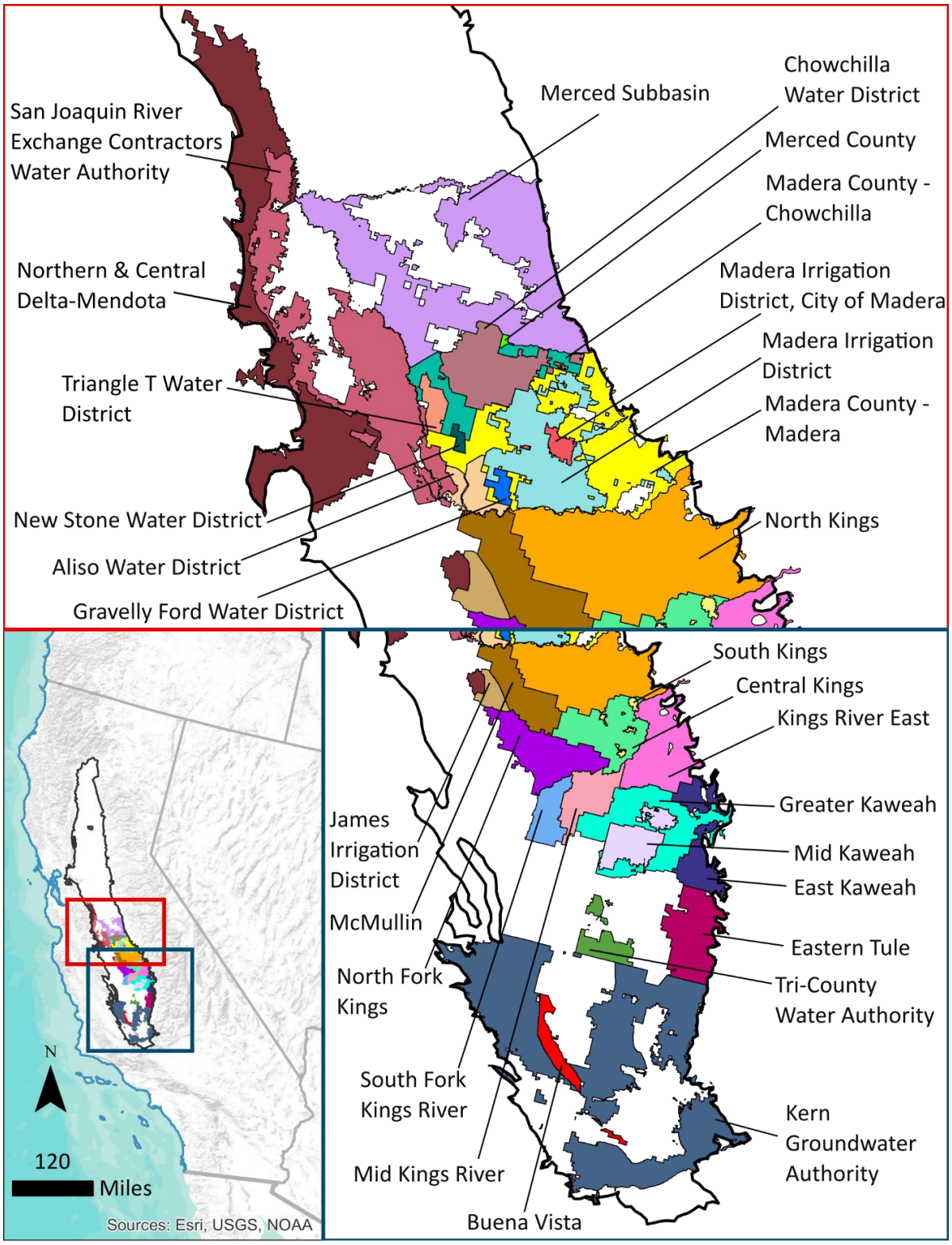

Figure 2.1: Map of GSAs in critically overdrafted basins in the Central Valley requiring land for recharge (DWR, n.d.; DWR, 2020c) (Benjamin Gooding, DWR, personal communication).

One potential approach to groundwater sustainability is through managed aquifer recharge (MAR). MAR is the deliberate infiltration of water into aquifers for storage; storing water in aquifers tends to have less evaporative loss and fewer adverse effects on rivers than storing water in surface reservoirs. MAR can mitigate aquifer depletion, enhance dry-season streamflows, and improve the quality of recycled water used for infiltration (Bekele et al., 2011; Kourakos et al., 2019). Analysis of the GSPs submitted for basins in critical overdraft revealed that 29 of 36 GSAs have plans for using surface water to meet recharge objectives, resulting in ~200 MAR projects (Ulibarri et al., 2021). Recharge with high magnitude streamflows has shown promise for flood and overdraft mitigation, but the uncertain timing, amount, and location of these flows poses logistical challenges (Dahlke and Kocis, 2018; Alam et al., 2020). Lack of nearby source water is a major factor preventing MAR projects from reaching recharge goals (Perrone and Rohde, 2016). In fact, unallocated surface water is insufficient to fulfill the requirements of the ~200 proposed MAR projects during a typical water year, suggesting that proposed MAR projects may need to reconsider their water source (Alam et al., 2020; Ulibarri et al., 2021).

One alternative water source for MAR is recycled water. Title 22 of the California Code of Regulations allows disinfected tertiary recycled municipal wastewater to be used for MAR, subject to water quality and residence time requirements (State of California, 2018). Under California Water Code, the owner of a wastewater treatment facility has exclusive rights to the treated water, though they must receive approval for new uses from the State Water Resources Control Board if a change might result in reduced flow to a watercourse (California Water Code, 2002). Because treatment facilities are often owned by public utilities, it may be easier for a municipality to obtain treated wastewater than water from

other sources (SWRCB, 2021b). Conventional wastewater treatment plants may be replaced by facilities producing recycled water at the end of their lifespan or may be upgraded to produce recycled water for improved effluent quality (Cooley and Phurisamban, 2016; Crook, 2004). MAR projects using recycled water, called Groundwater Replenishment Reuse Projects in Title 22, have been implemented in the Orange County Water District and Montebello Forebay in Los Angeles County (McDermott et al., 2008; Mills and Watson, 1994).

Despite the widespread interest in MAR siting and the potential of recycled water for recharge, few studies have examined the suitability of locations in California for recycled water MAR. Those that do focus largely on economic and logistical optimization (Bradshaw and Luthy, 2017; Fournier et al., 2016; Merayyan and Safi, 2014). Nevertheless, planning recycled water MAR requires consideration of unique criteria, such as natural attenuation of potential contaminants and proximity to a treatment plant for water supply (Ahmadi et al., 2017; Pedrero et al., 2011). In this paper, we identify areas in the CV suitable for recycled water MAR and locations where future projects could be developed if existing wastewater infrastructure is upgraded to produce recycled water. Additionally, we evaluate the current recycled water produced at existing treatment facilities and compare it to predicted needs by each GSA as outlined in their Plans.

Methods

Suitability Mapping--Overview

Suitability mapping was used to identify land within the CV which might be ideal for recycled water MAR. Criteria were compiled in the form of ArcGIS raster maps of the

valley, with each 100-meter by 100-meter pixel evaluated for each criterion. Each criterion was evaluated in one of two forms: (1) numerical or (2) binary. Numerical suitability scores were used for soil suitability and source proximity; binary suitability scores were used for land cover and proximity to drinking water sources. The binary score maps were multiplied by the averaged numerical score map to exclude unsuitable areas, resulting in a map giving an overall suitability score.

Numerical Suitability Scores

Land within the CV was numerically scored—from 1 to 100, where 1 is unsuitable, and 100 is ideal—using two criteria: (1) relative suitability for MAR based on soil and (2) proximity to a potential recycled water source. The soil suitability and source proximity scores were combined with equal weighting.

Soil suitability was determined using the modified Soil Agricultural Groundwater Banking Index (SAGBI), which scores suitability of land for MAR on agricultural land (ag-MAR) in terms of deep percolation, root zone residence time, topography, soil salinity, and soil surface conditions (O'Geen et al., 2015) (Figure 2.2). The modified version assumes deep tillage in restrictive soil horizons, increasing infiltration potential.

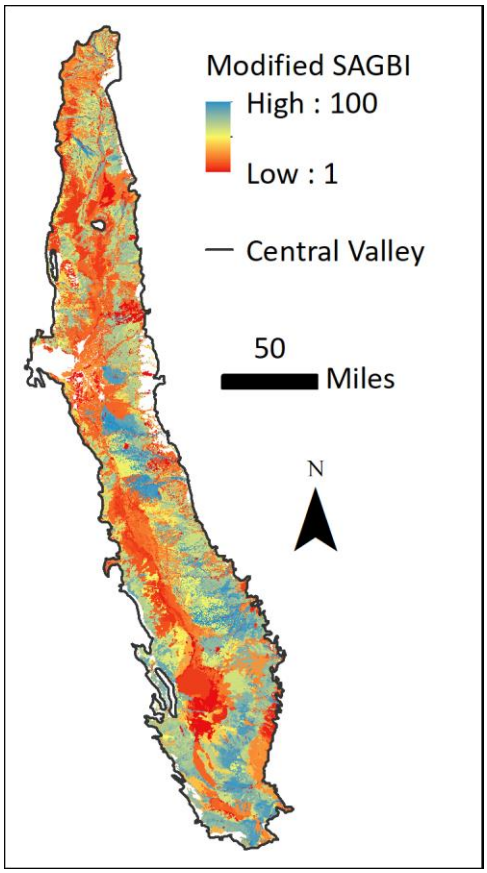

Figure 2.2: Modified SAGBI for the Central Valley. A value of 100 indicates optimum recharge conditions; a value of 1 indicates recharge is unfeasible.

Proximity to a potential source of recharge water was scored linearly from 1 (three or more miles (4.8 km) away; least suitable) to 100 (at source; most suitable) based on the distance to the nearest treatment facility (Figure 2.3). Beyond three miles, transporting the water is usually infeasible (Appendix A.6.4). Facilities were identified from the State Water Resources Control Board's 2019 Volumetric Annual Report of Wastewater and Recycled Water (SWRCB, 2021a). The proximity score was calculated under three scenarios, considering (1) only facilities producing disinfected tertiary water, (2) any facility with recycled water, and (3) any treatment facility, including those only producing wastewater.

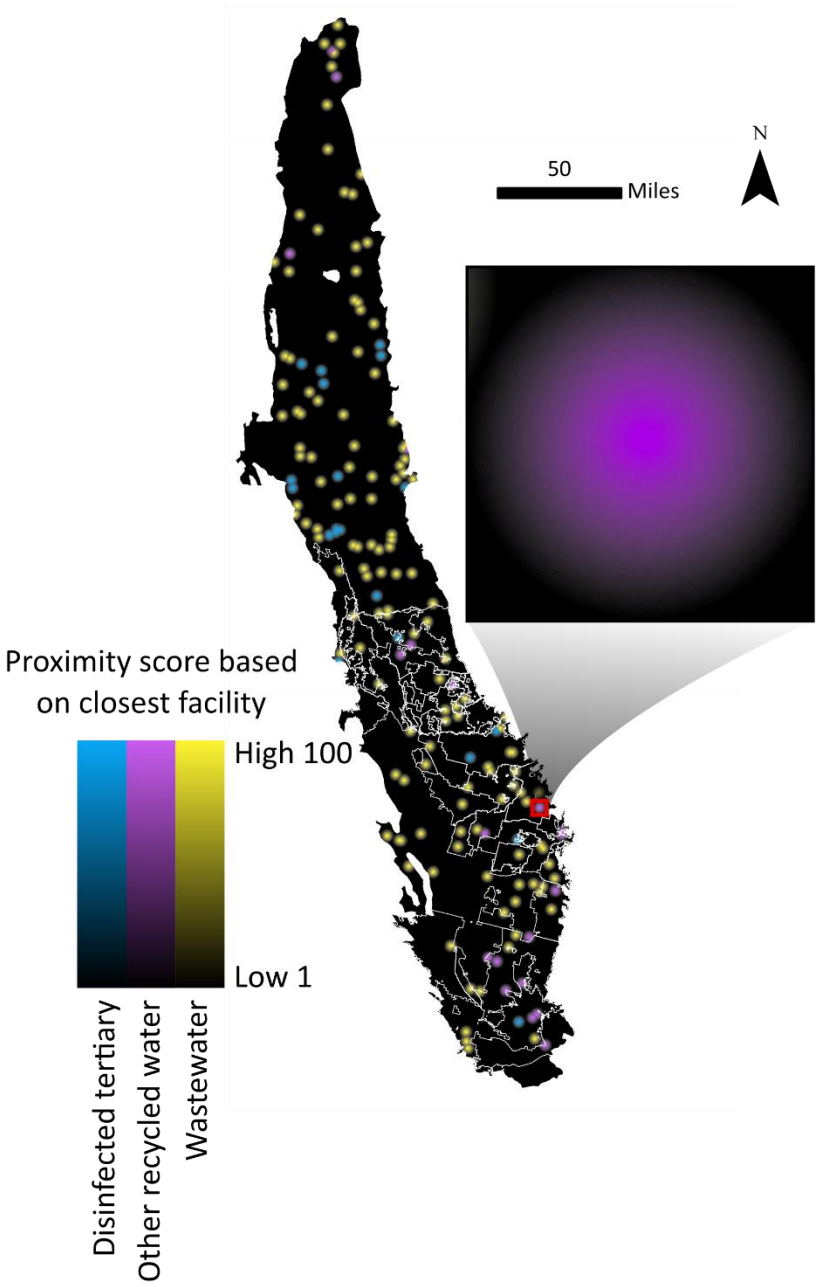

Figure 2.3: Source water proximity scores considering three classes of potential water sources. Color indicates highest treatment level produced in the nearest facility. Locations closest to potential sources are shown in bright color, and any location three or more miles (4.8 km) away from a facility is shown in black. GSA boundaries outlined in white.

Binary Suitability Scores

Some areas cannot be used for recycled water MAR due to existing land cover or proximity to drinking water supplies; therefore, a binary assessment of suitability (i.e., suitable, unsuitable) was performed for (1) land cover and (2) proximity to drinking water sources.

Land cover: Land cover was determined using the Land IQ 2018 crop map; the National Land Cover Database (NLCD) 2016 map of the Coterminous United States was used to fill gaps (Land IQ and DWR, 2021; USGS, 2021). Areas identified as undifferentiated urban (Land IQ) or as open water, wetlands, forest, or developed (except for "Developed, Open Space"; NLCD) were deemed unsuitable for MAR operations and excluded from further consideration (Figure 2.4).

Proximity to drinking water sources: We exclude some areas from consideration for MAR in order to protect drinking water sources. Recycled water MAR requires a minimum residence time between recharge and recovery for potable use (State of California, 2018). Areas where surface recharge would reach a potable well or major river within a year were deemed unsuitable for recycled water MAR. Title 22 requires that recycled water undergo a 12-log virus reduction before being incorporated into a potable supply; i.e., finished water must contain one trillion times fewer active viruses than the original wastewater (State of California, 2018). Six-log reductions can be credited to subsurface residence time, with 1-log reduction credited to each month spent underground (State of California, 2018). Residence time demonstrated with a model as opposed to a tracer study receives only half credit; because we use a model, we considered residence times of at least one year (State of California, 2018).

To determine residence times prior to arrival at wells and rivers, the groundwater system was modeled using the C2VSimFG groundwater model (Hatch et al., 2020). Then, the particle tracking software, ICHNOS, was used to identify where surface recharge would arrive at any well or flow into a river within one year (Kourakos, 2021) (Appendix A.4-A.5. For alternative methods see Appendix A.9.5). Any location in the CV where surface recharge would reach well or river within one year was excluded from further consideration (Figure 2.4). Additionally, Title 22 forbids impoundment of disinfected tertiary water, including in recharge basins, within 100 feet (30.5 m) of a domestic well (State of California, 2018). Accordingly, all wells classified as domestic were assigned a 100-foot buffer in which the land was deemed unsuitable (Figure 2.4).

To determine the location of domestic wells within the CV, we used well completion reports (CNRA, 2021). The data were quality controlled using methods by Jasechko and Perrone (2017). Records were retained for unique, active wells, producing water for human consumption (i.e., public, domestic, and transient non-community wells) with data for latitude, longitude, and completed depth (Appendix A.3). Wells for other purposes were not considered for protection, as MAR uses disinfected tertiary water. Disinfected tertiary water may be used for most non-potable uses, including irrigation of food crops, without further treatment (State of California, 2018). Of the 243,983 well completion records in the CV, 50,031 were retained. Domestic wells received the required distance buffer, and then all classes of potable wells were evaluated using the groundwater models noted above.

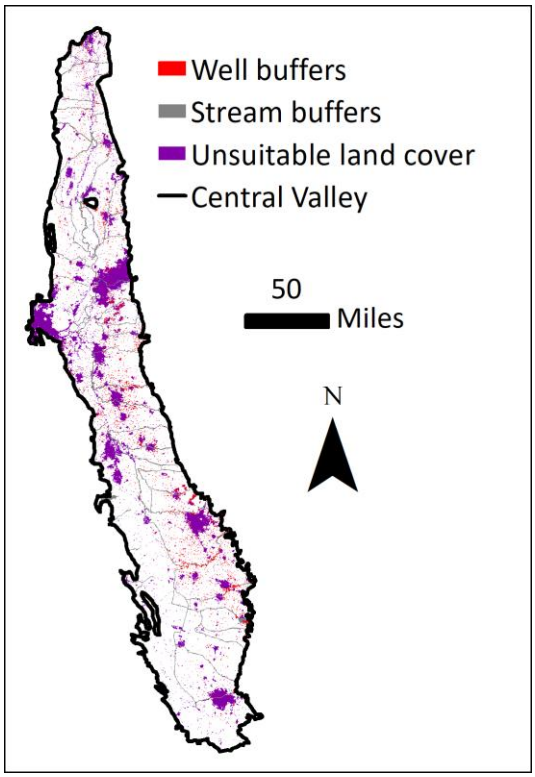

Figure 2.4: Excluded locations in the Central Valley; reason for exclusion indicated by color.

Modelling groundwater transport requires knowing the screened interval of each well. Screen depths should be recorded in the Online System for Well Completion Reports (OSWCR) but are missing from approximately 45% of the retained well reports. Linear models of screen bottom depth as a function of total well depth and top of screen depth as a function of bottom of screen depth were developed for each subbasin to fill the missing data (Appendix A.3). The depths of the wells were then compared to the depths of the aquifer units used in the models. 3,906 wells could not be modeled as they were either too shallow or too deep, resulting in a total of 46,125 wells included in the models. We also simulate a more conservative scenario in which the wells are modeled as fully screened to account for possible leaks in the casing (Appendix A.9.3).

The majority of exclusions are due to land cover and are near major population centers, resulting in exclusion of several otherwise suitable areas. Particle tracking indicates that 1,086 wells (of 46,125) capture water within a year of its infiltration. Combining this with the 100-ft domestic well buffer results in the exclusion of 21 mi^2 (60 km^2) for well protection (Fig 4).

Overall suitability scores and comparison with recharge goals

Following the exclusion of all unsuitable areas in the CV, the final scores of the remaining land in the Valley were divided into three equal intervals classified as "Good", "Moderate" or "Poor" recycled water MAR potential (For alternative classification, see Appendix A.9.4). The total area of land with good suitability within the boundary of each of the 29 critically overdrafted GSAs with plans for MAR was compared with the area needed to meet its recharge goals, as determined from GSP project descriptions or estimated based on recharge type where land needs are not defined (Appendix A.7). The feasibility of meeting the stated goals was evaluated based on the availability of enough suitable land.

Water availability

The main focus of this analysis is the identification of suitable land; however, suitable land requires available water if a GSA is to consider MAR feasible. The quantity of potentially available recycled water was determined from the 2019 discharge volumes of each treatment facility in the CV (SWRCB, 2021a). Totals for each facility were calculated for disinfected tertiary water, all recycled water, and all effluent (including wastewater). This allows for consideration of the amount of disinfected tertiary water currently being produced, as well as the amount that could potentially be produced if existing facilities were upgraded

to provide a higher treatment level. Water from the treatment facilities was divided among GSAs in proportion to the total amount of good suitability land surrounding the facility falling within their boundaries. Average annual water needs for surface recharge (excluding flood projects) were determined from estimates included in GSPs. These estimates were then compared with the amount of potential recycled water. For analyses considering water needs for different types of MAR, see Appendix A.9.7.

Limitations

The suitability mapping process is subject to six limitations, underscoring the importance of local assessments as part of proposed MAR projects.

1. SAGBI is a powerful tool for evaluating the physical suitability of land for MAR, but it addresses only surface conditions. It does not address the ability of the underlying aquifer to store water in terms of thickness and specific yield of water-bearing units or depth to the existing water table (Russo et al., 2015; Fisher et al., 2017). While SAGBI incorporates soil salinity, it does not consider other potential contaminants that may be leached from agricultural soil, such as nitrate or pesticides, or geogenic contaminants like uranium, chromium, or arsenic (O'Geen et al., 2015; Lopez et al., 2021; Murphy et al., 2021; McClain et al., 2019). To the best of our knowledge, maps of soil contamination covering the entire CV are not publicly available. (For a low-resolution analysis including estimates of groundwater arsenic and nitrate, see Appendix A.9.1.) Because SAGBI was not developed for use with recycled water, it does not evaluate the potential of the soil to attenuate residual pathogens or chemicals. While MAR has been successful with a variety of source water qualities

and environmental conditions, specific water quality improvements will depend on local soil properties (Miller et al., 2006; Bekele et al., 2011; Sharma et al., 2008; Fox et al., 2001).

2. Delineation of well protection buffers is limited by the resolution of reported locations and of C2VSimFG. Well completion reports submitted prior to 2015 report locations by township, range, and section, introducing an uncertainty of 0.7 miles (1.1 km) to these wells' locations (Appendix A.2.1).
3. C2VSimFG has an average element area of 407 acres, which is a fine resolution relative to the size of the Valley, but cannot capture local heterogeneities that could result in faster than expected arrival times (Hatch et al., 2020; Gerenday, 2022). This is one reason for the reduced log-reduction credits assigned to modeled residence times by Title 22 and highlights the need for local testing (State of California, 2018).
4. The 100-foot domestic well buffers are smaller than the 100-meter raster cells used for suitability calculations (Appendix A.6.2).
5. For the sake of simplicity, this analysis assumes that all water from the treatment facilities could be available for MAR; however, high quality recycled water generally already has a use from which it would need to be diverted for MAR. Consideration of the total water budget within a GSA and whether such diversion is feasible is beyond the scope of this study.
6. While linear distance to facilities is considered, it is not known whether the water can be practically transported over intervening topography.

Results

Suitability of land for recycled water MAR is dependent on recycled water proximity, as the poor proximity score of any land not within three miles of a treatment facility overrides the other factors and results in a low overall suitability score (Figure 2.5). The majority of land is rated as poorly or moderately suitable (Table 2.1). Land of good suitability is more likely to be found on the eastern side of the Valley, where soils tend to be better for infiltration and there is a higher density of recycled water sources. Areas in the southwest tend to be unsuitable due to a relative scarcity of treatment facilities and limited deep percolation capacity. The majority of land rated as suitable (87-91%) is agricultural with deciduous fruit and nut crops making up one of the largest portions (Appendix A.8.3).

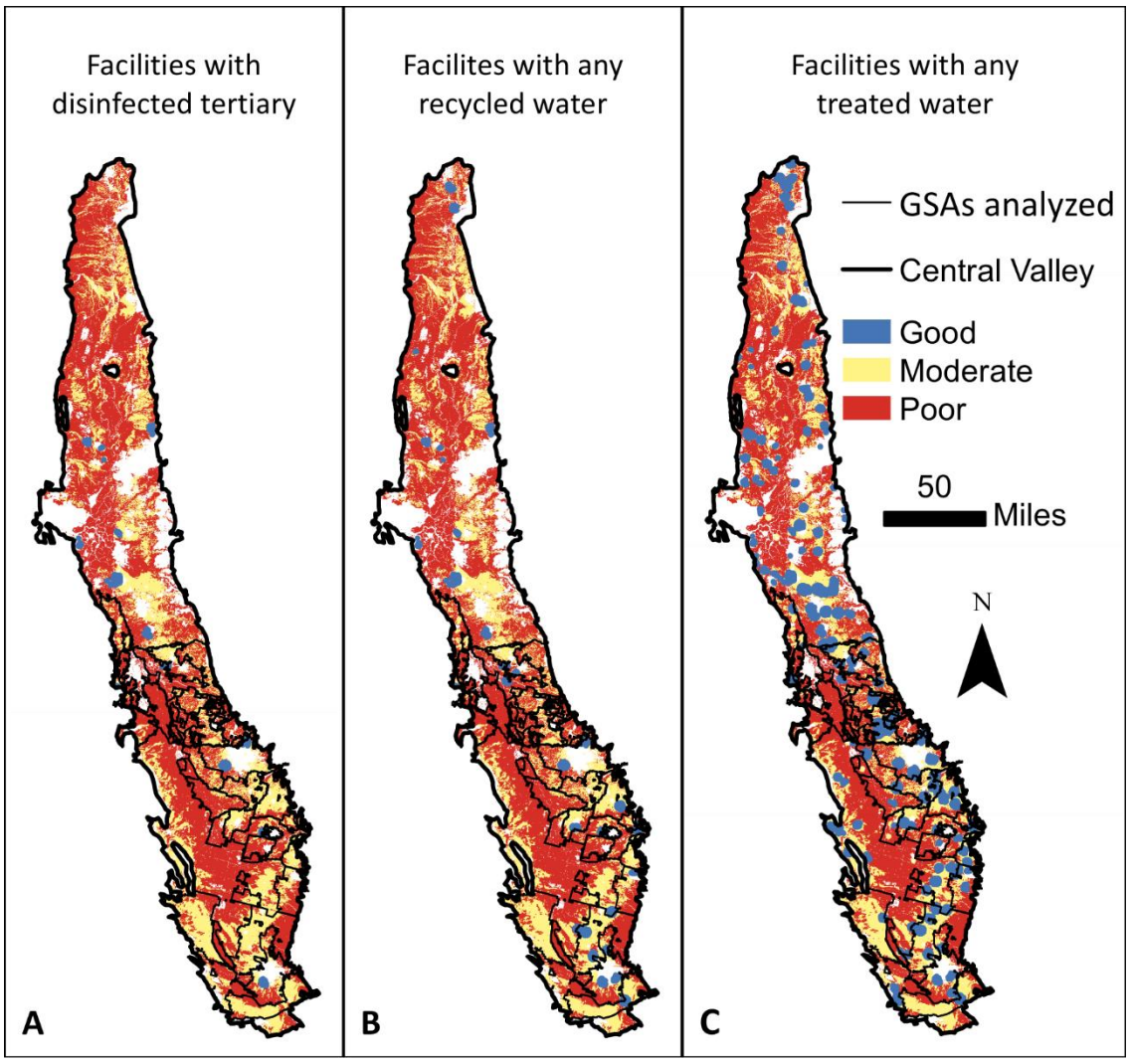

Figure 2.5: Suitability of potentially available land considering (A) only facilities producing disinfected tertiary, (B) any facility with recycled water, (C) any treatment facilities, including those with only wastewater. Good areas (blue) are emphasized; for a map with all areas to scale or for regional maps, see Appendix A.8.1.

Table 2.1: Area (mi^2; 1 mi^2 = 2.6 km^2) available to each GSA. Colors indicate facilities required to meet land needs (Blue = facilities with disinfected tertiary, Purple = facilities with any recycled water, Yellow = facilities with any treated water, Gray = needs not met)

GSA	Facilities with disinfected tertiary water			Facilities with any recycled water			Facilities with any treated water		
	Good	Moderate	Poor	Good	Moderate	Poor	Good	Moderate	Poor
Aliso Water District	0	7.6	33	0	7.6	33	0.035	7.9	33
Buena Vista	0	0.24	79	0	0.24	79	0.089	4.9	74
Central Kings	0	160	66	0	160	66	24	150	50
Chowchilla Water District	0	48	78	0	49	77	2.8	53	70
East Kaweah	0	100	68	2.2	100	64	11	97	61
Eastern Tule	0	80	140	0.25	80	140	5.0	84	130
Gravelly Ford Water District	0	3.5	9.6	0	3.5	9.6	0.0	3.5	9.6
Greater Kaweah	2.2	88	230	4.5	91	220	4.9	100	210
James Irrigation District	0	0.9	42	0	0.9	42	0	6.7	37
Kern Groundwater Authority	0	890	580	21	880	570	34	870	570
Kings River East	0	170	100	5.9	160	98	20	150	94
Madera County - Chowchilla	0	14	52	0	16	50	0.097	17	49
Madera County - Madera	0.11	49	190	1.4	58	180	5.0	67	170
Madera Irrigation District	0	110	94	0.94	110	89	15	120	68
Madera Irrigation District, City of Madera	0	1.9	2.2	0	1.9	2.2	1.8	2.2	0.14
McMullin	0	73	110	0	73	110	4.5	77	100
Merced County	0	1.7	0.12	0	1.7	0.12	0	1.7	0.12
Merced Subbasin	0.78	140	320	3.3	150	310	11	160	290
Mid Kaweah	0.86	18	98	0.86	18	98	1.3	26	90
Mid Kings River	0	77	57	2.7	80	52	7.8	76	50
New Stone Water District	0	0.31	6.2	0	0.31	6.2	0	0.31	6.2
North Fork Kings	0	36	220	0	36	220	0.98	45	210
North Kings	5.9	160	150	5.9	160	150	18	160	130
Northern & Central Delta-Mendota	0.37	96	310	0.37	96	310	2.9	110	300
San Joaquin River Exchange Contractors Water Authority	0	25	360	0	25	360	1.1	36	350
South Fork Kings	0	17	85	0	17	85	0.10	30	72
South Kings	0	2.4	1.0	0	2.4	1.0	1.5	1.6	0.34
Tri-County Water Authority	0	41	53	0	41	53	0.089	41	53
Triangle T Water District	0	0.86	22	0	0.86	22	0	0.86	22
Central Valley Total	25	5500	11000	87	5500	11000	400	5900	10000

If treatment plants currently producing disinfected tertiary water are the only water source, two of 29 GSAs have enough suitable land, assuming average land needs (Figure 2.6 – Figure 2.7). If all facilities producing any kind of recycled water are considered, six GSAs have enough suitable land. If facilities only producing wastewater are also considered, an additional eight GSAs would have suitable land to meet their needs. Several others may have enough land under these conditions assuming the lowest land requirements (Figure 2.6 – Figure 2.7).

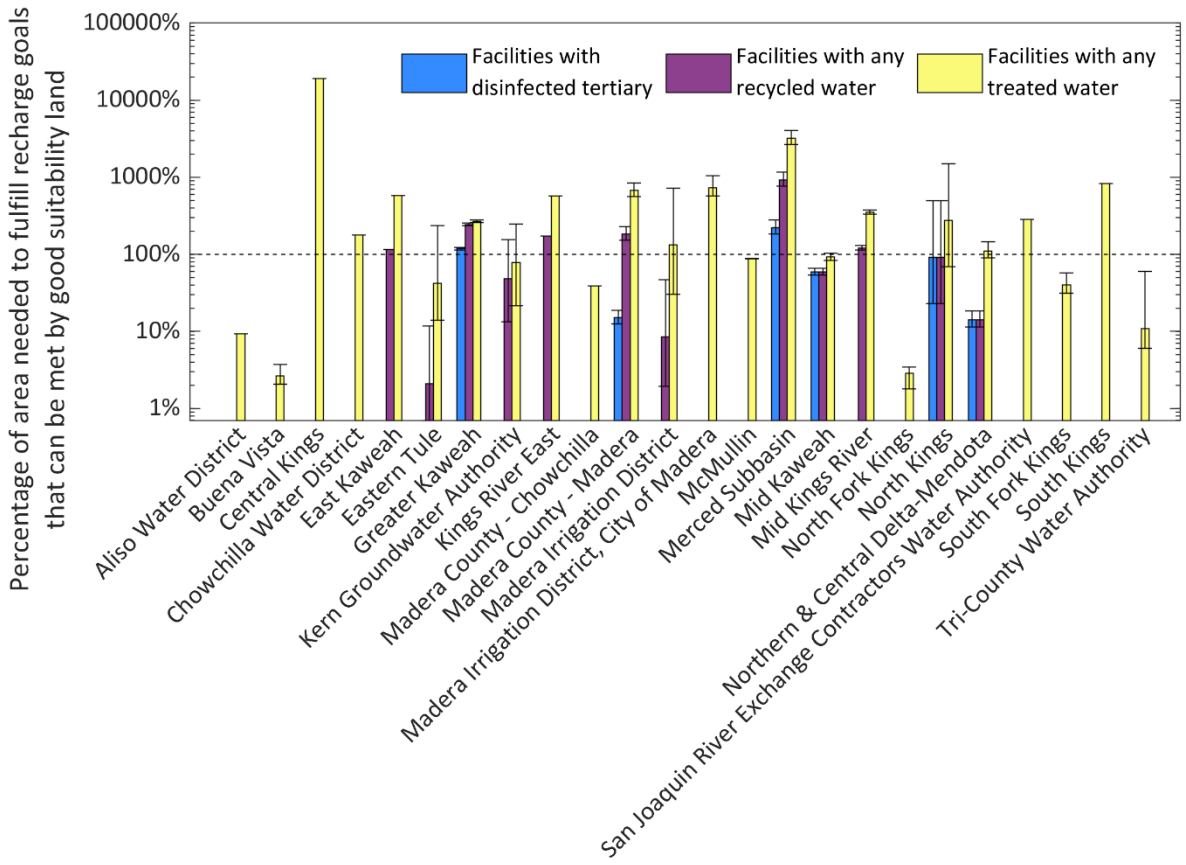

Figure 2.6: Land with proximity to facility assessment. Percentage of area needed by each GSA to fulfill recharge goals that can be met by good suitability land considering proximity to different types of treatment facilities (e.g., facilities with disinfected tertiary, facilities with any recycled water, and facilities with any treated water). Some Plans did not explicitly state land needs; for these Plans, we estimated a mean, min, and max amount of land based on proposed MAR projects. For these GSAs, bars represent the mean land; minimum and maximum estimated land requirements are shown with error bars. GSAs without suitable area not shown. Dashed line indicates 100% of area needed to fulfill recharge goals can be met by good suitability land within proximity to treatment facilities.

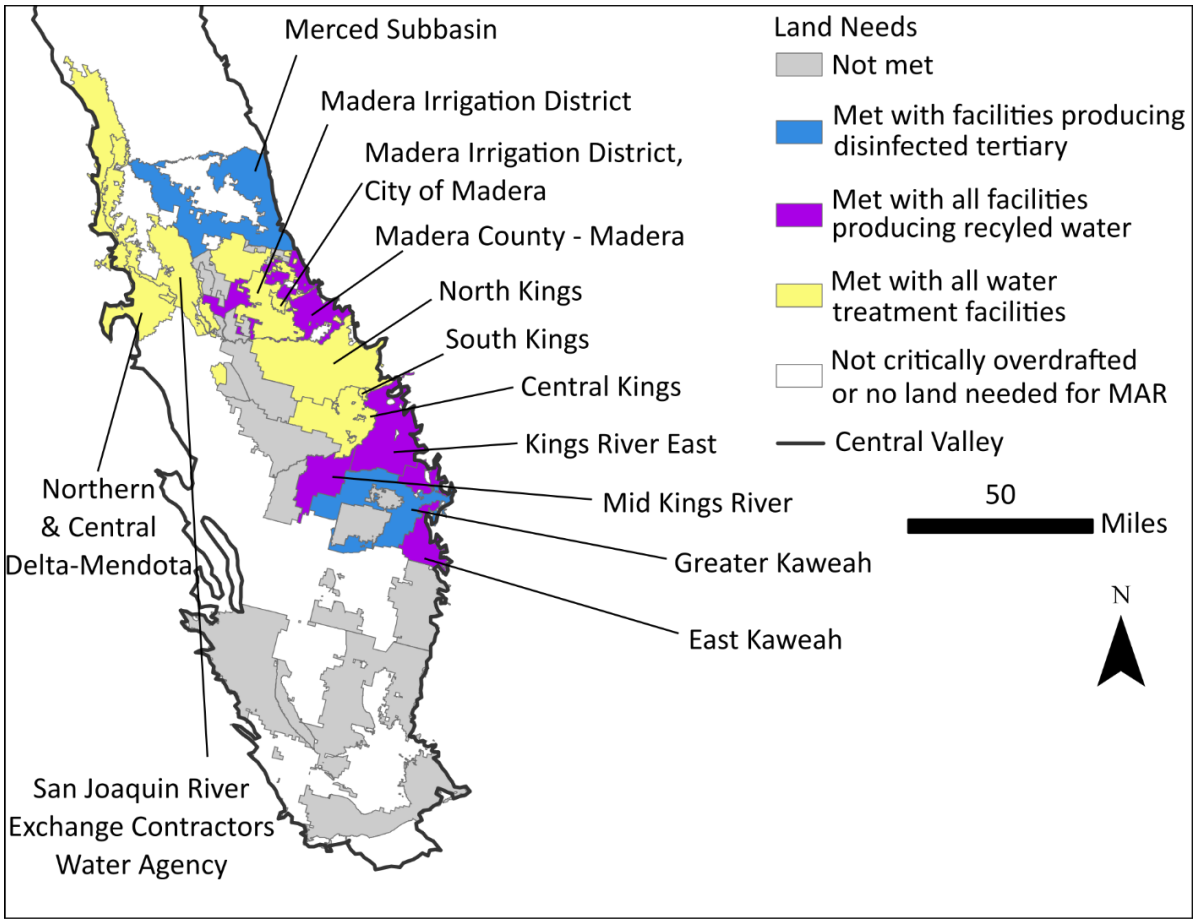

Figure 2.7: GSAs by most conservative scenario in which land needs can be met (if any). GSAs needs met by: disinfected tertiary facilities only shown in blue; all facilities with any recycled water shown in purple; and all treatment facilities, including those with only wastewater, shown in yellow. GSAs without enough suitable land given their current facilities shown in gray.

We also assess if recycled water could be used as a potential source to meet the water needs of MAR projects proposed within each GSP (Figure 2.8). North Kings could have access to enough total recycled water to supply its recharge goals if water treatments were upgraded. Similarly, if all treated water, including wastewater, is considered, North and Central Kings, as well as Madera Irrigation District - City of Madera could access enough recycled water to meet their goals. These three GSAs also have enough potentially suitable land when all facilities are considered. Sensitivity analyses considering water needs for different types of projects yield the same result in terms of which GSAs have sufficient

recycled water but do show a difference in terms of how close some GSAs are to meeting their goals (Appendix A.9.7).

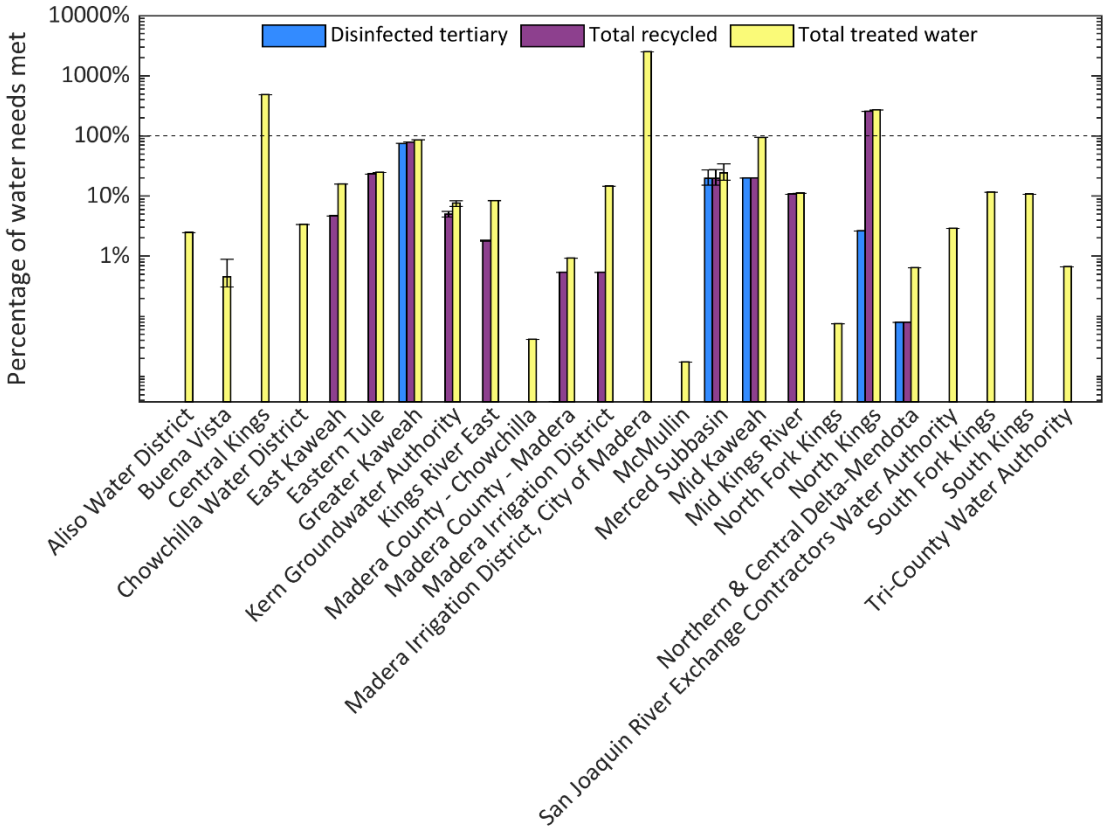

Figure 2.8: Water needs assessment based on recharge goals set in GSPs and types of water produced in facilities near or within each GSA. Percentage of water needed by each GSA to fulfill recharge goals that can be met by different types of available water, assuming treatment processes can be upgraded where needed. Some Plans did not explicitly state water needs; for these Plans, we estimated a mean, min, and max amount of water based on proposed MAR projects. For these GSAs, the bars represent the mean; minimum and maximum estimated water requirements are presented with error bars. GSAs without available water are not shown. Dashed line indicates 100% water needs are met by available water.

Discussion

Local recycled water availability is the most limiting factor in siting recycled water MAR projects. This is evident from the fact that recharge for recycled water MAR projects tends to be conducted at the treatment facility, and many MAR operators cite limited water availability as their greatest challenge (Al-Otaibi and Al-Senafy, 2004; Bennani et al., 1992;

Lopes and dos Santos, 2012; Pi and Wang 2006; Perrone and Rohde, 2016). In order for a project to be successful, suitable land and water must be available in the same location. Constructing or retrofitting facilities to produce disinfected tertiary water can result in more potential for recharge. Costs of upgrading wastewater treatment plants to produce recycled water suitable for MAR may range from $140,000 to $620,000 per acre-foot over 30 years (Cupps and Morris, 2005). If patterns of groundwater extraction remain the same, increased water recycling capacity will likely be needed to balance overdraft in the CV (Badiuzzaman et al., 2017). The majority of facilities currently producing disinfected tertiary water in the CV are not located in critically overdrafted basins (Figure 2.3); however, they may provide a future opportunity for lower priority basins as they continue to develop their water management strategies.

It is possible to recharge farther from the source if transporting water is more feasible than obtaining suitable land nearby or if a regional facility distributes water to many decentralized sites. For instance, the Chino Basin Recycled Water Groundwater Recharge Program distributes recycled water to 11 infiltration sites distributed throughout Chino Basin (Campbell and Fan, 2021). When completed, the Metropolitan Water District of Southern California's Regional Recycled Water Program will deliver recycled water for recharge through 60 miles (96.6 km) of pipe to four regional groundwater basins (MWD, 2016).

Major factors influencing the maximum acceptable distance include local land values and the cost and energy use of transporting water (Bradshaw and Luthy, 2017). Costs of land acquisition for recharge basins and conveyance right-of-ways estimated in GSPs range from $15,000 to $42,000 per acre, resulting in normalized costs of $5-42 per acre-foot of recharge over a 30-year period (Aliso Water District GSA, 2020; McMullin Area GSA, 2019; Central

Kings GSA, 2019; South Kings GSA, 2019). Factors including the availability of existing conveyance networks and topography along the transport route affect costs (Fournier et al., 2016; Trussell et al., 2012). The cost of constructing new conveyance systems has been estimated at $2.3-34 million per mile or $25-1,100 per acre-foot, while the operation and maintenance costs range from $25-29 per acre-foot per mile (Bradshaw and Luthy, 2017; Cooley and Phurisamban, 2016; McMullin Area GSA, 2019). Water savings due to recycled water MAR may be negated by water consumption for power generation if excessive uphill pumping is required to move recycled water (Fournier et al., 2016). Recycled water MAR projects more than one to two miles (1.6 – 4.8 km) from their source tend to make use of gravity flow or are integrated with a wastewater system (Hutchinson, 2013; Johnson, 2009; Kanarek and Michail, 1996; Page et al., 2010).

Although this study demonstrates the power of suitability mapping and groundwater modeling for evaluating large land areas for potential recycled water MAR, selecting locations is best done at the local level. GSAs are more likely to know the statuses and exact locations of wells and availability of land and water. If a GSA does not have a source of recycled water within its boundaries, they will have to negotiate with other entities. This is not surprising, as water recycling projects often require partnerships with multiple agencies, but it could be a challenge if another GSA already has plans for the water (Sokolow et al., 2019). Additionally, while mapping is a useful tool for selecting candidate sites, any recycled water MAR project will require local soil studies, pilot testing, and tracer experiments before operating at scale.

Finally, the value of groundwater recharge must be weighed against that of other uses for water and land. For instance, 700,000 acre feet (860 million m^3) of recycled water was

used for irrigation in California in 2019, comprising 50% of total reported reuse (SWRCB, 2021a), and surface outflows from treatment plants can support riparian ecosystems (Rohde et al., 2021). Currently, the majority of suitable land is in use for agriculture, particularly deciduous fruits and nuts. Growing seasons and limits on how long perennial crops can tolerate flooding constrain the total time infiltration can occur on active farmland (Ganot and Dahlke, 2021). Recharging recycled water on agricultural land is still largely unexplored (Grinshpan et al., 2021). Given the scarcity of available recharge water, it is unlikely that there will be an excess at times when MAR is impossible, and the relative predictability of recycled water supplies can facilitate planning of water allocations (SWRCB, 2021a; Perrone and Rohde, 2016). Nevertheless, focusing recharge efforts on agricultural areas may require land fallowing. This can assist in bringing water budgets into balance and benefit habitats but will be expensive and require compensating farmers (Bourque et al., 2019). (For required MAR area broken down by whether plans include on-farm recharge, see Appendix A.9.6). Given that fruit and nut crops are among the state's most valuable, the cost of acquiring land may be high (CDFA, 2021).

Conclusion

Recycled water MAR is feasible in many locations in the CV, but more recycled water sources are necessary for recycled water MAR to be implemented across the CV. Highly populated areas are more likely to have access to recycled water but tend to have less suitable land and a greater density of wells, excluding more areas. Suitability mapping and particle tracking are useful tools for GSAs considering recycled water MAR. Areas under serious consideration for recycled water MAR will need infiltration studies and tracer tests to ground truth results and receive project approval. Recycled water MAR can help GSAs that

have sufficient suitable land and access to water achieve their recharge goals, enabling them to comply with SGMA and maintain a sustainable water supply.

Chapter 3 Sulfur hexafluoride and potassium bromide as groundwater tracers for managed aquifer recharge

Abstract

Sulfur hexafluoride (SF_6) is an established tracer for use in managed aquifer recharge projects. SF_6 exsolves from groundwater when it encounters trapped air according to Henry's Law. This results in its retardation relative to groundwater flow, which can help determine porous media saturation and flow dynamics. SF_6 and the conservative, non-partitioning tracer, bromide (Br^- added as KBr), were introduced to recharge water infiltrated into stacked glacial aquifers in Thurston County, Washington, providing the opportunity to observe SF_6 partitioning. Br^-, which is assumed to travel at the same velocity as the groundwater, precedes SF_6 at most monitoring wells. Average groundwater velocity in the unconfined aquifer in the study area ranges from 3.9 – 40 m/d, except in the southwestern corner where it is slower. SF_6 in the shallow aquifer exhibits an average retardation factor of 2.5 ± 3.8, suggesting an air to water ratio on the order of 10^{-3} to 10^{-2} in the pore space. Notable differences in tracer arrival times at adjacent wells indicate very heterogeneous conductivity. One monitoring well exhibits double peaks in concentrations of both tracers with different degrees of retardation for the first and second peaks. This suggests multiple flowpaths to the well with variable saturation. The confining layer between the upper two aquifers appears to allow intermittent connection between aquifers but serves as an aquitard in most areas. This study demonstrates the utility of SF_6 partitioning for evaluating hydrologic conditions at prospective recharge sites.

Introduction

Increasing populations and climate insecurity are forcing many municipalities to reevaluate how they manage their water supplies. One available strategy is to use treated wastewater for managed aquifer recharge (MAR) and eventual reuse. MAR is the addition of water into aquifers by infiltration or injection at engineered facilities to prevent their depletion. MAR can be an efficient way of storing water and can provide an opportunity for contaminants to be removed or degraded through interaction with matrix materials and microbes (Bouwer, 2002; P. Dillon, 2005).

An important step in MAR projects planning to recharge reclaimed wastewater is to conduct a tracer study to establish subsurface residence times, as this timing affects the degree to which residual chemicals and pathogens in the reclaimed water will be attenuated before the water is re-extracted or discharges to surface water. Tracer data also serve to establish hydraulic connections between recharge and extraction facilities. Furthermore, tracers can be used to evaluate subsurface flow, groundwater ages, and hydrologic properties of aquifers.

This paper evaluates the behaviors of two tracers added to MAR water: sulfur hexafluoride (SF_6), a relatively insoluble gas tracer, and bromide (Br^-), a common ionic tracer. These chemicals are easy to distinguish from their background concentrations, and SF_6 can be detected at concentrations ranging over several orders of magnitude (Wanninkhof et al., 1987). Both tracers are non-toxic at the concentrations used and are chemically non-reactive. As an insoluble gas, SF_6 exsolves in the presence of trapped air, retarding its transport, while behaving conservatively under saturated conditions (Fry et al., 1995; Vulava et al., 2002). Bromide, on the other hand, behaves conservatively regardless of porous media

saturation as demonstrated by numerous studies in the unsaturated zone (e.g., Flury and Wai, 2003). The use of these two tracers allows comparison of the behaviors of ionic and gas tracers and the evaluation of gas partitioning, which will aid in selecting the appropriate tracers in subsequent environmental investigations.

Although there have been several studies of SF_6 partitioning in laboratory experiments (Balcke et al., 2007; Bullister et al., 2002; Vulava et al., 2002) and various field studies employing the gas as a tracer (Clark et al., 2004, 2005; McDermott et al., 2008; K.Dillon et al., 1999), there have been few studies that make use of SF_6 partitioning in the field. Typically, it is assumed that SF_6 is conservative in groundwater; however, it is known that small pockets of air are routinely trapped in otherwise saturated porous media with implications for biological processes and infiltration rates (Christiansen, 1944; Heilweil et al., 2004). Therefore, some degree of SF_6 partitioning may occur, which can provide a useful tool for understanding air distribution in porous media. This study examines SF_6 transport and partitioning in a set of stacked glacial aquifers with localized heterogeneities, which provides the opportunity to observe tracer behaviors in a natural setting and to shed light on the site's hydrologic properties.

Study location

This study was conducted at the Hawks Prairie Reclaimed Water Ponds and Recharge Basins managed by the LOTT Clean Water Alliance in Thurston County, Washington (Figure 3.1). At the site are eight one-acre infiltration basins, two of which were used in the study. The Hawks Prairie site is underlain by the Vashon formation, which consists of Quaternary glacial siliciclastic deposits (Figure 3.2). In the Vashon advance outwash is a shallow, unconfined aquifer. Flow is restricted in some locations by occurrence of Vashon

Till. The shallow aquifer is separated by a confining unit of pre-Vashon sand and finer sediment, which is sometimes referred to as the Kitsap formation, from a gravel layer forming the sea level aquifer. The sea level aquifer is underlain by Tertiary mixed glacial and non-glacial deposits in which a deep aquifer occurs. Groundwater flow through the study area determined from monitoring well head measurements in the shallow aquifer is predominately to the south and southwest, and flow in the sea level aquifer is to the east (HDR Engineering, Inc., 2018a). The shallow aquifer is used for private residential water supply, while the sea level and deep aquifers serve as sources of public water supplies for the cities of Lacey, Olympia, and Tumwater (HDR Engineering, Inc., 2017; Logan et al., 2003). The shallow aquifer near Hawks Prairie is monitored with 21 wells across 2 km^2, and the sea level aquifer is monitored with four wells. The deep aquifer is not monitored in this study, as the effects of MAR on it are thought to be negligible.

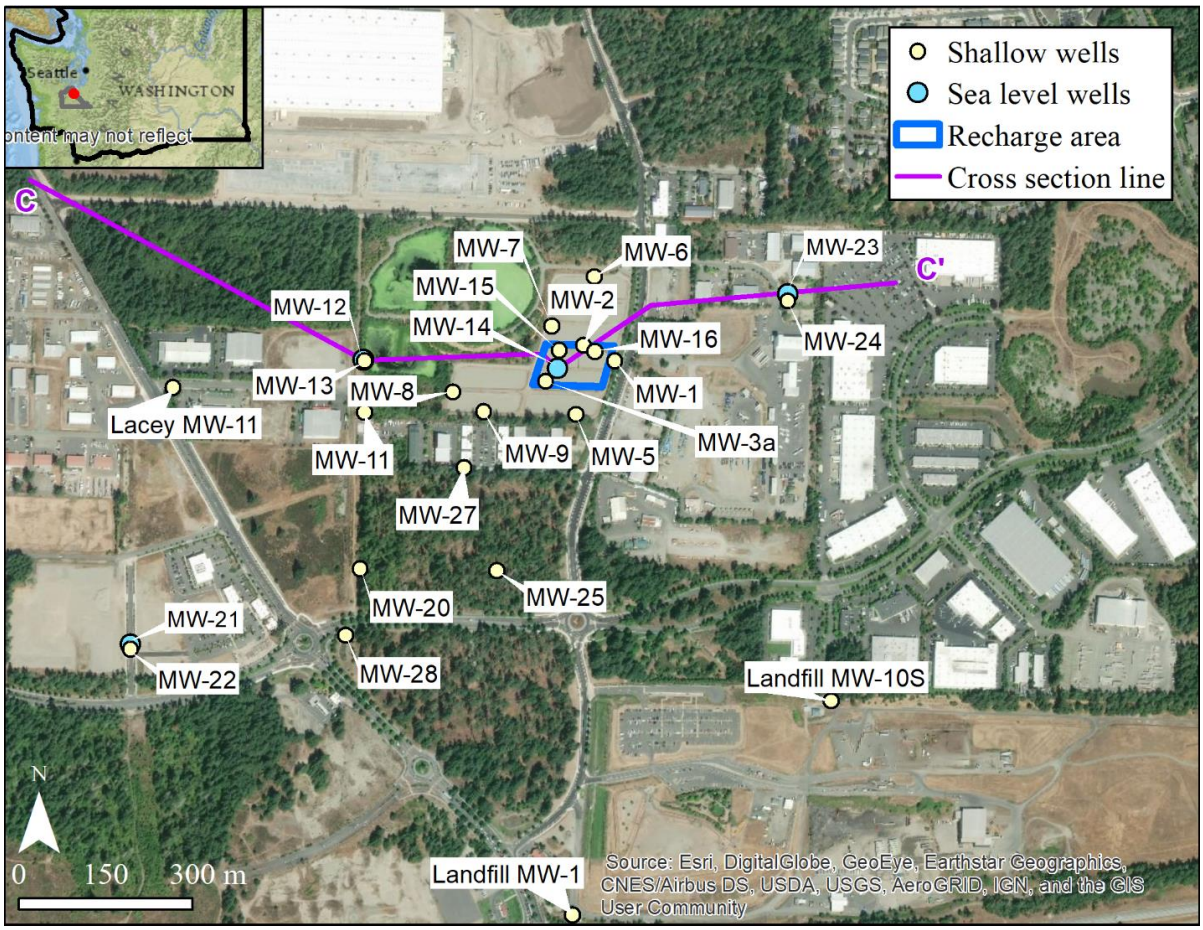

Figure 3.1: Aerial photo of the Hawks Prairie Facility showing the locations of the basins used for recharge and monitoring wells (MW). Purple line indicates location of cross section shown in Figure 3.2. Inset map: Washington State outlined in black; Thurston County outlined in gray; study area marked in red.

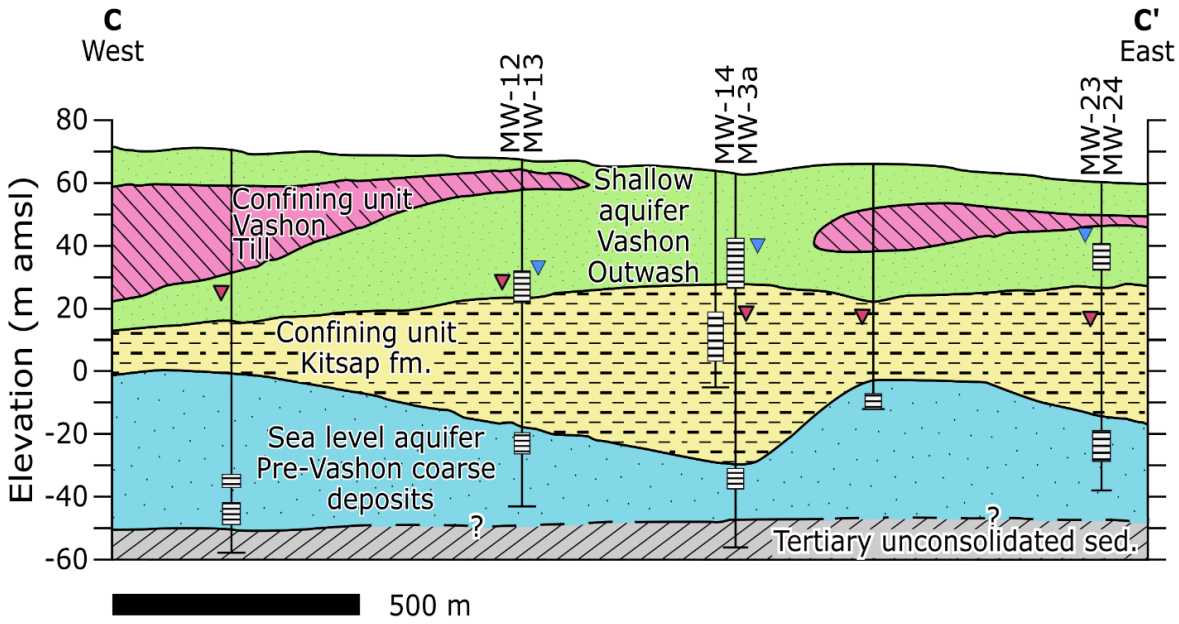

Figure 3.2: Cross section of study area. Blue triangles denote piezometric surface of the shallow aquifer, as measured during prior hydrogeological characterization, and red, bold edged triangles represent that of the sea level aquifer. Unlabeled wells are preexisting and were not monitored in the study (after HDR Engineering, Inc., 2018a).

Theoretical Background

Since SF_6 is a chemically non-reactive gas, it behaves conservatively in saturated aquifers and travels by advection and dispersion at a linear velocity similar to that of the groundwater (Vulava et al., 2002). However, groundwater flow may encounter air in the vadose zone, as well as small, immobile air bubbles that are trapped in aquifers due to water table or pressure fluctuations and remain in gas phase. When dissolved SF_6 encounters trapped air, it exsolves until its concentration in the air pockets is in equilibrium with the groundwater. Then, it is slowly redissolved as the local SF_6 concentration declines. This exsolution – dissolution process results in the retardation of SF_6, which is the reduction in the velocity of a solute relative to the groundwater's mean linear velocity. This retardation is similar to that caused by sorption and desorption of more reactive compounds (Fry et al.,

1995). Ideally, this retardation can be described as a linear function of the aquifer's gas content using the equation

$$R_f = 1 + H * \frac{V_a}{V_w} \quad (2.1)$$

where R_f is the retardation factor or ratio of the effective velocity of the groundwater to that of the dissolved gas tracer, where V_a and V_w are the volumes of air and water in the aquifer respectively (Fry et al., 1995; Vulava et al., 2002). *H* is the Henry's law constant defined as the equilibrium ratio of the tracer gas concentration in the gas and aqueous phase, which for SF_6 at 12° C is equal to 121 (See appendix B for calculation). This effect has been demonstrated in lab experiments with SF_6, Kr, and ^3H_2O in variously saturated media by Vulava et al. (2002).

The retardation of SF_6 can be calculated from its arrival time at a monitoring well compared to the arrival of a highly soluble and non-reactive tracer such as Br^-. Aquifer saturation is more difficult to measure, and the goal of a tracer study using SF_6 partitioning is to estimate the aquifer's trapped air content. Thus, equ. (2.1) is rearranged to calculate V_a/V_w as a function of R_f and *H*.

$$\frac{V_a}{V_w} = \frac{R_f - 1}{H} \quad (2.2)$$

Using this equation, it is possible to calculate the average degree of saturation between the release and monitoring points using an observed R_f, assuming *H* is known.

Methods

Prior to the experiment, all of the recharge basins were regularly used, saturating most of the underlying porous media. The basins were allowed to drain, and reclaimed water

was fed into the northern and southern edges of two of the basins via pipes. A few meters of the basins adjacent to the pipes were inundated to a maximum depth of approximately 10 cm. The remaining area remained dry. From January 16 to February 3, 2018, 2100 kg of potassium bromide (KBr) were dissolved in potable grade water and released into the inflow to the infiltration basins at a rate of 5.5 to 8.2 m^3/d. The Br^- concentration flowing into the basins was measured at 9,800 – 42,500 μg/L. To prepare the SF_6 tracer, 76 L of pure SF_6 and 380 L of water were injected into each of two nylon bags and allowed to equilibrate. Using the equations of Bullister et al. (2002) and assuming ideal gas behavior at a mean air temperature of 6.7 °C, the maximum solubility of SF_6 is 0.459 mmol/L, so about 0.35 mol or 8 L of SF_6 would have gone into solution while the rest remained in the headspace. The equilibrated solution was then added to the recharge water with an average frequency of 1.4 times per day. In total, 207 L (9.0 mol) of SF_6 were added to the recharge water from January 16 to February 2, 2018. Since much of the SF_6 was expected to degas from the infiltration basins before reaching the groundwater, an additional 48 L (2.1 mol) of SF_6 was injected into each of the injection wells: MW-1, MW-2, MW-7, MW-15, and MW-16, between February 7 and 14, 2018. It should be noted that SF_6 is a potent greenhouse gas with the highest greenhouse warming potential named in the IPCC reports; however, the amount used in this study is miniscule compared to the amount used in electrical applications. Furthermore, due to its low mole fraction in the atmosphere, the total radiative forcing due to SF_6 is 0.23% of that of the total CO_2 forcing (Myhre, 2013).

During the calendar year 2018, water samples were collected from wells on a daily to weekly basis during January and February, weekly to semimonthly in March, semimonthly in April, and monthly through October. Sampling at MW-1, MW-2, MW-6, and MW-7 was

discontinued in late February 2018 following the injection of SF_6 into these wells. Samples tested for bromide were bottled onsite and sent to Eurofins Eaton Analytical for ion chromatography analysis. SF_6 samples were collected in four pre-weighed and sealed 10 mL Vacutainers (blood collection tubes). SF_6 was then analyzed in the headspace of the Vacutainers by gas chromatography equipped with an electron capture detector at University of California, Santa Barbara following the procedure outlined by Clark et al. (2004). At least two replicates must agree within 10% for the measurement to be accepted. The headspace method can be used to analyze water samples containing SF_6 at concentrations ranging from 0.05 pmol/L to 23.6 nmol/L (23,600 pmol/L). In samples with SF_6 concentrations exceeding what can be measured by the headspace method, a small quantity of the equilibrated solution, which has a lower concentration than what was originally sampled due to Henry's law exsolution, can be transferred to a new container for measurement and the initial concentration calculated (See appendix B).

Average velocity from basin to well is determined by dividing the direct distance from the edge of the nearest infiltration basin to the well screen by travel time. Travel time is calculated starting with the date on which 50% of each tracer had been added to the infiltrating water and ending with the arrival of the peak tracer concentration or tracer center of mass (COM), which is determined by integrating under the breakthrough curve. COM can only be accurately determined for complete breakthrough curves, while the peaks can be identified when concentrations start to decline, even if they have not returned to background levels.

Results

Tracer concentrations were measured in monitoring wells from January to October 2018, and breakthrough curves are available for several wells (Figure 3.3 - Figure 3.6). Following the beginning of infiltration, both tracers were first detected above background levels at MW-5 in the shallow aquifer. Both tracers exhibit distinctive double peaks in the breakthrough curve at this well in January to early February (Figure 3.3). In the case of Br^-, the tracer patch then spread predominately to the west and additionally to the north and south (Figure 3.7). High Br^- levels were measured in shallow wells MW-3a and MW-16 in late January, but concentrations above background level were not detected at nearby MW-15 until late March and were not detected at MW-2. The SF_6 injected into wells MW-1, MW-2, MW-7, MW-15, and MW-16 in early February quickly overshadowed the signature from SF_6 infiltration observed in MW-5. The SF_6 migrated downgradient in a southwesterly direction, but concentrations at MW-3a remained low relative to nearby MW-5 and to downgradient MW-8, MW-9, and MW-27 until late March (Figure 3.4 and Figure 3.8). The farthest that SF_6 spread during the study period was to MW-13 and MW-27, approximately 300 m downgradient in the shallow aquifer (Figure 3.8). With the exception of MW-12 which has breakthroughs occurring at similar times to its nested partner MW-13, detections in the sea level aquifer were small and isolated (Figure 3.5).

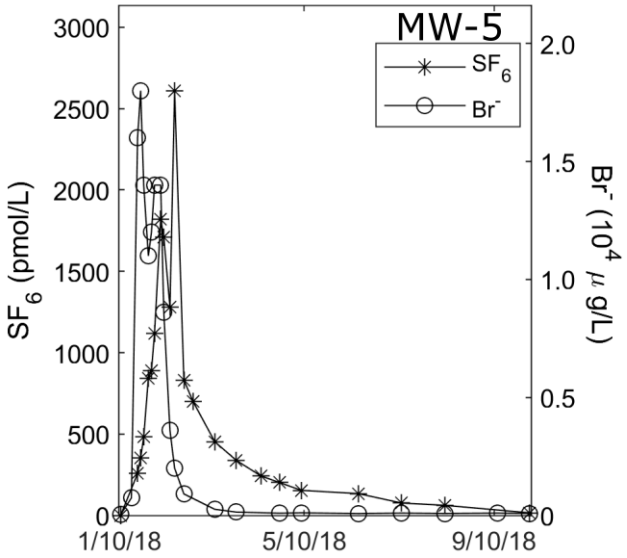

Figure 3.3: Breakthrough curve at MW-5 showing double peaks for both tracers.

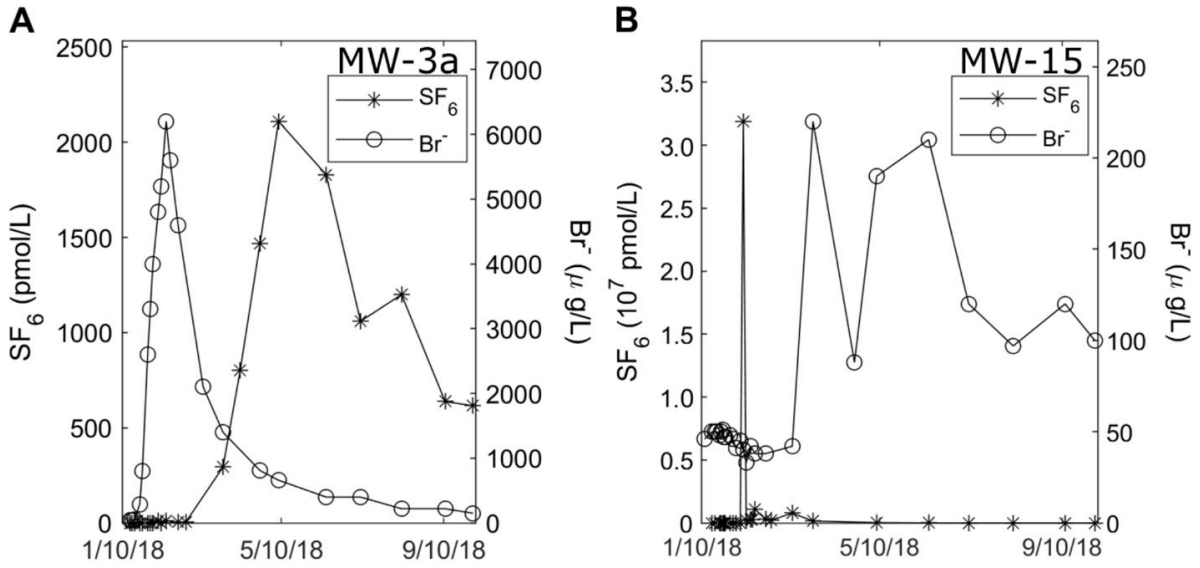

Figure 3.4: Breakthrough curves for (A) MW-3a and (B) MW-15. Note that Br^- at MW-3a significantly precedes that at MW-15, while SF_6, which was added directly to MW-15, is late to arrive at MW-3a.

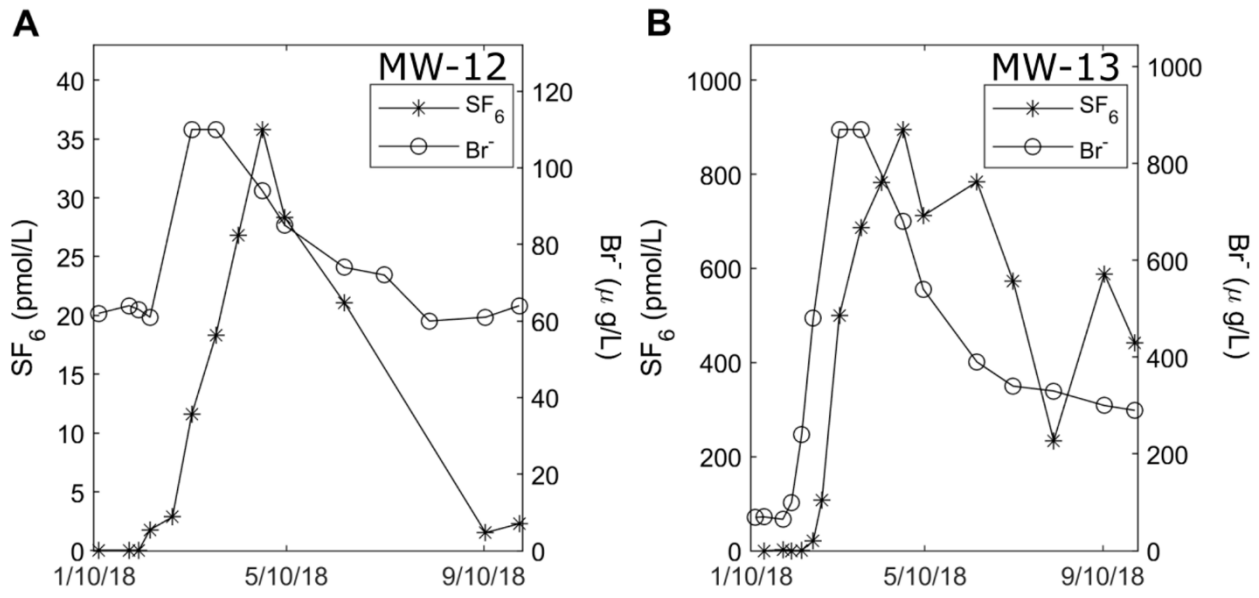

Figure 3.5: Breakthrough curves for (A) MW-12 and (B) MW-13. Arrivals of both tracers at MW-12 follow those at MW-13 closely even though MW-12 is screened in the sea level aquifer and MW-13 is screened in the shallow.

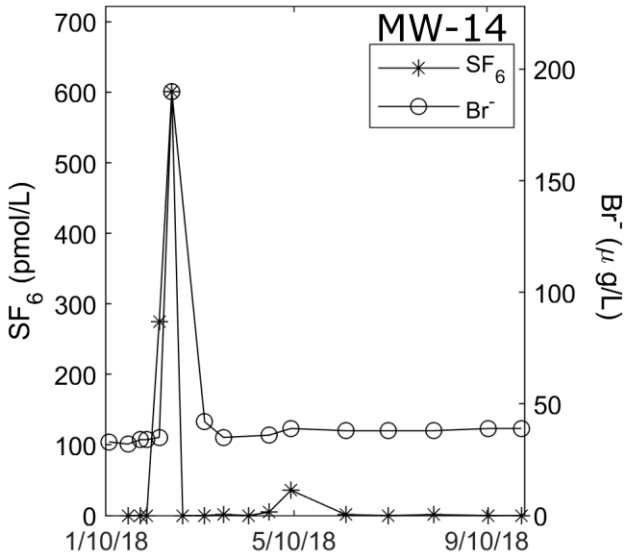

Figure 3.6: Breakthrough curve for MW-14 showing isolated spikes of both tracers.

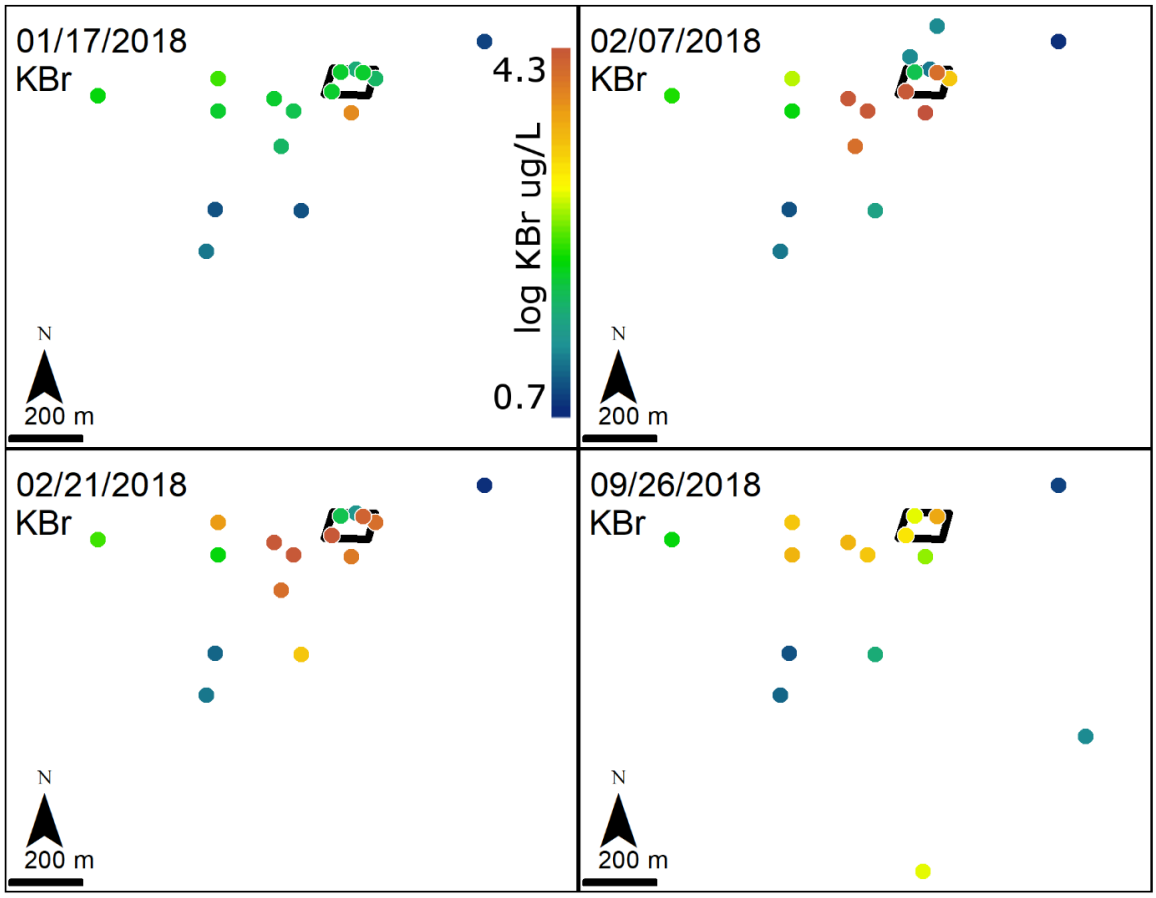

Figure 3.7: Br^- concentration measured in shallow aquifer monitoring wells with infiltration basins outlined in black. Color scale is the same for all dates. Br^- first appears in MW-5, shown on January 31st in orange, to the south of the basins. Br^-, which unlike SF_6 was not injected into any wells, is low in February at MW-2 and MW-15 relative to surrounding wells. By September, Br^- concentrations are representative of the end of the monitoring period.

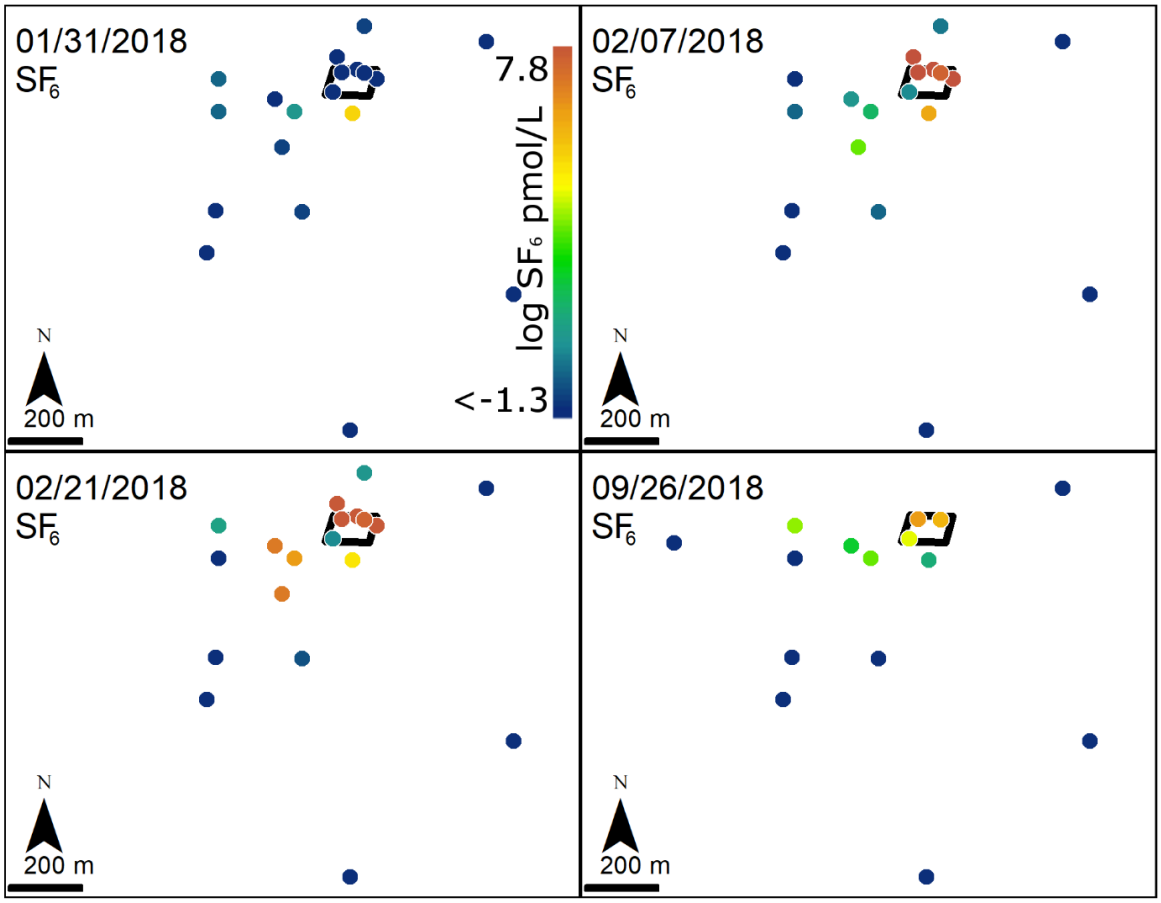

Figure 3.8: Like Br^-, SF_6 is first detected at MW-5, though at a later date. High concentrations can be observed in injection wells indicated in red along the north edge of the basins on February 7th. Concentrations remain low at MW-3a in the southwest corner of the basins, despite being surrounded by wells with higher concentrations. Concentrations in September are representative of the end of the monitoring period.

In monitoring wells where arrivals of both tracers can be detected, Br^- precedes SF_6. The exception to this is MW-14, where detections of both tracers are questionable due to their brevity (Figure 3.6). In wells where tracer concentrations have begun to decline, the peak concentration are used to approximate the mean velocity of the tracer arriving at that well (Figure 3.9). Among the wells where both tracers have peaked, SF_6 has peaked later than Br^- in all but MW-14, where the peaks arrived on the same date. If a breakthrough curve is relatively complete, its mean velocity can be more accurately determined from its COM.

Eight monitoring wells have sufficiently complete breakthrough curves to approximate a COM for both tracers, all of which except for MW-14 and MW-27 show retardation of SF_6 relative to Br^-. Injection wells are excluded from tracer velocity analysis.

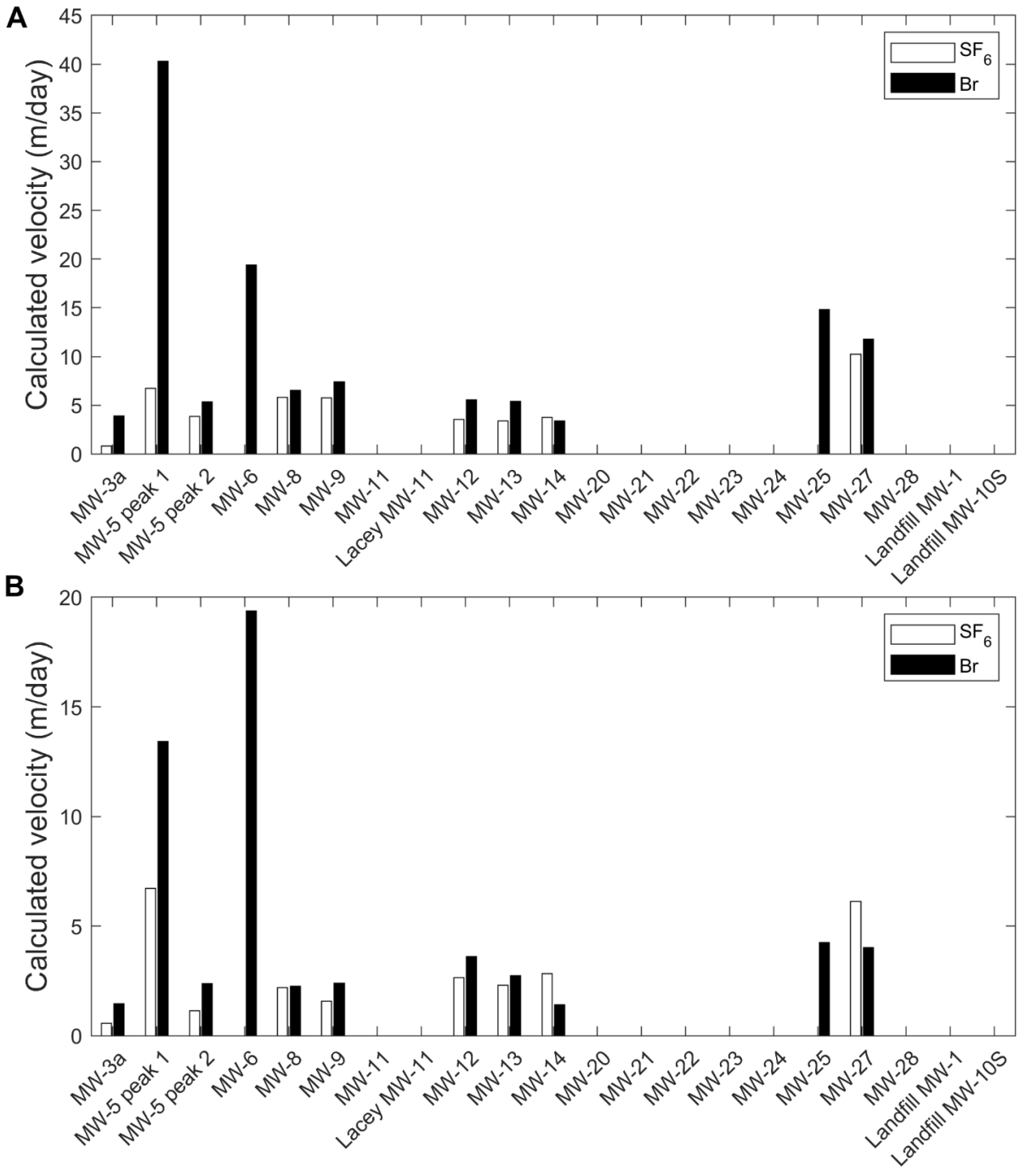

Figure 3.9: Mean linear tracer velocities estimated from (A) peak and (B) center of mass arrivals. Only those wells with complete enough break through curves to identify a peak or approximate a center of mass are shown.

Since Br^- travels at the same velocity as the groundwater and both tracers can be assumed to reach a well by the same flow paths, the average retardation of SF_6 along the flow path that it takes to reach the well can be determined by dividing the arrival time of SF_6 by that of Br^- (Figure 3.10). The average retardation across the study site determined from peak arrivals is 2.2±3.5. For the shallow aquifer only, the average retardation is 2.5±3.8. Using COM, average retardation is 1.4±1.3 or 1.6±1.2 for the shallow aquifer only (Table 3.1).

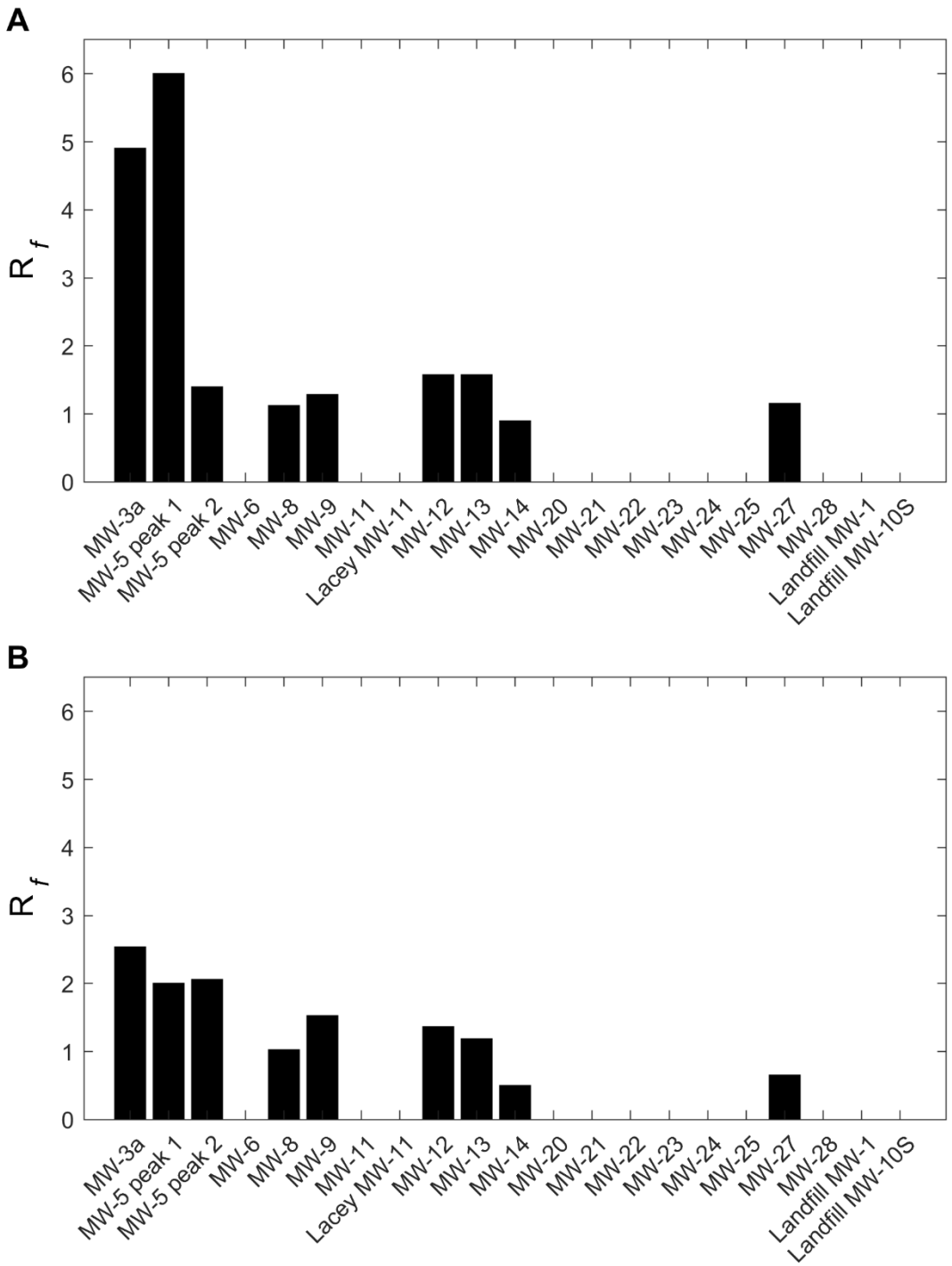

Figure 3.10: Retardation of SF_6 relative to Br^- (assumed to travel at the same velocity as groundwater) based on (A) peak and (B) center of mass arrivals. An R_f value of 1 indicates no retardation, while an R_f greater than one indicates that the SF_6 has been slowed.

Table 3.1: Arrival times and retardation factors by well

Well		Distance (m)	$t_{peak\ SF6}$ (days)	$t_{peak\ Br-}$ (days)	Peak retardation	$t_{COM\ SF6}$ (days)	$t_{COM\ Br-}$ (days)	COM retardation
MW-3a		82	103	21	4.90	142	56	2.54
MW-5	peak 1	81	12	2	6.00	12	6	2.00
	peak 2	81	21	15	1.40	70	34	2.06
MW-6		155	-	8	-	-	8	-
MW-8		156	27	24	1.13	71	69	1.03
MW-9		155	27	21	1.29	99	65	1.52
MW-11		308	-	-	-	-	-	-
Lacey MW-11		763	-	-	-	-	-	-
MW-12		318	90	57	1.58	120	88	1.36
MW-13		308	90	57	1.58	133	112	1.19
MW-14		102	27	30	0.90	36	72	0.50
MW-20		459	-	-	-	-	-	-
MW-21		826	-	-	-	-	-	-
MW-22		1067	-	-	-	-	-	-
MW-23		316	47	-	-	-	-	-
MW-24		306	12	-	-	-	-	-
MW-25		459	-	31	-	-	109	-
MW-27		307	30	26	1.15	50	76	0.66
MW-28		611	-	-	-	-	-	-
Landfill MW-1		764	-	-	-	-	-	-
Landfill MW-10S		1068	-	-	-	-	-	-

Discussion

COM arrivals are considered a more reliable measure of tracer velocity than peak arrivals, as they take into account breakthrough curve asymmetry. However, measurements at the site were terminated due to budget constraints before tracers at most wells returned to background concentrations. Thus, the COM times should be considered minimums and velocities calculated from them maximums. Both methods suggest moderate retardation of SF_6 to varying degrees along different flow paths to wells. The variation in retardations calculated at different wells indicates that trapped air is distributed heterogeneously across the Hawks Prairie site. Hydraulic conductivity also seems to be heterogeneous, given the

extremely broad range in flow velocities along different flow paths and the disparities between tracer levels at wells such as MW-15 and MW-3a. Drilling logs indicate that Vashon Till is interfingered with the Vashon outwash below the infiltration basins. It is possible that the till is acting locally as a barrier to shallow flow beneath the basins. The arrival of the tracers at MW-5 above background concentrations before the wells in the infiltration basins suggests a preferential pathway to MW-5 and possibly effects of differential saturation within the basins. Its unique double peak may be indicative of two separate flow paths leading to the well as discussed by McDermott et al. (2008). Since two adjacent basins were used for recharge and were only inundated on the northern and southern edges, it is also possible that the first set of peaks represents arrival of tracers from the nearer basin and the second set from the farther one. The breakthrough curve for each tracer was separated into two single peak curves (appendix C) for analysis, and the first peak was found to exhibit significantly greater retardation than the second. This suggests that there is more trapped air along the first flow path. Applying equation (2.2) to the calculated retardations provides an estimated ratio of trapped air to groundwater along each flow path (Table 3.2). Flow paths for which $R_f \leq 1$ are assumed to have no trapped air. Pore space air to water ratios are calculated in the 10^{-3} to 10^{-2} range (Figure 3.11).

Table 3.2: Trapped air to water ratios along flow paths to each well calculated with equ. (2.2), assuming a temperature of 12° C.

Well		V_a/V_w (peak)	V_a/V_w (COM)
MW-3a		0.0323	0.0127
MW-5	peak 1	0.0413	0.0083
	peak 2	0.0033	0.0088
MW-6		-	-
MW-8		0.0010	0.0002
MW-9		0.0024	0.0043
MW-11		-	-
Lacey MW-11		-	-
MW-12		0.0048	0.0030
MW-13		0.0048	0.0015
MW-14		0	0
MW-20		-	-
MW-21		-	-
MW-22		-	-
MW-23		-	-
MW-24		-	-
MW-25		-	-
MW-27		0.0013	0
MW-28		-	-
Landfill MW-1		-	-
Landfill MW-10S		-	-

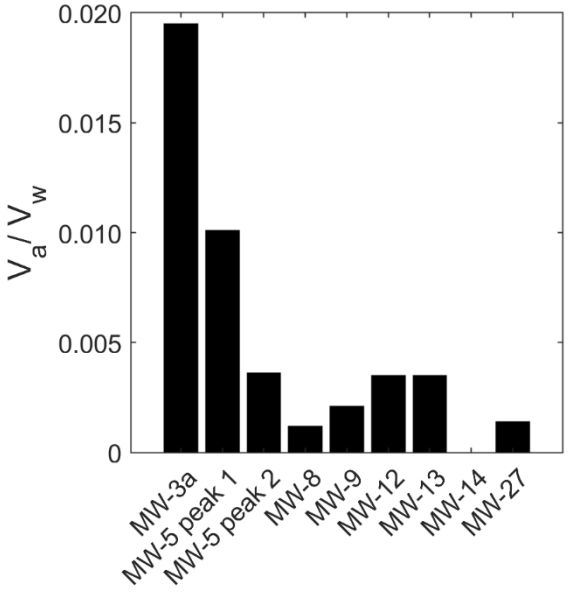

Figure 3.11: Trapped air to water ratios encountered along paths to wells in pore space calculated from peak arrival time ratios. Trapped air quantities are small but variable between paths.

Based on the hydraulic gradient, HDR Engineering, Inc. (2018b) divided the shallow aquifer into two zones. Zone 1, which is located northeast of MW-20, has a horizontal hydraulic gradient of 0.023, while zone 2, which is located southwest of MW-20 has gradient of 0.002. Water recharged at the basins must travel through zone 1 to reach zone 2. Slug and pump tests suggest a hydraulic conductivity of 30 – 60 m/d, and effective porosity has been estimated at 0.18 – 0.25 (HDR Engineering, Inc., 2018b; Truex et al., 2011). Using Darcy's law, this yields an expected linear velocity in the shallow aquifer of 2.8 – 7.7 m/d in zone 1 and 0.24 – 0.67 m/d in zone 2. Previous measurements of temperature and salinity changes in response to recharge at the site yield a velocity of 4.0 – 13 m/d (HDR Engineering, Inc., 2018b). Given that groundwater must travel through the much slower zone 2 to arrive at wells MW-22, MW-28 and Landfill MW-1, it is not surprising that there were no confirmed tracer detections at these wells (Table 3.3). Calculated linear velocities in zone 1 are highly

variable, suggesting that flow paths differ considerably in conductivity and sinuosity (Table 3.4). The majority of wells with detections of Br^- exhibited velocities in the previously measured range, though MW-6, MW-25, and most dramatically, the first peak of MW-5 were higher. Meanwhile, MW-11, MW-20, and MW-24 had no detections during the monitoring period, even though they are close enough for recharge water to reach if it were traveling at least at the minimum calculated velocity. Velocities calculated from tracer centers of mass are slower than those calculated from peaks due to the asymmetric shapes of the breakthrough curves (Table 3.5).

Table 3.3: Distances to zone 2 wells, separated into distances which must be travelled through zone 1 and distances which must subsequently be travelled in zone 2 along the most direct path from basin to well. None of these wells saw tracer detections during the monitoring period, so the maximum possible velocity that would not result in a detection is compared with the expected velocity.

Well	Zone 1 distance (m)	Zone 2 distance (m)	Comparison to expected velocity
MW-22	480	587	Undetermined
MW-28	425	186	Lower
Landfill MW-1	470	294	Undetermined

Table 3.4: Br- velocities from peak arrivals at zone 1 wells compared to calculated and previously measured groundwater velocity ranges. Wells with no breakthrough are determined to have lower than expected velocities if linear travel at the minimum expected velocities if linear travel at the minimum expected velocity would have brought the tracer to the well by the last measurement date.

Well		Distance (m)	Br^- velocity (m/d)	Comparison to expected velocity
MW-3a		82	3.9	Calculated range
MW-5	peak 1	81	40	Higher
	peak 2	81	5.4	Both ranges
MW-6		155	19	Higher
MW-8		156	6.5	Both ranges
MW-9		155	7.4	Previous range
MW-11		308	-	Lower
Lacey MW-11		763	-	Undetermined
MW-13		308	5.4	Both ranges
MW-20		459	-	Lower
MW-24		306	-	Lower
MW-25		459	15	Higher
MW-27		307	12	Previous range
Landfill MW-10S		1068	-	Undetermined

Table 3.5: Br- velocities from center of mass arrivals at zone 1 wells compared to calculated and previously measured groundwater velocity ranges as in Table 3.4.

Well		Distance (m)	Br^- velocity (m/d)	Comparison to expected velocity
MW-3a		82	1	Lower
MW-5	peak 1	81	13.4	Higher
	peak 2	81	2.4	Lower
MW-6		155	19	Higher
MW-8		156	2.3	Lower
MW-9		155	2.4	Lower
MW-11		308	-	Lower
Lacey MW-11		763	-	Undetermined
MW-13		308	2.7	Lower
MW-20		459	-	Lower
MW-24		306	-	Lower
MW-25		459	4.2	Both ranges
MW-27		307	4.0	Both ranges
Landfill MW-10S		1068	-	Undetermined

Prior measurements indicate a vertical gradient of -0.09 to -0.45 between the shallow and sea level aquifers, which would suggest a less permeable confining layer throughout most of the study site than the breakthrough at MW-12 appears to indicate. (HDR Engineering, Inc., 2018b). Given that the breakthrough at MW-12 seems to approximately coincide with that at MW-13, with which it is nested, it is likely that there is preferential pathway through the Kitsap Formation nearby. The apparently identical retardations calculated from the two wells' peak arrivals also suggest that groundwater travelling to the two wells follows very similar flow paths, since it appears to encounter similar amounts of trapped air. Additionally, since MW-12 is upgradient of recharge in the sea level aquifer, it is far more feasible for the tracer to have travelled most of the way in the shallow aquifer than for it to have travelled primarily in the sea level aquifer. Among the other sea level wells, only MW-14 has both SF_6 and Br^- detections at similar times, and these only occur for one or two measurements. This suggests that the majority of detections at sea level wells are either false positives or the result of minor, intermittent transmission of water.

The sea level aquifer has a hydrologic gradient of 0.01 with groundwater flowing eastward. Its hydraulic conductivity as determined from slug and pump tests is 0.6 – 12 m/d (HDR Engineering, Inc., 2018b). If it is assumed to have a similar effective porosity to the shallow aquifer, then the resulting groundwater velocity would be 0.03 – 0.67 m/d. Given that any tracer arriving at a well screened in the sea level aquifer would have to first travel down through the confining layer, the mean velocity along the entire flow path should be even slower. MW-12 and possibly MW-14 are the only sea level wells with reliable detections and have mean Br^- velocities of 5.6 and 3.4 m/d respectively. These velocities are

an order of magnitude higher than predicted, lending credence to the idea that any water traveling from the surface to the sea level aquifer must follow preferential pathways.

Conclusion

The application of SF_6 and Br^- as groundwater tracers at the Hawks Prairie site in Thurston County, Washington demonstrates how the use of paired gas and ionic tracers can reveal the distribution of trapped air in the subsurface. Flow velocity in the shallow aquifer ranges from 3.9 to 40 m/d. Water flow velocities and concentration disparities between nearby wells suggest that groundwater at the site follows several non-linear flow paths. Retardation of SF_6 relative to Br^- was observed at most wells, indicating partitioning of the gas tracer into trapped air. Average retardation of SF_6 in the shallow aquifer based on peak arrivals was 2.5±3.8, reflecting differing trapped air contents along different flow paths. Connection between the shallow and sea level aquifers is highly localized and largely intermittent.

Chapter 4 Evolution of groundwater chemistry in Thurston County, Washington

Abstract

Modern and historical data were evaluated to determine potential processes affecting groundwater chemistry in Thurston County Washington. Potential influences include evapotranspiration of meteoric water, deposition of sea salt aerosols, seawater intrusion, septic contamination, microbial processes, and mineral weathering. Sodium, chloride, and nitrate levels suggest contamination by seawater in some wells and septic effluent in others, while the majority are largely uncontaminated. Samples were grouped into representative endmembers based on chemistry and hydrologic relationships and used to develop inverse models. Modeling suggests that weathering of aluminosilicates and iron-bearing minerals, in addition to cation exchange and the incorporation of organic matter and halite, can explain most of the evolution of groundwater in the area. Potential effects of reclaimed water MAR are discussed and are expected to be minimal.

Introduction

When conducting MAR operations, it is critical to understand the existing geochemistry of the target aquifers. To avoid degrading high quality aquifers, recharge water must be of a quality equal to or better than what is currently in the aquifer by the time it reaches the groundwater (State of Washington, 1990). The minimum acceptable quality of the recharge water therefore depends in part on the background water quality in the aquifer. Interactions with soil and aquifer matrix materials can improve the quality of the recharge water, which can help with meeting groundwater quality requirements (Drewes, 2009;

Bekele et al., 2011). Alternatively, recharging high quality water can dilute contaminants existing in the aquifer, or in areas prone to seawater intrusion, prevent their introduction (Dillon et al., 2009). On the other hand, disequilibrium between recharge water and the aquifer could mobilize contaminants (Fakhreddine et al., 2015). Finally, knowing potential sources of existing contaminants can help MAR operators avoid being incorrectly blamed for them. This chapter investigates potential factors affecting the background geochemistry of both the shallow and sea level aquifers in Thurston County, WA prior to, or in areas unaffected by, MAR at LOTT's Hawks Prairie site from chapter 3.

Several previous investigations of the groundwater in the region have been conducted by the U.S. Geological Survey (USGS) and other agencies. Van Denburgh and Santos (1965) assess the quality of groundwater resources throughout the state of Washington, separating the state along the Cascade Divide. The authors note that west of the Divide, where Thurston County is located, groundwater is generally of good quality, though iron may be elevated in areas with low dissolved oxygen, and some locations are impacted by saltwater intrusion (Van Denburgh and Santos, 1965). Two decades later, Turney (1986) conducted an investigation of groundwater quality in the Puget Sound region. He observed continued good water quality with low total dissolved solids (TDS) in most locations. Where EPA water quality violations occurred, they were typically the result of elevated iron or manganese (Turney, 1986). A pair of USGS Water Resource Investigations focus specifically on the groundwater of northern Thurston County. Drost et al. (1998) describes the aquifers and water chemistry in detail, noting, like investigators before them, that the most frequent issues are locally elevated iron and manganese, along with anthropogenic nitrate pollution and seawater intrusion. Drost et al. (1999) used MODFLOW to create a numerical model of the

same location investigated by Drost et al. (1998). The authors demonstrate that recharge is primarily from precipitation and infiltration from surface water bodies, while discharge occurs when water feeds into other surface bodies, springs, or Puget Sound or when it is withdrawn from wells. Meanwhile, Vaccaro et al. (1998) develops a broader hydrologic framework of the Puget Sound aquifers, which they describe as being governed by subregional flow systems defined by bedrock, topography, and saltwater bodies. Most locally and most recently, HDR Engineering, Inc. (2017) analyzed the groundwater in all of the aquifer units tapped by domestic and municipal wells in the Hawks Prairie and Tumwater areas as a part of the LOTT study. This study revealed water chemistry in line with previous studies except where impacted by septic effluent.

In this chapter, I will synthesize historical groundwater quality data and data collected during the 2018 LOTT tracer study described in chapter 3 (HDR Engineering, Inc., 2019) in order to shed light on the processes affecting major solutes in northern Thurston County groundwater in the shallow and sea level aquifers. These processes form the background conditions for MAR at the Hawks Prairie site. Potential processes include mixing, evapotranspiration, anthropogenic contamination, microbial activity, and mineral interactions. To investigate this, I will identify and characterize potential endmembers and create inverse models using the USGS program PHREEQC (Parkhurst and Appelo, 2021).

Methods

Groundwater datasets

This chapter focuses on water samples from three studies. The largest dataset are wells sampled by Drost et al. (1998) drawing from the Vashon Advance (Qva) and

Recessional (Qvo) Outwashes, which comprise the shallow aquifer, and from the Salmon Springs Drift and Penultimate deposits (Qc), which comprise the sea level aquifer. These are investigated alongside slightly more recent data on the shallow and sea level aquifers at the Hawks Prairie Site and in the nearby city of Tumwater from the groundwater characterization associated with the LOTT study (HDR Engineering, Inc., 2017). In addition to this, I will compare the water represented in existing data with wells measured during the LOTT tracer study believed to represent primarily background groundwater.

Group identification

Within datasets, wells were grouped by hierarchical clustering analysis (HCA) using Ward's linkage method with Euclidean distances (Güler and Thyne, 2004; Belkhiri et al., 2010). For the LOTT wells, separate rounds of HCA were conducted with the data from each quarter of sampling (Figure 4.1 and Figure 4.2). Separate rounds were also conducted with different sets of variables. The first set of variables consisted of the analytes detected in all wells for the quarter in question. The second set consisted of all analytes detected in a given quarter in at least half of the wells, with non-detects filled in with 0.5 times the method detection limit (MDL). Finally, principal component analysis (PCA) was conducted using analytes detected in all wells and the PCA scores were the used as another set of HCA variables (Figure 4.3) (Mahlknecht et al., 2004). The HCA results were used to create dendrograms for all wells with at least three quarters of data, the leaves of which were each divided into three groups.

Wells MW-8, MW-9, and MW-16 consistently clustered together and tended to have higher concentrations of constituents associated with the reclaimed water, as reported in HDR Engineering, Inc. (2019). These wells also all exhibited significant tracer detections

during the tracer study. These three wells were designated the high-recharge wells due to the high influence of the Hawks Prairie MAR. Similarly, wells MW-20, MW-23, MW-25, and MW-28 consistently grouped together but had low concentrations of reclaimed water constituents and lacked detections of one or both tracers. These wells were designated as low-recharge. Well MW-5 typically, though not exclusively, stood apart from the others, while MW-27 switched between being more closely related to the high or low-recharge groups. Both of these wells were labeled as inconsistent. MW-26 clustered with the low-recharge wells, except in the plain HCA of quarter 4, when it was apart from them. Since it is upgradient and not directly affected by the recharge, it was considered part of the low-recharge group. Likewise, MW-3a clustered with the high-recharge wells except in the HCA with PCA variables for quarter 2. Since it had robust detections of both tracers, it was considered high recharge. While MW-14 did consistently cluster with the low recharge wells, it had (questionable) detections of both tracers during the tracer study and was therefore deemed inconsistent (Figure 4.1 - Figure 4.3, Table 4.1). The low recharge wells are the main group of LOTT wells included in this analysis, as they are the ones most likely to represent the background geochemistry.

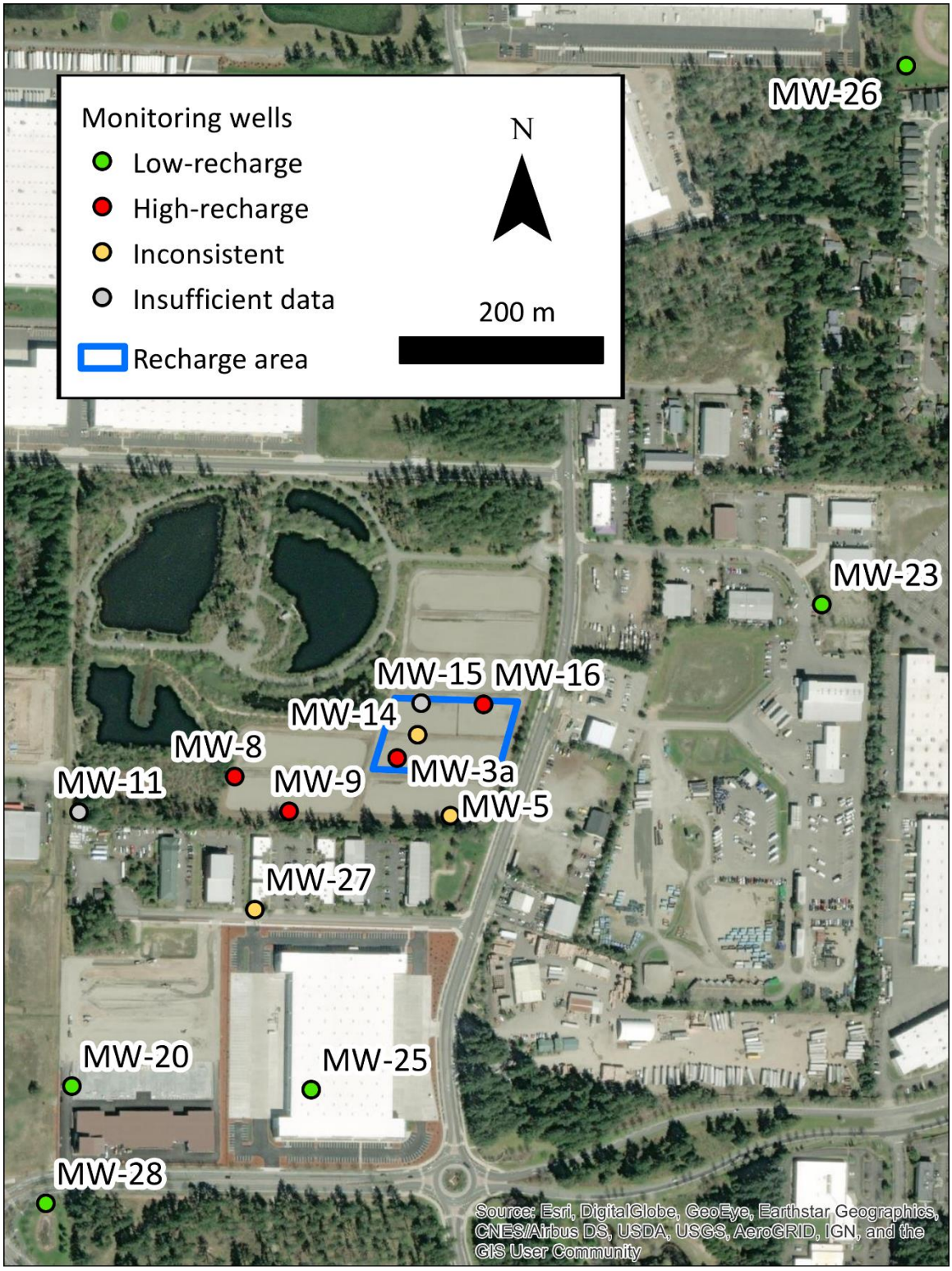

Figure 4.1: Wells monitored for water quality during the LOTT tracer study. Wells MW-20, 23, 25, 26, and 28 are designated low-recharge. MW-3a, 8, 9, and 16 are high-recharge. MW-5, 14, and 27 are inconsistent, and MW-11 and 15 have insufficient data for classification.

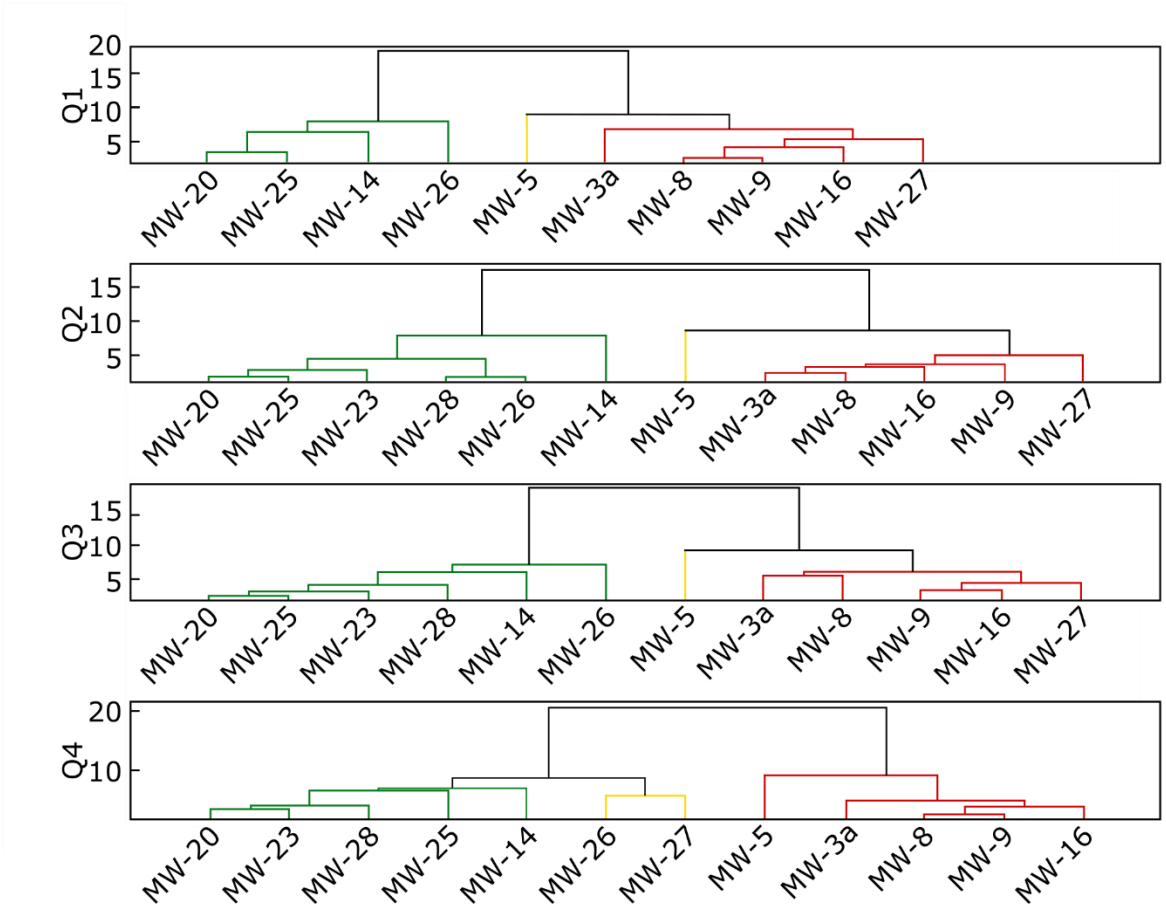

Figure 4.2: Dendrograms showing the results of unweighted HCA of LOTT monitoring well samples using measured analytes for variables. Colors indicate groups assigned by cutoff at whatever height produced three groups. Note that MW-23 and MW-28 were not measured during quarter 1, but were added to the set of wells being measured in quarters 2 through 4 in place of MW-11 and MW-15 (not shown due to limited data) for better spatial coverage of the study area (HDR Engineering, Inc., 2019).

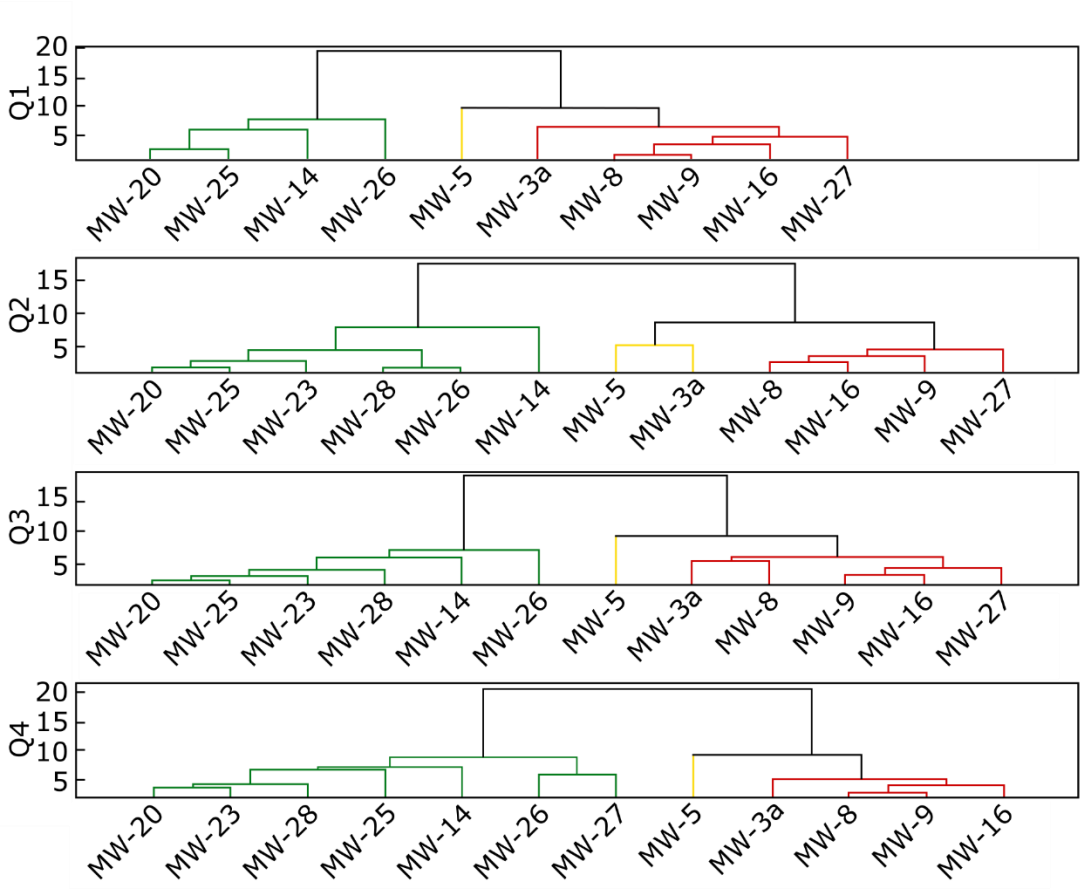

Figure 4.3: Dendrograms showing unweighted HCA of LOTT samples using PCA variables. Colors indicate groups assigned by cutoff at whatever height produced three groups. Note that MW-23 and MW-28 were not measured during quarter 1, but were added to the set of wells being measured in quarters 2 through 4 in place of MW-11 and MW-15 (not shown due to limited data) for better spatial coverage of the study area (HDR Engineering, Inc., 2019).

Table 4.1: Groupings of LOTT monitoring wells based on HCA and presumed influence of MAR operations.

Low-Recharge Wells	High-Recharge Wells	Inconsistent Wells
MW-20	MW-3a	MW-5
MW-23	MW-8	MW-14
MW-25	MW-9	MW-27
MW-26	MW-16	
MW-28		

Table 4.2: Selected data for LOTT low-recharge wells averaged across all quarters measured.

Well	MW-20	MW-23	MW-25	MW-26	MW-28	Average
Specific Conductance (µS/cm)	156.72	211.5	180.33	140.82	127.39	163.35
Hardness (as $CaCO_3$)	86.75	112.05	91.24	57.81	63.1	82.19
Alkalinity (as $CaCO_3$)	85.1	96.42	81.1	45.74	62.87	74.25
Ca	18.25	22.33	16.75	14	14	17.07
Mg	10	13.67	12	5.55	6.83	9.61
Na	7.38	8.2	7.98	6.58	6	7.23
K	1.73	2.4	2.5	0	1.23	1.57
SO_4^{2-}	5.2	9.7	9.63	6.55	4.1	7.04
Cl	5.88	15.14	9.69	5.56	5.77	8.41
SiO_2	25.25	27.33	29.25	20	22	24.77
NO_3^- (as N)	0.82	1.31	0.98	1.45	0.62	1.04
P	0	0.01	0.02	0.01	0.03	0.01
Fe (µg/L)	0	0	6.5	0	0	1.3
Mn (µg/L)	2.75	0.87	5.1	5.2	0.9	2.96
O_2	6.29	6.42	8	7.56	5.8	6.82
Temperature (°C)	11.14	11.17	10.82	10.78	12.03	11.19
pH	7.11	7.32	7.22	6.23	7.04	6.98

The LOTT low recharge wells were observed to have a linear relationship between Na^+ and Mg^{2+}, Mg^{2+} and SiO_2, and SiO_2 and Na^+. The same species were plotted against each other for the other datasets and observed to be distributed roughly between two to three endmembers on each two-species plot (Figure 4.4 - Figure 4.6). Wells from the Drost et al. (1998) and HDR Engineering, Inc. (2017) datasets were selected for modeling based on hierarchical clustering analysis (HCA) of Ca, Mg, Na, K, SO_4^{2-}, Cl^-, SiO_2, NO_3^- – N, P, Fe, Mn, and alkalinity (as $CaCO_3$). Mg, Na, and SiO_2 were given a weight of 2, as they were the main solutes of interest in terms of end members, while NO_3 was given a weight of 0.5, as it is a reflection primarily of surface inputs and not of *in situ* geochemical processes. All other

analytes were given a weight of 1. HCA was performed using Ward's linkage method and Euclidean distances. Samples were grouped into 30 leaves on the resulting dendrogram, where the samples within each leaf were more similar to each other than to the samples in any other leaf (Figure 4.7). Plotting of Na vs Mg and Na vs SiO_2 revealed that the wells of Leaf 7 are consistently low in the solutes of interest, while Leaf 1 wells formed a distinct high-SiO_2 group. Leaf 7 wells with NO3-N ≤ 1 mg/L and DO > 1 mg/L were averaged to use as a low endmember (Figure 4.8, Table 4.4 - Table 4.5), and Leaf 1 wells with DO ≤ 2 mg/L (where measured) were averaged to use as a high-SiO_2 endmember (Figure 4.9, Table 4.6).

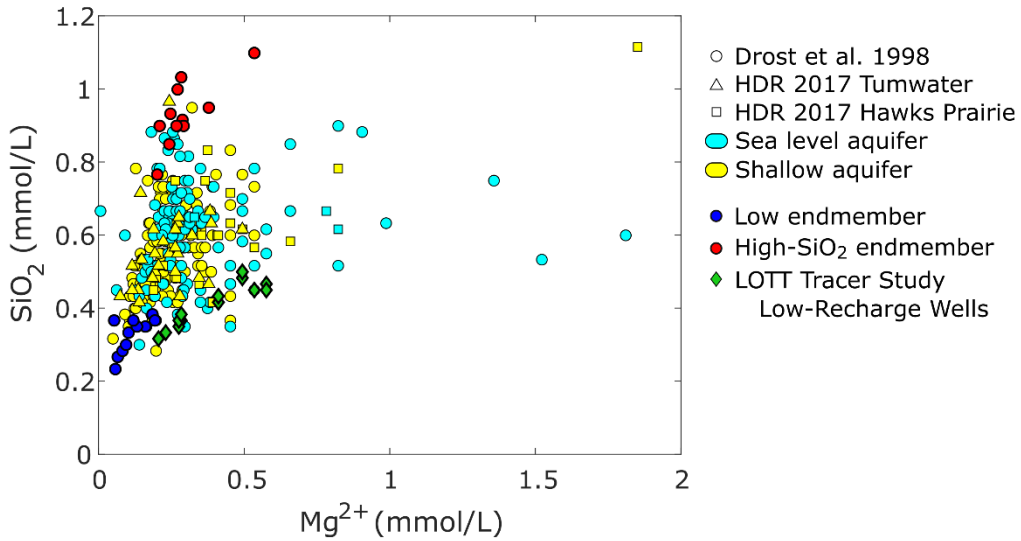

Figure 4.4: Mg^{2+} vs SiO_2 in groundwater samples with LOTT low-recharge wells and wells selected to represent the low endmember and high-SiO_2 endmember highlighted.

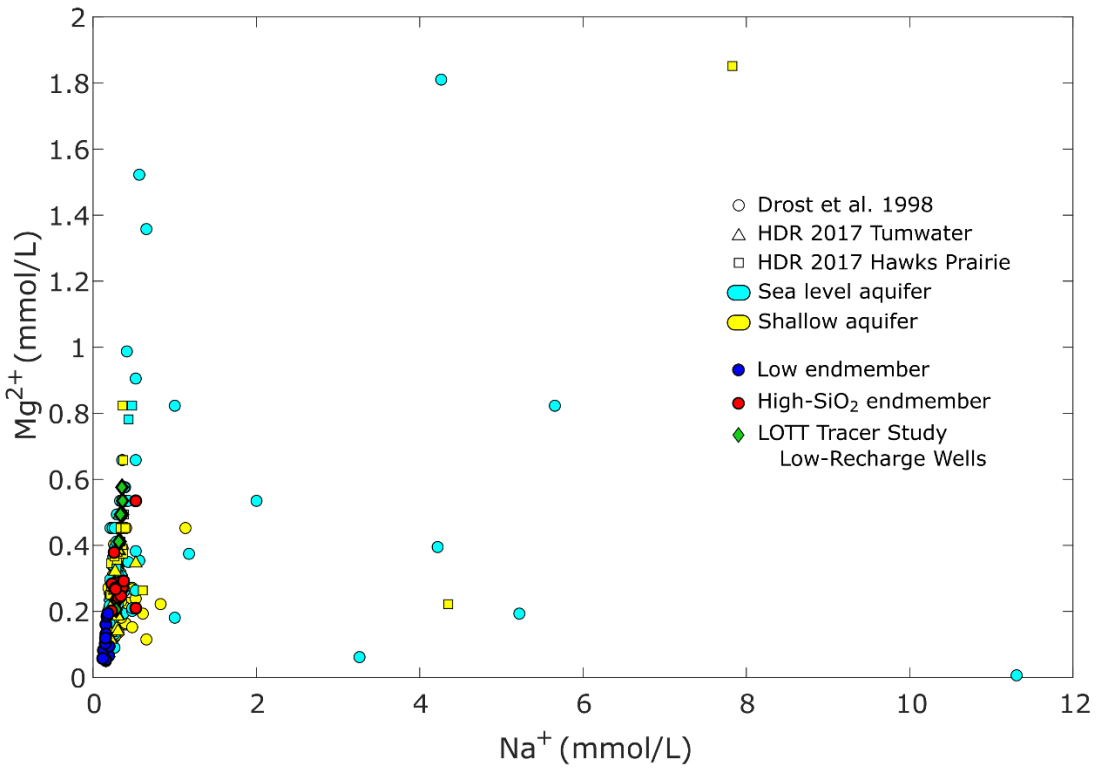

Figure 4.5: Na^+ vs Mg^{2+} in groundwater samples with LOTT low-recharge wells and wells selected to represent the low endmember and high-SiO_2 endmember highlighted.

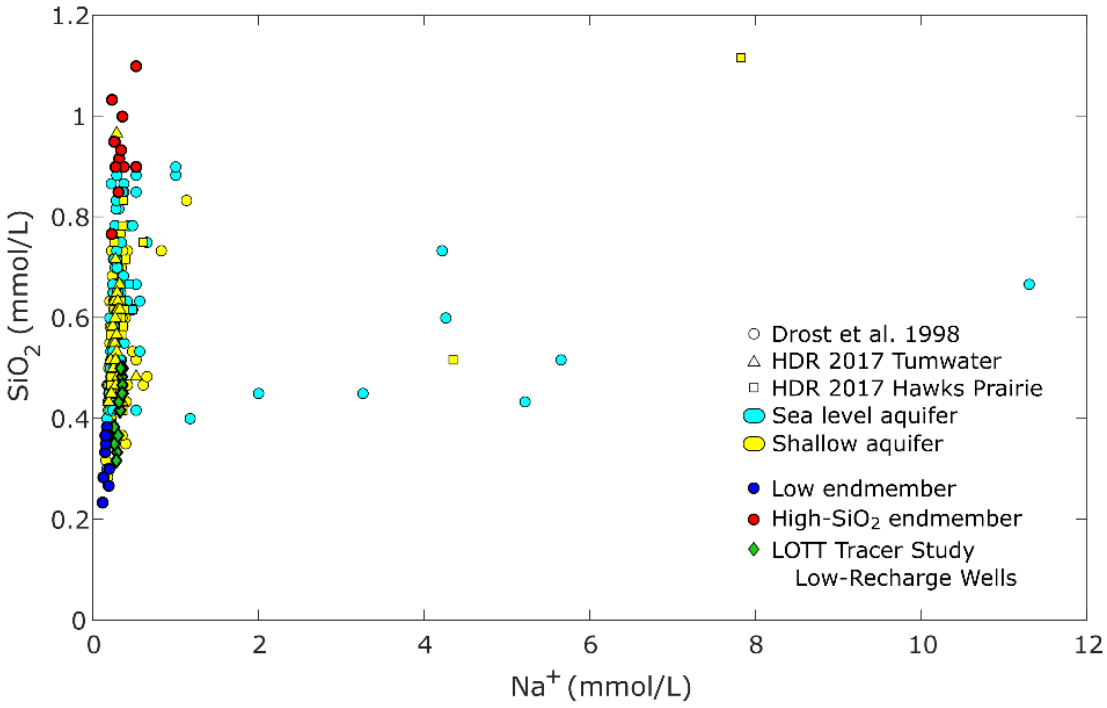

Figure 4.6: Na^+ vs SiO_2 in groundwater samples with LOTT low-recharge wells and wells selected to represent the low endmember and high-SiO_2 endmember highlighted.

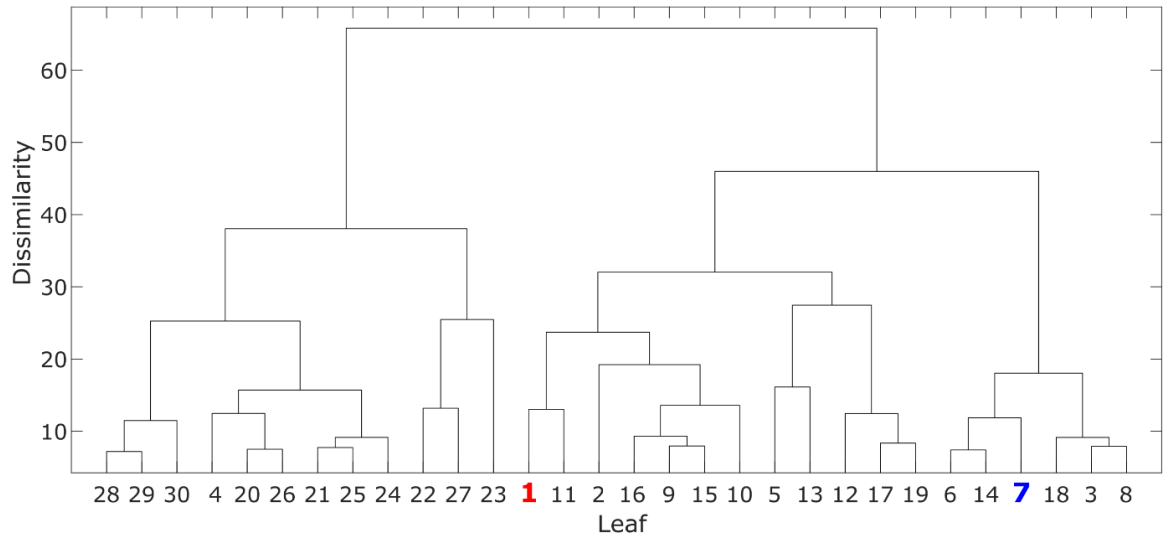

Figure 4.7: Dendrogram of weighted HCA of Drost et al. (1998), HDR Engineering, Inc., (2017), and LOTT reclaimed water study data. Leaves of interest highlighted. Connections at greater height indicate greater difference between leaves.

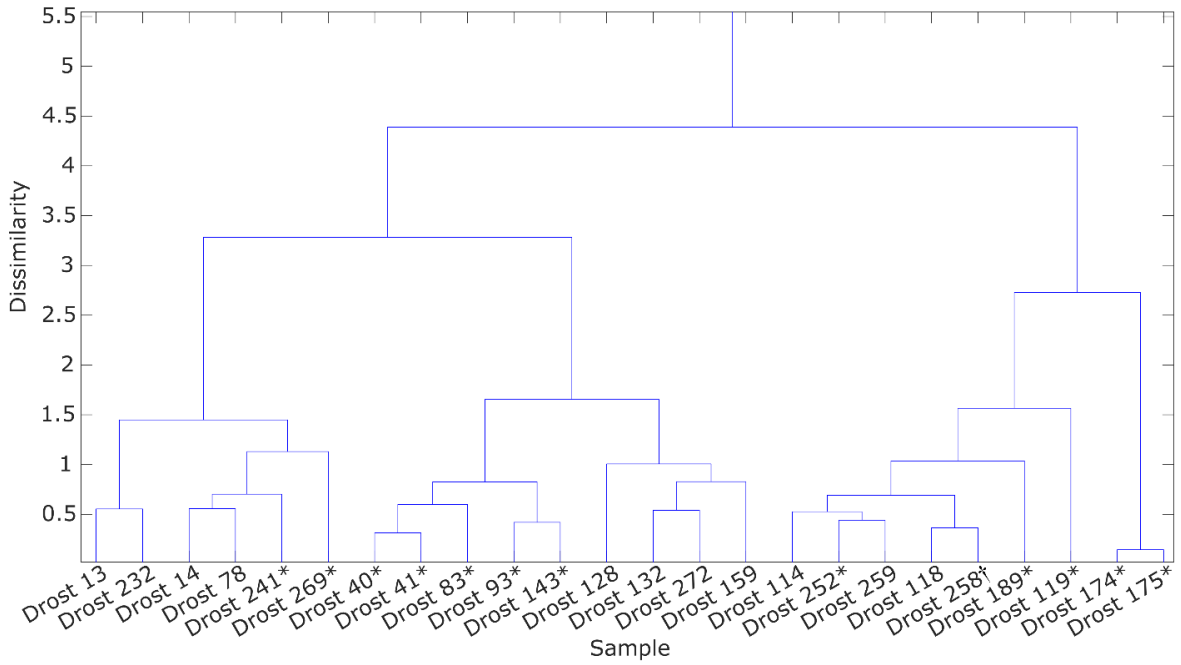

Figure 4.8: Dendrogram from Figure 4.7 zoomed in to show Leaf 7 samples. *excluded from low endmember due to elevated nitrate; †excluded from low endmember due to low oxygen.

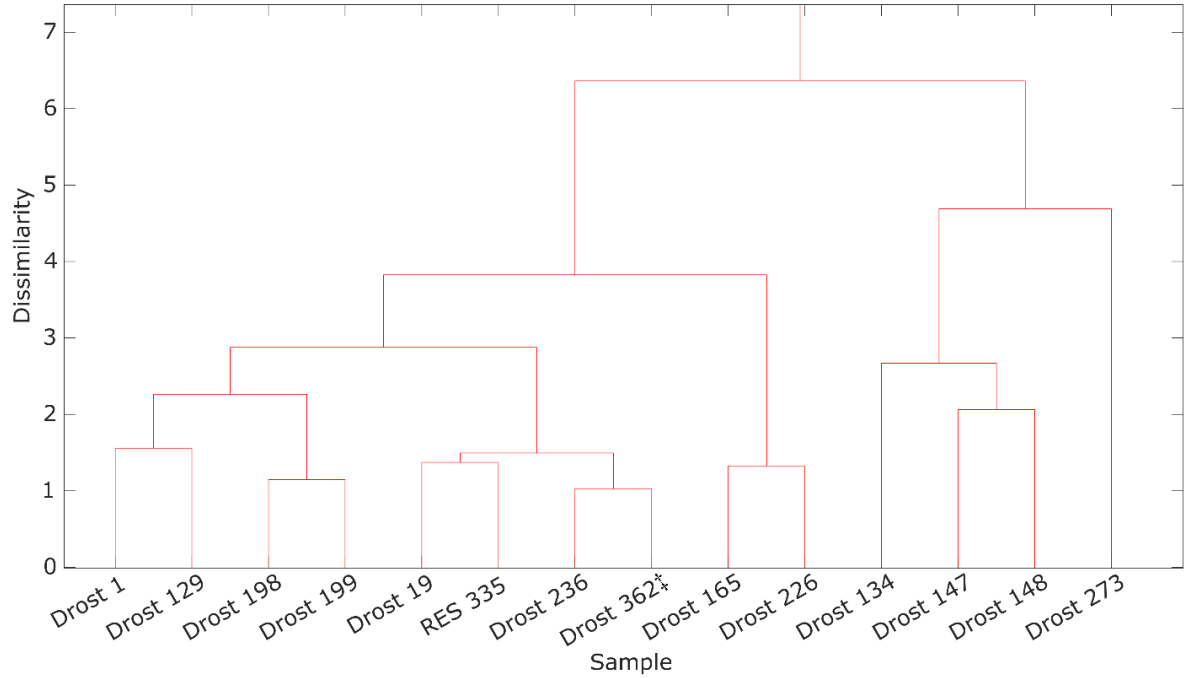

Figure 4.9: Dendrogram from Figure 4.7 zoomed in to show Leaf 1 samples. ‡excluded from high-SiO_2 endmember due to elevated oxygen.

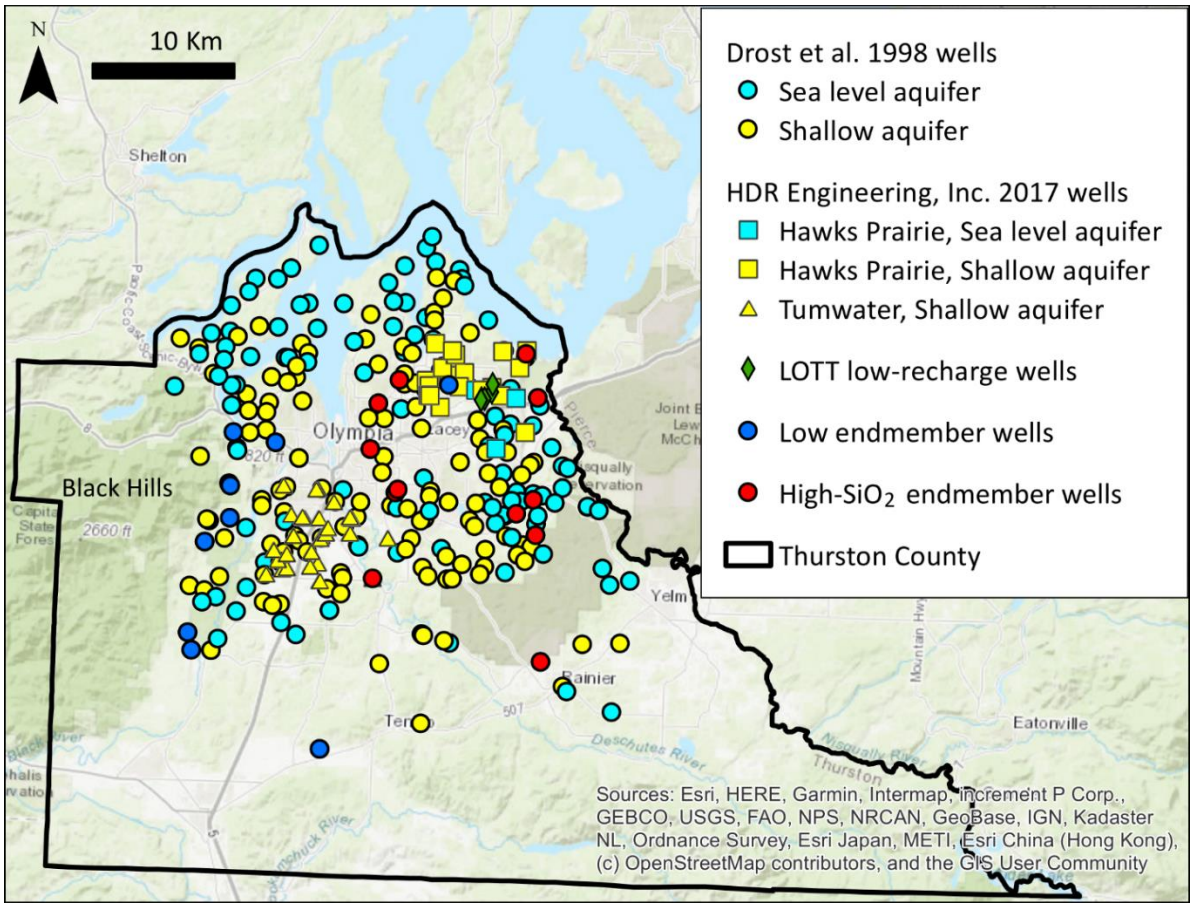

Figure 4.10: Locations of wells included in this study.

Table 4.3: Endmember wells selected from Drost et al. (1998) and HDR Engineering, Inc. (2017)

Endmember	Well Number (this study)	Data Source	Original well ID	Hydrogeologic Unit
Low	Drost 13	Drost et al., (1998)	16N/02W-27H02	Qva
	Drost 14	Drost et al., (1998)	16N/03W-02E01	Qc
	Drost 78	Drost et al., (1998)	17N/02W-06P03	Qva
	Drost 114	Drost et al., (1998)	17N/03W-01G02	Qva
	Drost 118	Drost et al., (1998)	17N/03W-11K01	Qva
	Drost 128	Drost et al., (1998)	17N/Q3W-25R04	Qc
	Drost 132	Drost et al., (1998)	17N/03W-34J01	Qva
	Drost 159	Drost et al., (1998)	18N/01W-03E01	Qva
	Drost 232	Drost et al., (1998)	18N/02W-20C01	Qva
	Drost 259	Drost et al., (1998)	18N/03W-13K01	Qc
	Drost 272	Drost et al., (1998)	18N/03W-36B01	Qc
High-SiO_2	Drost 1	Drost et al., (1998)	16N/01E-05F01	Qc
	Drost 19	Drost et al., (1998)	17N/01E-05N01	Qc
	Drost 129	Drost et al., (1998)	17N/Q3W-25R05	Qc
	Drost 134	Drost et al., (1998)	18N/01E-06R01	Qc
	Drost 147	Drost et al., (1998)	18N/01E-31H03	Qc
	Drost 148	Drost et al., (1998)	18N/01E-31N01	Qva
	Drost 165	Drost et al., (1998)	18N/01W-06A03	Qc
	Drost 198	Drost et al., (1998)	18N/01W-31A02	Qva
	Drost 199	Drost et al., (1998)	18N/01W-31A03	Qva
	Drost 226	Drost et al., (1998)	18N/02W-12H01	Qc
	Drost 236	Drost et al., (1998)	18N/02W-24B01	Qva
	Drost 273	Drost et al., (1998)	19N/01E-30P06	Qc
	RES 335	HDR Engineering, Inc., (2017)	RES335	Qva

Table 4.4: Selected chemistry for Leaf 7 wells included in low endmember. Units in mg/L unless otherwise specified.

Well	Drost 13	Drost 14	Drost 78	Drost 114	Drost 118	Drost 128	Drost 132	Drost 159	Drost 232	Drost 259	Drost 272
Ca^{2+}	5.9	4.7	7.6	12	13	3.7	5.9	5	5.4	10	7.2
Mg^{2+}	1.6	2	2.3	3.9	4.5	1.3	2.5	3.2	1.4	4.7	2.9
Na^{+}	4.4	2.9	4.5	3.6	3.9	3.5	3.4	3.6	2.7	4.2	3.5
K^{+}	0.6	0.2	0.5	0.6	0.5	0.5	0.4	0.9	0.4	0.6	0.5
SO_4^{2-}	5.7	1	2.5	1.9	2.5	3.5	1.2	6.5	4.4	3.3	1.9
Cl^{-}	3.4	2.6	3.2	2.7	2.3	3.5	2.7	2.4	2.3	2.2	2.2
SiO_2	16	17	18	21	23	22	20	21	14	22	22
NO_3^{-}-N	1	0.58	0.91	0.93	0.43	0.32	0.49	0.64	0.23	0.55	0.67
P	0.01	0	0.01	0.01	0	0.01	0.01	0.02	0	0.02	0
Fe (µg/L)	16	29	7	6	5	8	8	8	24	7	12
Mn (µg/L)	4	2	0	0	0	0	1	2	3	0	2
Alkalinity (as $CaCO_3$)	17	20	29	46	51	14	26	22	17	47	32
O_2	7.1	7.7	8.9	10.1	9.2	6.1	5.7	8.7	7.3	9.8	3.9
T (°C)	10	10	11.5	10.5	10.5	9.5	10.5	10	14.5	10.5	10
pH	6.2	6.8	6.5	7.4	6.9	6.4	6.7	6.8	6.5	7.3	6.5

Table 4.5: Selected chemistry for Leaf 7 wells excluded from low endmember. Units in mg/L unless otherwise noted. Reasons for exclusion: *excluded due to elevated nitrate, †excluded due to low oxygen, - not measured

Well	Drost 40*	Drost 41*	Drost 83*	Drost 93*	Drost 119*	Drost 143*	Drost 174*	Drost 175*	Drost 189*	Drost 241*	Drost 252*	Drost 258†	Drost 269*
Ca^{2+}	10	9.6	9.4	7.9	13	11	16	16	13	5	13	13	8.9
Mg^{2+}	2.6	2.5	2.2	3	4.8	3.1	3.9	4	4.5	1.2	4.8	4.4	3.4
Na^{+}	4.6	4.7	4.5	4.7	4.1	5	9.1	9.1	5.4	3.6	4.7	4.6	3.9
K^{+}	0.7	0.7	0.6	0.8	0.8	0.7	0.9	0.9	0.9	0.5	0.4	0.8	0.4
SO_4^{2-}	6	7	3.7	6	1.7	7	9	8	5	1.7	2.8	3.4	1.8
Cl^{-}	3.4	2.6	3.6	3.8	2.7	4.2	7.7	7.6	4.2	3.6	3.1	2.3	5
SiO_2	22	21	23	24	17	24	21	21	22	19	22	23	18
NO_3^{-}-N	2.1	1.6	2.2	1.5	1.5	2.2	5.6	5.4	3.2	1.1	1.5	0	2.9
P	0.01	0.01	0.01	0.02	0.01	0.01	0	0	0.02	0.02	0.01	0.11	0.01
Fe (µg/L)	4	4	0	5	3	7	5	10	5	6	9	33	15
Mn (µg/L)	0	16	0	0	8	1	0	0	0	0	1	11	10
Alkalinity (as $CaCO_3$)	28	29	28	27	52	29	34	35	40	15	50	57	26
O_2	9.2	8.4	8.5	6.8	8.7	7.4	7.9	7.9	8.6	-	7.3	0.1	7.8
T (°C)	10	10.5	10.5	11	10.5	13	12.5	12.5	11.5	9.5	11	11	11.5
pH	6.6	6.6	6.8	6.6	8.2	6.2	6.6	6.6	7.1	6.5	6.5	8	6.2

Table 4.6: Selected chemistry for all Leaf 1 wells. Well numbers refer to Drost wells except RES 335 from HDR Engineering, Inc., 2017. Units in mg/L unless otherwise specified (note Fe units different from Table 4.4 and Table 4.5.)

‡excluded from high-SiO_2 endmember due to elevated oxygen, - not measured

Well	**1**	**19**	**129**	**134**	**147**	**148**	**165**	**198**	**199**	**226**	**236**	**273**	**362‡**	**RES 335**
Ca^{2+}	9.8	10	10	12	11	7.8	11	11	7.5	12	13	17	11	11
Mg^{2+}	5.9	7	4.9	5.1	9.2	6.9	6.6	6.6	7.1	6	6.5	13	6.2	5.9
Na^{+}	7.1	7.3	5.2	12	5.9	5.3	8.2	6.3	8.6	7.8	6.3	12	6.6	6.6
K^{+}	2.1	2.1	1.7	1.8	2.2	2.2	1.8	2.1	1.9	1.6	2.5	3.5	2	2.1
SO_4^{2-}	7	2	5.5	0	2	2	0	9	4	0	3.2	0	0	4.5
Cl^{-}	7.1	2.6	3.8	3.1	2.8	3.3	3.8	5.3	2.2	2.9	3.6	3.2	3.3	2.2
SiO_2	51	55	46	54	57	62	60	54	54	56	54	66	53	58
NO_3^{-}-N	0	0	0	0	0	0	0	0	0	0	0	0	0	0
P	0.1	0.2	0.2	0.7	0.2	0.3	0.4	0.1	0.1	0.7	0.3	0.7	0.6	0.1
Fe	0.9	0.02	2.1	0.2	0.2	0.1	4.4	3.2	2.2	3.3	0.9	1.3	1.3	0.9
Mn (µg/L)	140	300	230	630	600	390	260	250	170	230	130	370	240	160
Alkalinity (as $CaCO_3$)	49	67	49	73	72	55	70	54	60	72	68	116	65	63
O_2	0.1	0.1	2	0.1	0.1	0.1	0	0	0	0	0.1	0	6.4	-
T (°C)	12	11	12	12	11	11	12	10	11	10	11	12	10	-
pH	7.5	7.9	7.3	7.7	7.6	7.1	7.1	7.1	7.4	7.3	7.1	7	7.1	-

Bicarbonate calculation

The dissolved species in the water were compared using Piper diagrams and scatter plots. In order to plot the water compositions on a Piper diagram, it is necessary to know the bicarbonate content; however, this was not directly reported in most of the datasets. The bicarbonate content of the Drost et al. (1998) wells was estimated as 0.61 times the carbonate alkalinity, which is the that relationship the authors state generally holds true in the measured pH range. For HDR Engineering, Inc. (2017) data, the reported bicarbonate alkalinity as

HCO_3 was used as is. The HDR Engineering, Inc. (2019) data reported neither bicarbonate nor alkalinity. CO_3 was measured but not detected above the MDL of 2 mg/L. In order to estimate the bicarbonate content, the water samples were speciated in PHREEQC with an initial CO_3 value set to 1 mg/L. This initial value was allowed to adjust for charge balance, and the resulting values remained lower than the MDL. The bicarbonate from the speciation was then used to plot the LOTT water on the Piper diagram.

Data representing potential water inputs

Precipitation chemistry was obtained from the National Atmospheric Deposition Program – National Trends Network (NADP-NTN) site WA21 in La Grande, WA (46.8353 N, 122.2867 W) from the period of 1984 – 2021 (Figure 1.3) (US EPA and University of Washington, 1984). Measurements of Ca^{2+}, Mg^{2+}, K^{+}, Na^{+}, NH_4^{+}, NO_3^{-}, Cl^{-}, SO_4^{2-}, pH, and conductivity are reported from the site. Dissolved oxygen was calculated using PHREEQC, assuming equilibrium with atmospheric oxygen at 9.3 °C (as inert species Oxg, to avoid reacting to equilibrium with dissolved nitrogen species). This station is the nearest to the study area and has the most complete monitoring record. Unfortunately, the average reported composition has a significant charge imbalance, -26.18% as determined by PHREEQC speciation (Figure 4.11). It is common for precipitation measurements to have unbalanced charges; however, the excess charge is usually positive, which is sometimes attributed to a lack of HCO_3^{-} and organic acid measurements (Edmonds et al., 1991; Johansen et al., 2019). A slightly better balance can be achieved by taking the median values of all weekly measurements for which the magnitude of manually summed charges exhibited an imbalance less than or equal to 10%. The magnitude of charge imbalance tended to decrease over the course of the monitoring period, such that the exclusion of highly imbalanced measurements

biases the samples towards younger dates. Station WA99, which is the second closest NADP-NTN site, located to the southeast near Tahoma Woods (46.7582 N, 122.1243 W), has a greater proportion of weekly measurements with a charge imbalance less than 10%, but its record is less complete (US EPA and University of Washington, 2021b). Also, the solute concentrations tend to differ significantly but unsystematically between the two sites, suggesting that the data from the farther station should not be considered representative of local conditions.

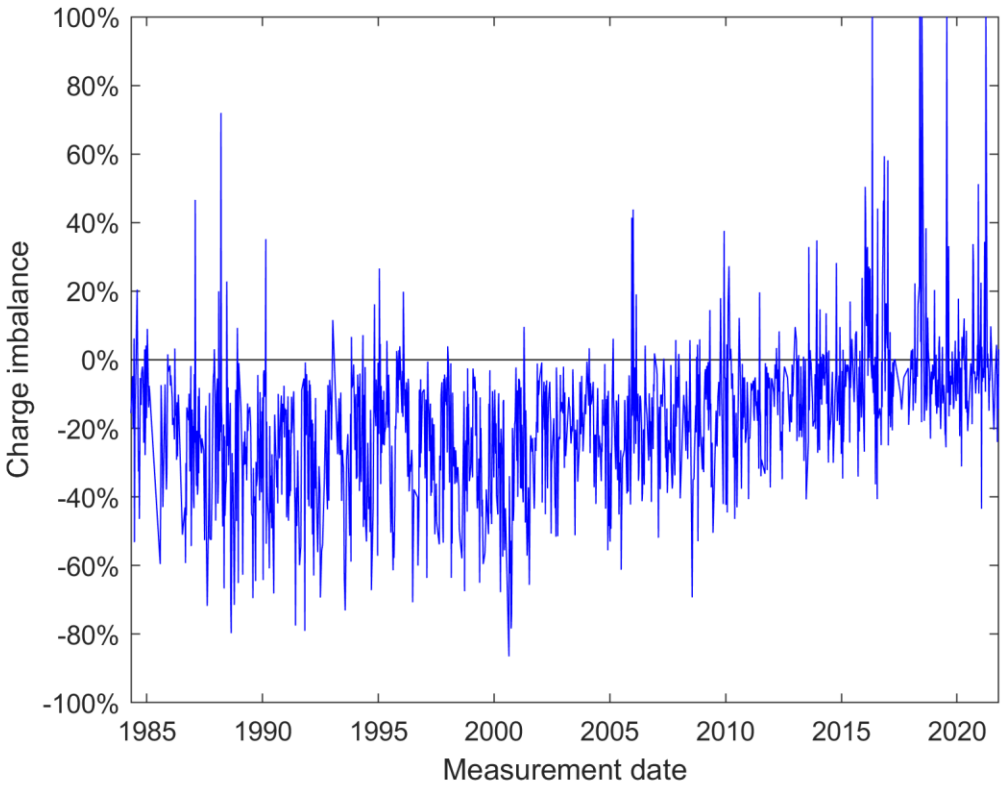

Figure 4.11: Charge imbalance in weekly wet deposition measurements at NADP-NTN station WA21.

Another potential input is water intruding from Puget Sound (Dion and Sumioka, 1984; Drost et al., 1998). A comprehensive dataset of dissolved ions in the Sound does not appear to be available, so concentrations were estimated based on the average seawater

compositions published by Sverdrup et al. (1942), Voutchkov (2010), MBARI (2015) and Lenntech (n.d.). The reported concentrations were linearly adjusted to a salinity of 28.18 practical salinity units, the average measured in the upper 14 meters of Budd Inlet in 1999, 2002, and 2014 (Bos, 2015). Nitrate levels were obtained from Collias and Lincoln (1977).

Finally, some of the water may be affected by septic effluent. Some local data is available on the five-day biochemical oxygen demand (BOD_5), total suspended solids, oil and grease, and pH of septic effluents, but other solutes are not available. Richards et al. (2016) provides broad averages of solutes in effluent which are used here. When determining possible nitrate contributions from septic effluent, the total dissolved nitrogen value is used, because it is likely be oxidized to nitrate in the leach field and during travel through the vadose zone (Costa et al., 2002).

Table 4.7: Representative solutions considered to explain groundwater chemistry in the shallow and sea level aquifers. Units in mg/L unless otherwise specified.

Solution	Meteoric water	Puget Sound water	Septic effluent	Low endmember	High-SiO_2 endmember	LOTT low-recharge
Ca^{2+}	0.036	-	21	7.3	11	17
Mg^{2+}	0.026	1000	6.6	2.8	7	9.6
Na^{+}	0.021	8700	53	3.7	7.6	7.2
K^{+}	0.21	-	24	0.5	2.1	1.6
S^{6+}	0.21	-	6.2	3.1	3	7
Cl^{-}	0.36	16000	51	2.7	3.5	8.4
SiO_2	-	1.4	6.6	20	56	25
N^{3-}	0.027	-	55	-	-	-
N^{5}	0.15	0.013	0.44	0.61	0	1
P	-	-	9.3	0.01	0.3	0.014
Fe	-	-	200	0.012	1.5	0.0013
Mn (µg/L)	-	-	74	1	300	3
O^{0}	56	-	-	7.7	0.22	6.8
Alkalinity (as $Ca(CO_3)$)	-	-	0.0066	29	67	-
pH	5.3	-	7	6.7	7.3	7
Temperature (°C)	9.3	-	24	11	11	11

Inverse models

Potential mechanisms that could produce the observed endmembers include mixing, concentration from evapotranspiration, and mineral interactions. Inverse models were developed in PHREEQC to help determine what geochemical processes may be feasible. In an inverse model, an initial solution or set of solutions and a final solution are given as inputs, along with a list of minerals that could dissolve or precipitate. PHREEQC then outputs all of the possible combinations of starting solutions and mineral dissolutions or

precipitations (referred to as phase mole transfers) that can produce the desired ending solution within user-specified tolerances.

Models were constructed to explain the evolution of meteoric water to the low endmember, the low endmember to the high-SiO_2 endmember, and the low endmember to the LOTT low-recharge wells. The models were required to balance pH, alkalinity, Al, C, Ca, Cl, Fe, H, K, Mg, Mn, Na O^0, P, S^{6+}, and Si. Global uncertainties were given the default value of ±0.05 (±5%). Modeling the evolution of the rainwater to the low endmember requires that the rainwater pH be allowed to adjust for charge balance and that its alkalinity be allowed an uncertainty of ±100%. Alkalinity was not included in the rainwater measurements, and the alkalinity initially calculated by PHREEQC is very low (on the order of $-1x10^{-5}$ mol/L as $Ca_{0.5}(CO_3)_{0.5}$). It can also be expected to change due to soil zone CO_2 inputs from organic matter degradation (Drever, 1982). Given this, and the fact that the adjusted pH is still well within the measured range, these allowances seem reasonable.

Potential dissolving or precipitating phases were determined from a number of sources. XRD analysis of soil samples taken during lysimeter installation at the Hawks Prairie site indicate the presence of chlorite, illite, kaolinite, smectite, and Ca-Na feldspar (HDR Engineering, Inc., 2018b). Additional minerals were identified from the literature. In order to better represent the local mineralogy, stoichiometries determined by Easterbrook et al. (1981) for andesine, hornblende, and ilmenite found in tephra beds of the Salmon Springs Drift were used. All other mineral phases were left as defined in the default phreeqc.dat database if available, or from sit.dat or llnl.dat if not. Organic matter was defined as CH_2O.

Reasonable mineral phases were included as needed to balance the solutions and were removed if they did not contribute significantly to any plausible models. Pyrite, andesine,

albite, K-mica, hornblende, ilmenite, organic matter, O_2 gas, and CaX_2 were allowed as dissolve-only phases. Kaolinite, Ca-montmorillonite, amorphous $Fe(OH)_3$, TiO_2, and NaX were allowed as precipitate-only phases. Vivianite, halite, FeX_2 and MnX_2 were allowed to dissolve or precipitate as needed. MgX_2 and KX were also included as precipitate-only phases for the low endmember to LOTT low-recharge well models. The phases with X represent cation exchange, where dissolution of a phase (e.g. CaX_2) results in the release of the associated cation, most likely from a clay, while precipitation of an X phase (e.g. NaX) indicates that the cation in question has replaced the one just released. A version of the meteoric water to low-endmember was also tested allowing H_2O gas to precipitate to represent evapotranspiration.

Evolution from rainwater to the low endmember and from the low endmember to the LOTT low recharge endmember requires an increase in nitrate, which would presumably be leached from the soil or produced via nitrification of other N species. Meanwhile evolution from the low endmember to the high-SiO_2 endmember requires a loss of nitrate. Since the groundwater samples generally do not contain NO_2 or NH_4, the nitrate is presumably being denitrified and off-gassed as N_2. The inverse modeling setup in PHREEQC can model the exsolution or dissolution of N_2 gas but not the input of other N species. There is therefore a choice of whether to model NO_3 inputs as dissolution of N_2 and O_2 gas or to exclude N from inverse modeling and address it separately. Both types of models were initially constructed, with the nitrogen-free models eventually selected.

When processing the inverse models produced by PHREEQC, models were only accepted if the ratio to initial and final solutions was in the range of 0.99-1.01 and, if possible, the magnitude of all phase mole transfers was less than 10^{-3}. If no models were

produced meeting these criteria, the phase mole transfer cutoff was raised to 10^{-2} for all phases except FeX_2 and MnX_2. The limit for these two was left in place, as Fe and Mn cation exchange at the millimolar level would indicate the involvement of a geologically improbable Fe or Mn dominated clay (David Parkhurst, USGS, personal communication).

Results

Water groupings and types

HCA with the LOTT wells resulted in the same groupings regardless of whether variables or PCA scores were used. The high and low recharge wells can be distinguished most easily by their Na^+ and, in most cases, Cl^- content, which is much higher in the high recharge wells than in the low ones. Inconsistent wells generally have Na^+ concentrations falling between the two groups, though not always. The Drost et al. (1998), HDR Engineering, Inc. (2017), and LOTT low recharge samples are predominantly Ca-Mg-HCO_3 type water, though the Drost wells exhibit a greater spread in Cl^- and SO_4. Meanwhile, the reclaimed, lysimeter, and high-recharge well waters are of a mixed type with higher Na^+ (Figure 4.12).

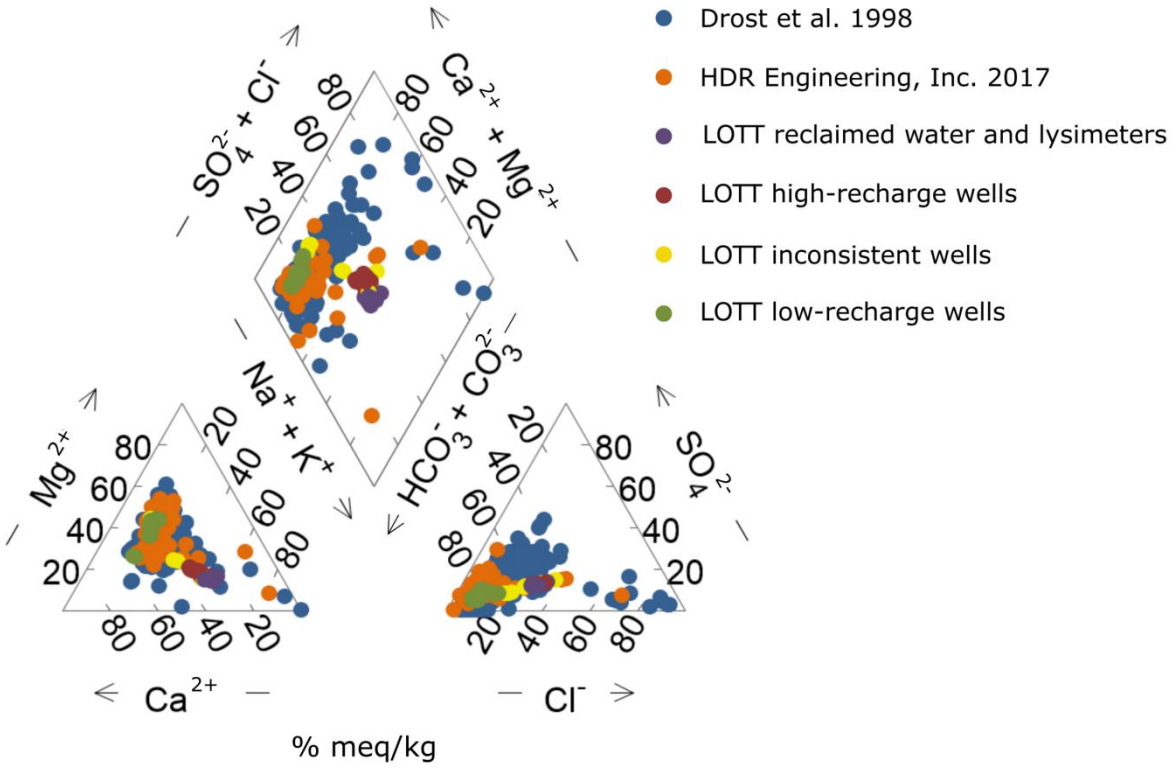

Figure 4.12: Piper diagram of Drost et al. (1998), HDR Engineering, Inc. (2017), and LOTT tracer study samples (including reclaimed water, lysimeters, and high recharge wells).

Solute relationships

The relationships between Na^+ and Mg^{2+}, Mg^{2+} and SiO_2, and Na^+ and SiO_2 form roughly linear or triangular distributions with the low endmember and high-SiO_2 endmember arranged along an edge. Meteoric water plots near the origin, slightly below the low endmember wells. Puget Sound water exhibits significantly less Mg^{2+} and SiO_2 relative to its Na^+ levels than the groundwater. Typical septic effluents contain far less SiO_2 than the groundwater and average Na^+ and Mg^{2+} levels slightly below the lower bounding line. Molar Mg^{2+}/ Na^+ and Ca/ Na^+ ratios in groundwater fall approximately into the range of 0 to 2.5, which matches the bulk composition of Vashon Outwash material (Figure 4.13) (Booth, Derek, personal communication Feb. 2021). The Vashon Outwash material, in turn, exhibits

ratios that fall between those of Crescent Formation basalts and various tephras found in Thurston County (Bowman et al., 2015).

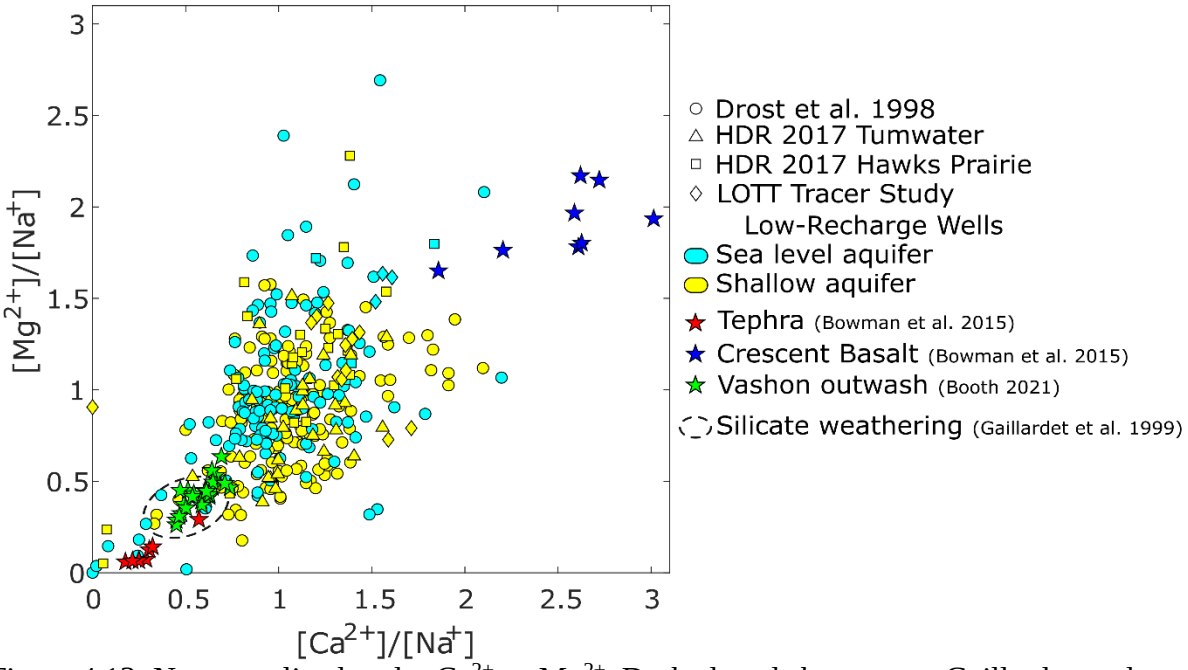

Figure 4.13: Na-normalized molar Ca^{2+} vs Mg^{2+}. Dashed oval shows zone Gaillardet et al. (1999) attribute to silicate weathering.

The majority of groundwater samples exhibit Cl^- concentrations less than 15 mg/L (0.42 mmol/L) and Na^+ below 20 mg/L (0.87 mmol/L). The selected endmember wells fall in this range. The mixing line from meteoric water to Puget Sound water has a roughly 1:1 ratio for molarities and bounds the lower Na^+ to Cl^- ratio groundwaters in the main cluster. Concentrated precipitation also falls along this line. Samples with Cl^- greater than approximately 15 mg/L extend approximately in the direction of Puget Sound water with a high degree of scatter (Figure 4.14).

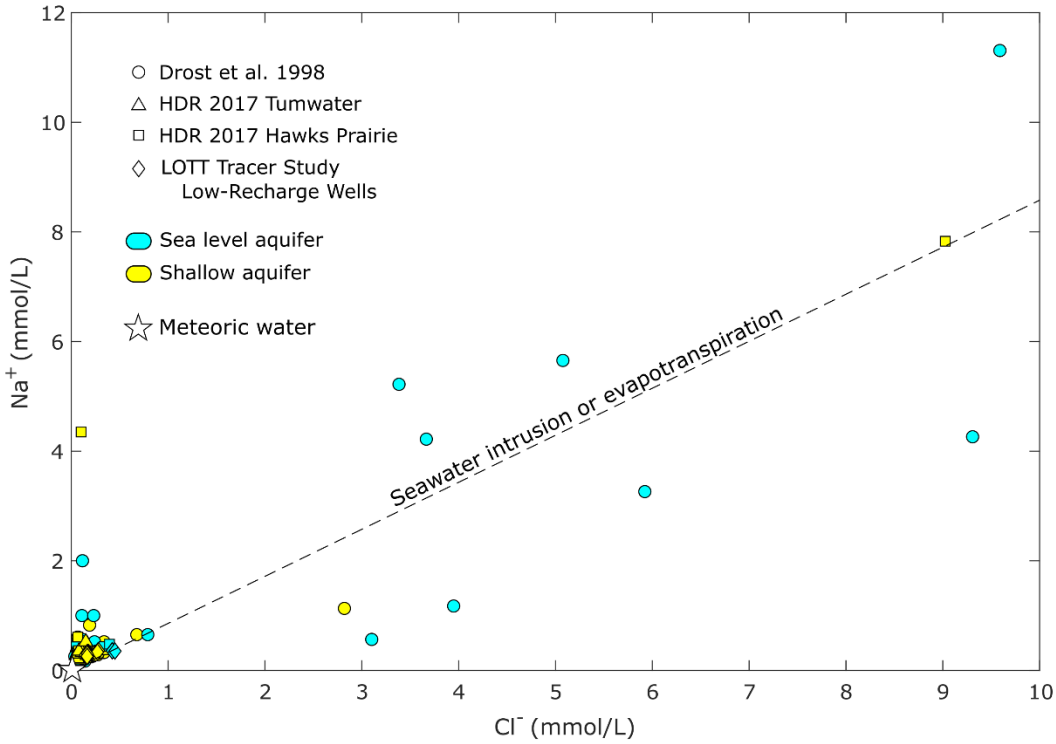

Figure 4.14: Molar Cl^- vs Na^+ in groundwater samples compared with meteoric water. Concentration by evapotranspiration or mixing with seawater will move concentrations up the dashed line.

Nitrate appears to increase with Cl^- for wells with elevated nitrate in the shallow and sea level aquifers, with NO_3 roughly bounded by the mixing line between local precipitation and average septic discharge from Richards et al. (2016) (Figure 4.15). Low NO_3 can be found in Drost wells of any temperature; however, higher temperatures are associated with higher maximum NO_3 concentrations (Figure 4.16). LOTT low recharge wells do not exhibit any trend with regard to NO_3 and temperature, and HDR Engineering, Inc. (2017) measurements do not include temperature. Evolving meteoric water to low endmember water or low endmember water to low recharge water requires an input of additional nitrogen, while evolving from the low endmember to the high-SiO_2 endmember requires that nitrogen exit the solution.

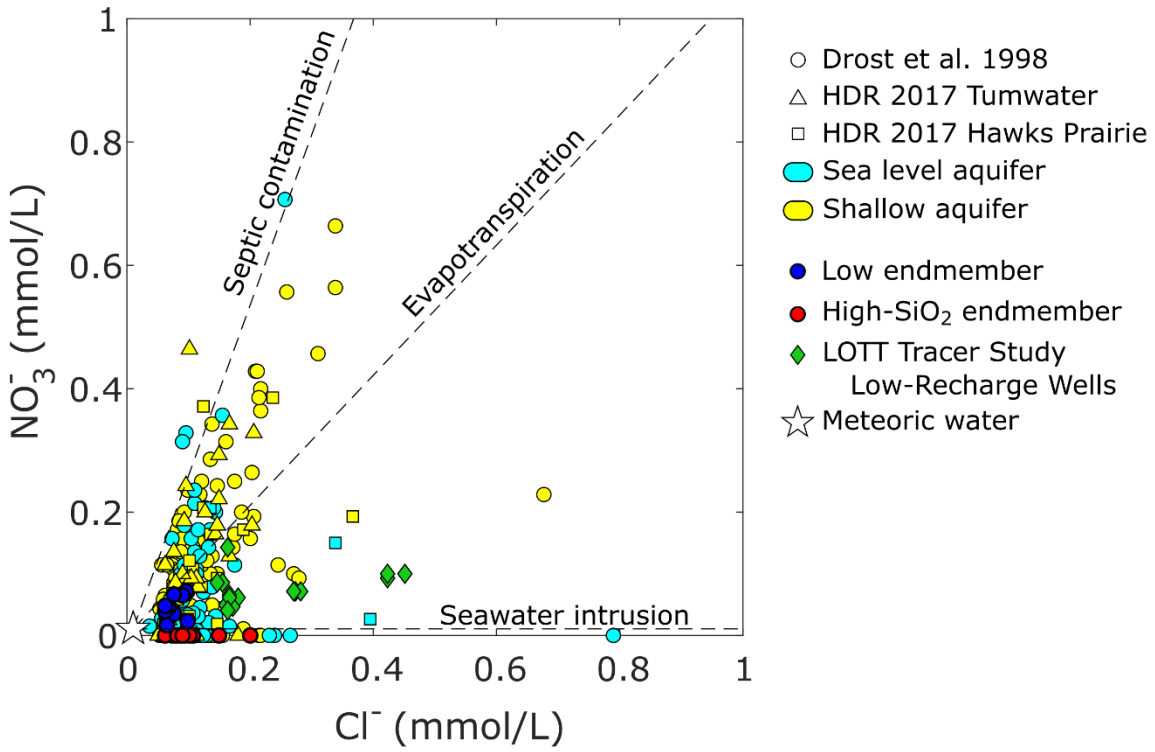

Figure 4.15: Molar Cl^- vs NO_3^- in groundwater samples (zoomed to focus on majority of data). Mixing lines for seawater intrusion and septic contamination and concentration by evapotranspiration trend shown by dashed lines.

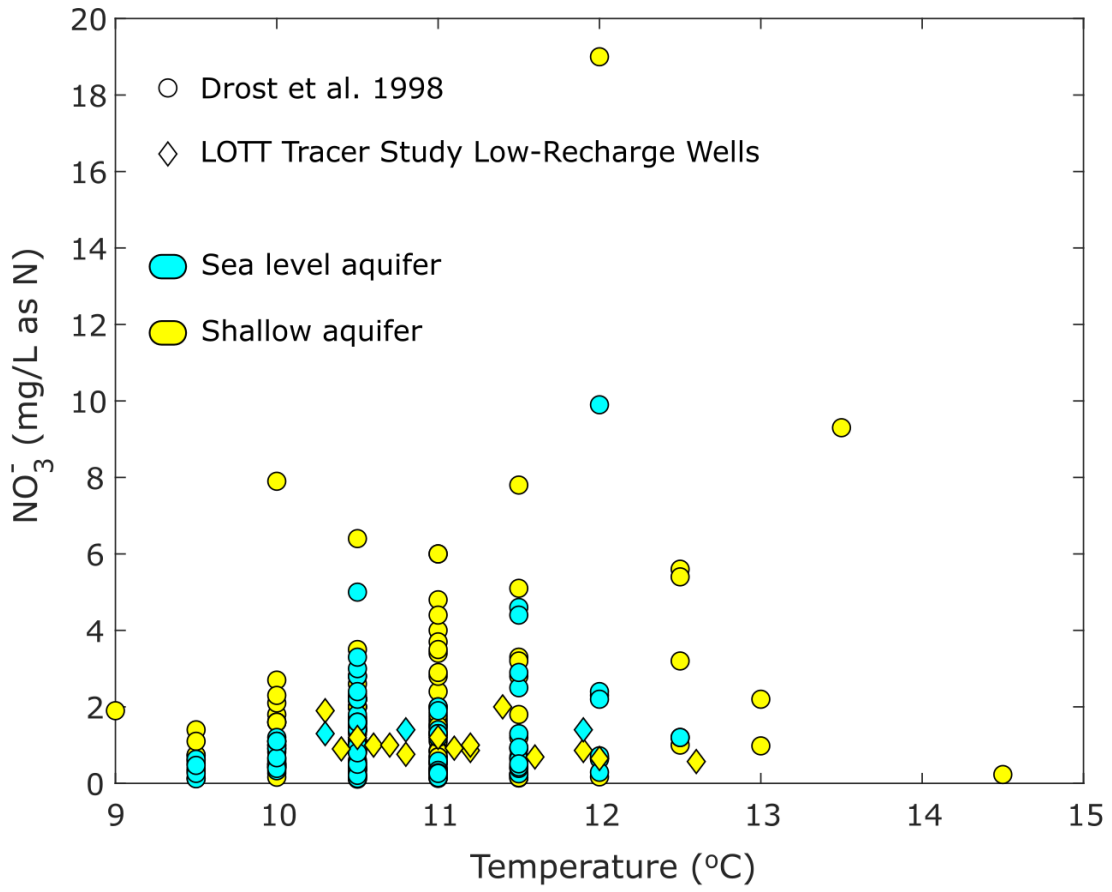

Figure 4.16: Groundwater temperature vs NO_3 for Drost et al. (1998) and LOTT low-recharge wells. (Temperature not measured in HDR Engineering, Inc. (2017).)

Oxygen is undersaturated in all endmember wells and in all LOTT samples. Oxygen levels in the low endmember (7.7 mg/L) are similar to LOTT low recharge levels and higher than in the high endmember (0.2 mg/L). Among the Drost et al. (1998) wells, the high-SiO_2 wells have some of the lowest oxygen levels. Oxygen can be consumed through the microbially mediated oxidation of organic matter (Eq. 3-1) or metals such as iron or titanium in the form of pyrite or other mafic minerals (Eq. 3-2) (Appelo and Postma, 2005).

$$CH_2O + O_2 \rightarrow CO_2 + H_2O \qquad \text{Equation 3-1}$$

$$FeS_2 + {}^{15}/_4\, O_2 + {}^{7}/_2\, H_2O \rightarrow Fe(OH)_3 + 2SO_4^{2-} + 4H^+ \qquad \text{Equation 3-2}$$

The greatest loss of dissolved oxygen is required in the evolution of meteoric water to low-endmember water, followed by the evolution of low endmember water to high-SiO_2 endmember water. The evolution of low endmember water to LOTT low-recharge water requires the least loss of dissolved oxygen.

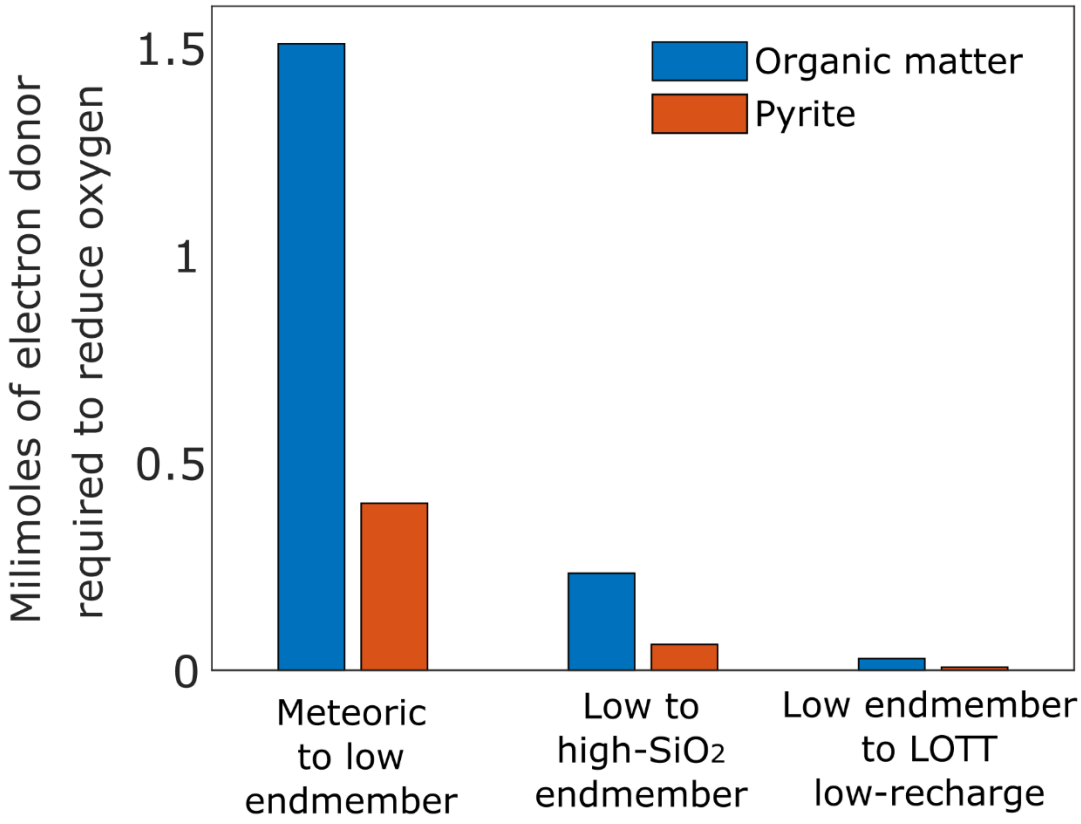

Figure 4.17: Amount of organic matter or pyrite stoichiometrically required to reduce oxygen, assuming (hypothetically) that it is the only electron donor

Concentration of meteoric water via evapotranspiration can increase concentrations of solutes such as Cl^- and nitrogen species. Producing the chloride levels found in the selected endmember wells by evapotranspiration of meteoric water requires a minimum concentration factor of 6.1 for Drost wells 199, 259, and 272 and RES335 or as high as 19.7 for Drost well

1 (Figure 4.18). Other solutes, if assumed to behave conservatively, can be corrected for meteoric inputs using the equation:

$$[X]_{\text{concentrated meteoric}} = [X]_{\text{meteoric}}([Cl^-]_{\text{sample}}/ [Cl^-]_{\text{meteoric}}) \qquad \text{Equation 4-3}$$

where brackets indicate molarity (Moulton, 2000; Jin et al., 2016). Calculated concentrated meteoric NO_3 nitrogen equals or exceeds measured NO_3 in all endmember wells and LOTT tracer study samples.

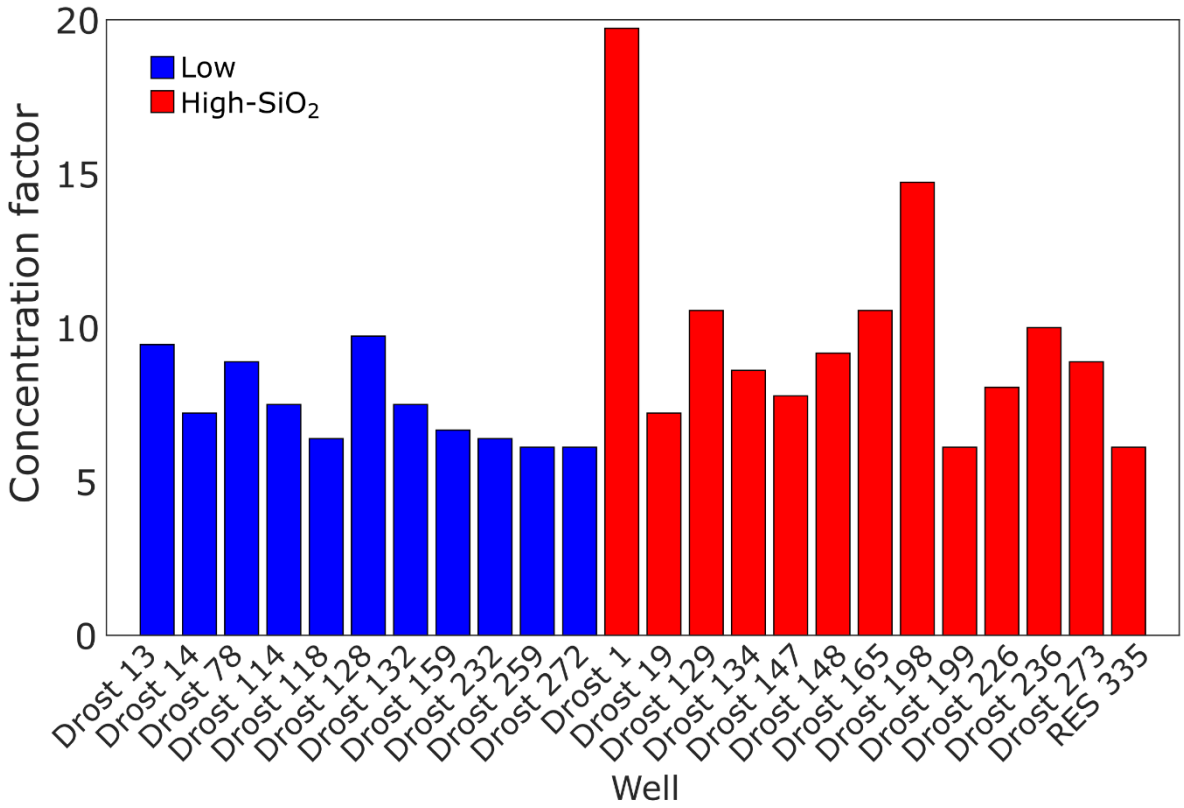

Figure 4.18: Concentration of meteoric water needed to account for chloride in groundwater samples.

Inverse modeling

The evolution of meteoric water to the low endmember can be modeled with the dissolution of pyrite, ilmenite, organic matter, vivianite, halite, and some combination of andesine, albite, and K-mica, and the precipitation of amorphous $Fe(OH)_3$, TiO_2 and either

kaolinite or Ca-montmorillonite. Cation exchange occurs among Ca, Na, Mn, and Fe (Table 4.8). Though evaporation was allowed, it did not occur in any model.

The high-SiO_2 endmember can be produced from the low endmember via the dissolution of K-mica, hornblende, organic matter, oxygen, vivianite, halite, and albite, in addition to ilmenite in some models, and the precipitation of amorphous $Fe(OH)_3$, TiO_2 and either kaolinite or Ca-montmorillonite. Cation exchange occurs among Ca, Na, Mn, and Fe (Table 4.9).

The evolution of low endmember water to LOTT low recharge water could be modeled as the dissolution of pyrite, hornblende, organic matter, oxygen, vivianite, halite, and in some cases andesine, in addition to the precipitation of Ca-montmorillonite, $Fe(OH)_3$, and TiO_2. Ca, Na, Mg, K, Mn, and Fe participate in cation exchange. The LOTT models were the only ones to require the inclusion of KX and MgX_2 (Table 4.10).

The evolution of the low endmember water to the high-SiO_2 endmember could be achieved with all phase mole transfers under 10^{-3}, while meteoric water to low endmember and low endmember to LOTT required raising the threshold to 10^{-2} for species other than FeX_2 and MnX_2.

Models in which nitrogen balance was considered gave largely equivalent results to models in which it was not. Minor differences were observed in O_2, NaX, $Fe(OH)_3$, and FeX_2 in the low endmember to high-SiO_2 or LOTT low-recharge models, in addition to albite in the low to high-SiO_2 models and andesine, K-mica, Ca-montmorillonite, MgX_2, and KX in the low to LOTT models. The sum of residuals was slightly lower for models with nitrogen, ranging 0.55 – 8.79 as opposed to 3.44 – 8.88.

Comparing the amount of organic matter dissolved in the models with the amount of iron and titanium oxides and hydroxides precipitated suggests that for the evolution of meteoric water to the low endmember and the evolution of the low endmember to the LOTT low-recharge water, oxygen reduction in the models occurs mostly due to oxidation of metals. For models of the evolution of low endmember water to high-SiO_2 endmember water, oxygen reduction is more evenly divided between organic matter oxidation and metal oxidation.

Table 4.8: Inverse model details and phase mole transfers for evolution of meteoric water to low endmember. Positive values indicate dissolution; negative values indicate precipitation.

Model number	1	2	3	4
Sum of residuals	3.44E+00	3.53E+00	3.80E+00	3.92E+00
Sum of delta/ uncertainty limit	3.44E+00	3.53E+00	3.80E+00	3.92E+00
Maximum fractional error	9.23E-01	9.23E-01	9.23E-01	9.23E-01
Fraction meteoric (input)	1.00E+00	1.00E+00	1.00E+00	1.00E+00
Fraction low endmember (output)	1.00E+00	1.00E+00	1.00E+00	1.00E+00
Pyrite	1.51E-05	1.51E-05	1.51E-05	1.51E-05
Andesine	5.84E-04	2.52E-04	0.00E+00	0.00E+00
Kmica	0	6.88E-06	1.23E-05	1.23E-05
Hornblende	0	0	0	0
Ilmenite	1.84E-03	1.84E-03	1.85E-03	1.85E-03
Organic Matter	8.98E-04	8.98E-04	9.06E-04	9.12E-04
O_2 (g)	0	0	0	0
Kaolinite	0	-1.81E-04	0	-1.07E-04
Ca-Montmorillonite	-3.36E-04	0.00E+00	-1.29E-04	0.00E+00
Vivianite	1.61E-07	1.61E-07	1.61E-07	1.61E-07
Halite	6.60E-05	6.60E-05	6.60E-05	6.60E-05
CaX_2	2.90E-05	8.67E-05	1.93E-04	1.72E-04
NaX	-2.61E-04	-6.37E-05	-1.72E-04	-8.55E-05
$Fe(OH)_3$ (amorph)	-2.75E-03	-2.59E-03	-2.55E-03	-2.53E-03
TiO_2	-1.20E-03	-1.20E-03	-1.21E-03	-1.21E-03
Albite	0	0	2.57E-04	1.70E-04
MnX_2	-8.26E-04	-8.27E-04	-8.31E-04	-8.31E-04
FeX_2	9.28E-04	7.72E-04	7.24E-04	7.02E-04

Table 4.9: Inverse model details and phase mole transfers for evolution of low endmember to high-SiO_2 endmember. Positive values indicate dissolution; negative values indicate precipitation.

Model number	1	2	3	4	5	6	7
Sum of residuals	7.53E+00	4.46E+00	7.67E+00	4.74E+00	4.76E+00	8.20E+00	8.88E+00
Sum of delta/ uncertainty limit	7.53E+00	4.46E+00	7.67E+00	4.74E+00	4.76E+00	8.20E+00	8.88E+00
Maximum fractional error	5.00E-02	5.00E-02	5.00E-02	5.00E-02	5.00E-02	5.00E-02	5.00E-02
Fraction meteoric (input)	1.00E+00	1.00E+00	1.00E+00	1.00E+00	1.00E+00	1.00E+00	1.00E+00
Fraction low endmember (output)	1.00E+00	1.00E+00	1.00E+00	1.00E+00	1.00E+00	1.00E+00	1.00E+00
Pyrite	0	0	0	0	0	0	0
Andesine	0	0	0	0	0	0	0
Kmica	3.76E-05	3.79E-05	3.76E-05	3.79E-05	3.79E-05	3.82E-05	3.82E-05
Hornblende	6.46E-05	5.88E-05	6.44E-05	5.88E-05	5.87E-05	5.30E-05	5.29E-05
Ilmenite	0	0	6.75E-06	0	7.22E-06	0	7.70E-06
Organic Matter	6.08E-04	6.08E-04	6.08E-04	6.08E-04	6.08E-04	6.08E-04	6.08E-04
O_2 (g)	3.91E-04	3.78E-04	3.92E-04	3.77E-04	3.79E-04	3.77E-04	3.78E-04
Kaolinite	0	-1.61E-04	0	-1.58E-04	-1.58E-04	0	0
Ca-Montmorillonite	-1.85E-04	0	-1.84E-04	0	0	-1.93E-04	-1.90E-04
Vivianite	4.68E-06	4.68E-06	4.68E-06	4.68E-06	4.68E-06	4.68E-06	4.68E-06
Halite	2.26E-05	2.26E-05	2.23E-05	2.26E-05	2.26E-05	2.26E-05	2.26E-05
CaX_2	0	0	0	0	0	5.76E-05	5.73E-05
NaX	-1.03E-04	-6.47E-06	-1.02E-04	0	0	-1.22E-04	-1.15E-04
$Fe(OH)_3$ (amorph)	-1.26E-04	-6.88E-05	-1.34E-04	-6.56E-05	-7.58E-05	-6.08E-05	-6.81E-05
TiO_2	-1.11E-05	-1.01E-05	-1.55E-05	-1.01E-05	-1.48E-05	-9.12E-06	-1.41E-05
Albite	2.29E-04	1.27E-04	2.28E-04	1.21E-04	1.21E-04	2.63E-04	2.56E-04
MnX_2	3.02E-06	3.24E-06	0	3.24E-06	0	3.45E-06	0
FeX_2	4.86E-05	0	5.08E-05	-3.24E-06	0	0	0

Table 4.10: Inverse model details and phase mole transfers for evolution of low endmember to LOTT low-recharge. Positive values indicate dissolution; negative values indicate precipitation.

Model number	1	2	3
Sum of residuals	4.86E+00	4.41E+00	4.41E+00
Sum of delta/ uncertainty limit	4.86E+00	4.41E+00	4.41E+00
Maximum fractional error	5.00E-02	5.00E-02	5.00E-02
Fraction meteoric (input)	1.00E+00	1.00E+00	1.00E+00
Fraction low endmember (output)	1.00E+00	1.00E+00	1.00E+00
Pyrite	2.05E-05	2.05E-05	2.05E-05
Andesine	0	7.33E-04	0
Kmica	2.02E-04	4.46E-04	5.19E-04
Hornblende	9.42E-05	9.19E-05	2.15E-04
Ilmenite	0	0	0
Organic Matter	9.97E-04	9.97E-04	9.97E-04
O_2 (g)	1.06E-03	1.17E-03	1.24E-03
Kaolinite	0	0	0
Ca-Montmorillonite	-3.15E-04	-1.05E-03	-7.95E-04
Vivianite	7.06E-08	7.06E-08	7.06E-08
Halite	1.61E-04	1.61E-04	1.61E-04
CaX_2	1.19E-04	0	0
NaX	-5.30E-05	-4.84E-04	-1.04E-04
$Fe(OH)_3$ (amorph)	-1.52E-04	-6.19E-04	-9.98E-04
TiO_2	-1.62E-05	-1.58E-05	-3.70E-05
Albite	0	0	0
MnX_2	-3.41E-06	-3.33E-06	-7.83E-06
FeX_2	0	4.65E-04	6.78E-04
MgX2	0	0	-3.67E-04
KX	-1.79E-04	-4.39E-04	-5.03E-04

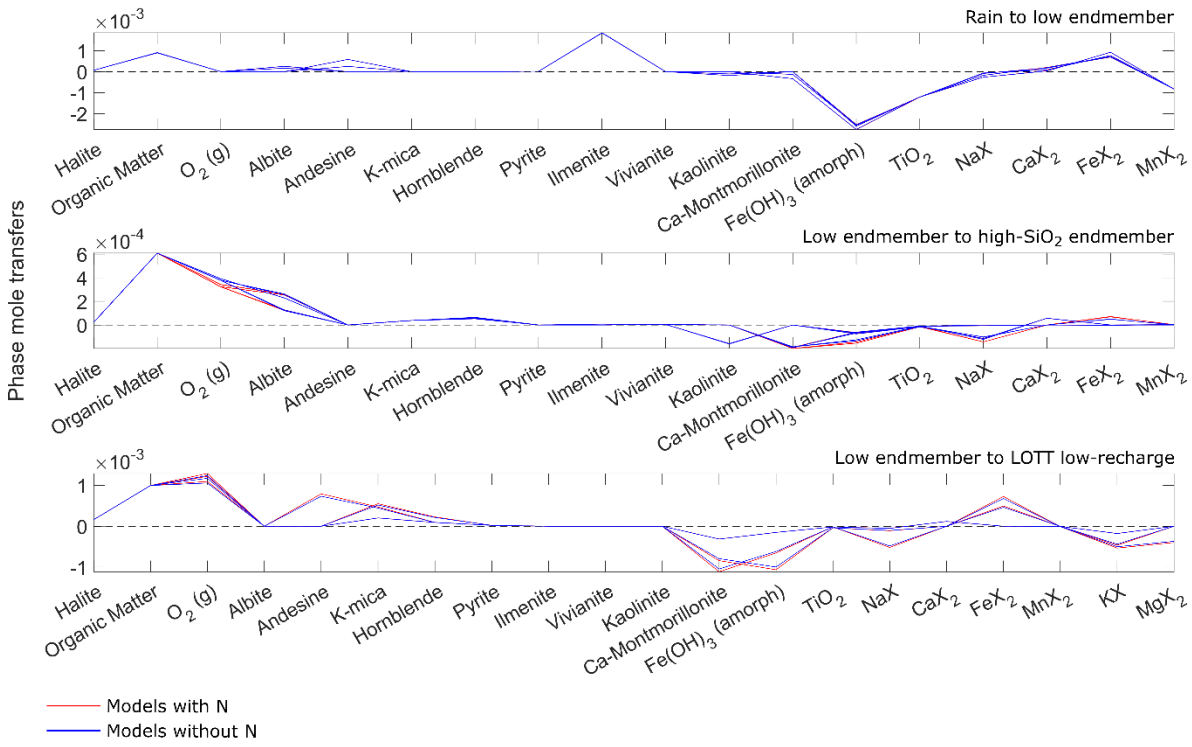

Figure 4.19: Phase mole transfers in PHREEQC inverse models

Discussion

Spatiotemporal distribution of water samples

Tritium dating of water in the Puget Sound aquifer system broadly suggests that most groundwater in the region is no more than a few decades old (Vaccaro et al., 1998). Accompanying flow models indicate that some locations might have water that is even younger or as old as several centuries, though the younger end of the range is believed to be more likely (Vaccaro et al., 1998). Well sampling for the Drost et al. (1998) studies and the HDR Engineering, Inc. (2017) and HDR Engineering, Inc. (2019) studies occurred approximately two decades apart; however, there should not have been any major geochemical shifts during this time. The only changes to be expected are anthropogenic shifts in climate, seawater intrusion, and land use change. SO_4 has decreased and pH increased in

local precipitation since the early 1990's, in agreement with national trends, while other ions have remained fairly constant (Lehmann et al., 2005; US EPA and University of Washington, 2021a). Over the period of 1991 – 2016, Thurston County experienced a 24% growth in developed areas, while undeveloped areas shifted from forests towards shrub lands (TRPC, n.d.). In spite of this, water quality assessments document fairly consistent conditions during the period of 1981 – 2015 (Turney, 1986; Drost et al., 1998; Vaccaro et al., 1998; TCSSWP and TCEHD, 1999; HDR Engineering, Inc., 2017). Given that the Drost et al. (1998), HDR Engineering, Inc. (2017), and LOTT low recharge samples tend to exhibit the same water types, and the selected wells have very similar overall geochemistry, it is probably safe to consider them together. In addition, the endmember samples contain little to no nitrate, suggesting minimal anthropogenic inputs.

The low endmember wells are located primarily to the west, at the base of the Black Hills (Figure 4.10), which form one of the upper boundaries of the Vashon deposits containing the aquifer system (Berris, 1995). Meanwhile, the high-SiO_2 endmember wells are more scattered to the east (Figure 4.20 - Figure 4.21). Mapping of the wells in comparison to the groundwater flow models of Drost et al. (1999) suggests that the high-SiO_2 wells have a slight tendency to be towards the ends of longer flow paths. It therefore makes sense that the water would be older and have more solutes than the low endmember wells positioned in more upgradient areas. The low oxygen content of these wells compared to the others also suggests that the high-SiO_2 wells draw older water. Since the same minerals are likely to be present throughout the study area, it is probable that after remaining in the ground for a sufficient amount of time, water similar to the low endmember could develop a composition similar to that of the high-SiO_2 endmember. Simulations by Drost et al. (1999) indicate

different flow paths for the wells; however, they can still be assumed to represent the endmembers for potential paths of chemical evolution that water in the aquifers can take. This assumption is likely valid for elements derived from minerals or atmospheric deposition where land cover does not vary too greatly, given that they are all located within the same area. In terms of LOTT monitoring wells, the high-recharge wells were determined to be strongly influenced by the reclaimed water infiltrated at the Hawks Prairie site, while the low-recharge wells were the downgradient wells determined to reflect primarily background conditions. Therefore, only low-recharge wells are considered in analysis of the local geochemistry.

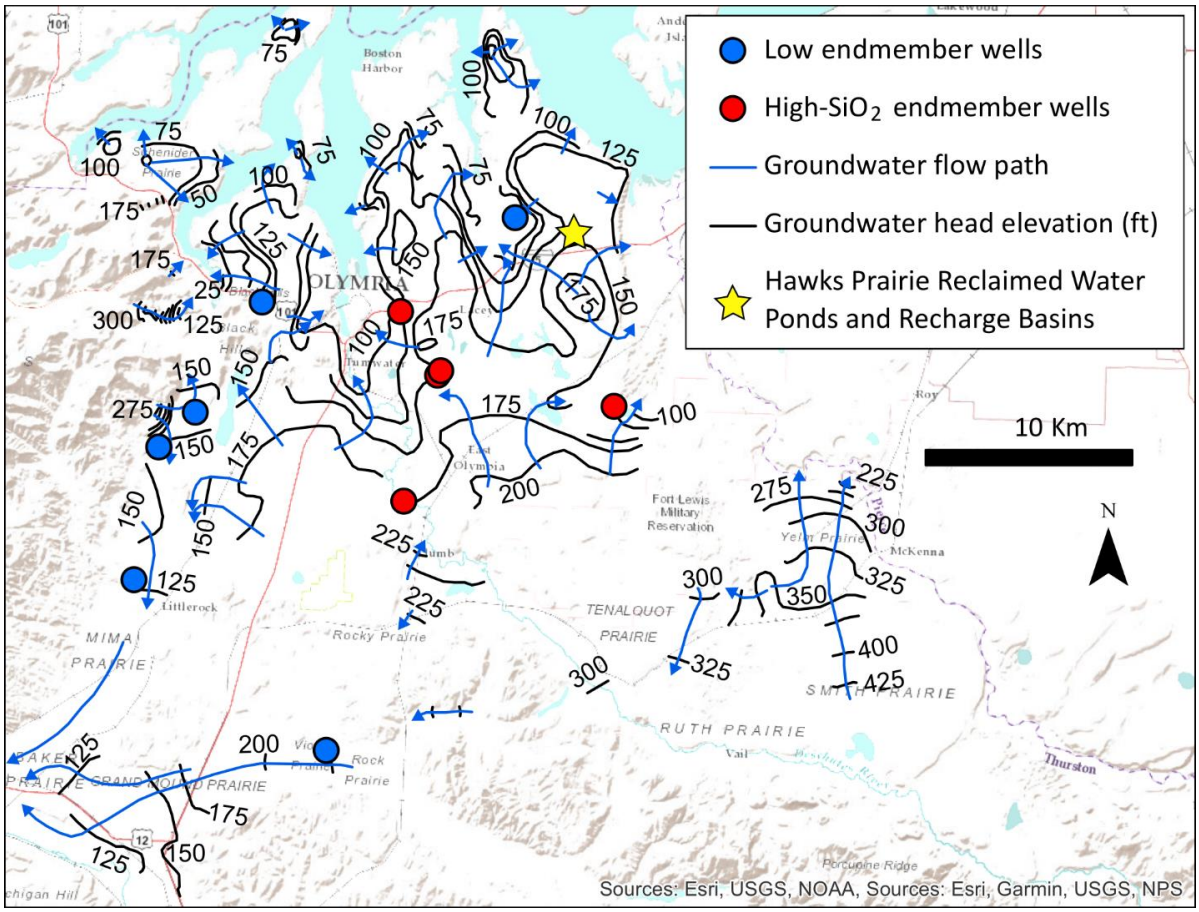

Figure 4.20: Groundwater heads and flow directions in the shallow aquifer. Locations of endmember wells screened in the shallow aquifer marked with circles. Contours and flow lines from Drost et al. (1999).

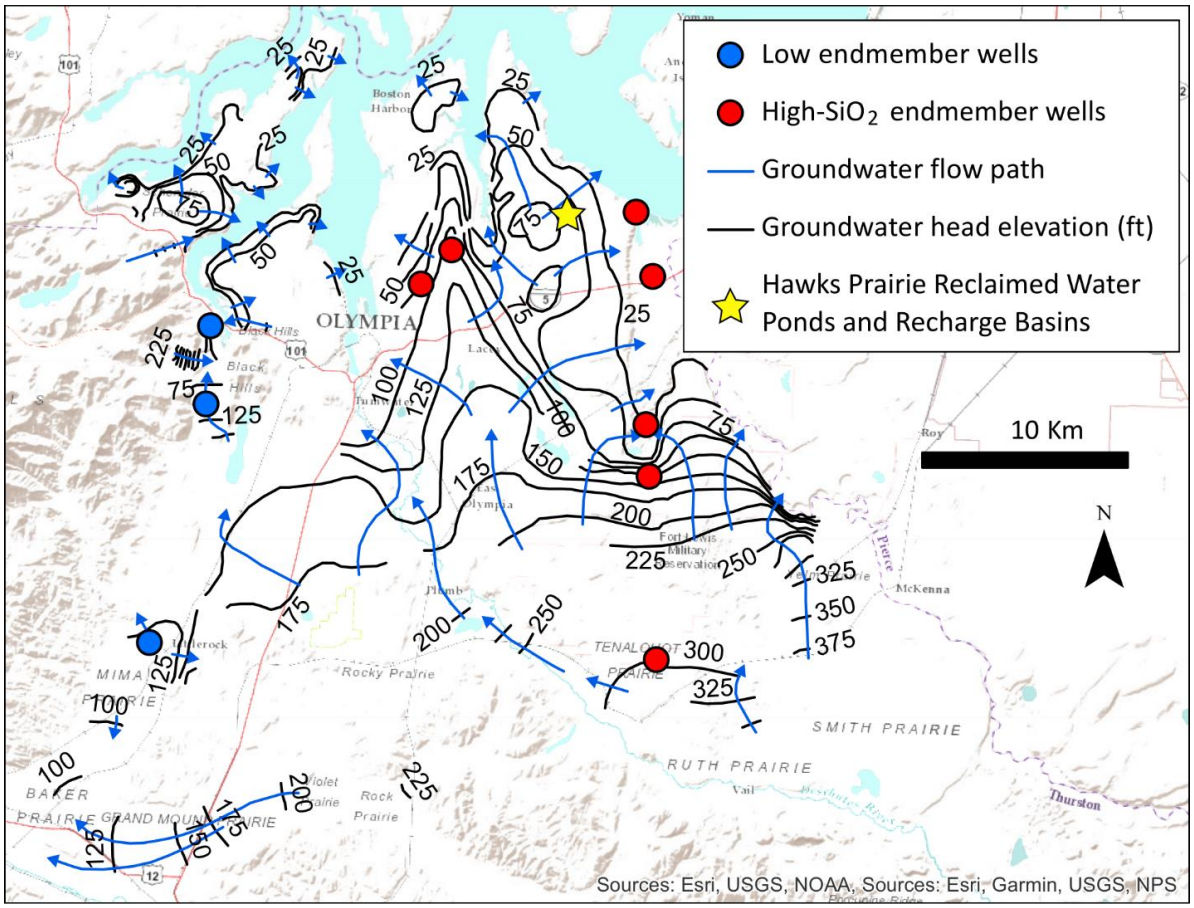

Figure 4.21: Groundwater heads and flow directions in the sea level aquifer. Locations of endmember wells screened in the sea level aquifer marked with circles. Contours and flow lines from Drost et al. (1999).

Potential influences to groundwater chemistry

The wells measured by Drost et al. (1998) and HDR Engineering, Inc. (2017) exhibit a fairly wide range of Cl^- concentrations, which holds true for the selected endmembers. Since Cl^- is a conservative ion, this is likely to represent different inputs as opposed to variation in geochemical evolution. One potential source of Cl^- is seawater intrusion. The sea level aquifer is in hydrologic connection with Puget Sound (Drost et al., 1999; TCSSWP and TCEHD, 1999), and seawater intrusion has been observed to occur (Dion and Sumioka, 1984; Drost et al., 1998). Drost et al. (1998) suggest that Cl^- concentrations over 50 mg/L in Thurston County groundwater or Cl-type waters in general could be suggestive of seawater

intrusion, while Dion and Sumioka (1984) only consider the possibility of seawater intrusion if Cl^- exceeds 100 mg/L. The majority of groundwater samples, including the endmember wells, fall below both of these thresholds. The roughly concomitant increases in Na^+ and Cl^- in wells with high Cl^- are suggestive of a seawater influence, even in waters that fall short of the 50 mg/L threshold (Figure 4.14).

Septic effluent is believed to be a major source of nitrate in the area and can also be a source of chloride (Turney, 1986; Drost et al., 1998; HDR Engineering, Inc., 2017); Drost et al. (1998) suggests that Cl^- concentration greater than 5 mg/L in wells located away from the coast may be the result of septic effluent. Elevated nitrate appears roughly correlated with Cl^- for most wells in the shallow and sea level aquifers, on a trend that roughly follows the mixing line between local precipitation and average septic discharge (Figure 4.15). It should be noted that the potential range of septic concentrations is quite wide, and the values used are not specific to the area; nevertheless, it does support the hypothesis that wells with elevated Cl^- and nitrate could be affected by septic discharge. The wells selected for modeling fall at the low end of this range, with some exhibiting a different trajectory due to excess chloride. Three of the low-recharge wells measured during the LOTT tracer study, MW-20, MW-26, and MW-28 also agree reasonably with the aforementioned trend, while MW-23 and MW-25 exhibit higher Cl^-. Drost wells 1 and 198 have Cl^- slightly greater than 5 mg/L, the threshold described by Drost et al. (1998) for potential septic influence, though less than 50 mg/L, the criteria for seawater. The nitrate levels in these wells, like in the others selected for modeling, fall below 1 mg N/L. Drost et al. (1998) only focus on wells with nitrate above this level with regard to septic contamination, so the selected wells can be assumed to be unaffected. It is interesting to note that the maximum nitrate levels observed

by Drost et al. (1998) in wells of a given temperature appears to increase with the temperature of the water (Figure 4.16). This is interesting, given that increased temperature has been shown to increase denitrification rates, which would result in an inverse, not a positive, correlation (Hiscock et al., 1991; Addy et al., 2016; Hoover et al., 2016; Robertson et al., 2017; Xiong et al., 2017). It is common for septic effluent to exhibit higher temperatures than ambient groundwater due to indoor hot water usage, which may explain this trend (Viraraghavan and Warnock, 1976; Humphrey et al., 2013). In wells with low but nonzero nitrate, such as some of the low endmember wells, the nitrate may simply be concentrated from meteoric water. This nitrate is derived largely from fossil fuel emissions (Elliott et al., 2007). These findings suggest that septic effluent does affect some wells in the study area, but that the impact to the selected endmember wells is minimal.

Nitrate concentrations in groundwater may vary for a number of reasons. Firstly, there is the spatial distribution of septic systems and variations in their nitrogen removal efficiency. Sewer connections are generally available to residents of urban areas in the north county and Grand Mound, which are served by LOTT, and to residents of Yelm and Tenino (Thurston Sewerage Plan, 1990; Blinn, 2012; City of Tenino, 2016; Parametrix and FCS Group, 2016). Meanwhile, rural areas and properties developed prior to local expansion of sewer systems generally rely on septic systems (Thurston Sewerage Plan, 1990; TRPC, 2016; Schuyler, 2015). This results in an uneven distribution in the location of septic sites, while factors such as the design of the system, type of soil, unsaturated zone thickness, loading rate, and lot size all determine how much nitrate leaves these sites (Cogger et al., 1988; Costa et al., 2002; McQuillan, 2004). Nitrogen also falls as dry deposition, while forest canopies have been shown to take up nitrogen from precipitation that filters through them, so varying

vegetative cover could result in differing amounts of nitrate in throughfall water reaching the ground (Fenn et al., 2013). In groundwater, the persistence of nitrate depends on the oxygen content of the water and the presence of an electron donor such as organic matter (Appelo and Postma, 2005). Denitrification will only occur after all of the oxygen has been consumed or in anoxic microsites, and there must be labile organic matter remaining to reduce the nitrogen (McClain et al., 2003; Kedziorek et al., 2008). This is typically mediated by heterotrophic bacteria, such as those of the *Pseudomonas* genus (Knowles, 1982). The required organic matter could be dissolved in the water or be present in the soil and sediment. Drost et al. (1998) does not include measurements of organic carbon, though HDR Engineering, Inc. (2017) finds total organic carbon at concentrations less than 1 mg/L in most shallow and sea level wells. The exact amount of carbon needed to reduce oxygen and potentially nitrate to observed levels may not align with the amount measured in the water, as what is measured may be recalcitrant, residual carbon, or more might be incorporated during transport (Kedziorek et al., 2008; Holch, 2008; Jiménez, 2011). Additionally, oxygen typically becomes more depleted with time when not in contact with the atmosphere, such that residence time can affect redox sensitive species such as nitrogen (Appelo and Postma, 2005).

It is somewhat surprising that the models indicate a greater role of metal oxidation than organic matter oxidation in oxygen depletion for the evolution of meteoric water to low endmember groundwater and the opposite for the evolution of low endmember groundwater to the high-SiO_2 endmember. In a typical system, more labile organic matter is usually present closer to the surface and becomes depleted with time spent in the aquifer, resulting in organic matter oxidation preceding metal oxidation (Kedziorek et al., 2008). Given that the

inverse modeling process evaluates reactions in terms of their stoichiometry, not their plausibility, it may be that the modeled order of electron donors is not representative of reality.

With regard to whether nitrogen should be included in the inverse models of the water chemistry, the main issue is how the model handles electron balance. If organic matter is available, it should be the primary electron acceptor for denitrification (Korom, 1992); however, the inclusion of nitrogen in models requiring denitrification does not result in a change to the amount of organic matter required. Instead, a slight decrease in the amount of amorphous $Fe(OH)_3$ precipitated suggests that the models may be using iron. The inclusion of N in the models does result in a slightly lower sum of residuals in most cases, but the difference is small, and the phase mole transfers of all non-nitrogen species remain very similar. Therefore, simplification of the models by excluding nitrogen balance is justified.

One way for chloride levels to exceed that of precipitation in uncontaminated groundwater is by concentration via evaporation and transpiration. Mundorff et al. (1955) states that there is little runoff in the Yelm area, and that precipitation in well drained areas either recharges or is returned to the atmosphere via evapotranspiration. They estimate that in Yelm Prairie, 75% of annual precipitation recharges the aquifers, with the remaining 25% going to evapotranspiration. This would result in a 1.3x concentration of solutes. In more poorly drained areas where water sits at the surface for longer periods, evapoconcentration would be greater. As the groundwater evolves, some evaporation or transpiration may still occur when the water table is close to the surface, but it is much less significant (Berris, 1995; Drost et al., 1999). PHREEQC inverse models do not show evaporation occurring and instead rely on halite dissolution. Given that evaporation is known to occur in the area, it is

likely that the lack of evaporation in the models is a mathematical artifact caused by the modeled phases not having exactly the right stoichiometries to account for the other changes that must occur when evaporation is included. Halite may be present in soils and sediments as a result of the continuous deposition of sea salt aerosols over time. Dissolution of halite may therefore contribute to chloride in the groundwater, though probably not to as great of an extent as indicated by the models.

Evapotranspiration of meteoric water produces molar concentrations Na^+ approximately equal to Cl^-, which can be a confounding factor in distinguishing among the effects of evapotranspiration, halite dissolution, or seawater intrusion; however, seawater intrusion has the potential to yield much higher concentrations than the other processes. This is to be expected, as the primary source of both ions in the atmosphere is sea salt aerosols (Vong et al., 1988). It is assumed that most of the samples start with evapotranspiration along with possible halite dissolution to produce the observed Cl^- content, which should raise Na^+ to equal levels, but Na^+ is greater than Cl^- in most samples. This suggests that additional Na^+ is obtained from the dissolution of other minerals. Inverse models suggest phases such as plagioclase feldspars and hornblende could supply additional sodium, while cation exchange may serve as a sink for excess.

The weathering of aluminosilicate minerals to clays has been broadly documented to influence groundwater chemistry and has previously been proposed to determine the water types found in the shallow and sea level aquifers (Drever, 1982; Appelo and Postma, 2005; Drost et al. 1998). Plagioclase feldspars, K-micas, kaolinite, and montmorillonite have all been documented in the region and likely participate in these reactions (Easterbrook et al., 1981; Snavely, 1958; Mullineaux, 1967; Gault, 2015).

Authors such as Gaillardet et al. (1999) and Jin et al. (2016) have used molar ratios in surface water samples to broadly identify different types of rock weathering in catchments. Plotting molar Ca/ Na^+ and Mg^{2+}/ Na^+ ratios in groundwater samples and local rocks and minerals after Gaillardet et al. (1999) suggests water chemistry most closely aligned with Vashon Outwash deposits, as is to be expected, since these deposits host the aquifers (Figure 4.13). The positioning of the Vashon deposits between Crescent Basalts and various bulk tephras suggests their origin includes volcanic source rocks. The water samples tend to cluster towards the ratios Gaillardet et al. (1999) associate with silicate weathering, supporting the importance of silicate weathering in influencing groundwater compositions.

Phosphorous has multiple potential sources but is most likely derived through mineral weathering. Van Denburgh and Santos (1965) note that phosphates in groundwater often originate from wastewater or fertilizers but that elevated phosphates in Washington groundwater are widespread and not necessarily spatially correlated with sources of contamination. Concentrations have also been observed to increase with depth and groundwater age in some locations (Van Denburgh and Santos, 1965). HDR Engineering, Inc. (2017) observed elevated nutrients such as NO_3^- and PO_4^{3-} primarily in areas with a high density of septic systems, but the concentrations of the two anions in the shallow and sea level aquifers do not show any particular correlation. When also considering data from Drost et al. (1998), it becomes apparent that the wells with the highest NO_3^- levels have the lowest concentrations of phosphorus and vice versa. This suggests that either the two come from different sources (nitrate from surface inputs and phosphorus from minerals) or that if PO_4^{3-} is derived from septic effluent, then extensive denitrification must occur.

As with all of the minerals used in modeling, it is not certain that the source of phosphorus is vivianite specifically. Apatite, another phosphorus bearing mineral, is known to be present in some pre-Vashon deposits that might be found in the study area, but generally only as an accessory mineral (Mullineaux et al., 1964; Easterbrook et al., 1981). It also tends to resist weathering and is therefore considered less likely to be a major contributor (Drever, 1982). Alternatively, phosphorus may also be released from clays or metal oxyhydroxides (Loewald et al., n.d.).

Iron and manganese are highly redox sensitive with solubilities dependent on the presence of reducing conditions (Hem, 1972). This is reflected in the marked increase in both elements from the oxic low endmember water to the high-SiO_2 water with little to no oxygen. Iron and manganese do not have any known major surface sources and thus are likely geogenic. The metals are virtually absent from meteoric water and seawater, and the concentrations in typical septic effluent are too low to explain the concentrations found in the high-SiO_2 wells. The models suggest that dissolution of mafic minerals such as ilmenite and hornblende, along with pyrite, is a major source of iron in the groundwater. Hornblendes and other amphiboles have been identified in local Vashon and pre-Vashon deposits, while ilmenite is present known to be present in the Northcraft formation, which is the source of some Vashon deposits (Gault, 2015; Troost, 2016; Mullineaux, 1967; Easterbrook et al., 1981). Pyrite can commonly be found throughout the state (Shedd, 1924). Iron may also be released via cation exchange from clays such as smectites, which have been documented as significant in other Washington aquifers (Appelo and Postma, 2005; Hearn et al., 1985; Steinkampf et al., 1985). Precipitation of amorphous iron oxyhydroxides appears to be a major control on iron concentrations (Hearn et al., 1985; Steinkampf et al., 1985; Sharif et

al., 2008; Zhu, 2013). Manganese has also been demonstrated to be present at low levels in several local minerals, including ilmenite and hornblende, which may provide the required concentrations with their dissolution (Easterbrook et al., 1981). Models suggest additional manganese being released by cation exchange, though dissolution of manganese oxides is a better documented source (Z. Zhang et al., 2020; Kedziorek et al., 2008).

The magnitudes of phase mole transfers in the inverse models are similar to those reported in other mass balance or inverse modeling studies of basalt and siliciclastic aquifers (Locsey et al., 2012; Mahlknecht et al., 2004). Whether the magnitudes reflect a reasonable rate of reaction depends on the age of the water. Studies of other aquifers suggest that a weathering flux of approximately 10^{-8} to 10^{-5} mol/L/year for plagioclase feldspars, 10^{-8} mol/L/year of K-micas, or 10^{-6} to 10^{-7} for hornblende could be considered typical, though, obviously, this would vary depending on the composition of the aquifer matrix and the existing water chemistry (Kenoyer and Bowser, 1992; G. Zhang et al., 2016; Rademacher et al., 2001). Assuming a groundwater age of 40 years, based on Vaccaro et al.'s (1998) tritium dating, puts most of the modeled weathering fluxes for plagioclase and hornblende in these ranges, though the K-mica flux is significantly higher.

Potential influence of MAR

Given the high treatment level of the class A reclaimed water used for MAR at the Hawk's Prairie site, the main concern is with particularly recalcitrant residual chemicals (HDR Engineering, Inc., 2021, 2019). In terms of major ions, there may be benefits and drawbacks. The addition of reclaimed water to the aquifer can be expected to locally raise chloride levels; indeed, chloride was a significant factor in differentiating between the low- and high-recharge wells. However, the chloride levels in the reclaimed water are not high

enough to impair the aquifer (State of Washington, 2019, 1990), and raising the water table may help prevent future seawater intrusion. Nitrate levels associated with MAR at the LOTT site are not significantly different than the background, so there should be little immediate effect. In the long run, if recharging reclaimed water enables the expansion of wastewater services, the number of active septic systems could decrease, resulting in eventual improvements to nitrate levels. The recharge water contains enough oxygen to prevent iron and manganese mobilization. While raising oxygen levels can mobilize arsenic (Fakhreddine et al., 2020), elevated iron and manganese cause significantly more water quality violations in the area (Turney, 1986; Drost et al., 1998; HDR Engineering, Inc., 2017). Also, since the water is infiltrated, not injected, it is unlikely to encounter any particularly substantial deposits of reduced metals before its oxygen is depleted.

Conclusions

Changes to land use and wastewater treatment have resulted in shifts in the quality of recharge water in Thurston County; however, background groundwater compositions have remained fairly consistent for the past few decades. Nitrate in the study area is largely due to pollution, most likely from septic effluents. Oxidation of organic matter or metals results in diminished oxygen in more evolved water and may facilitate denitrification. Septic effluents can also be source of chloride, but in most of the shallow and sea level aquifer, chloride is primarily derived from sea salt aerosols which are concentrated by evapotranspiration of rainwater or accumulation in soils. Other solutes are primarily derived from the dissolution of minerals such as aluminosilicates and mafic minerals. Reclaimed water MAR is likely to be a net benefit to the aquifer system.

Chapter 5 Conclusions

This dissertation has explored many aspects of reclaimed water MAR projects and the aquifers that they recharge to demonstrate their viability in the western United States. Chapter 2, began with motivation and site selection. In this chapter, I employed GIS-based suitability mapping and backwards particle tracking to identify suitable locations for recycled water MAR in the Central Valley of California. Based on proximity to potential recycled water supplies, soil suitability, land cover, and exclusion zones for potable well protection, seven to fourteen out of 29 Groundwater Sustainability Plans include enough potentially suitable land within their boundaries to meet their recharge goals using recycled water, though only three have enough recycled water to do it. This study was conducted at a regional level, and may be followed by more localized aquifer characterization, tracer studies, and ongoing monitoring once prospective MAR sites are located.

Chapter 3 was an example of one such tracer study. While chapters 3 and 4 are set in a different aquifer system than chapter 2, both locations have water management needs that can be addressed by reclaimed water MAR. Chapter 3 showed that the use of sulfur hexafluoride and bromide as paired tracers can be used to estimate the amount of air encountered along groundwater flow paths based on the retardation of the sulfur hexafluoride. Using these, it was demonstrated that the shallow and sea level aquifers at the Hawks Prairie recharge site in Thurston County, Washington have localized connectivity and water travels along several, nonlinear preferential pathways.

Chapter 4 put this study in the broader hydrogeologic context of Thurston County. An understanding of the background geochemistry is necessary for reclaimed water MAR projects in order to ensure that MAR provides a net benefit to the ecosystem. Chapter 4

showed that elevated nitrate is generally attributable to septic contamination, while elevated chloride is often due to seawater intrusion. Uncontaminated groundwater receives its character from sea salt aerosols and mineral weathering. The aquifer system appears to be reasonably suited to recycled water MAR, which can help with maintaining good quality groundwater into the future.

Together, these three studies demonstrate how the development of recycled water MAR projects can progress and provide water management benefits. Many factors must be considered to make such projects successful. These studies show the importance of groundwater transport, geochemical character, and the joint consideration of environmental and logistical factors in planning and developing reclaimed water MAR projects. Careful attention to these factors can make reclaimed water MAR a valuable strategy for maintaining a high quality water supply in the present and the future.

References

Addy, K., A. J. Gold, L. E. Christianson, M. B. David, L. A. Schipper, and N. A. Ratigan. 2016. Denitrifying Bioreactors for Nitrate Removal: A Meta-Analysis. *Journal of Environmental Quality* 45, no. 3: 873–81, https://doi.org/10.2134/jeq2015.07.0399.

Ahmadi, M. M., H. Mahdavirad, and B. Bakhtiari. 2017. Multi-criteria analysis of site selection for groundwater recharge with treated municipal wastewater. *Water Science and Technology* 76, no. 4, https://doi.org/10.2166/wst.2017.273.

Alam, S., M. Gebremichael, R. Li, J. Dozier, and D. P. Lettenmaier. 2020. Can Managed Aquifer Recharge Mitigate the Groundwater Overdraft in California's Central Valley? *Water Resources Research* 56, no. 8: e2020WR027244, https://doi.org/10.1029/2020WR027244.

Aliso Water District GSA. 2020. Aliso Water District Groundwater Sustainability Agency Groundwater Sustainability Plan.

Al-Otaibi, M., and M. Al-Senafy. 2004. Recharging Aquifers Through Surface Ponds: Hydraulic Behaviour. *Emirates Journal for Engineering Research* 9, no. 1: 21–27.

Appelo, C. A. J., and D. Postma. 2005. *Geochemistry, groundwater and pollution*. 2nd edition. Boca Raton London New York: CRC Press, Taylor & Francis Group.

Badiuzzaman, P., E. McLaughlin, and D. McCauley. 2017. Substituting freshwater: Can ocean desalination and water recycling capacities substitute for groundwater depletion in California? *Journal of Environmental Management* 203, December: 123–35, https://doi.org/10.1016/j.jenvman.2017.06.051.

Balcke, G.U., S. Meenken, C. Hoefer, and S.E. Oswald. 2007. "Kinetic Gas-Water Transfer and Gas Accumulation in Porous Media during Pulsed Oxygen Sparging." *Environmental Science and Technology* 41 (12): 4428–34.

Bekele, E., S. Toze, B. Patterson, and S. Higginson. 2011. Managed aquifer recharge of treated wastewater: Water quality changes resulting from infiltration through the vadose zone. *Water Research* 45, no. 17: 5764–72, https://doi.org/10.1016/j.watres.2011.08.058.

Belkhiri, L., A. Boudoukha, L. Mouni, and T. Baouz. 2010. Application of multivariate statistical methods and inverse geochemical modeling for characterization of groundwater — A case study: Ain Azel plain (Algeria). *Geoderma* 159, nos. 3–4: 390–98, https://doi.org/10.1016/j.geoderma.2010.08.016.

Bennani, A. C., J. Lary, A. Nrhira, L. Razouki, J. Bize, and N. Nivault. 1992. Wastewater Treatment of Greater Agadir (Morocco): An Original Solution for Protecting the Bay of Agadir by Using the Dune Sands. *Water Science and Technology* 25, no. 12: 239–45, https://doi.org/10.2166/wst.1992.0355.

Berris, S. N. 1995. Conceptualization and simulation of runoff generation from rainfall for three basins in Thurston County, Washington. Water-Resources Investigations Report 94–4038, https://doi.org/10.3133/wri944038.

Bertoldi, G., R. Johnston, and K. D. Evenson. 1991. Ground water in the Central Valley, California - a summary report. Professional Paper 1401-A. Professional Paper.

Blinn, R. 2012. Grand Mound water system plan Grand Mound service area. 07158–0, https://www.co.thurston.wa.us/publicworks/Library/PDF/GrandMoundWaterSystemPlan2012.pdf.

Borchers, J., M. Carpenter, V. K. Grabert, B. Dalgish, and D. Cannon. 2014. Land subsidence from groundwater use in California, https://cawaterlibrary.net/wp-content/uploads/2017/04/1397858208-SUBSIDENCEFULLREPORT_FINAL.pdf.

Bos, J. 2015. Long-term marine water column monitoring 1999-present. Location BUD002. Ecy Environmental Assessment Program, https://apps.ecology.wa.gov/eim/search/Eim/EIMSearchResults.aspx?ResultType=WaterColumnProfileList&EIMSearchResultsFirstPageVisit=false&StudySystemIds=99970619&StudySystemIds=99970618&StudyUserIds=MarineWater-P&StudyUserIds=MarineWater&StudyUserIdSearchType=Equals&LocationUserIds=BUD002&LocationUserIdSearchType=Equals&LocationUserIDAliasSearchFlag=True&ResultParameterName=Salinity&ResultParameterNameSearchType=Equals&ResultParameterNameAliasSearchFlag=True.

Bostic, D. 2021. At Risk: Public Supply Well Vulnerability Under California's Sustainable Groundwater Management Act, https://pacinst.org/publication/at_risk_wells_SGMA.

Bourque, K., A. Schiller, C. Loyola Angosto, L. McPhail, W. Bagnasco, A. Ayres, and A. Larsen. 2019. Balancing agricultural production, groundwater management, and biodiversity goals: A multi-benefit optimization model of agriculture in Kern County, California. *Science of The Total Environment* 670, June: 865–75, https://doi.org/10.1016/j.scitotenv.2019.03.197.

Bouwer, H. 2002. "Artificial Recharge of Groundwater: Hydrogeology and Engineering." *Hydrogeology Journal* 10 (1): 121–42.

Bouwer, H., R. D. G. Pyne, and J. Brown. 2008. Design, Operation, and Maintenance for Sustainable Underground Storage Facilities.

Bowman, J. D., J. L. Czajkowski, S. P. Reidel, D. E. Boschmann, and L. A. Fusso. 2015. Geochemistry. Geodatabase. Washington State Rock Geochemistry Database--GIS Data: Washington Geological Survey Digital Data Series 5, http://www.dnr.wa.gov/publications/ger_portal_geochemistry.zip.

Bradshaw, J. L., and R. G. Luthy. 2017. Modeling and optimization of recycled water systems to augment urban groundwater recharge through underutilized stormwater spreading basins. *Environmental Science & Technology* 51, no. 20: 11809–19, https://doi.org/10.1021/acs.est.7b02671.

Bullister, J.L., D.P. Wisegarver, and F.A. Menzia. 2002. "The Solubility of Sulfur Hexafluoride in Water and Seawater." *Deep-Sea Research Part I: Oceanographic Research Papers* 49 (1): 175–87.

Campbell, A., and B. Fan. 2021. Chino Basin Recycled Water Groundwater Recharge Program 2020 Annual Report, https://18x37n2ovtbb3434n48jhbs1-wpengine.netdna-ssl.com/wp-content/uploads/2021/05/CBRW-GRP-2020-Annual-Report-Final.pdf.

[CDFA] California Department of Food and Agriculture. 2021. County agricultural commissioners' reports crop year 2018-2019, https://www.nass.usda.gov/Statistics_by_State/California/Publications/AgComm/2019/CAC_2019_actual_final.pdf.

Christiansen, J.E. (USDA). 1944. "Effect of Entrapped Air upon the Permeability of Soils." *Soil Science* 58 (5): 355–65.

City of Tenino. 2016. Tenino comprehensive plan 2016-2036 - Joint comprehensive plan with Thurston County, https://www.ezview.wa.gov/Portals/_1976/Documents/ElementExamples/Tenino%20Comprehensive%20Plan.pdf.

Clark, J.F., G.B. Hudson, and D. Avisar. 2005. "Gas Transport below Artificial Recharge Ponds: Insights from Dissolved Noble Gases and a Dual Gas (SF6 and 3He) Tracer Experiment." *Environmental Science and Technology* 39 (11): 3939–45.

Clark, J.F., G.B. Hudson, M.L. Davisson, G. Woodside, and R. Herndon. 2004. "Geochemical Imaging of Flow Near an Artificial Recharge Facility, Orange County, California." *Ground Water* 42 (2): 167–74.

[CNRA] California Natural Resources Agency. 2021. Well Completion Reports.

[CNRA, CDFA, Cal EPA] California Natural Resources Agency, California Department of Food and Agriculture, and California Environmental Protection Agency. 2014. California Water Action Plan, https://resources.ca.gov/CNRALegacyFiles/docs/california_water_action_plan/2014_California_Water_Action_Plan.pdf.

Cogger, C. G., L. M. Hajjar, C. L. Moe, and M. D. Sobsey. 1988. Septic System Performance on a Coastal Barrier Island. *Journal of Environmental Quality* 17, no. 3: 401–8, https://doi.org/10.2134/jeq1988.00472425001700030009x.

Collias, E. E., and J. H. Lincoln. 1977. A study of the nutrients in the main basin of Puget Sound. Puget Sound Interim Studies.

Costa, J. E., G. Heufelder, S. Foss, N. P. Milham, and B. Howes. 2002. Nitrogen Removal Efficiencies of Three Alternative Septic System Technologies and a Conventional Septic Systema. *Environment Cape Cod* 5, no. 1: 15–24.

Crook, J. 2004. Innovative Applications in Water Reuse: Ten Case Studies.

Cupps, K., and E. Morris. 2005. Case Studies in Reclaimed Water Use. 05-10–013.

Dahlke, H., and T. Kocis. 2018. Streamflow availability ratings identify surface water sources for groundwater recharge in the Central Valley. *California Agriculture* 72, no. 3: 162–69, http://calag.ucanr.edu/Archive/?article=ca.2018a0032.

Dieter, C., M. Maupin, R. Caldwell, M. Harris, T. Ivahnenko, J. Lovelace, N. Barber, and K. Linsey. 2018. Estimated use of water in the United States in 2015. Circular 1441. Circular, https://doi.org/10.3133/cir1441.

Dillon, K.S., D.R. Corbett, J.P. Chanton, W.C. Burnett, and D.J. Furbish. 1999. "The Use of Sulfur Hexafluoride (SF_6) as a Tracer of Septic Tank Effluent in the Florida Keys." *Journal of Hydrology* 220 (3-4): 129–40.

Dillon, P. 2005. "Future Management of Aquifer Recharge." *Hydrogeology Journal* 13 (1): 313–16.

Dillon, P., P. Pavelic, D. Page, H. Beringen, and J. Ward. 2009. Managed aquifer recharge: an introduction. 13. Waterlines.

Dion, N. P., and S. S. Sumioka. 1984. Seawater intrusion into coastal aquifers in Washington, 1978. Water Supply Bulletin 56, https://apps.ecology.wa.gov/publications/SummaryPages/WSB56.html.

Drever, J. I. 1982. *The geochemistry of natural waters Surface and groundwater environments*. 3rd ed. Upper Saddle River, NJ: Prentice-Hall.

Drewes, J. E. 2009. Ground Water Replenishment with Recycled Water-Water Quality Improvements during Managed Aquifer Recharge. *Ground Water* 47, no. 4: 502–5, https://doi.org/10.1111/j.1745-6584.2009.00587_5.x.

Drost, B. W., D. M. Ely, and W. E. Lum. 1999. Conceptual Model and Numerical Simulation of the Ground-Water-Flow System in the Unconsolidated Sediments of Thurston County, Washington. 99–4165. Water-Resources Investigations, https://doi.org/10.3133/wri994165.

Drost, B. W., G. L. Turney, N. P. Dion, and M. A. Jones. 1998. Hydrology and Quality of Ground Water in Northern Thurston County, Washington (Revised). Water Resources Investigation 92–4109, https://doi.org/10.3133/wri924109.

[DWR] California Department of Water Resources. 2020a. Adjudicated area map viewer. Web map, https://sgma.water.ca.gov/webgis/index.jsp?appid=adjbasin.

[DWR] California Department of Water Resources. 2020b. B118 SGMA 2019 Basin Prioritization. Shapefile.

[DWR] California Department of Water Resources. 2020c. C2VSimFG boundary. C2VSimFG GIS Files. California Natural Resources Agency.

[DWR] California Department of Water Resources. 2022. California Groundwater Projects Tool. ESRI mapping tool, 2022, https://experience.arcgis.com/experience/00197adac22f4b06a3f410068d43a641/page/Page/.

[DWR] California Department of Water Resources. n.d., a. GSA notice submitted. Shapefile. SGMA Data Viewer, https://sgma.water.ca.gov/webgis/?appid=SGMADataViewer#boundaries.

[DWR] California Department of Water Resources. n.d., b. Sustainable Groundwater Management (SGMA) Portal, https://sgma.water.ca.gov/portal/gsp/status, retrieved 3/5/2022.

Easterbrook, D. J., N. D. Briggs, J. A. Westgate, and M. P. Gorton. 1981. Age of the Salmon Springs Glaciation in Washington. *Geology* 9, no. 2: 87, https://doi.org/10.1130/0091-7613(1981)9<87:AOTSSG>2.0.CO;2.

Edmonds, R. L., T. B. Thomas, and J. J. Rhodes. 1991. Canopy and Soil Modification of Precipitation Chemistry in a Temperate Rain Forest. *Soil Science Society of America Journal* 55, no. 6: 1685–93, https://doi.org/10.2136/sssaj1991.03615995005500060031x.

Elliott, E. M., C. Kendall, S. D. Wankel, D. A. Burns, E. W. Boyer, K. Harlin, D. J. Bain, and T. J. Butler. 2007. Nitrogen Isotopes as Indicators of NOx Source Contributions to Atmospheric Nitrate Deposition Across the Midwestern and Northeastern United States. *Environmental Science & Technology* 41, no. 22: 7661–67, https://doi.org/10.1021/es070898t.

Fakhreddine, S., H. Prommer, S. M. Gorelick, J. Dadakis, and S. Fendorf. 2020. Controlling Arsenic Mobilization during Managed Aquifer Recharge: The Role of Sediment Heterogeneity. *Environmental Science & Technology* 54, no. 14: 8728–38, https://doi.org/10.1021/acs.est.0c00794.

Fakhreddine, S., J. Dittmar, D. Phipps, J. Dadakis, and S. Fendorf. 2015. Geochemical Triggers of Arsenic Mobilization during Managed Aquifer Recharge. *Environmental Science & Technology* 49, no. 13: 7802–9, https://doi.org/10.1021/acs.est.5b01140.

Fenn, M. E., C. S. Ross, S. L. Schilling, W. D. Baccus, M. A. Larrabee, and R. A. Lofgren. 2013. Atmospheric deposition of nitrogen and sulfur and preferential canopy consumption of nitrate in forests of the Pacific Northwest, USA. *Forest Ecology and Management* 302, August: 240–53, https://doi.org/10.1016/j.foreco.2013.03.042.

Flury, M. and N. N. Wai. 2003. "Dyes as tracers for vadose zone Hydrology" *Reviews in Geophysics* 41(1): 1002.

Fox, P., K. Narayanaswamy, A. Genz, and J. E. Drewes. 2001. Water quality transformations during soil aquifer treatment at the Mesa Northwest Water Reclamation Plant, USA. *Water Science and Technology* 43, no. 10: 343–50, https://doi.org/10.2166/wst.2001.0658.

Fry, V.A., J.D. Istok, L. Semprini, K.T. O'Reilly, and T.E. Buscheck. 1995. "Retardation of Dissolved Oxygen Due to a Trapped Gas Phase in Porous Media." *Groundwater* 33 (3): 391–98.

Gaillardet, J., B. Dupré, P. Louvat, and C. J. Allègre. 1999. Global silicate weathering and CO2 consumption rates deduced from the chemistry of large rivers. *Chemical Geology* 159, nos. 1–4: 3–30, https://doi.org/10.1016/S0009-2541(99)00031-5.

Ganot, Y., and H. E. Dahlke. 2021. A model for estimating Ag-MAR flooding duration based on crop tolerance, root depth, and soil texture data. *Agricultural Water Management* 255, September: 107031, https://doi.org/10.1016/j.agwat.2021.107031.

Gault, A. 2015. The Mineralogy and Strength Characteristics of Selected Glaciolacustrine Clays in the Puget Sound Region. Master of Science, University of Washington, https://digital.lib.washington.edu/researchworks/bitstream/handle/1773/36251/Gault_MESSAGeReport019.pdf?sequence=1&isAllowed=y.

Grinshpan, M., A. Furman, H. E. Dahlke, E. Raveh, and N. Weisbrod. 2021. From managed aquifer recharge to soil aquifer treatment on agricultural soils: Concepts and challenges. *Agricultural Water Management* 255, September: 106991, https://doi.org/10.1016/j.agwat.2021.106991.

Groundwater Monitoring Program. 2015. *California Water Code*. Vol. WAT section 10933(b), https://leginfo.legislature.ca.gov/faces/codes_displayText.xhtml?lawCode=WAT&division=6.&title=&part=2.11.&chapter=3.&article=.

Güler, C., and G. D. Thyne. 2004. Hydrologic and geologic factors controlling surface and groundwater chemistry in Indian Wells-Owens Valley area, southeastern California, USA. *Journal of Hydrology* 285, nos. 1–4: 177–98, https://doi.org/10.1016/j.jhydrol.2003.08.019.

Hatch, T. 2020. DWR Report: California Central Valley Groundwater-Surface Water Simulation Model - Fine Grid (C2VSimFG) Development and Calibration Version 1.0.

Hatch, T., H. Guobiao, A. Guillien, and E. Behrooz. 2020. C2VSimFG. California Department of Water Resources.

HDR Engineering, Inc. 2017. Groundwater quality characterization. 1.1. Reclaimed Water Infiltration Study.

HDR Engineering, Inc. 2018a. Work plan: Tracer testing and water quality monitoring of treatment effectiveness (task 2.1.3) Hawks Prairie area. Work plan. Reclaimed Water Infiltration Study.

HDR Engineering, Inc. 2018b. Hydrogeologic characterization report: On-site wells and lysimeter installation, Off-site monitoring wells, Hawks Prairie area. 2.1.1A, 2.1.2.C. Reclaimed Water Infiltration Study.
HDR Engineering, Inc. 2019. Tracer Test and Water Quality Monitoring Report. 2.1.3. Reclaimed Water Infiltration Study.
HDR Engineering, Inc. 2021. Residual chemical fate and transport analysis. Task 2.1.5. Reclaimed Water Infiltration Study.
Hearn, P. P., W. C. Steinkampf, G. C. Bortleson, and B. W. Drost. 1985. Geochemical controls on dissolved sodium in basalt aquifers of the Columbia Plateau, Washington. Water-Resources Investigations Report 84–4304, https://doi.org/10.3133/wri844304.
Heilweil, V.M., D.K. Solomon, K.S. Perkins, and K.M. Ellett. 2004. "Gas-Partitioning Tracer Test to Quantify Trapped Gas during Recharge." *Groundwater* 42 (4): 589–600.
Hem, J. 1972. Chemical factors that influence the availability of iron and manganese in aqueous systems. *Geological Society of America Bulletin* 83, February: 443–50, https://doi.org/10.1130/0016-7606(1972)83[443:CFTITA]2.0.CO;2.
Hiscock, K. M., J. W. Llyod, and D. N. Lerner. 1991. Review of natural and artificial denitrification of groundwater. *Water Research* 25, no. 9: 1099–1111, https://doi.org/10.1016/0043-1354(91)90203-3.
Holch, J. 2008. Thermodynamic and kinetic degradation reactions of organic substances in groundwater modelled with phreeqc. Master, Institut für Hydrologie Albert-Ludwigs Universität Freiburg i. Br.
Hoover, N. L., A. Bhandari, M. L. Soupir, and T. B. Moorman. 2016. Woodchip Denitrification Bioreactors: Impact of Temperature and Hydraulic Retention Time on Nitrate Removal. *Journal of Environmental Quality* 45, no. 3: 803–12, https://doi.org/10.2134/jeq2015.03.0161.
Humphrey, C. P., M. A. O'Driscoll, N. E. Deal, D. L. Lindbo, S. C. Thieme, and M. A. Zarate-Bermudez. 2013. Onsite Wastewater System Nitrogen Contributions to Groundwater in Coastal North Carolina. *Journal of environmental health* 76, no. 5: 16–22, https://www.ncbi.nlm.nih.gov/pmc/articles/PMC4849129/.
Hutchinson, A. S. 2013. 2011-12 Report on Groundwater Recharge in the Orange County Groundwater Basin, https://www.ocwd.com/media/2414/11-12-annual-recharge-report-final.pdf.
Jasechko, S., and D. Perrone. 2017. Hydraulic fracturing near domestic groundwater wells. *Proceedings of the National Academy of Sciences* 114, no. 50: 13138–43, https://doi.org/10.1073/pnas.1701682114.
Jiménez, R. A. 2011. A Geochemical Model of Redox Reactions in a Tropical Rain Forest Stream Riparian Zone:
Jin, Z., A. J. West, F. Zhang, Z. An, R. G. Hilton, J. Yu, J. Wang, G. Li, L. Deng, and X. Wang. 2016. Seismically enhanced solute fluxes in the Yangtze River headwaters following the A.D. 2008 Wenchuan earthquake. *Geology* 44, no. 1: 47–50, https://doi.org/10.1130/G37246.1.
Johansen, A. M., C. Duncan, A. Reddy, N. Swain, M. Sorey, A. Nieber, J. Agren, et al. 2019. Precipitation chemistry and deposition at a high-elevation site in the Pacific Northwest United States (1989–2015). *Atmospheric Environment* 212, September: 221–30, https://doi.org/10.1016/j.atmosenv.2019.05.021.

Johnson, T. A. 2009. Ground Water Recharge Using Recycled Municipal Waste Water in Los Angeles County and the California Department of Public Health's Draft Regulations on Aquifer Retention Time. *Ground Water* 47, no. 4: 496–99, https://doi.org/10.1111/j.1745-6584.2009.00587_3.x.

Kanarek, A., and M. Michail. 1996. Groundwater recharge with municipal effluent: Dan region reclamation project, Israel. *Water Science and Technology* 34, no. 11: 227–33.

Kedziorek, M. A. M., S. Geoffriau, and A. C. M. Bourg. 2008. Organic Matter and Modeling Redox Reactions during River Bank Filtration in an Alluvial Aquifer of the Lot River, France. *Environmental Science & Technology* 42, no. 8: 2793–98, https://doi.org/10.1021/es702411t.

Kenoyer, G. J., and C. J. Bowser. 1992. Groundwater chemical evolution in a sandy silicate aquifer in northern Wisconsin: 2. Reaction modeling. *Water Resources Research* 28, no. 2: 591–600, https://doi.org/10.1029/91WR02303.

Knowles, R. 1982. Denitrification. Microbiol Rev. 46, no. 1: 43–70, https://doi.org/10.1128/mr.46.1.43-70.1982.

Korom, S. 1992. Natural denitrification in the saturated zone: a review. *Water Resources Research* 28, no. 6: 1657–68.

Kourakos, George. (2020) 2021. Ichnos. C++, https://github.com/giorgk/ichnos.

Kourakos, George, H. E. Dahlke, and T. Harter. 2019. Increasing groundwater availability and seasonal base flow through agricultural managed aquifer recharge in an irrigated basin. *Water Resources Research* 55, no. 9: 7464–92, https://doi.org/10.1029/2018WR024019.

Land IQ and California Department of Water Resources. 2021. i15 Crop Mapping 2018. File geodatabase feature class.

Lehmann, C. M. B., V. C. Bowersox, and S. M. Larson. 2005. Spatial and temporal trends of precipitation chemistry in the United States, 1985–2002. *Environmental Pollution* 135, no. 3: 347–61, https://doi.org/10.1016/j.envpol.2004.11.016.

Lenntech. n.d. Major ion composition of seawater, https://www.lenntech.com/composition-seawater.htm, retrieved 28/2/2022.

Locsey, K. L., M. Grigorescu, and M. E. Cox. 2012. Water–Rock Interactions: An Investigation of the Relationships Between Mineralogy and Groundwater Composition and Flow in a Subtropical Basalt Aquifer. *Aquatic Geochemistry* 18, no. 1: 45–75, https://doi.org/10.1007/s10498-011-9148-x.

Loewald, A., P. Ryan, and J. Kim. n.d. A Review of Phosphorous and Nitrogen in Groundwater and Lakes, 36.

Logan, R. L., T. J. Walsh, H. W. Schasse, and M. Polenz. 2003. Geologic Map of the Lacey 7.5-minute Quadrangle, Thurston County, Washington. Washington Division of Geology and Earth Resources.

Lopes, R. L., and A. S. dos Santos. 2012. Característica do Solo da Área de Infiltração de Efluentes Domésticos de uma ETE. In , 6.

LOTT Clean Water Alliance. 2022. Reclaimed water infiltration study overview fact sheet.

Mahlknecht, J., B. Steinich, and I. Navarro de León. 2004. Groundwater chemistry and mass transfers in the Independence aquifer, central Mexico, by using multivariate statistics and mass-balance models. *Environmental Geology* 45, no. 6: 781–95, https://doi.org/10.1007/s00254-003-0938-3.

[MBARI] Monterey Bay Aquarium Research Institute. 2015. Periodic Table of Elements in the Ocean, November 19, 2015, https://www.mbari.org/science/upper-ocean-systems/chemical-sensor-group/periodic-table-of-elements-in-the-ocean/.
McClain, M. E., E. W. Boyer, C. L. Dent, S. E. Gergel, N. B. Grimm, P. M. Groffman, S. C. Hart, et al. 2003. Biogeochemical Hot Spots and Hot Moments at the Interface of Terrestrial and Aquatic Ecosystems. *Ecosystems* 6, no. 4: 301–12, https://doi.org/10.1007/s10021-003-0161-9.
McDermott, J. A., D. Avisar, T. A. Johnson, and J. F. Clark. 2008. Groundwater Travel Times near Spreading Ponds: Inferences from Geochemical and Physical Approaches. *Journal of Hydrologic Engineering* 13, no. 11: 1021–28, https://doi.org/10.1061/(ASCE)1084-0699(2008)13:11(1021).
McMullin Area GSA. 2019. McMullin Area Groundwater Sustainability Agency Groundwater Sustainability Plan.
McQuillan, D. 2004. Ground-water quality impacts from on-site septic systems. In *National Onsite Wastewater Recycling Association*, 13. Albuquerque, NM.
Merayyan, S., and S. Safi. 2014. Feasibility of Groundwater Banking under Various Hydrologic Conditions in California, USA. *Computational Water, Energy, and Environmental Engineering* 03, no. 03: 79–92, https://doi.org/10.4236/cweee.2014.33009.
Mid Kaweah GSA. 2019. Groundwater Sustainability Plan Mid-Kaweah Groundwater Sustainability Agency.
Miller, J. H., W. P. Ela, K. E. Lansey, P. L. Chipello, and R. G. Arnold. 2006. Nitrogen Transformations during Soil–Aquifer Treatment of Wastewater Effluent—Oxygen Effects in Field Studies. *Journal of Environmental Engineering* 132, no. 10: 1298–1306, https://doi.org/10.1061/(ASCE)0733-9372(2006)132:10(1298).
Moulton, K. 2000. Solute flux and mineral mass balance approaches to the quantification of plant effects on silicate weathering. *American Journal of Science* 300, September: 539–70, https://doi.org/10.2475/ajs.300.7.539.
Mukherjee, M., and O. Jensen. 2020. Making water reuse safe: A comparative analysis of the development of regulation and technology uptake in the US and Australia. *Safety Science* 121, January: 5–14, https://doi.org/10.1016/j.ssci.2019.08.039.
Mullineaux, D. 1967. Gross composition of Pleistocene clays in Seattle, Wash. Professional Paper 575-B.
Mullineaux, D., T. Nichols, and R. Speirer. 1964. A zone of montmorillonitic weathered clay in Pleistocene deposits at Seattle, Washington. Professional Paper 501-D, https://pubs.usgs.gov/pp/0501d/report.pdf.
Mundorff, M. J., J. M. Weigle, and G. D. Holmberg. 1955. Ground water in the Yelm area, Thurston and Pierce Counties, Washington. Geological Survey Circular 356, https://doi.org/10.3133/cir356.
[MWD] The Metropolitan Water District of Southern California. 2016. Potential Regional Recycled Water Program Feasibility Study. 1530, https://www.ocwd.com/media/4888/wic05xcarson-rrwp-feasibility-main-report.pdf.
Myhre, G., D. Shindell, F.-M. Breon, W. Collins, J. Fuglestvedt, J. Huang, D. Koch, et al. 2013. “Anthropogenic and Natural Radiative Forcing.” In *Climate Change 2013 the Physical Science Basis: Working Group I Contribution to the Fifth Assessment Report of the Intergovernmental Panel on Climate Change*, edited by T. F. Stocker,

D. Qin, G.-K. Plattner, M. Tignor, S. K. Allen, J. Boschung, A. Nauels, Y. Xia, V. Bex, and P. M. Midgley, 659–740. Cambridge, United Kingdom and New York, NY, USA: Cambridge University Press.

O'Geen, A. T., M. Saal, H. Dahlke, D. Doll, R. Elkins, A. Fulton, G. Fogg, et al. 2015. Soil suitability index identifies potential areas for groundwater banking on agricultural lands. *California Agriculture* 69, no. 2: 75–84, https://doi.org/10.3733/ca.v069n02p75.

Page, R. W. 1986. Geology of the fresh ground-water basin of the Central Valley, California, with texture maps and sections. Professional Paper 1401–C. Regional Aquifer-System Analysis.

Parametrix and FCS Group. 2016. Sewer facilities plan, https://files4.revize.com/yelmwa/document_center/Reports%20and%20plans/Infrastructure/FacilityPlanExecSummary.pdf.

Parkhurst, D. L., and C. A. J. Appelo. 2021. PHREEQC. C++. U.S. Geological Survey.

Pedrero, F., A. Albuquerque, H. Marecos do Monte, V. Cavaleiro, and J. J. Alarcón. 2011. Application of GIS-based multi-criteria analysis for site selection of aquifer recharge with reclaimed water. *Resources, Conservation and Recycling* 56, no. 1: 105–16, https://doi.org/10.1016/j.resconrec.2011.08.003.

Perrone, D., and M. Rohde. 2016. Benefits and Economic Costs of Managed Aquifer Recharge in California. *San Francisco Estuary and Watershed Science* 14, no. 2, https://doi.org/10.15447/sfews.2016v14iss2art4.

Pi, Y., and J. Wang. 2006. A field study of advanced municipal wastewater treatment technology for artificial groundwater recharge. *Journal of Environmental Sciences* 18, no. 6: 1056–60, https://doi.org/10.1016/S1001-0742(06)60038-7.

PPC Land Consultants, Inc. 2017. An overview of laws and regulations governing water reuse in California, Arizona, Nevada, and Texas, https://foundation.caionline.org/wp-content/uploads/2018/07/smart_water_project_ppc_laws.pdf.

Rademacher, L. K., J. F. Clark, G. B. Hudson, D. C. Erman, and N. A. Erman. 2001. Chemical evolution of shallow groundwater as recorded by springs, Sagehen basin; Nevada County, California. *Chemical Geology* 179, nos. 1–4: 37–51, https://doi.org/10.1016/S0009-2541(01)00314-X.

Richards, S., E. Paterson, P. J. A. Withers, and M. Stutter. 2016. Septic tank discharges as multi-pollutant hotspots in catchments. *Science of The Total Environment* 542, January: 854–63, https://doi.org/10.1016/j.scitotenv.2015.10.160.

Robertson, A., J. Cordova, A. Teeple, J. Payne, and R. Carruth. 2017. Hydrogeologic and geochemical characterization and evaluation of two arroyos for managed aquifer recharge by surface infiltration in the Pojoaque River Basin, Santa Fe County, New Mexico. Scientific Investigations Report 2017–5007. Scientific Investigations Report.

Rohde, M. M., J. C. Stella, D. A. Roberts, and M. B. Singer. 2021. Groundwater dependence of riparian woodlands and the disrupting effect of anthropogenically altered streamflow. *Proceedings of the National Academy of Sciences* 118, no. 25: e2026453118, https://doi.org/10.1073/pnas.2026453118.

Sallwey, J., J. P. B. Valverde, F. V. López, R. Junghanns, and C. Stefan. 2018. Suitability maps for managed aquifer recharge: a review of multi-criteria decision analysis studies. *Environmental Reviews*, October, https://doi.org/10.1139/er-2018-0069.

Sanchez-Flores, R., A. Conner, and R. A. Kaiser. 2016. The regulatory framework of reclaimed wastewater for potable reuse in the United States. *International Journal of Water Resources Development* 32, no. 4: 536–58, https://doi.org/10.1080/07900627.2015.1129318.

Schuyler, A. 2015. Wastewater comprehensive plan update, http://www.ci.lacey.wa.us/Portals/0/docs/Public_Works/Water%20Comp%20Plan/2015/wastewater_comprehensive_plan_update_2015.pdf.

[SGMA] *Sustainable Groundwater Management Act*. 2014. *California*, https://www.counties.org/sites/main/files/file-attachments/2014_sustainable_groundwater_management_act__--_combined_bills_00263584xa1c15.pdf?1412350612.

Shaleen-Hansen, M. n.d. Guidance for Aquifer Storage and Recovery AKART Analysis and Overriding Consideration of Public Interest Demonstration, 71.

Sharif, M. U., R. K. Davis, K. F. Steele, B. Kim, T. M. Kresse, and J. A. Fazio. 2008. Inverse geochemical modeling of groundwater evolution with emphasis on arsenic in the Mississippi River Valley alluvial aquifer, Arkansas (USA). *Journal of Hydrology* 350, nos. 1–2: 41–55, https://doi.org/10.1016/j.jhydrol.2007.11.027.

Sharma, S. K., C. M. Harun, and G. Amy. 2008. Framework for assessment of performance of soil aquifer treatment systems. *Water Science and Technology* 57, no. 6: 941–46, https://doi.org/10.2166/wst.2008.188.

Shedd, S. 1924. The mineral resources of Washington with statistics for 1922. Bulletin no. 30.

Snavely, P. D. 1958. *Geology and Coal Resources of the Centralia-Chehalis District, Washington*. U.S. Government Printing Office.

Sokolow, S., H. Godwin, and B. Cole. 2019. Perspectives on the future of recycled water in California: results from interviews with water management professionals. *Journal of Environmental Planning and Management* 62, no. 11: 1908–28, https://doi.org/10.1080/09640568.2018.1523051.

Springhorn, S., B. Wyckoff, R. Hull, S. Edmunds, S. Najmus, J. Uecker, and F. Qian. 2021. California's Groundwater Update 2020. Bulletin 118.

State of California. 1980. *Treated waste water*. *California Water Code*, https://leginfo.legislature.ca.gov/faces/codes_displayText.xhtml?lawCode=WAT&division=2.&title=&part=2.&chapter=1.&article=1.5.

State of California. 2015a. Groundwater Monitoring Program. California Water Code. Vol. WAT section 10933(b), https://leginfo.legislature.ca.gov/faces/codes_displayText.xhtml?lawCode=WAT&division=6.&title=&part=2.11.&chapter=3.&article=.

State of California. 2015b. Title 17 Code of regulations. California Code of Regulations. Vol. Title 17 Div. 1 Chapt. 5 Subchapter 1 Group 4.

State of California. 2018. *Water Recycling Criteria*. *California Code of Regulations*. Vol. Title 22, Div. 4, Chapt. 3.

State of Washington 1990. *Water quality standards for groundwaters of the State of Washington*. *Washington Administrative Code*. Vol. WAC 173-200.

State of Washington. 2000a. *Reservoir permits—Secondary permits—Expedited processing—Underground artificial storage and recovery project standards and rules—*

Exemptions—Report to the legislature. 2000. *Reformed Code of Washington*. Vol. RCW 90.03.370.
State of Washington. 2000b. *Reservoir permits*. *Reformed Code of Washington*. Vol. RCW 90.44.460.
State of Washington. 2003. *Underground artificial storage and recovery*. *Washington Administrative Code*. Vol. WAC 173-157.
State of Washington. 2008. *Underground injection control program*. 2008 *Washington Administrative Code*. Vol. WAC 173-218.
State of Washington. 2011. *Reclaimed water use*. *Reformed Code of Washington*. Vol. RCW 90.46.
State of Washington. 2018 *Reclaimed water*. *Washington Administrative Code*. Vol. WAC 173-219.
State of Washington. 2019. *Group A public water supplies*. *Washington Administrative Code*. Vol. WAC 246-290, https://apps.leg.wa.gov/wac/default.aspx?cite=246-290.
Steinkampf, W. C., G. C. Bortleson, and F. A. Packard. 1985. Controls on ground-water chemistry in the Horse Heaven Hills, south-central Washington. Water-Resources Investigations Report 85–4048, https://doi.org/10.3133/wri854048.
Sverdrup, H. U., M. W. Johnson, and R. H. Flemming. 1942. Chemistty of Seawater. In *The Oceans, Their Physics, Chemistry, and General Biology*. New York: Prentice-Hall, https://publishing.cdlib.org/ucpressebooks/view?docId=kt167nb66r&chunk.id=ch06&toc.depth=1&toc.id=ch06&brand=eschol.
[SWRCB] California State Water Resources Control Board. 2020. Volumetric annual report data dictionary, https://data.ca.gov/dataset/volumetric-annual-report-of-wastewater-and-recycled-water/resource/5a02e86e-537e-4d93-9523-9b9f51c9f2cb.
[SWRCB] California State Water Resources Control Board. 2021a. 2019 Volumetric annual report of wastewater and recycled water.
[SWRCB] California State Water Resources Control Board. 2021b. Regulated facility report. California Integrated Water Quality System, November 8, 2021, https://ciwqs.waterboards.ca.gov/ciwqs/readOnly/CiwqsReportServlet?inCommand=reset&reportName=RegulatedFacility.
[SWRCB] California State Water Resources Control Board. 2022. Water Conservation and Production Reports. California Water Boards, 2022, https://public.tableau.com/views/CaliforniaUrbanWaterProduction_15785959527960/StatewideUseandProduction?:embed=y&:showVizHome=no&:host_url=https%3A%2F%2Fpublic.tableau.com%2F&:embed_code_version=3&:tabs=yes&:toolbar=no&:animate_transition=yes&:display_static_image=no&:display_spinner=no&:display_overlay=yes&:display_count=yes&:loadOrderID=0.
[SWRCB and Cal EPA] California State Water Resources Control Board and California Environmental Protection Agency. 2018. Water quality control policy for recycled water, https://www.waterboards.ca.gov/board_decisions/adopted_orders/resolutions/2018/121118_7_final_amendment_oal.pdf.
[TCSSWP and TCEHD] Thurston County Storm and Surface Water Program and Thurston County Environmental Health Division. 1999. Groundwater monitoring report 1997-1998 water year. Water resources monitoring report,

https://www.co.thurston.wa.us/health/ehsc/documents/GroundWaterMonitoringReport-97-98.pdf.
[Thurston Sewage Plan] Thurston County sewerage general plan for unincorporated urban growth management area. 1990, https://www.co.thurston.wa.us/health/ehadm/pdf/SewerageGenPlan.pdf.
Toze, S., and E. Bekele. 2009. Determining Requirements for Managed Aquifer Recharge in Western Australia. 022/04G. Water Foundation Project, https://publications.csiro.au/rpr/download?pid=changeme:422&dsid=DS1.
Troost, K. G. 2016. Chronology, Lithology and Paleoenvironmental Interpretations of the Penultimate Ice-Sheet Advance into the Puget Lowland, Washington State. Doctor of Philosophy, University of Washington.
Troost, K. G., and D. B. Booth. 2008. Geology of Seattle and the Seattle area, Washington. In *Landslides and Engineering Geology of the Seattle, Washington, Area*, edited by R. L. Baum, J. W. Godt, and L. M. Highland, 20:1–35. Reviews in Engineering Geology. Geological Society of America, https://doi.org/10.1130/2008.4020(01).
[TRPC] Thurston Regional Planning Council. 2016. Map 17: Septic and Sewer Access. Deschutes watershed: Thurston Regional Planning Council, https://www.thurstoncountywa.gov/planning/planningdocuments/map-17-sewer.pdf.
[TRPC] Thurston Regional Planning Council. n.d. Land Cover and Impervious Surfaces, https://trpc.org/434/Land-Cover-and-Impervious-Surfaces, retrieved 20/5/2022.
Truex, M.J., V.R. Vermeul, D.P. Mendoza, B.G. Fritz, R.D. Mackley, M. Oostrom, T.W. Wietsma, and T.W. Macbeth. 2011. "Water Level Monitoring Pressure Transducers : A Need for Industry-Wide Standards." *Ground Water Monitoring & Remediation* 31 (1): 50–58.
Trussell, R., H. Anderson, E. Archuleta, J. Crook, J. E. Drewes, D. Fort, C. Haas, et al. 2012. *Water Reuse: Potential for Expanding the Nation's Water Supply Through Reuse of Municipal Wastewater*. Washington, D.C.: National Academies Press, https://doi.org/10.17226/13303.
Turney, G. L. 1986. Quality of ground water in the Puget sound region, Washington, 1981. Water-Resources Investigations Report 84–4258, https://doi.org/10.3133/wri844258.
Ulibarri, N., N. E. Garcia, R. L. Nelson, A. E. Cravens, and R. J. McCarty. 2021. Assessing the feasibility of managed aquifer recharge in California. *Water Resources Research* 57, no. 3, https://doi.org/10.1029/2020WR029292.
US Census Bureau. 2011. Census Bureau Releases 2010 Census Demographic Profiles for Alaska, Arizona, California, Connecticut, Georgia, Idaho, Minnesota, Montana, New Hampshire, New York, Ohio, Puerto Rico and Wisconsin, May 12, 2011, https://www.census.gov/newsroom/releases/archives/2010_census/cb11-cn137.html.
[US EPA] U.S. Environmental Protection Agency. 2012. *Guidelines for Water Reuse*. Vol. EPA/600/R-12/618.
[US EPA] U.S. Environmental Protection Agency. 2015. Primary Enforcement Authority for the Underground Injection Control Program, May 22, 2015, https://www.epa.gov/uic/primary-enforcement-authority-underground-injection-control-program.
[US EPA] U.S. Environmental Protection Agency. 2021. Aquifer Recharge and Aquifer Storage and Recovery. Other Policies and Guidance, October 16, 2021, https://www.epa.gov/uic/aquifer-recharge-and-aquifer-storage-and-recovery.

US EPA and University of Washington. 2021a. Site NTN WA21. National Atmospheric Deposition Program - National Trends Network, https://nadp.slh.wisc.edu/sites/ntn-WA21/.
US EPA and University of Washington. 2021b. Site NTN WA99. National Atmospheric Deposition Program - National Trends Network, https://nadp.slh.wisc.edu/sites/ntn-WA99/.
[USGS] United States Geological Survey. 2021. NLCD 2016 Land Cover Conterminous United States. Raster. National Land Cover Database.
Vaccaro, J. J., A. J. Hansen Jr., and M. A. Jones. 1998. Hydrogeologic framework of the Puget Sound Aquifer System, Washington and British Columbia. Professional Paper 1424-D. Regional Aquifer-System Analysis Program, https://doi.org/10.3133/pp1424D.
Van Denburgh, A. S., and J. F. Santos. 1965. Groundwater in Washington Its chemical and physical quality. Water Supply Bulletin 24, https://apps.ecology.wa.gov/publications/documents/wsb24.pdf.
Viraraghavan, T., and R. g. Warnock. 1976. Groundwater Quality Adjacent to a Septic Tank System. *Journal AWWA* 68, no. 11: 611–14, https://doi.org/10.1002/j.1551-8833.1976.tb02505.x.
Vong, R. J., H.-C. Hansson, H. B. Ross, D. S. Covert, and R. J. Charlson. 1988. Northeastern Pacific submicrometer aerosol and rainwater composition: A multivariate analysis. *Journal of Geophysical Research: Atmospheres* 93, no. D2: 1625–37, https://doi.org/10.1029/JD093iD02p01625.
Voutchkov, N. 2010. Introduction to Reverse Osmosis Desalination - A SunCam online continuing education course, https://doi.org/10.13140/RG.2.2.13908.60801.
Vulava, V.M., E.B. Perry, C.S. Romanek, and J.C. Seaman. 2002. “Dissolved Gases as Partitioning Tracers for Determination of Hydrogeological Parameters” 36 (2): 254–62.
Wanninkhof, R., J.R. Ledwell, W.S. Broecker, and M. Hamilton. 1987. “Gas Exchange on Mono Lake and Crowley Lake, California.” *Journal of Geophysical Research: Oceans* 92 (C13): 14567–80.
Washington Department of Ecology. 2009. Water rights impairment standards for reclaimed water: Stakeholder views and ecology recommendations. Report to the legislature 09-11–027.
Wells, R. E., C. S. Weaver, and R. J. Blakely. 1998. Fore-arc migration in Cascadia and its neotectonic significance. *Geology* 26, no. 8: 759–62.
Wetch, N., 2015, Watewater Treatment Facility Engineering Report.
Williamson, A. K., D. E. Prudic, and L. A. Swain. 1989. Ground-Water Flow in the Central Valley, California. Professional Paper 1401-D. Regional Aquifer-System Analysis - Central Valley, California, https://doi.org/10.3133/pp1401D.
Wilson, A. M., G. Garven, and J. Boles. 1999. Paleohydrogeology of the San Joaquin basin, California. *Geological Society of America Bulletin*, 19.
Xiong, Z., L. Guo, Q. Zhang, G. Liu, and W. Liu. 2017. Edaphic Conditions Regulate Denitrification Directly and Indirectly by Altering Denitrifier Abundance in Wetlands along the Han River, China. *Environmental Science & Technology* 51, no. 10: 5483–91, https://doi.org/10.1021/acs.est.6b06521.

Zhang, G., P. Lu, X. Wei, and C. Zhu. 2016. Impacts of Mineral Reaction Kinetics and Regional Groundwater Flow on Long-Term CO $_2$ Fate at Sleipner. *Energy & Fuels* 30, no. 5: 4159–80, https://doi.org/10.1021/acs.energyfuels.5b02556.

Zhang, Z., C. Xiao, O. Adeyeye, W. Yang, and X. Liang. 2020. Source and Mobilization Mechanism of Iron, Manganese and Arsenic in Groundwater of Shuangliao City, Northeast China. *Water* 12, no. 2: 534, https://doi.org/10.3390/w12020534.

Zhu, N. 2013. Geochemical Modeling of an Aquifer Storage and Recovery Project in Union County, Arkansas. Master of Engineering, Massachusetts Institute of Technology.

Appendix A: Additional material for Chapter 2

Contents

A.1. A note about units

Metric units are used in the modeling and calculations done in this study for consistency with scientific standards and existing models. Surface distances and tabulated areas are presented in feet, miles, or square miles, as these are standard when discussing United States geography.

A.2. Well locations

A.2.1 Determining well locations from state databases

For the sake of modeling, wells are located based on the latitude and longitude assigned to them in the Well Completion Reports dataset published by the California Natural Resources Agency (CNRA 2021). Wells completed in 2019 or later are located by their actual latitude and longitude. Those completed earlier but following the rollout of the Online System for Well Completion Reports (OSWCR) in October 2015 are located primarily by latitude and longitude, address, or assessor's parcel number. The majority of earlier records are located only by public land survey system and are assigned the coordinates of the center of the section in which they are located (Benjamin Brezing, California Department of Water Resources, personal communication). This introduces an uncertainty of up to 0.7 miles (~1.1 km, the distance from the section center to the corner) to earlier well locations and causes wells located in different parts of the same section to be assigned the same coordinates. The methods of determining the coordinates included in the database for wells in the Central Valley are shown in Figure C 1.

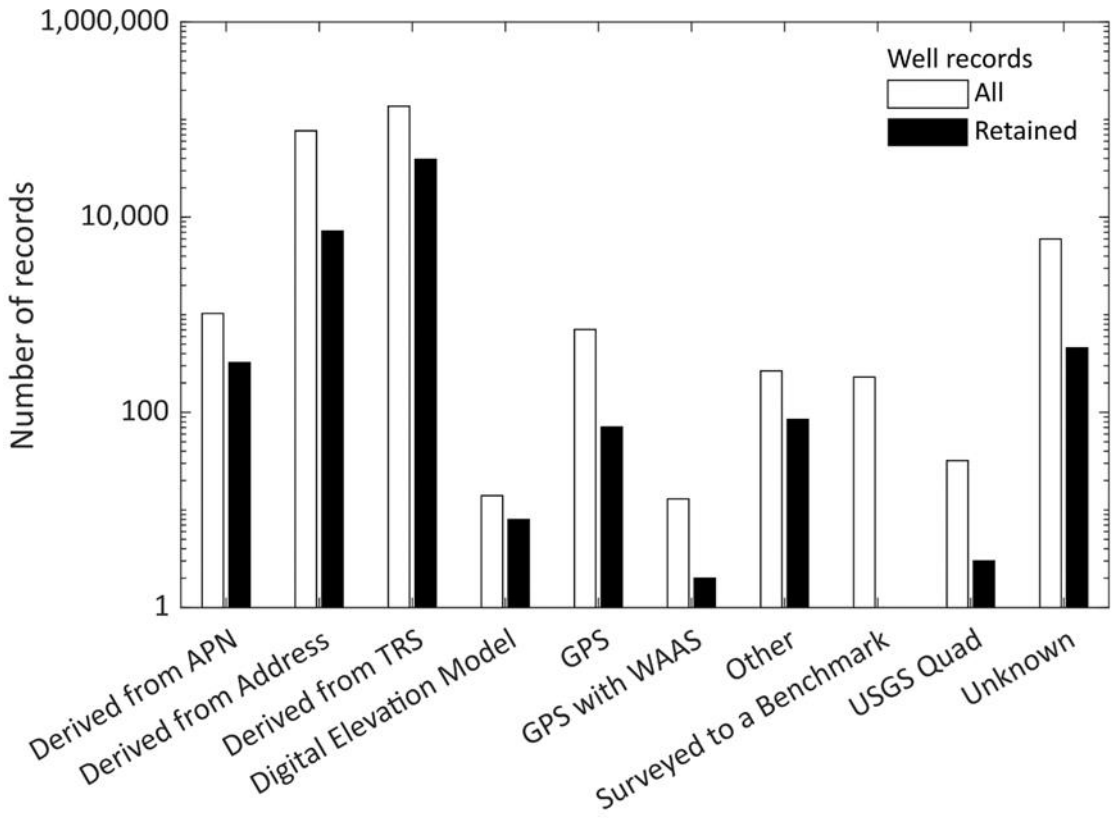

Figure C 1: Method of determining well coordinates for records within the Central Valley. Retained records are those that remain after cleaning as described in sections A.2.2 and A.2.3. (APN - Assessor's Parcel Number, TRS – Township, Range, Section, GPS – Global Positioning System, WAAS – Wide Area Augmentation System, USGS – United States Geological Survey)

A.2.2 MATLAB code for cleaning well reports

```
function
[retained_logs,clusters_abandoned,total_retained_clusters,total_discarded_clusters,reason_dis
carded,initial_num]=clean_CA_logs(all_reports)

% a function to take input table all_reports and clean according to the
% Jasecko and Perrone 2017 methodology for California. all_reports comes from OSWCR data
converted to a shapefile and should contain variables PlannedUse, LegacyLogN, CountyName,
DecimalLat, DecimalLon, TotalCompletedDepth, originalFID, RecordType, DateWorkEnded,
TopPerforated, and BottomPerforated

initial_num=size(all_reports,1);
all_reports.PlannedUse=strtrim(all_reports.PlannedUse); %remove leading and trailing
whitespaces from the planned use column
all_reports.LegacyLogN(ismember(all_reports.LegacyLogN,{'',' ','0000NONE','N'}))={'NN'};
%Converts some common missing lln values to values easier to find with regexp
```

```
retained_logs=[];
retained_logs.all=[];
clusters_abandoned=[];
total_retained_clusters=0;
total_discarded_clusters=0;
counties=unique(all_reports.CountyName); %get all county names
counties=counties(~ismember(counties,'')); %remove blank counties
reason_discarded.clusters=array2table(zeros(length(counties),5)); %make a table to count
reasons for discarding clusters
reason_discarded.single=array2table(zeros(length(counties),6)); %make a table to count
reasons for discarding single reports
reason_discarded.clusters.Properties.VariableNames={'no_new','abandoned','pre_1970','not_for_
humans','total'}; %assign variable names for discarded clusters table
reason_discarded.single.Properties.VariableNames={'no_new','pre_1970','missing_xy','missing_z
','not_for_humans','total'}; %assign variable names for discarded single records table
reason_discarded.clusters.Properties.RowNames=counties;
reason_discarded.single.Properties.RowNames=counties;
allowed_uses = {' Domestic', 'Other Community Well', 'Other COMMUNITY/PWS/CITY', 'Other
MunicipalWell', 'Other Municipial Well', ' Public', 'Water Supply Domestic', 'Water Supply
Public', 'Other  TNC well', 'Other  Domestic/Agricultural', 'Other  Agricultural/Domestic'};

for c = 1:length(counties) %for each county

    county_name=cellstr(counties(c)); %get county name as cell array
    county_name=county_name{:}; %get county name as string
    county_name= county_name(find(~isspace(county_name))); %remove whitespace
    county_reports=all_reports(ismember(all_reports.CountyName,counties{c}),:); %select
reports for that county
    notlln=regexp(county_reports.LegacyLogN,'\D\D*\D\>','match'); %finds lln entries that
don't contain numbers
    notlln=[notlln{:}]; %removes some nesting
    county_reports.with_lln=~ismember(county_reports.LegacyLogN,notlln); %identifies records
with legacy log number

county_reports.with_latlon=((county_reports.DecimalLat~=0)+(county_reports.DecimalLon~=0))==2
; % identifies records with lat and lon
    reason_discarded.single.missing_xy(c)=sum(~county_reports.with_latlon); %counts single
records of wells missing latitude and longitude

county_reports.with_depth=(ismissing(county_reports.TotalCompletedDepth)+(county_reports.Tota
lCompletedDepth<=0)+(county_reports.TotalCompletedDepth>9998))==0; %identifies records with
recorded depths
    reason_discarded.single.missing_z(c)=sum(~county_reports.with_depth); %counts single
records of wells missing depth
    county_reports.xyz=(county_reports.with_latlon+county_reports.with_depth==2); %identifies
records with lat, lon, and depth recorded
    almost=(county_reports.xyz+~county_reports.with_lln==2); %identifies records with lat,
lon, and depth, but no lln
    keep=(county_reports.with_lln+county_reports.with_latlon+county_reports.with_depth==3);
%identifies records with legacy log number, lat, lon, and depth
    almost_complete=county_reports(almost,:); %keeps a separate table of records with lat,
lon, and depth, but no lln
    county_reports=county_reports(keep,:); %retains records with legacy log number, lat, lon,
```

```
and depth
    connected=county_reports(:,'originalFID'); %make table to track which logs are connected
    [~,ia.lln,ic.lln]=unique(county_reports(:,'LegacyLogN'),'stable'); %find unique tag
numbers (and logs with no tag)
    connected(:,2)=county_reports(ia.lln(ic.lln),'originalFID'); %For each log, finds the
originalFID of the first log with its legacy log number and records it in Connected (receives
its own ID if it is the only one or the first)

[~,ia.coord,ic.coord]=unique(county_reports(:,{'DecimalLat','DecimalLon','TotalCompletedDepth
'}),'stable'); %find unique lat, lon, and depth
    connected(:,3)=county_reports(ia.coord(ic.coord),'originalFID'); %For each log, finds the
originalFID of the first log with its lat and lon and records it in Connected (receives its
own ID if it is the only one or the first)

    conn_mat=zeros(length(county_reports.originalFID)); %make a matrix of zeros to be
adjacency matrix
    for L = 1:length(county_reports.originalFID) %for each log
        common=sum((connected{:,2:end}==county_reports.originalFID(L)),2); %count number of
criteria in common out of legacy log number and lat-lon-depth
        conn_mat(common==2,L)=1; %find logs that meet all of the above criteria
    end

    cluster_graph=graph(conn_mat,'lower','omitselfloops'); %make networks of all connected
logs
    county_reports.samewell=conncomp(cluster_graph)'; %create column in criteria_tab with a
unique number for logs of each cluster indicating that they refer to the same well.
net_same=unique(county_reports.samewell); %get all well group numbers
    total_wells=0; %variable to count the number of wells represented by the logs

    retained_logs.(county_name)=table();%creates a table to hold logs for the resulting wells
    warning('off','MATLAB:table:RowsAddedExistingVars') %suppresses warning that woul be
displayed when first column of a new row is added to table
    for t = 1:length(net_same) %for each group number
        if sum(county_reports.samewell==net_same(t)) > 1 % if the log has been grouped with
any others

            thisgroup=strcat('t',num2str(net_same(t))); %makes a name with t and tag number
            log_clusters.(thisgroup)=county_reports(county_reports.samewell==net_same(t),:);
%make a table in a structure for all records with that group
            county_reports(county_reports.samewell==net_same(t),:)=[]; %remove those records
from the original data set (does not alter the actual data outside the function)
            if
sum(ismember(log_clusters.(thisgroup).RecordType,'WellCompletion/New/Production or
Monitoring/NA')) >0 % if there is at least one new well log
                if
(sum(ismember(log_clusters.(thisgroup).RecordType,'WellCompletion/Destruction/NA/NA')) +
sum(ismember(log_clusters.(thisgroup).RecordType,'WellCompletion/Drill and Destroy/NA/NA')))
==0 %if there are no abandonment logs in the cluster
                    if max(log_clusters.(thisgroup).DateWorkEnded)>=datetime(1970,01,01) %if
last log in cluster was from 1970 or later

log_clusters.(thisgroup)=sortrows(log_clusters.(thisgroup),'DateWorkEnded','ascend'); %sort
records in cluster by increasing date
```

```
                        recorded=~ismember(log_clusters.(thisgroup).PlannedUse,{'Not
Specified','Unknown','',' '}); %get indicies of recorded uses
                        rec_lat=~isnan(log_clusters.(thisgroup).DecimalLat); %checks for
recorded coordinates (logs have both Lat and Lon or neither)
                        rec_depth = ~isnan(log_clusters.(thisgroup).TotalCompletedDepth);
%checks for recorded depth
                        if sum(recorded)>0 and rec_lat>0 and rec_depth>0 % if there are
recorded uses and coordinates
                            if
ismember(log_clusters.(thisgroup).PlannedUse(find(recorded,1,'last')),allowed_uses) %if last
recorded use was for an allowed use
                                total_wells=total_wells+1; %counts a well
                                if size(log_clusters.(thisgroup),1)>1
                                    total_retained_clusters=total_retained_clusters + 1; %
counts total retained well clusters that are actually clusters
                                end

retained_logs.(county_name).originalFID(total_wells)=log_clusters.(thisgroup).originalFID(1);
%get an originalFID

retained_logs.(county_name).PlannedUse(total_wells)=log_clusters.(thisgroup).PlannedUse(find(
recorded,1,'last')); %last recorded use

retained_logs.(county_name).DateWorkEnded(total_wells)=log_clusters.(thisgroup).DateWorkEnded
(find(recorded,1,'last')); %last recorded date

retained_logs.(county_name).DecimalLat(total_wells)=log_clusters.(thisgroup).DecimalLat(find(
rec_lat,1,'last')); %get last recorded lat

retained_logs.(county_name).DecimalLon(total_wells)=log_clusters.(thisgroup).DecimalLon(find(
rec_lat,1,'last')); %get recorded lon

retained_logs.(county_name).TotalCompletedDepth(total_wells)=log_clusters.(thisgroup).TotalCo
mpletedDepth(find(rec_depth,1,'last')); %get last recorded depth

retained_logs.(county_name).TopPerforated(total_wells)=log_clusters.(thisgroup).TopPerforated
(find(rec_depth,1,'last')); %get top of perforation associated with last recorded depth

retained_logs.(county_name).BottomPerforated(total_wells)=log_clusters.(thisgroup).BottomPerf
orated(find(rec_depth,1,'last')); %get bottom of perforation associated with last recorded
depth
                            elseif size(log_clusters.(thisgroup),1)>1
                                total_discarded_clusters=total_discarded_clusters + 1; %
counts total discarded well clusters that are actually clusters

reason_discarded.clusters.not_for_allowed_use(c)=reason_discarded.clusters.not_for_allowed_us
e(c)+1; %counts a cluster that is not for an allowed use
                            else

reason_discarded.clusters.not_for_allowed_use(c)=reason_discarded.clusters.not_for_allowed_us
e(c)+1; %counts a cluster that is not for an allowed use
                            end
                        end
```

```
                    else

reason_discarded.clusters.pre_1970(c)=reason_discarded.clusters.pre_1970(c)+1; %counts a
cluster with last work later than 1970
                    end
                else
                    clusters_abandoned.(county_name).(thisgroup)=log_clusters.(thisgroup); %
if there is an abandonment record, records the logs as being associated with an abandoned
well

reason_discarded.clusters.abandoned(c)=reason_discarded.clusters.abandoned(c)+1; %counts a
cluster with abandonment record
                end
            else
                reason_discarded.clusters.no_new(c)=reason_discarded.clusters.no_new(c)+1;
%counts a cluster with no new wells
            end
        end
    end

    resid.county_reports=county_reports; %outputs remaining unmatched records

resid.county_reports=[resid.county_reports(:,{'originalFID','PlannedUse','DateWorkEnded','Rec
ordType','DecimalLat','DecimalLon','TotalCompletedDepth','TopPerforated','BottomPerforated'})
;
almost_complete(:,{'originalFID','PlannedUse','DateWorkEnded','RecordType','DecimalLat','Deci
malLon','TotalCompletedDepth','TopPerforated','BottomPerforated'})]; %appends the records
with lat, lon, and depth but no legacy log number to unmatched records
    new=ismember(resid.county_reports.RecordType,'WellCompletion/New/Production or
Monitoring/NA'); %finds unmatched new well records
    recent=resid.county_reports.DateWorkEnded>=datetime(1970,01,01); %finds unmatcehd records
from 1970 onwards
    allowed=ismember(resid.county_reports.PlannedUse,allowed_uses); %finds wells intended for
an allowed use
    all_num=(~isnan(resid.county_reports.DecimalLat)+ ~isnan(resid.county_reports.DecimalLon)
+ ~isnan(resid.county_reports.TotalCompletedDepth))==3; %finds logs with lat, lon, and depth
included
    resid.keep=resid.county_reports((new+recent+allowed+all_num==4),:); %finds records
meeting all criteria
    reason_discarded.single.no_new(c)=sum(~new); %counts single records not for new wells
    reason_discarded.single.pre_1970(c)=sum(~recent); %counts single records prior to 1970
    reason_discarded.single.not_for_allowed_use(c)=sum(~allowed); %counts single records of
wells not for an allowed use
    reason_discarded.single.total(c)=sum((new+recent+allowed+all_num<4)); %count total number
of single records discarded
    if ~isempty(resid.keep) %if the table isn't empty

retained_logs.(county_name)(size(retained_logs.(county_name),1)+1:size(retained_logs.(county_
name),1)+size(resid.keep,1),:)=resid.keep(:,{'originalFID','PlannedUse','DateWorkEnded','Deci
malLat','DecimalLon','TotalCompletedDepth','TopPerforated','BottomPerforated'}); %add
unmatched logs to retained_logs.(county_name)
        retained_logs.all=[retained_logs.all; retained_logs.(county_name)]; % add logs to
whole list
```

```
    end
    warning('on','MATLAB:table:RowsAddedExistingVars') %turns warning back on
    reason_discarded.clusters.total(c)=sum(reason_discarded.clusters{c,1:5}); %count total
number of clusters discarded

end

% plot reasons for discarding single records

figure
bar(reason_discarded.single{reason_discarded.single.total>0,1:end-1})
xticks(1:sum(reason_discarded.single.total>0))
xticklabels(reason_discarded.single.Properties.RowNames(reason_discarded.single.total>0))
legend('not a new well record','pre-1970','missing x, y','missing z', 'not for
humans','Location','EastOutside')
title({'Reasons for discarding single records', '(note: all reasons for discarding any record
counted)'})
set(gca,'FontSize',20)
xtickangle(45)
% plot reasons for discarding clustered records
figure
bar(reason_discarded.clusters{reason_discarded.clusters.total>0,1:end-1})
xticks(1:sum(reason_discarded.clusters.total>0))
xticklabels(reason_discarded.clusters.Properties.RowNames(reason_discarded.clusters.total>0))
legend('no new well records','abandonded','pre-1970', 'not for
humans','Location','EastOutside')
title({'Reasons for discarding clustered records', '(note: Only first reason for discarding
any cluster counted. Priority same as legend order.)'})
set(gca,'FontSize',20)
```

Published with MATLAB® R2021a

A.2.3 Reasons for discarding well reports

Reasons for discarding well reports are indicated below. Single records are reports that do not refer to the same well as any other report (or cannot be proven to refer to the same well). Clustered records refer to a set of two or more reports determined to refer to the same well on the basis of latitude, longitude, depth, and possibly legacy log number. Single records are discarded if they do not refer to a new well, the work was completed prior to January 1, 1970, they are missing latitude or longitude, they were missing depth, or the primary use is not for human consumption (Figure C 2). Clustered records are discarded if the cluster did not contain a new well report, the cluster contained an abandonment report, the most recent report is dated prior to 1970, or the primary use is not for human consumption (Figure C 3). Since records are matched by location in three dimensions, missing positional data is not a relevant criterion for discarding clustered records. Note that due to the different ways in which single and clustered records are processed, the single records plot shows all reasons that a given well report would be ineligible, while the clustered records plot shows only the first reason. Clusters are evaluated first by whether they contained a new report, secondly

whether they have been abandoned, thirdly by date, and lastly by whether they were intended for human consumption. The most common reasons for records to be excluded were lack of depth data (for single records) and primary use not for human consumption.

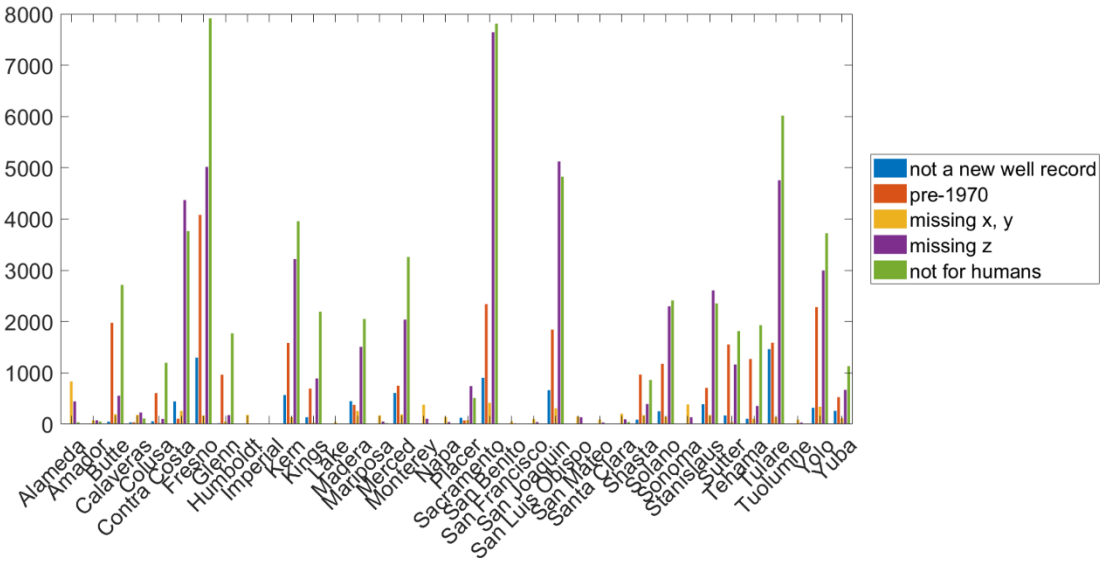

Figure C 2: Reasons for discarding single well records. Note: all reasons for discarding any record counted.

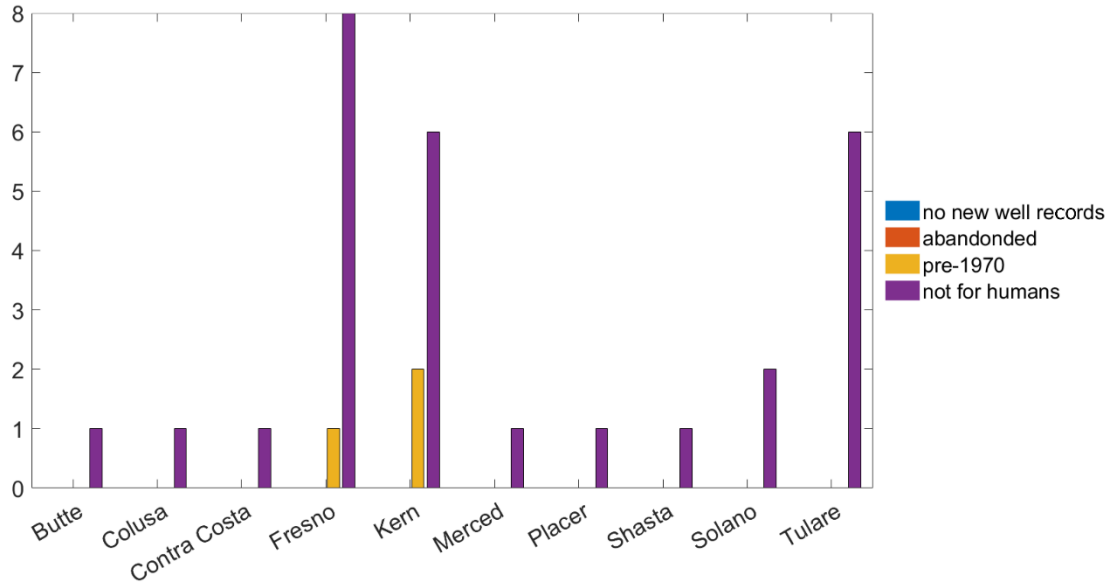

Figure C 3: Reasons for discarding clustered well records. Note, only first reason for discarding any cluster counted. Priority same as legend order.

A.3. Estimating missing screen depths

A.3.1 Process

Approximately 45% of the retained well reports are missing depths for the tops and bottoms of their screens. In order to fill in the missing bottom depths, wells are divided by bulletin 118 subbasins, and a linear regression of screen bottom depth as a function of total completed depth is fitted to all wells for which both numbers are defined. Subbasins containing fewer than 75 retained well records are grouped with adjacent basins until their combined number of retained wells is at least 75, and the data for the whole group is used for the regression (Table C 1, Figure C 4). In some cases, subbasins with 75 or more wells are included in a group; however, the combined regression is used only for the subbasins in the group with fewer than 75 wells. The regression for basins with 75 or more wells is based solely on data from that subbasin.

Table C 1: Retained wells by subbasin with regression groups

Name	Retained Wells	Group
Arroy del Hambre Valley*	0	
Clayton Valley	24	C
Pittsburg Plain	16	C
Redding Area - Anderson	1107	
Redding Area - Bowman	940	
Redding Area - Enterprise	828	
Redding Area - Millville	410	D
Redding Area - South Battle Creek	16	D
Sacramento Valley - Antelope	531	
Sacramento Valley - Bend	113	
Sacramento Valley - Butte	475	
Sacramento Valley - Colusa	1617	
Sacramento Valley - Corning	1247	
Sacramento Valley - Los Molinos	492	
Sacramento Valley - North American	1018	
Sacramento Valley - North Yuba	255	
Sacramento Valley - Red Bluff	2428	
Sacramento Valley - Solano	1206	
Sacramento Valley - South American	931	
Sacramento Valley - South Yuba	261	
Sacramento Valley - Sutter	1042	
Sacramento Valley - Vina	1727	
Sacramento Valley - Wyandotte Creek	415	
Sacramento Valley - Yolo	1225	
San Joaquin Valley - Chowchilla	272	
San Joaquin Valley - Cosumnes	1338	

San Joaquin Valley - Delta-Mendota	1354	
San Joaquin Valley - East Contra Costa	827	C
San Joaquin Valley - Eastern San Joaquin	5193	
San Joaquin Valley - Kaweah	1958	
San Joaquin Valley - Kern County	783	A
San Joaquin Valley - Kettleman Plain	6	B
San Joaquin Valley - Kings	7759	
San Joaquin Valley - Madera	2670	
San Joaquin Valley - Merced	2310	
San Joaquin Valley - Modesto	1689	
San Joaquin Valley - Pleasant Valley	5	B
San Joaquin Valley - Tracy	997	
San Joaquin Valley - Tulare Lake	941	B
San Joaquin Valley - Tule	845	
San Joaquin Valley - Turlock	2454	
San Joaquin Valley - Westside	27	B
San Joaquin Valley - White Wolf	5	A
Suisun-Fairfield Valley	249	
Ygnacio Valley	25	C

*Not included in further analysis due to lack of retained well records.

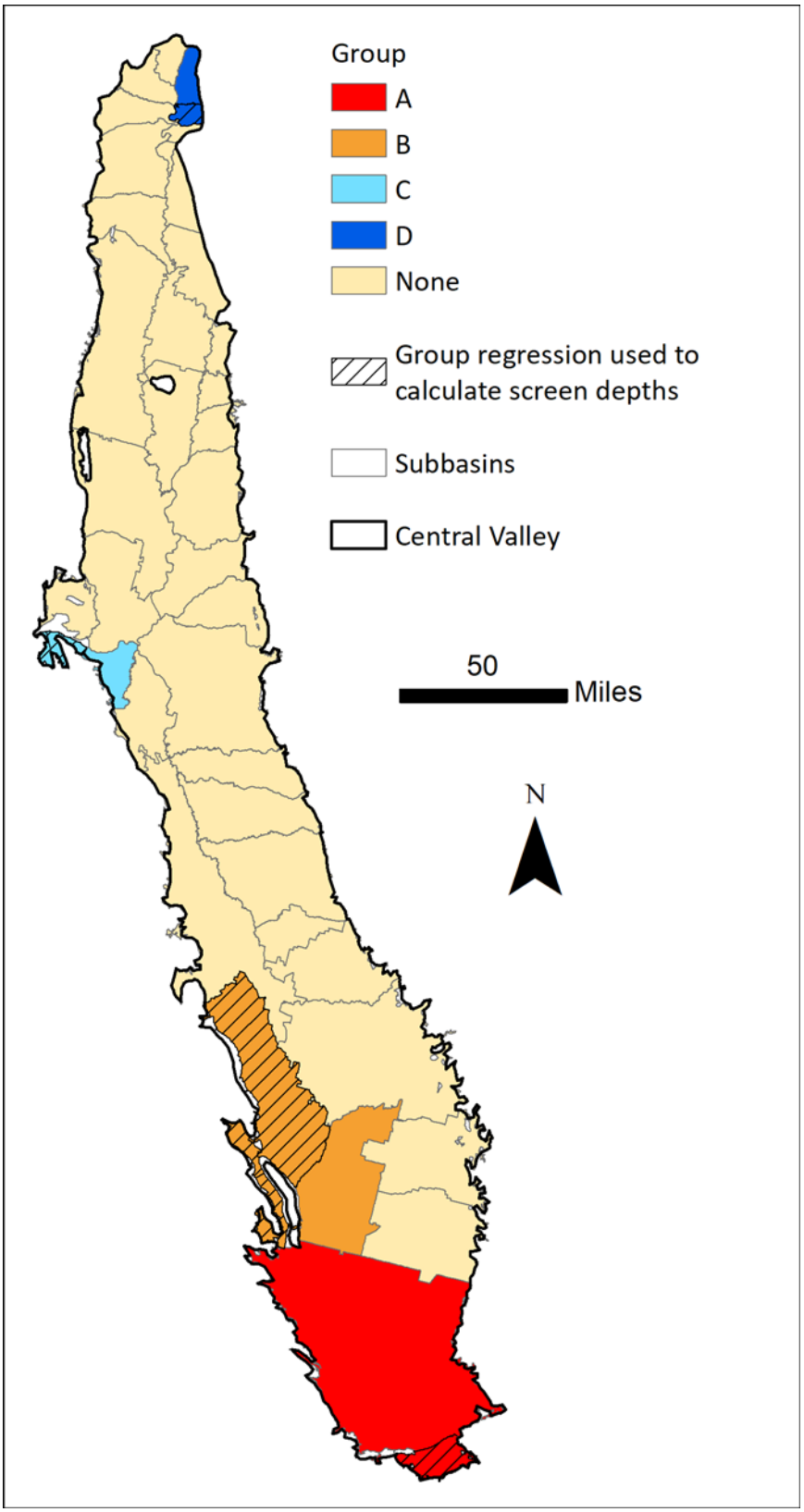

Figure C 4: Subbasins with groups used for calculating regressions.

A.3.2 MATLAB code for estimating screen depths

```
function [all_est,subbasin_tab]=estimate_screen_depths(all_data)
%Estimates screen depths for all wells in all_data, a table of wells with the following
variables
% Well_ID: A unique number for ech well (numeric)
% Total_depth: Total completed depth (numeric)
% Top_perf: Top of perforated interval (numeric, Nan where unknown)
% Bot_perf: Bottom of perforated interval (numeric, Nan where unknown)
% Subbasin: Subbasin name (categorical)
%Subbasin_name: Subbasin name (cell array of character vectors)
% X: X coordinate of well (numeric)
% Y: Y coordinate of well (numeric)

all_est=[]; %empty matrix for estimates

%select subbasins known to have fewer than 75 wells or to be adjacent to
%ones that are
SJVWW = all_data.Subbasin=='SAN JOAQUIN VALLEY - WHITE WOLF';
SJVKC = all_data.Subbasin=='SAN JOAQUIN VALLEY - KERN COUNTY';
SJVW = all_data.Subbasin=='SAN JOAQUIN VALLEY - WESTSIDE';
SJVPV = all_data.Subbasin=='SAN JOAQUIN VALLEY - PLEASANT VALLEY';
SJVKP = all_data.Subbasin=='SAN JOAQUIN VALLEY - KETTLEMAN PLAIN';
SJVTL = all_data.Subbasin=='SAN JOAQUIN VALLEY - TULARE LAKE';
YV = all_data.Subbasin=='YGNACIO VALLEY';
CV = all_data.Subbasin=='CLAYTON VALLEY';
PP = all_data.Subbasin=='PITTSBURG PLAIN';
SJVECC = all_data.Subbasin=='SAN JOAQUIN VALLEY - EAST CONTRA COSTA';
RASBC = all_data.Subbasin=='REDDING AREA - SOUTH BATTLE CREEK';
RAM = all_data.Subbasin=='REDDING AREA - MILLVILLE';

%group subbasins to make subbasin groups with at least 75 wells
all_data.group(SJVWW+SJVKC>0)=categorical({'A'});
all_data.group(SJVW+SJVPV+SJVKP+SJVTL>0)=categorical({'B'});
all_data.group(YV+CV+PP+SJVECC>0)=categorical({'C'});
all_data.group(RASBC+RAM>0)=categorical({'D'});

all_subb=unique(all_data.Subbasin); %all the subbasin codes
well_count=histcounts(all_data.Subbasin); % count wells in each subbasin
for subb=1:length(all_subb) %for each subbasin
    data=all_data(all_data.Subbasin==all_subb(subb),:); %get records from that subbasin
    if well_count(subb)<75 and ~isundefined(data.group(1))
        data=all_data(all_data.group==data.group(1),:); %get records from its group
        label{subb}=['group',char(data.group(1))]; %label with group code
    else
        label{subb}=regexprep(data.Subbasin_name{1},'\W','_'); %label with subbasin name
    end

    too_deep_top1=(data.Top_perf>=data.Bot_perf); %find wells with recorded top of screen
depth greater than bottom of screen depth
    too_deep_top2 = (data.Top_perf>=data.Total_depth); %find wells with recorded top of
```

```
screen depth greater than total completed depth
    too_deep_bottom = (data.Bot_perf>data.Total_depth); %find wells with recorded bottom of
screen depth greater than total completed depth
    top_zero = (data.Top_perf<=0); %find wells with recorded top of screen depth less than or
equal to 0
    bottom_zero = (data.Bot_perf<=0); %find wells with recorded bottom of screen depth less
than or equal to 0

    data.Top_perf(too_deep_top1 + too_deep_top2 + top_zero >0)=NaN; % set invalid top depths
to NaN
    data.Bot_perf(too_deep_bottom + bottom_zero >0)=NaN; % set invalid bottom depths to NaN
    data.scr_int=data.Bot_perf-data.Top_perf; %calculate screen interval

    top_specified = ~isnan(data.Top_perf); % find wells with top of casing interval specified
    bottom_specified = ~isnan(data.Bot_perf); % find wells with bottom of casing interval
specified
    bottom_gap = data.Bot_perf<data.Total_depth; %find wells with gap between bottom of
screen and total depth (this is normal)
    both_specified = top_specified+bottom_specified ==2; % find wells with top and bottom of
casing interval specified

    subbasin_data=data(data.Subbasin==all_subb(subb),:); %get records from that subbasin only
to estimate depths

    subbasin_bottom_unspec=isnan(subbasin_data.Bot_perf); %records from the subbasin missing
screen bottom depths
    subbasin_top_unspec=isnan(subbasin_data.Top_perf); %records from the subbasin missing
screen top depths

    bot_coeff.(label{subb})=
polyfit(data.Total_depth(bottom_gap),data.Bot_perf(bottom_gap),1); %fit linear model of total
depth vs bottom of casing depth to records with bottom of casing specified shallower than
total completed depth
    subbasin_data.bottom_est=subbasin_data.Bot_perf; %copy screen bottom depths as recorded
    subbasin_data.bottom_est(subbasin_bottom_unspec)=
polyval(bot_coeff.(label{subb}),subbasin_data.Total_depth(subbasin_bottom_unspec));
%calculate screen bottom depths where unspecified based on linear model

    too_deep_check=subbasin_data.bottom_est>subbasin_data.Total_depth; %find wells with
estimated screen bottom deeper than total depth
    too_shallow_check=subbasin_data.bottom_est<=subbasin_data.Top_perf |
subbasin_data.bottom_est<=0; %find wells with estimated screen bottom shallower than screen
top or surface
    subbasin_data.bottom_est(too_deep_check |
too_shallow_check)=subbasin_data.Total_depth(too_deep_check | too_shallow_check); %reasign
wells with illogical estimated bottom of screen depth with the total completed depth

     top_coeff.(label{subb}) =
polyfit(data.Bot_perf(both_specified),data.scr_int(both_specified),1); %fit linear model for
screen interval based on screen bottom to records with top and bottom of casing specified
     subbasin_data.top_est=subbasin_data.Top_perf; %copy screen top depths as recorded
     subbasin_data.top_est(subbasin_top_unspec)
=subbasin_data.bottom_est(subbasin_top_unspec)-
```

```
polyval(top_coeff.(label{subb}),subbasin_data.bottom_est(subbasin_top_unspec)); %estimate top
of screen where unspecified from linear model of interval based on bottom of screen depth

    all_est=[all_est;subbasin_data]; %put estimates in all_est
end
all_est.top_est(all_est.top_est>=all_est.bottom_est) =
all_est.bottom_est(all_est.top_est>=all_est.bottom_est)-5; %if top of screen estimate is as
deep as or deeper than the bottom of screen, reset to 5 ft shallower than bottom of screen
all_est.top_est(all_est.top_est<0)=0; %if top estimate is less than zero, reset to zero
subbasin_tab=table(); %make a table to hold counts of wells in each subbasin
subbasin_tab.Subbasin=unique(all_data.Subbasin); %get names
subbasin_tab.Wells=histcounts(all_data.Subbasin)'; %get well counts
```

Published with MATLAB® R2021a

A.4. C2VSimFG

Simulated groundwater heads and velocities were generated using version 1.0 of C2VSim fine grid (C2VSimFG) (Hatch et al. 2020). C2VSimFG simulates all pumping original to the model on an element level, except for groundwater substitution transfer pumping, which is simulated by individual well. The water supply wells identified from OSWCR were added to the model as additional individual wells. The OSWCR wells were divided into domestic and public supply wells. The two that did not fit directly into either category (described as "Other Agricultural/Domestic" and Other TNC well") were assumed to have the same pumping patterns as a domestic well, as they are not expected to support large amounts of potable use on a regular basis. Since the goal of the C2VSimFG modeling was to produce a multiyear average water table and velocity field, the OSWCR wells were assumed to continuously pump the same amount of water. Domestic wells were assigned a pumping rate of 0.020 acre-feet per month based on average California per capita residential water use in 2015 (California State Water Resources Control Board 2022) and 2010 average California household size (US Census Bureau 2011). Public supply wells were assigned a pumping rate of 5.272 acre-feet per month based on the same per capita water use, average number of people served and average number of wells per water system in the San Joaquin Valley (the largest hydrologic province in the Central Valley) (Bostic 2021) and average proportion of urban demand met by groundwater in the Central Valley (Springhorn et al. 2021).

Sixty-five wells had a screen top or bottom outside the model domain and were modeled in C2VSimFG with shortened screens to fit inside the domain. Six wells were not included in C2VSimFG modeling, as their screens were completely outside the model domain.

C2VSimFG can output a file of groundwater velocities at cell centers, though it is not produced by default. This option was enabled before running the model. The output units for groundwater velocity are set using a conversion factor (referred to as FACTVROU in the specification file) and a label (UNITVROU). The default settings for these is 0.000022957 (converting from cubic feet to acre feet) and AC-FT/MON; however, the velocity units

should actually be linear (Tyler Hatch, CA DWR, personal communication). FACTVROU is therefore changed to 1000.0 such that the output unit is thousand feet per month. Additionally, each element is designated as its own zone for the Z-budget calculation.

A.5. ICHNOS

ICHNOS version 2.10 was used for backwards particle tracking from wells to find the areas where recharging water would reach them within a year. The input files were prepared using the boundary shapefile, node file, and stratigraphy file which come with C2VSimFG. Additionally, the velocity and groundwater head files produced by running C2VSimFG were used. The outline, top and bottom (single file), processor polygon, velocity files were prepared according to the Getting Started guidance on the ICHNOS GitHub page for C2VSimFG single processor steady state (Kourakos 2022). In contrast to the published example, the average groundwater head in the top layer of the C2VSimFG model, as opposed to the top of the aquifer unit, was used as the top of the model domain for ICHNOS. In order to account for downward movement of water from the unsaturated zone to the saturated zone, an additional layer was added to the top of the model with the same horizontal velocity as the original top layer and a vertical velocity determined from the Z-budget calculated for each element by C2VSimFG. The net flux in each element to the groundwater zone from streams, deep percolation, diversions, bypasses, and small watersheds, and that required by constant head boundaries (used in C2VSimFG to represent certain water bodies), was divided by the element area to produce an element average vertical velocity. The surface layer was assigned 25% of the thickness of the original top layer, while the top layer of the saturated zone receives 75% of the original thickness. Groundwater levels and velocity from October 2005 through September 2015 were averaged to allow a steady state simulation.

A.5.1 Wells

Particles for tracking were released from 46,125 wells (all of those identified in OSWCR which passed the cleaning stage, minus 3,906 which were too shallow or too deep for the modified ICHNOS domain). Eighteen particles were released from each well, divided into six layers, at a distance of 1 meter from the well. Tracking was ended at 365 days, and any particles exiting the model domain via the top were determined to represent locations where recharge would reach a well within a year.

A.5.2 Rivers

Buffer areas for rivers were generated in a similar manner to buffers for wells. C2VSimFG nodes intersected by rivers delineated the shapefiles accompanying the model were selected. Flow lines from NHDplusV2 with associated bankfull depth estimates were also selected (US EPA and USGS 2012; Wieczorek et al. 2018). Selected nodes falling within 10 meters of selected NHDplusV2 flow lines were retained and given the bankfull depth associated with the line. These points were treated as fully screened wells in ICHNOS with 6 particles released per well from 3 layers at a distance of 1 meter from the virtual well.

Given that the river beds are shallower than the water table in many locations, the surface was used as the top of the model domain instead of the water table. Backwards particle tracking was conducted for 365 days. For each virtual well, the exit location of the farthest particle reaching the surface (if any) was selected to be used to calculate buffer distances as described in Section 6.2.

A.5.3 ICHNOS model configuration parameters

[Velocity]

XYZType = CLOUD

Type = STEADY

[Domain]

TopRadius = 3000

TopPower = 3

[StepConfig]

Method = RK45

Direction = -1

StepSize = 50

StepSizeTime = 100

nSteps = 10

nStepsTime = 0

minExitStepSize = 0.1

[AdaptStep]

MaxStepSize = 1000

MinStepSize = 0.1

increaseRateChange = 1.5

limitUpperDecreaseStep = 0.15

Tolerance = 1

[StoppingCriteria]

MaxIterationsPerStreamline = 3000

MaxProcessorExchanges = 50

AgeLimit = 365

StuckIter = 10

[InputOutput]

ParticlesInParallel = 5000

GatherOneFile = 0

[Other]

Version = 0.2.10

Nrealizations = 1

A.5.4 ICHNOS velocity configuration parameters

[Velocity]

Type = STEADY

Multiplier = 0.000001

Scale = 1

Power = 3.5

InitDiameter = 1500000

InitRatio = 20

[Porosity]

Value = 0.1

[General]

OwnerThreshold = 0.15

Threshold = 0.1

FrequencyStat = 100

A.6. Suitability Mapping

A.6.1 Land cover

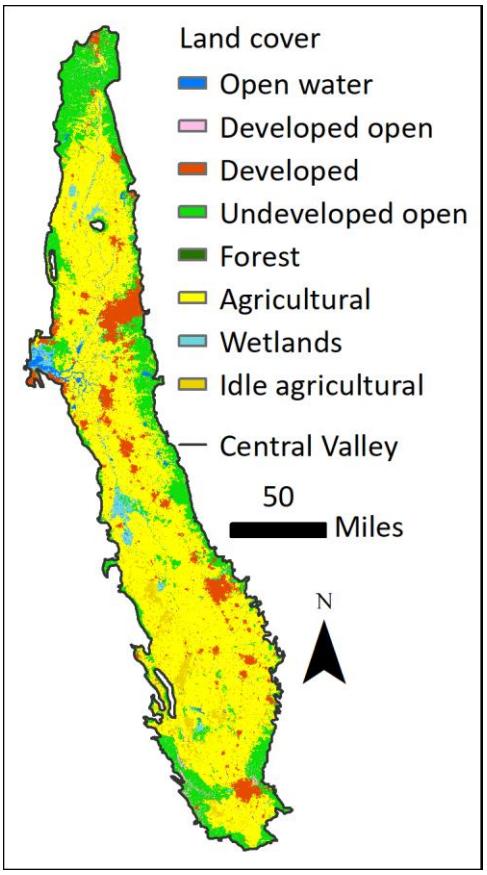

Figure C 5: Basic land cover classes. For detailed classes, see Table C 2 - Table C 5.

Land cover was determined based on the Land IQ 2018 map for 61% of the study area. Land cover for the remaining area, which the Land IQ map does not cover, was determined based on the National Land Cover Dataset 2016 data for the contiguous United States (*Figure C* 5) (Land IQ and DWR 2021; USGS 2021). Land covers were divided into those potentially compatible with recycled water MAR and those which are incompatible and therefore excluded from analysis. The map was converted to a raster with a value of 1 in all areas to be included and a value of 0 in all areas to be excluded. Land covers present in the study area are listed in Table C 2 - Table C 5, divided into those classes included in further analysis and those that are excluded.

Table C 2: Land IQ classes included in analysis

Class 2	Class 2 description	Subclass 2	Subclass 2 description

C	Citrus and subtropical		
G	Grain and hay crops		
T	Truck, nursery, and berry crops		
V	Vineyards		
X	Unclassified fallow (Idle status could not be determined solely within the 2018 calendar)		
YP	Young Perennial		
C	Citrus and subtropical	4	Dates
C	Citrus and subtropical	5	Avocados
C	Citrus and subtropical	6	Olives
C	Citrus and subtropical	7	Miscellaneous subtropical fruit
C	Citrus and subtropical	8	Kiwis
D	Deciduous fruits and nuts	1	Apples
D	Deciduous fruits and nuts	3	Cherries
D	Deciduous fruits and nuts	5	Peaches and nectarines
D	Deciduous fruits and nuts	6	Pears
D	Deciduous fruits and nuts	10	Miscellaneous deciduous
D	Deciduous fruits and nuts	11	Mixed deciduous
D	Deciduous fruits and nuts	12	Almonds
D	Deciduous fruits and nuts	13	Walnuts

D	Deciduous fruits and nuts	14	Pistachios
D	Deciduous fruits and nuts	15	Pomegranates
D	Deciduous fruits and nuts	16	Plums
F	Field crops	1	Cotton
F	Field crops	2	Safflower
F	Field crops	10	Beans (dry)
F	Field crops	11	Miscellaneous field
F	Field crops	12	Sunflowers
F	Field crops	16	Corn, Sorghum or Sudan grouped for remote sensing only
G	Grain and hay crops	2	Wheat
G	Grain and hay crops	6	Miscellaneous grain and hay
I	Idle	2	new lands being prepared for crop production
P	Pasture	1	Alfalfa and alfalfa mixtures
P	Pasture	3	Mixed pasture
P	Pasture	4	Native pasture
P	Pasture	6	Miscellaneous grasses
R	Rice	1	Rice
R	Rice	2	Wild Rice
T	Truck, nursery and berry crops	4	Cole crops (mixture of broccoli, cabbage, cauliflower, and Brussels sprouts)
T	Truck, nursery and berry crops	6	Carrots
T	Truck, nursery and berry crops	9	Melons, squash, and cucumbers (all types)
T	Truck, nursery and berry crops	10	Onions and garlic

T	Truck, nursery and berry crops	12	Potatoes
T	Truck, nursery and berry crops	15	Tomatoes (processing)
T	Truck, nursery and berry crops	16	Flowers, nursery and Christmas tree farms
T	Truck, nursery and berry crops	18	Miscellaneous truck
T	Truck, nursery and berry crops	19	Bush berries
T	Truck, nursery and berry crops	20	Strawberries
T	Truck, nursery and berry crops	21	Peppers (chili, bell, etc.)
T	Truck, nursery and berry crops	27	Greenhouse
T	Truck, nursery and berry crops	30	Lettuce or Leafy Greens grouped for remote sensing only
T	Truck, nursery and berry crops	31	Potato or Sweet potato grouped for remote sensing only

Table C 3: Land IQ classes excluded from analysis

Class 2	Class 2 description	Subclass 2	Subclass 2 description
U	Urban - residential, commercial, and industrial, unsegregated		

Table C 4: NLCD classes included in analysis

Class	Description

21	Developed, Open Space- areas with a mixture of some constructed materials, but mostly vegetation in the form of lawn grasses. Impervious surfaces account for less than 20% of total cover. These areas most commonly include large-lot single-family housing units, parks, golf courses, and vegetation planted in developed settings for recreation, erosion control, or aesthetic purposes.
31	Barren Land (Rock/Sand/Clay) - areas of bedrock, desert pavement, scarps, talus, slides, volcanic material, glacial debris, sand dunes, strip mines, gravel pits and other accumulations of earthen material. Generally, vegetation accounts for less than 15% of total cover.
52	Shrub/Scrub- areas dominated by shrubs; less than 5 meters tall with shrub canopy typically greater than 20% of total vegetation. This class includes true shrubs, young trees in an early successional stage or trees stunted from environmental conditions.
71	Grassland/Herbaceous- areas dominated by gramanoid or herbaceous vegetation, generally greater than 80% of total vegetation. These areas are not subject to intensive management such as tilling, but can be utilized for grazing.
81	Pasture/Hay-areas of grasses, legumes, or grass-legume mixtures planted for livestock grazing or the production of seed or hay crops, typically on a perennial cycle. Pasture/hay vegetation accounts for greater than 20% of total vegetation.
82	Cultivated Crops -areas used for the production of annual crops, such as corn, soybeans, vegetables, tobacco, and cotton, and also perennial woody crops such as orchards and vineyards. Crop vegetation accounts for greater than 20% of total vegetation. This class also includes all land being actively tilled.

Table C 5: NLCD classes excluded from analysis

Class	Description
11	Open Water- areas of open water, generally with less than 25% cover of vegetation or soil.
22	Developed, Low Intensity- areas with a mixture of constructed materials and vegetation. Impervious surfaces account for 20% to 49% percent of total cover. These areas most commonly include single-family housing units.
23	Developed, Medium Intensity -areas with a mixture of constructed materials and vegetation. Impervious surfaces account for 50% to 79% of the total cover. These areas most commonly include single-family housing units.

24	Developed High Intensity-highly developed areas where people reside or work in high numbers. Examples include apartment complexes, row houses and commercial/industrial. Impervious surfaces account for 80% to 100% of the total cover.
41	Deciduous Forest- areas dominated by trees generally greater than 5 meters tall, and greater than 20% of total vegetation cover. More than 75% of the tree species shed foliage simultaneously in response to seasonal change.
42	Evergreen Forest- areas dominated by trees generally greater than 5 meters tall, and greater than 20% of total vegetation cover. More than 75% of the tree species maintain their leaves all year. Canopy is never without green foliage.
43	Mixed Forest- areas dominated by trees generally greater than 5 meters tall, and greater than 20% of total vegetation cover. Neither deciduous nor evergreen species are greater than 75% of total tree cover.
90	Woody Wetlands- areas where forest or shrubland vegetation accounts for greater than 20% of vegetative cover and the soil or substrate is periodically saturated with or covered with water.
95	Emergent Herbaceous Wetlands- Areas where perennial herbaceous vegetation accounts for greater than 80% of vegetative cover and the soil or substrate is periodically saturated with or covered with water.

A.6.2 Well buffers

For residence time-based buffers, the vertices of streamlines that exited from the top of the domain in ICHNOS were imported to ArcGIS. Buffer zones were created from the point features using the minimum bounding geometry tool with the convex hull option, grouped by well number. The resulting polygons represent the area within which surface recharge would reach a well within a year and are thus to be excluded from consideration for recycled water MAR. The shapefile was then converted to a raster with a value of 0 for all of the buffer zones and a value of 1 everywhere else.

For distance-based buffers, each domestic well was given a circular buffer with a 100-ft radius. The buffer shapefile was then converted to a 100 m x 100 m raster for analysis consistent with other layers. Since the buffers were smaller than the raster pixels, the rasterization process gave buffer pixels to an apparently random selection of wells (Figure C 6). Therefore, the area excluded should be considered a minimum estimate.

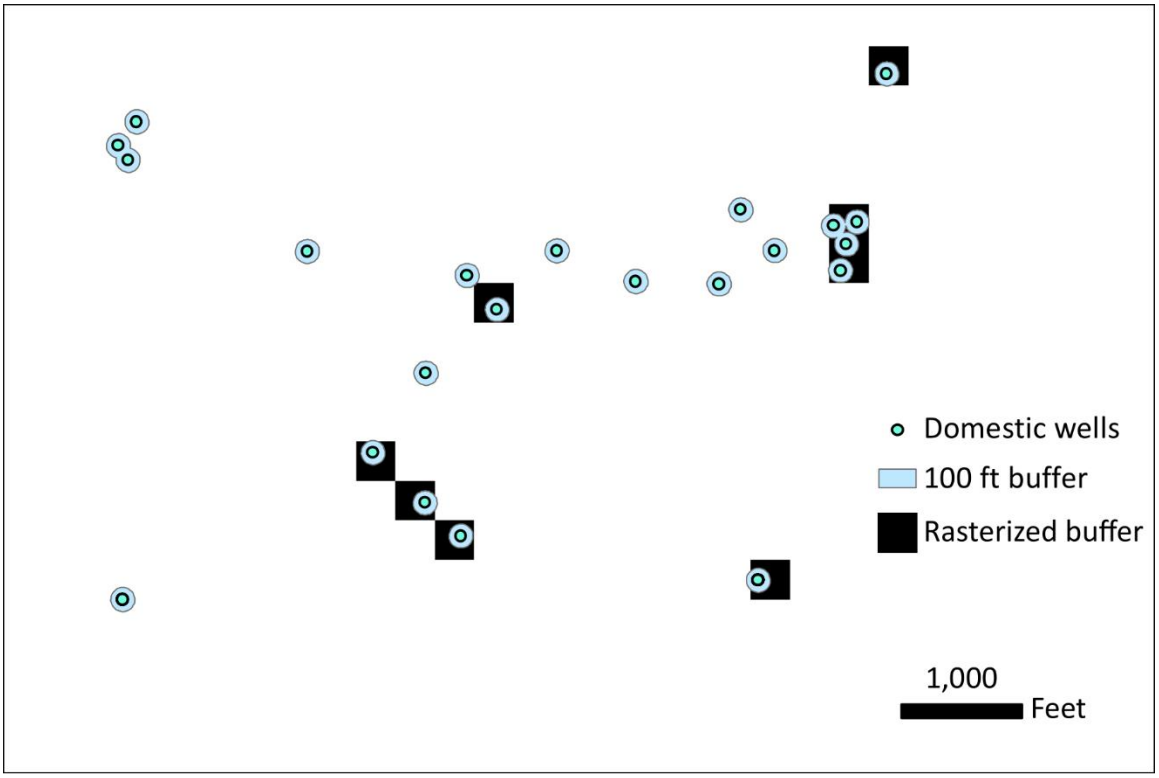

Figure C 6: Example of domestic wells with 100-ft buffers in original and rasterized form.

A.6.3 River buffers

Nodes from which backward tracked particles in ICHNOS reached the surface within a year were considered part of gaining reaches of rivers and therefore in need of protective buffers. A buffer distance was calculated at each of these nodes as:

$$B = 0.5W + D$$

where

B is the buffer distance.

W is the bankfull width.

D is the maximum distance travelled by a particle which was released from the node and reached the surface.

C2VSimFG river lines were split where they coincide with nodes. The resulting segments were given a buffer equal to the average of the values calculated for the nodes at either end.

A.6.4 Source water proximity

A.6.4.1 Previous studies

MAR suitability mapping studies often use a cutoff of 3 or 5 miles for source water proximity, generally citing cost to transport (Table C 6). These studies tend to cite previous studies using the same distance. The earliest sources in the chains of references are Reed and Crites (1984) and Brown et al. (2005). Brown et al. (2005) justifies the 3 mi cutoff based on cost of transport but does not give a reason for the specific number. Reed and Crites (1984) offers suitability scores for a range of distances, and it is not clear where the citing literature obtains the 5 mi (~8 km) cutoff. Several other works are cited for distance limits but do not actually contain any distance criteria.

In order to determine what distance is realistic, 31 MAR projects infiltrating reclaimed water were identified from the INOWAS global MAR map (Table C 7). Assuming that on-site infiltration had a distance of 0 miles, the average distance from reclaimed water source to infiltration site was 3 mi (~4.8 km) (Figure C 7).

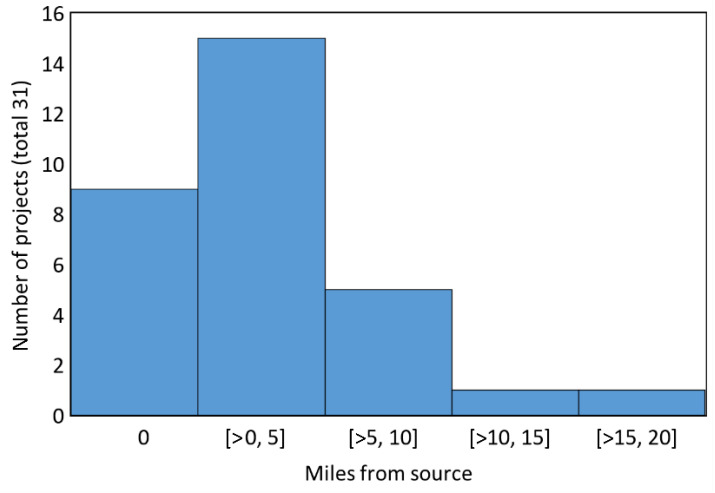

Figure C 7: Distance from reclaimed water source to infiltration locations in 31 MAR projects worldwide.

Table C 6: Review of literature pertaining to or referenced by others regarding maximum distance to source water

Study	Max distance (mi)	Reasoning	References
Gibson et al. (2018)	3	Assumes farther is cost prohibitive	Brown et al. (2016); Brown (2005) References also include Brown et al. (2005)
Tsangaratos et al. (2017)	5	Cost	US EPA (2004)
Smith et al. (2017)	20	None given, but also mentions feasible cities 32 km from aquifers, so the number might have some significance	None given
Ahmadi et al. (2017)	5	EPA guidance	US EPA (2006)
Brown et al. (2016)	None	States that source water availability and distance to surface water are important.	NA
Gdoura et al. (2015)	Stretched	Cost	None cited in text, but references include Anane et al. (2008); US EPA (1984); Kallali et al. (2007); Pedrero et al. (2011); Rahman et al. (2013)
Gibson and Campana (2014)	3	Following Woody (2007)	Woody (2007)
Rahman et al. (2013)	Indirect, probably stretched	Mentions cost of effluent transfer as subcriterion	None cited in text, but references include Anane et al. (2008)
Pedrero et al. (2011)	5	EPA guidance	US EPA (2006)
Anane et al. (2008)	Stretched	Cost	None cited in text, but references include US EPA (1984)
Woody (2007)	3	Cost. Notes that pipelines or canals could be expanded in future	Brown et al. (2005)
Kallali et al. (2007)	5	Cost. Notes that decision makers could choose to go farther	None cited in text, but references include US EPA (1984)
US EPA (2006)	Offers a range of scores. No maximum distance	Cost	Taylor (1981)
Brown et al. (2005)	3	Cost. Also allows 3 miles to canal, which could imply that the presence of conveyance would also satisfy requirement.	None given

Brown (2005)	None	Evaluates decision making process for aquifer storage and recovery projects. States that distance to source water is relevant.	NA
US EPA (2004)	None	Does not mention distance	NA
US EPA (1984)	Offers a range of scores. No maximum distance	Cost	Reed and Crites (1984)
Reed and Crites (1984)	Offers a range of scores. No maximum distance	Cost	None given
Taylor (1981)	None	Does not include table attributed to it by US EPA (2006)	NA

Table C 7: Reclaimed water infiltration projects with source water distance from INOWAS Global MAR Portal (Stefan and Ansems 2018)

Project	Location	Country	Dist. (mi)	Citation
Alice Springs SAT	-23.846, 133.857	Australia	3.7	Page et al. (2010)
Yanchep WWTP	-31.543, 115.648	Australia	0	McFarlane (2019)
Gordon Road WWTP	-32.503, 115.754	Australia	0	McFarlane (2019)
Caddadup WWTP	-32.617, 115.631	Australia	0	McFarlane (2019)
Floreat	-31.949, 115.791	Australia	0.3	Toze and Bekele (2009)
Halls Head	-32.54, 115.693	Australia	0	Toze and Bekele (2009)
Torreele/St-André	51.125, 2.666	Belgium	1.6	Van Houtte and Verbauwhede (2012)
ETE Ponta Negra	-5.897, -35.178	Brazil	0	Lopes and dos Santos (2012)
Gaobeidian WWTP	39.894, 116.526	China	0	Pi and Wang (2006)
Abu Rawash	29.669, 31.26	Egypt	0.1	El-Fakharany (2013)
Soreq-1	31.96, 34.764	Israel	1.2	Kanarek and Michail (1996)
Soreq-2	31.954, 34.769	Israel	1.2	Kanarek and Michail (1996)
Yavne-1	31.893, 34.724	Israel	4.0	Kanarek and Michail (1996)
Yavne-2	31.867, 34.72	Israel	6.2	Kanarek and Michail (1996)
Yavne-3	31.854, 34.713	Israel	6.8	Kanarek and Michail (1996)

Yavne-4	31.848, 34.706	Israel	7.8	Kanarek and Michail (1996)
Sulaibyia	29.282, 47.8	Kuwait	0	Al-Otaibi and Al-Senafy (2004)
Ben Sergao	30.386, -9.609	Morocco	0	Bennani et al. (1992)
Atlantis Water Resource Management Scheme (AWRMS)	-33.59, 18.369	South Africa	2.2	Towers and Hugman (2021)
Sedgefield	-33.907, 22.793	South Africa	0.6	Murray et al. (2010)
Blanes	41.674, 2.772	Spain	0.4	Sendrós et al. (2021)
Korba	36.639, 10.884	Tunisia	0.2	Chaieb (2014)
Nabeul-Hammamet	36.415, 10.635	Tunisia	17.4	Chaieb (2014)
LOTT Hawks Prairie	47.095, -122.813	USA	2.2	Washington Department of Ecology (2017)
Cochrane Park Rehabilitation Project	46.955, -122.666	USA	1.2	City of Yelm, WA n.d.
Whittier Narrows Water Reclamation Plant	34.036, -118.071	USA	2.5	Johnson (2009)
Brooks Street Basin*	34.061, -117.714	USA	8	Campbell (2020); Campbell and Fan (2021)
7th and 8th Street Basins	34.09, -117.635	USA	8	Campbell (2020); Campbell and Fan (2021)
Turner Basins	34.071, -117.6	USA	8	Campbell (2020); Campbell and Fan (2021)
San Sevaine Flood Control Basins	34.146, -117.491	USA	8	Campbell (2020); Campbell and Fan (2021)
Victoria Basin	34.128, -117.508	USA	8	Campbell (2020); Campbell and Fan (2021)
Hickory Basin	34.092, -117.512	USA	8	Campbell (2020); Campbell and Fan (2021)
Banana Basin	34.096, -117.499	USA	8	Campbell (2020); Campbell and Fan (2021)
IEUA RP3 Ponds	34.047, -117.477	USA	8	Campbell (2020); Campbell and Fan (2021)
Ely Basins	34.037, -117.615	USA	8	Campbell (2020); Campbell and Fan (2021)
Kraemer Basin	33.862, -117.857	USA	13	Hutchinson (2013)
Mesa Northwest Water Reclamation Plant (NWWRP)	33.427, -111.68	USA	6.8	Salt River Project n.d.
Fort Dix Land Application Site Infiltration Basin Project	39.976, -74.601	USA	0	Bouwer et al. (2008)
Honouliuli WWTP, OSC Field No. 049 – Sugarcane	21.329, -158.049	USA	0.6	Lau et al. (1989)

*Inland Empire Utilities Agency basin distances estimated. Considered one project for the purposes of average distance to avoid biasing result with uncertain numbers.

A.6.4.2 This study

The locations of water treatment facilities were determined from the 2019 Volumetric Annual Report of Wastewater and Recycled Water (California State Water Resources Control Board 2021). Facilities report volumes of effluent produced along with treatment levels, which can be "Full Advanced Treatment", "Disinfected Tertiary", "Disinfected Secondary-2.2", "Disinfected Secondary-2.3", "Undisinfected Secondary", "Tertiary Treatment", "Secondary Treatment", or "Primary Treatment". Out of these treatment levels, the first five are considered recycled water under Title 22 (California State Water Resources Control Board 2020). Eight facilities were flagged for review because they were designated as not producing recycled water in the Facility table of the report but reported some volume of recycled water in the Effluent table. At two of the flagged facilities, WDR100034219 and WDR100037211, it was observed that each reported 11 months of a single type of non-recycled water effluent and one month of recycled water, suggesting that the one month of recycled water was an error. These two entries were adjusted to match the effluent type for the other months from the respective facilities. All other effluent data was used as is. Facilities were classified by the highest treatment level of effluent that they produced in 2019, as indicated in Table C 8. Four facilities in the CV produced no effluent in 2019 and were excluded from further analysis.

Table C 8: Classification of treatment facilities

Classification	Highest treatment level	Facilities in Central Valley
Disinfected tertiary	Full Advanced Treatment	0
	Disinfected Tertiary	20
Other recycled water	Disinfected Secondary-2.2	3
	Disinfected Secondary-23	6
	Undisinfected Secondary	11
Wastewater	Tertiary Treatment	26
	Secondary Treatment	58
	Primary Treatment	52

The Euclidean distance tool was used to create a raster containing the distance from every location in the Central Valley to the nearest disinfected tertiary facility in the Valley. A second analysis was done including both disinfected tertiary and other recycled water, treating both the same. A third was conducted for all recycled water and wastewater facilities. Any location 3 or more miles (≥ 4.8 km) away from a facility was reassigned a value of 3 miles, as this is assumed to be the farthest that water could be feasibly transported. The locations in both rasters were then scored based on relative distance to the nearest facility with 1 being the farthest and 100 being the closest. Scores were assigned to points by:

$$\text{score} = (\text{maximum distance} - \text{distance at point})/\text{maximum distance} * 99 + 1$$

A.6.5 Compiling maps

A raster of the modified SAGBI for the Central Valley was averaged with the distance score for reclaimed water, giving both layers equal weight. This produced a numeric suitability score for recycled water MAR for the whole Valley. This raster was then multiplied by the land cover, well buffer, and river buffer exclusion rasters to remove areas that are off limits. All rasters had a cell size of 100 m by 100 m. Areas with a value of 0 are removed with the Set Null tool. The result is a raster with suitability scores for all potentially available areas in the Central Valley covered by the modified SAGBI (12% of the Valley does not have a modified SAGBI score). The same analysis was repeated with the distance raster containing both WWTP's and WRF's to evaluate potential for recycled water MAR if existing WWTP's are upgraded or replaced.

A.7. Required land areas and water volumes for MAR

Land areas required for each GSA to meet its stated recharge goals were estimated from the MAR project descriptions in the GSPs. Of the 207 proposed physical MAR projects in the Central Valley, 125 (60%) provided concrete estimates for the amount of land required. If a range of possible areas was provided, we used the minimum estimate. For projects without land areas stated in the GSP, we calculate the mean land area required for that MAR project type (as defined in Ulibarri et al. 2021) from other proposed projects. Lower and upper bounds were calculated for these projects with the formula:

$$\text{lower or upper bound} = \text{mean} \pm 1.96 \text{ standard error}$$

If 1.96 standard error was greater than the mean, then the minimum and maximum areas stated for that type of project were used as lower and upper bounds.

As some projects included multiple recharge approaches, we disaggregated areas where available (e.g., listing separate acreages for basins versus on farm recharge). For creekbed recharge, the GSPs estimated the miles of river, creek, or ditch along which recharge would take place. To convert this to an area, we estimated an average width of 10 ft. (likely an underestimate); the river miles were multiplied by 10 ft. and then converted to acres. Area required for projects intending to recharge with floodwater were calculated but not included in total land requirements used in the main analysis, as these projects would probably not have a need for recycled water. See GSP_MAR_land_area_water.xlsx

Planned average annual recharge volumes were also determined from GSPs with unstated volumes calculated in the same manner as unstated land areas, classifying projects by recharge type. Projects were also classified by water source. If more than one source was listed but disaggregated volumes were not given, the recharge volume associated with the project was assumed to come equally from all sources mentioned.

A.8. Additional results

A.8.1 Wells with residence time greater than one year

Out of the 46,125 wells included in the particle tracking model, 1,086 received surface recharge within one year, and 45,039 did not. Wells at which water had greater than one year of underground residence time are found at high density throughout the Valley except in areas such as the Western San Joaquin Valley, where wells in general are more scarce (Figure C 8).

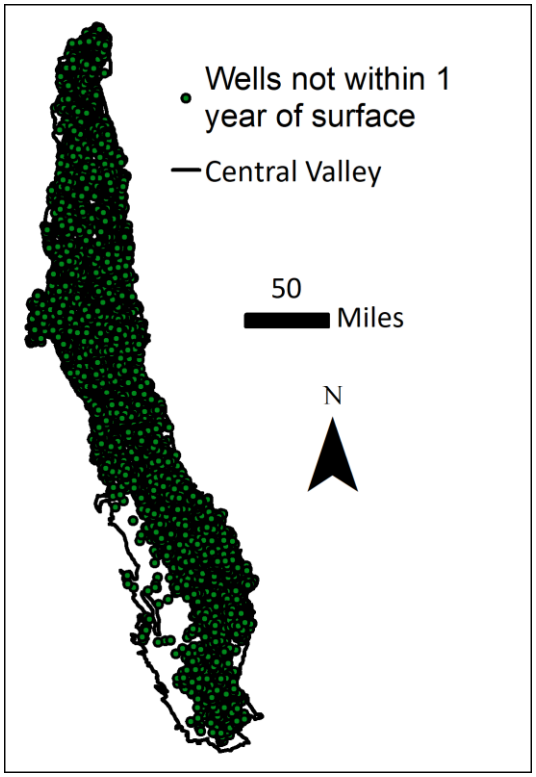

Figure C 8: Wells not receiving surface recharge within a year of its infiltration

A.8.2 Suitability classes shown to scale

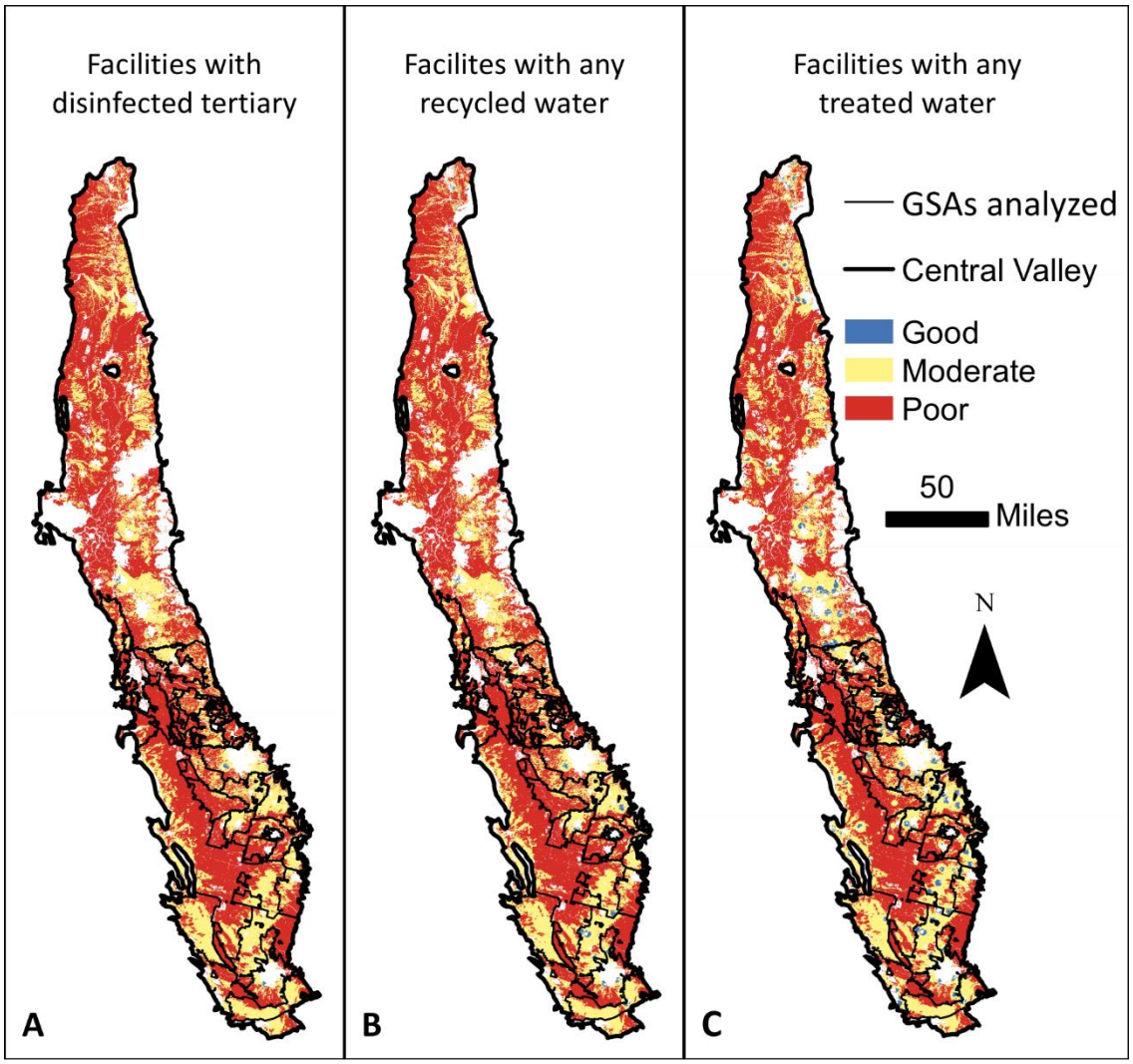

Figure C 9: Suitability of potentially available land considering (A) only facilities producing disinfected tertiary, (B) any facility with recycled water, (C) any treatment facilities, including those with only wastewater. This is the same map as Fig. 5 of the main text without highlighting. All areas are shown to scale.

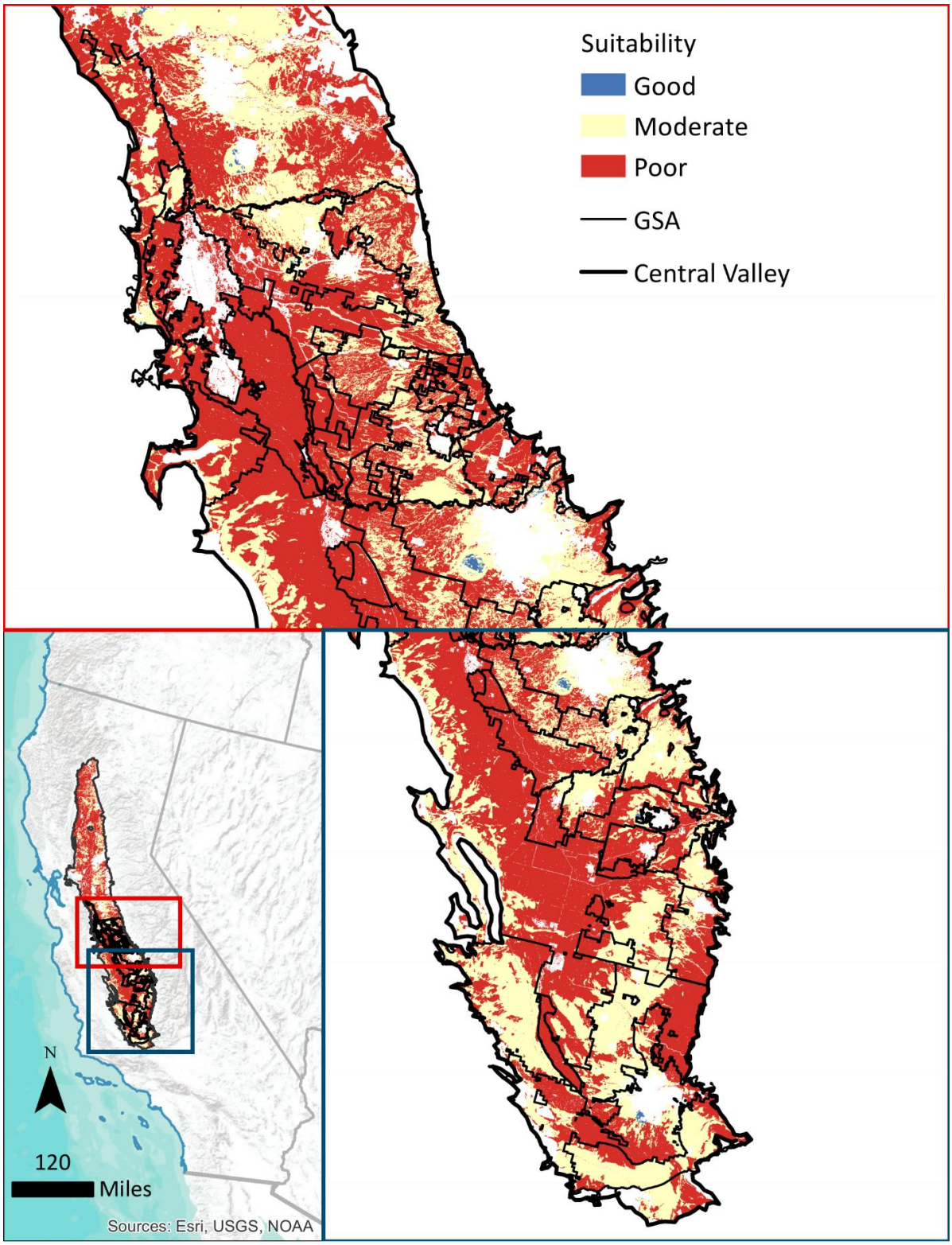

Figure C 10: Close up of suitability considering only treatment facilities producing disinfected tertiary water as potential sources of recharge water

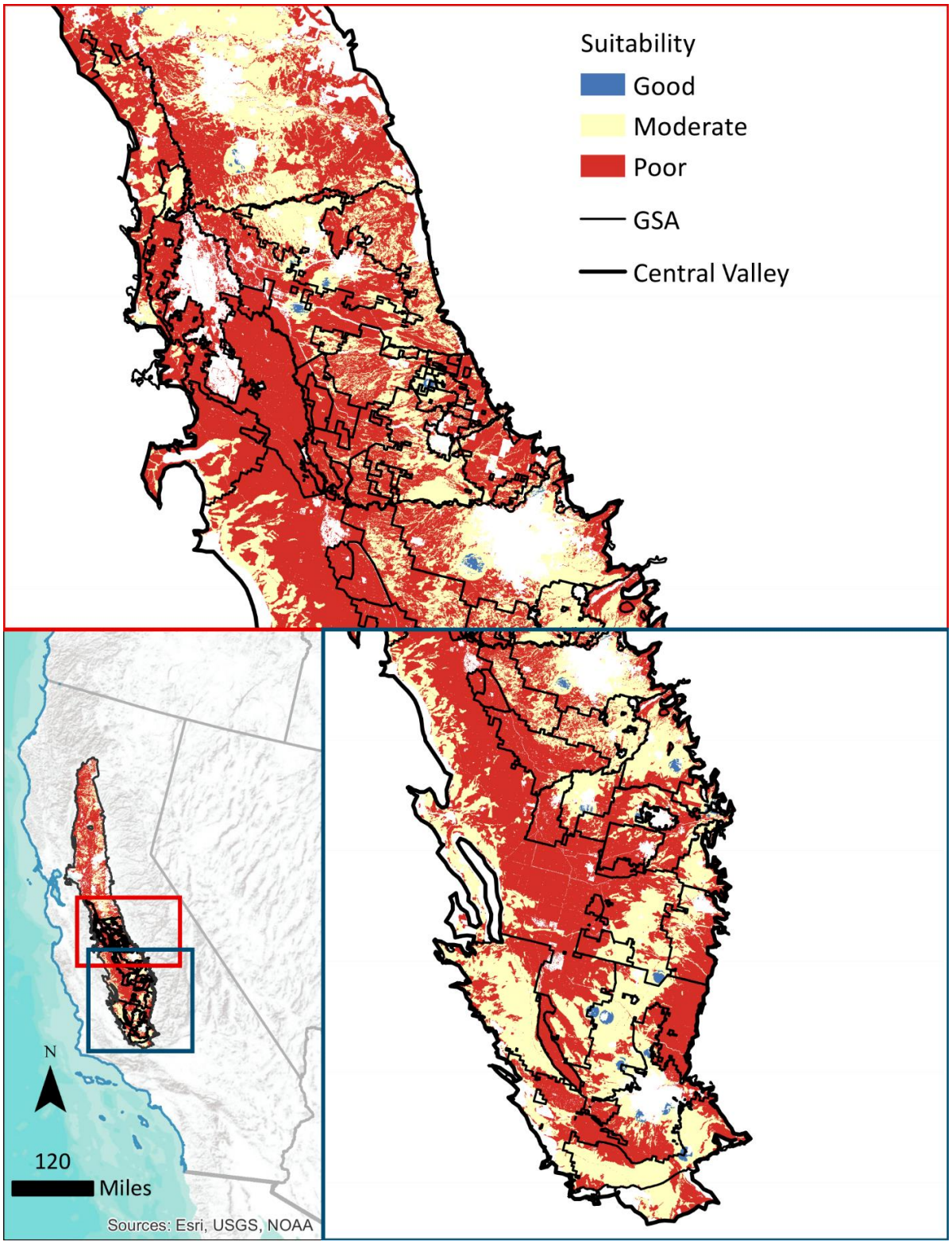

Figure C 11: Close up of suitability considering treatment facilities producing any kind of recycled water as potential sources of recharge water

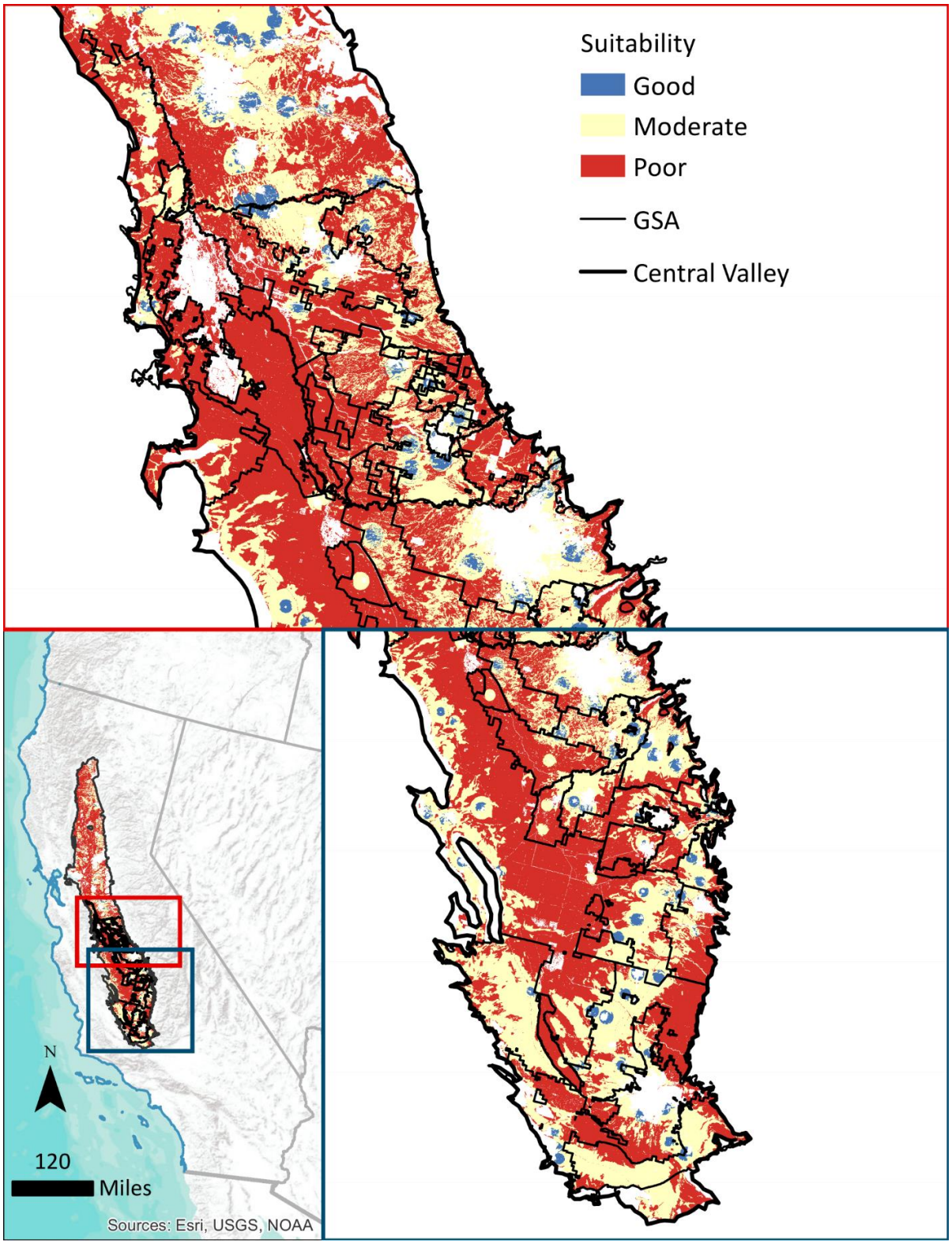

Figure C 12: Close up of suitability considering any treatment facilities, including those only producing wastewater, as potential sources of recharge water

A.8.3 Land use

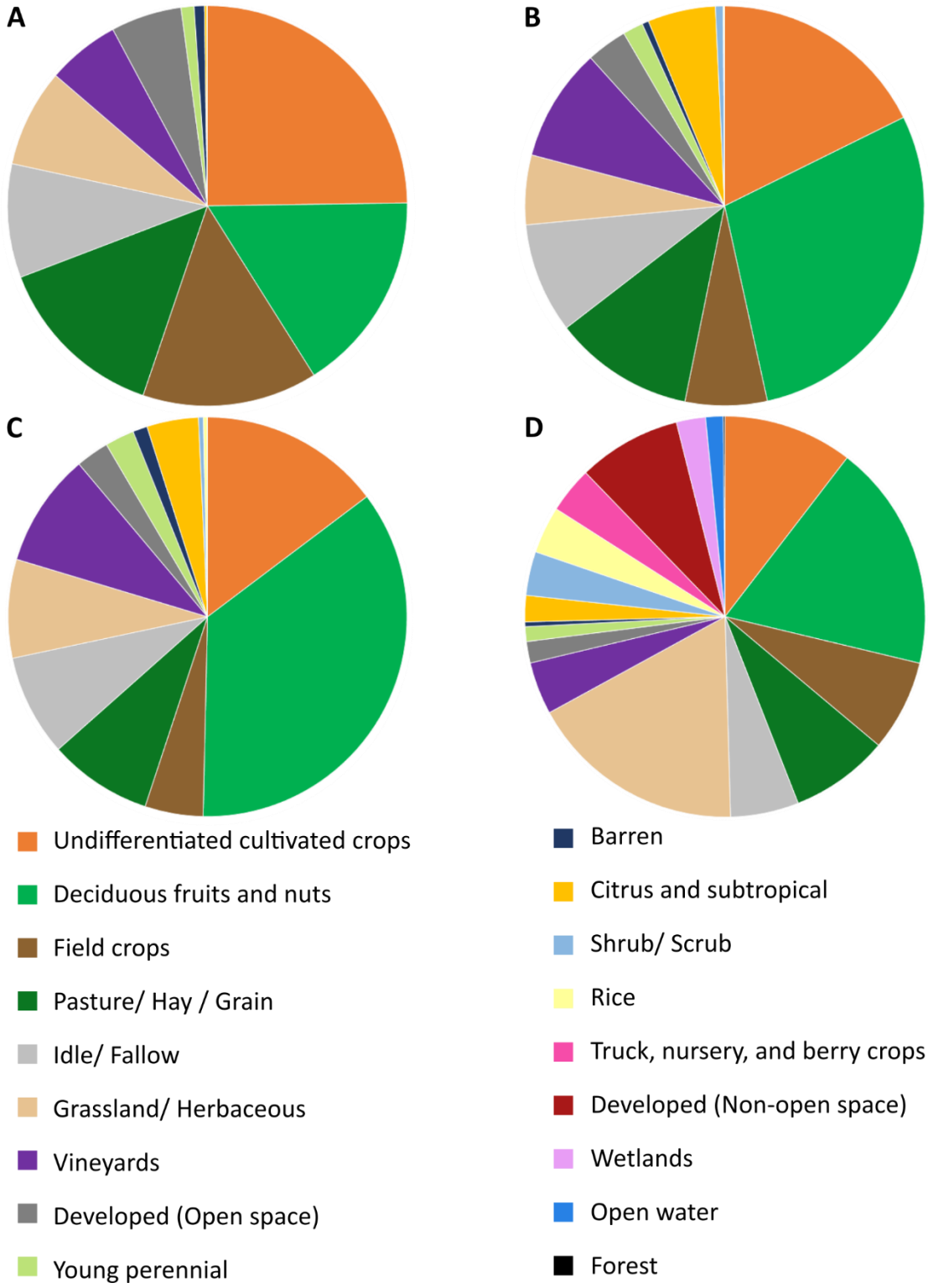
A
B
C
D
Undifferentiated cultivated crops
Deciduous fruits and nuts
Field crops
Pasture/ Hay / Grain
Idle/ Fallow
Grassland/ Herbaceous
Vineyards
Developed (Open space)
Young perennial
Barren
Citrus and subtropical
Shrub/ Scrub
Rice
Truck, nursery, and berry crops
Developed (Non-open space)
Wetlands
Open water
Forest

Figure C 13: Land use in good suitability areas considering facilities with (A) disinfected tertiary only (B) any recycled water (C) any effluent. (D) Shows the entire Central Valley. Legend items are listed clockwise. Developed (Non-open space), Wetlands, Open water, and Forest are present in the Central Valley but not in good suitability areas as they were excluded from consideration.

A.9. Alternatives

A.9.1 Chemical contaminants

A version of the suitability analysis was conducted including estimated arsenic and nitrate concentrations in groundwater using data from the USGS (McKinney 2012). Concentrations in the USGS geospatial dataset were given as ranges for 3 km x 3 km (1.8 mi x 1.8 mi) cells (Figure C 13). Lower concentrations of both chemicals are better, and neither is acceptable above its respective drinking water maximum contaminant level (MCL) (10 ug/L arsenic, 10 mg/L nitrate - N). Numerical suitability scores were assigned to each cell based on its concentration range. The lowest concentration range received a score of 100. Any concentrations greater than or equal to the MCL were given a score of 1. Intermediate scores were assigned proportionally to other cells based on the midpoint of their range (Table C 9). The arsenic and nitrate scores were then averaged for a combined chemical contaminant score. The chemical contaminant score was then averaged with the SAGBI and source water proximity scores to determine relative suitability. Additionally, any cell for which either compound was predicted to be present above its MCL was excluded as unsuitable. The remaining steps were conducted in the same manner as the main analysis. Results are shown below. Due to the lower resolution and less extensive coverage of the arsenic and nitrate geospatial data, the resulting map is less detailed and includes 20% less area than that produced by the main analysis (Figure C 14, Table C 9).

Table C 9: Concentration ranges for arsenic and nitrate with assigned suitability scores

Arsenic range (ug/L)	Arsenic score	Nitrate range (mg/L as N)	Nitrate score
<1.0	100	<0.50	100
1.0 – 1.9	95	0.50 – 0.99	97
2.0 – 2.9	84	1.0 – 1.9	90
3.0 – 4.9	68	2.0 – 4.9	69
5.0 – 9.9	29	5.0 – 9.9	28
10 – 24	1	≥10	1
≥25	1		

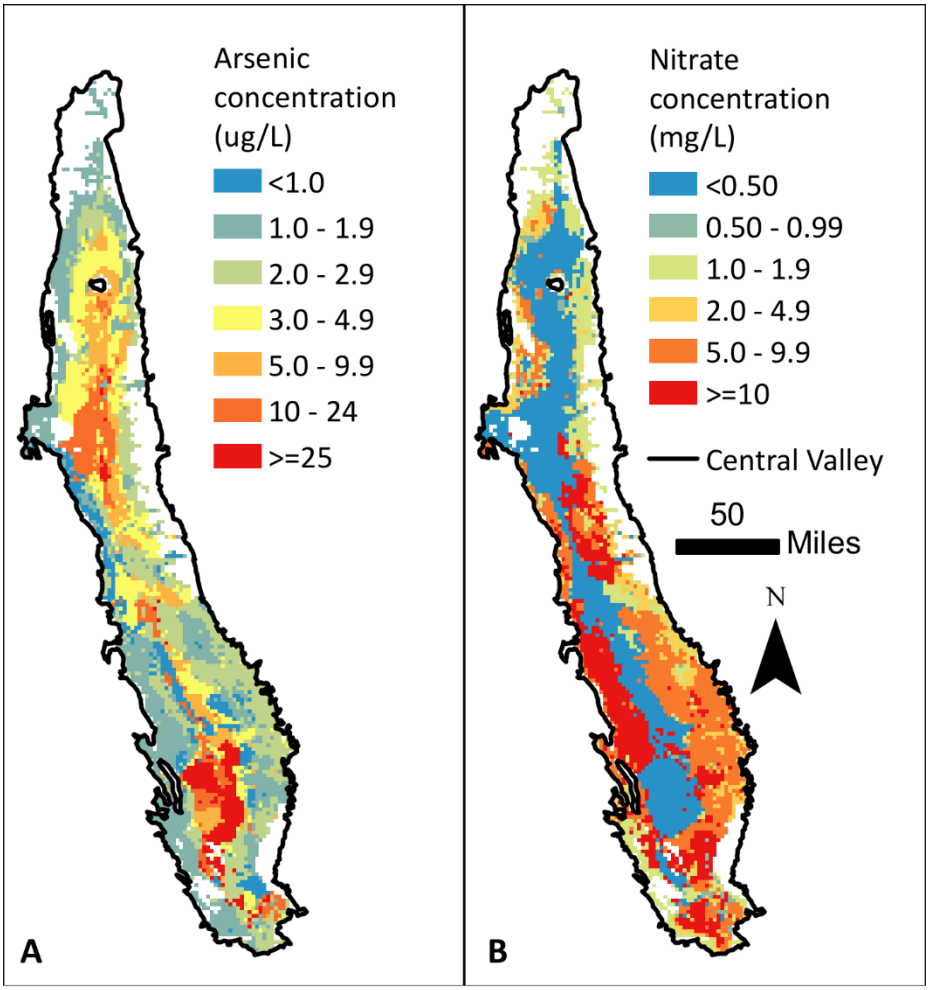

Figure C 14: Arsenic and nitrate concentrations predicted in Central Valley groundwater by McKinney (2012).

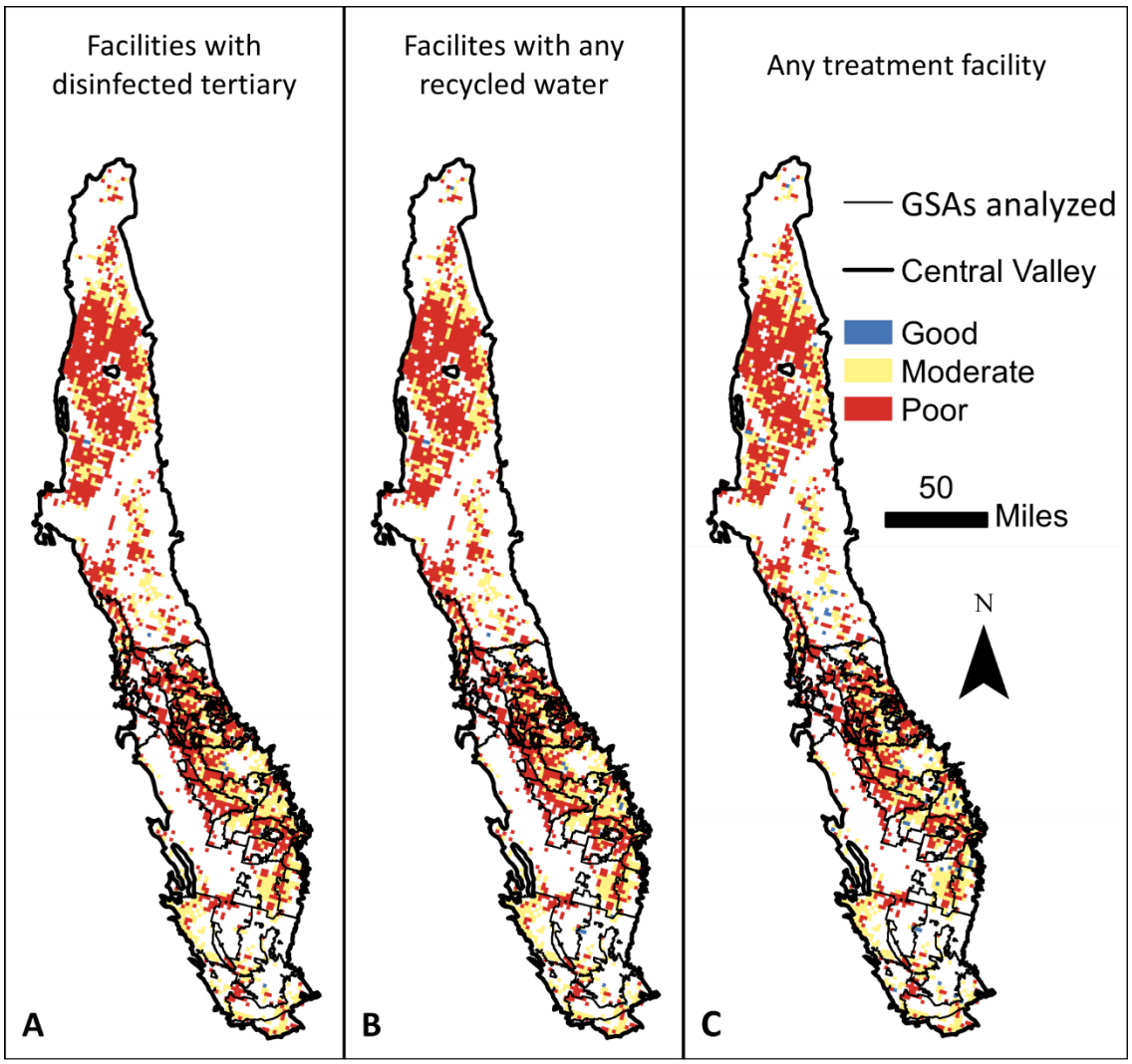

Figure C 15: Suitability of potentially available land considering chemical contaminants. (A) Only facilities producing disinfected tertiary, (B) any facility with recycled water, (C) any treatment facilities, including those with only wastewater as water sources.

Table C 10: Area (mi^2) available to each GSA by suitability considering chemical contaminants. (1 mi^2 = 2.6 km^2)

GSA	Disinfected tertiary			Any recycled water			Any effluent		
	Good	Moderate	Poor	Good	Moderate	Poor	Good	Moderate	Poor
Aliso Water District	0	3.5	28	0	3.5	28	0	3.5	28
Buena Vista	0	3.5	17	0	3.5	17	0	6.9	14
Central Kings	0	140	45	0	140	45	35	100	42
Chowchilla Water District	0	42	73	0	42	73	3.5	42	69
East Kaweah	0	76	59	3.5	73	59	10	73	52
Eastern Tule	0	76	42	0	80	38	6.9	73	38

Gravelly Ford Water District	0	3.5	10	0	3.5	10	0	3.5	10
Greater Kaweah	3.5	49	150	3.5	56	140	3.5	63	140
James Irrigation District	0	0	45	0	0	45	0	6.9	38
Kern Groundwater Authority	0	410	160	10	410	150	10	410	150
Kings River East	0	160	80	6.9	150	80	14	150	76
Madera County - Chowchilla	0	14	56	0	14	56	0	17	52
Madera County - Madera	0	73	170	0	87	160	3.5	97	140
Madera Irrigation District	0	87	94	0	90	90	6.9	100	73
Madera Irrigation District, City of Madera	0	0	3.5	0	0	3.5	0	3.5	0
McMullin	0	56	120	0	56	120	0	69	100
Merced County	0	0	3.5	0	0	3.5	0	0	3.5
Merced Subbasin	0	80	180	3.5	87	170	6.9	90	170
Mid Kaweah	0	28	56	0	28	56	0	38	45
Mid Kings River	0	73	24	0	73	24	6.9	66	24
New Stone Water District	0	0	6.9	0	0	6.9	0	0	6.9
North Fork Kings	0	42	160	0	42	160	3.5	49	150
North Kings	6.9	170	110	6.9	170	110	14	170	110
Northern & Central Delta-Mendota	0	49	130	0	49	130	3.5	56	120
San Joaquin River Exchange Contractors Water Authority	0	28	170	0	28	170	6.9	28	160
South Fork Kings	0	10	21	0	10	21	0	10	21
South Kings	0	10	0	0	10	0	3.5	6.9	0
Tri-County Water Authority	0	10	0	0	10	0	0	10	0
Triangle T Water District	0	3.5	17	0	3.5	17	0	3.5	17
Central Valley	24	3400	5600	63	3500	5500	300	3600	5100

A.9.2 Porosity

The default porosity used by ICHNOS is 10%. The model was also run with porosities of 20% and 30% for sensitivity analysis. Increasing porosity decreased the number of particles exiting the model domain within one year (Figure C 15). This is in agreement with Darcy's law, which states that linear velocity is inversely proportional to porosity. The total number of wells receiving surface recharge within a year decreased from 1086 with 10% porosity to 408 with 20% porosity and 227 with 30% porosity. None of the scenarios

change which of the GSA's have enough suitable land to meet their recharge goals with recycled water MAR.

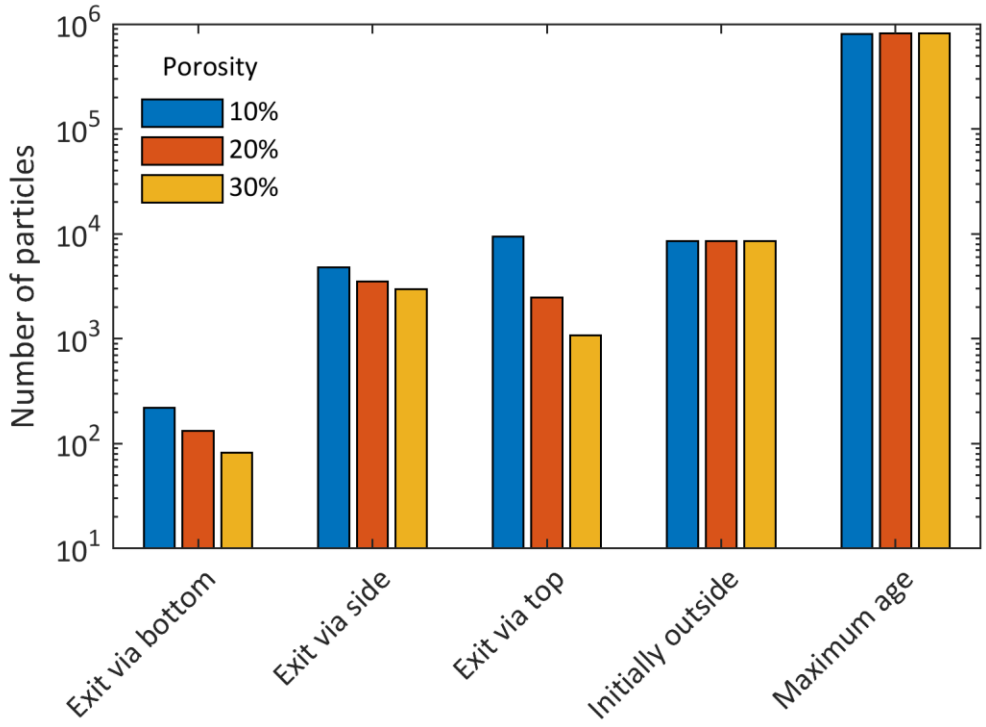

Figure C 16: Fate of particles in ICHNOS model runs with varying porosity. Particles exiting via the top of the model indicate a path along which a well receives surface recharge. A total of 830,250 particles were modeled.

A.9.3 Fully screened wells

The screen depth of a well plays a significant role in determining when water is captured (McDermott et al. 2008). Nevertheless, leaks in the casing could result in water entering the well from units in which it is not screened. To account for this, a scenario was modeled in ICHNOS in which all wells were assumed to have screens starting one meter below the top of the model domain and continuing down to the recorded or estimated screen bottom depth. The one meter offset from the top reduces the likelihood of errors from particles being released outside of the model domain.

Under this scenario, 11,271 wells received surface recharge within a year, resulting in an additional 2 mi^2 (5.1 km^2) of buffered area after the 100-ft default buffers for domestic wells are considered for both scenarios.

A.9.4 Natural breaks classification

Classification of recycled water MAR suitability scores was done by both equal intervals and natural breaks, with equal intervals ultimately being selected and reported in the main text. Breaks are shown in , and results of the natural breaks classification are shown in Table C 11. Natural breaks rates more areas as good and fewer as poor than equal intervals does (Table C 12, Figure C 16). Additionally, natural breaks rates more land as good when the number of potential recharge sources is lower (i.e. plants with disinfected tertiary vs any facility). This result is not logical in context and demonstrates why the use of equal interval is a more suitable form of analysis.

Table C 11: Classification breaks for recycled water MAR suitability scores

Facilities with disinfected tertiary		Facilities with any recycled water		Any treatment facility	
natural breaks	equal interval	natural breaks	equal interval	natural breaks	equal interval
35.45	33.27	35.45	33.27	21.45	33.61
47.76	66.03	47.76	66.03	43.95	66.71

Table C 12: Area (mi^2) available to each GSA of good, moderate, and poor recycled water MAR suitability using natural breaks. (1 mi^2 = 2.6 km^2)

GSA	Facilities with disinfected tertiary			Facilities with any recycled water			Any treatment facility		
	Good	Moderate	Poor	Good	Moderate	Poor	Good	Moderate	Poor
Aliso Water District	5.4	12	24	5.4	12	24	0.9	17	23
Buena Vista	0.11	0.37	79	0.11	0.37	79	1.8	10	67
Central Kings	160	59	9	150	63	9.0	150	59	13
Chowchilla Water District	30	48	48	31	47	48	24	58	44
East Kaweah	73	50	46	46	80	43	53	76	41
Eastern Tule	72	26	120	38	62	120	29	82	110
Gravelly Ford Water District	3.2	3.5	6.4	3.2	3.5	6.4	1.3	5.4	6.4
Greater Kaweah	83	100	130	82	110	130	35	170	110
James Irrigation District	0.43	0.62	42	0.43	0.62	42	1.9	12	29
Kern Groundwater Authority	640	430	400	630	450	400	330	710	420
Kings River East	150	47	76	120	69	76	100	95	68
Madera County - Chowchilla	6.9	27	32	8.5	25	32	5.7	28	32

Madera County - Madera	32	120	88	43	110	88	38	120	86
Madera Irrigation District	60	110	34	67	100	34	70	110	21
Madera Irrigation District, City of Madera	1.6	1.8	0.63	1.6	1.8	0.63	3.5	0.63	0.019
McMullin	36	110	44	33	110	44	40	91	55
Merced County	1.3	0.47	0.02	1.3	0.47	0.02	0.12	1.7	0.023
Merced Subbasin	50	200	210	57	210	200	58	210	190
Mid Kaweah	19	50	49	19	50	49	10	69	38
Mid Kings River	76	51	7.8	80	47	7.6	36	90	8.6
New Stone Water District	0.015	1.3	5.2	0.015	1.3	5.2	0	1.3	5.2
North Fork Kings	35	50	170	34	51	170	33	57	170
North Kings	140	130	42	120	150	42	110	170	37
Northern & Central Delta-Mendota	36	170	200	34	170	200	21	180	210
San Joaquin River Exchange Contractors Water Authority	14	73	300	13	74	300	11	93	280
South Fork Kings	17	8.1	77	17	8.1	77	7.5	43	51
South Kings	2.3	0.64	0.54	2.2	0.74	0.54	2.9	0.55	0.062
Tri-County Water Authority	18	24	52	18	24	52	17	25	52
Triangle T Water District	0.097	3.6	19	0.097	3.6	19	0	3.7	19
Central Valley Total	3900	5200	7600	3500	5600	7600	2800	6500	7400

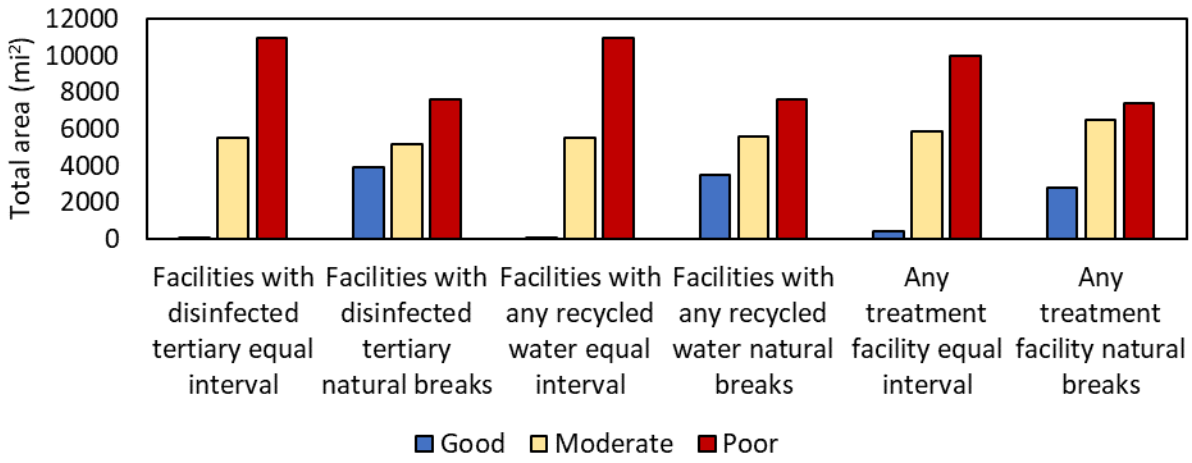

Figure C 17: Area of good, moderate, and poor recycled water MAR suitability for the whole Central Valley with classification by equal interval and natural breaks. (1 mi^2 = 2.6 km^2)

A.9.5 Darcy's law well buffers

Particle tracking results in residence time-based buffers for only some wells. These buffers are irregularly shaped and tend to trace a narrow track. For a simpler scenario in which all wells are buffered by approximate residence time, circular buffers can be created with Darcy's law.

$$v = \frac{K \frac{dh}{dl}}{n}$$

where *v* is linear velocity, *K* is hydraulic conductivity, *dh/dl* is hydraulic gradient, and *n* is porosity. For this scenario, hydraulic conductivity was taken from the top stratigraphic layer of C2VSimFG version 1.1. Water elevation point measurements from fall 2015 are taken from the SGMA data viewer and interpolated to form a water table (DWR n.d.). Unfortunately, measurements are not available for the entire study area, so the following analysis is restricted to the area where water level measurements are available. The slope of the water table at each well is used for the magnitude of the local hydraulic gradient, using the simplifying assumption that the slope of the overall water table is more significant than any cone of depression caused by the wells. Maximum and minimum shallow groundwater velocities are then calculated at each well location using the minimum and maximum porosities reported by Bertoldi et al. (1991). These velocities are multiplied by one year, and the resulting distances are used to create circular buffers around each well. The results are shown in Table C 13 and Table C 14.

This method assumes that shallow groundwater reaching the horizontal location of a well could be captured by it regardless of screen depth. This assumption can be useful in the event of leaks in a well's casing or vertical transmission of water within the borehole, but it also excludes areas for the protection of wells that may not receive any local surface recharge. Under Title 22, basic conceptual models such as Darcy's law receive only 0.25 credits for virus removal (State of California 2018). Thus, to demonstrate that a desired area is truly suitable for recycled water MAR, either the travel time must be extended to two years, or more detailed analysis must be performed.

Table C 13: Suitable land by subbasin using Darcy's law for well buffers, assuming maximum porosity (note that only areas with water level measurements are included).

GSA	Maximum porosity (0.65)								
	Facilities with disinfected tertiary			Facilities with any recycled water			Any treatment facility		
	Good	Moderate	Poor	Good	Moderate	Poor	Good	Moderate	Poor
Aliso Water District	0	7.6	33	0	7.6	33	0.03	7.8	33
Buena Vista	0	0.062	15	0	0.062	15	0	0.47	14

Central Kings	0	160	65	0	160	65	23	150	49
Chowchilla Water District	0	44	74	0	46	73	2.2	49	67
East Kaweah	0	83	43	0.87	84	41	9.8	78	38
Eastern Tule	0	54	36	0.32	54	36	4.1	54	33
Gravelly Ford Water District	0	3.5	9.5	0	3.5	9.5	0	3.5	9.5
Greater Kaweah	2.2	73	190	2.9	73	180	3.4	82	170
James Irrigation District	0	0.83	42	0	0.83	42	0	6.7	36
Kern Groundwater Authority	0	300	140	17	290	140	27	280	140
Kings River East	0	140	65	5.8	140	63	19	130	59
Madera County - Chowchilla	0	13	51	0	15	49	0.07	16	48
Madera County - Madera	0.11	37	120	1.3	46	110	4.4	52	110
Madera Irrigation District	0	100	88	0.93	110	83	14	120	62
Madera Irrigation District, City of Madera	0	1.9	2.1	0	1.9	2.1	1.7	2.1	0.15
McMullin	0	73	110	0	73	110	4.5	76	100
Merced County	0	1.7	0.13	0	1.7	0.13	0	1.7	0.13
Merced Subbasin	0.78	52	210	3.3	63	190	7.9	67	190
Mid Kaweah	0.88	18	97	0.88	18	97	1.4	25	89
Mid Kings River	0	7.2	5.2	0	7.2	5.2	0	7.2	5.2
New Stone Water District	0	0.31	6.2	0	0.31	6.2	0	0.31	6.2
North Fork Kings	0	35	220	0	35	220	1.1	43	210
North Kings	5.7	140	120	5.7	140	120	16	140	110
Northern & Central Delta-Mendota	0	57	170	0	57	170	0.40	68	160

San Joaquin River Exchange Contractors Water Authority	0	23	350	0	23	350	0.16	32	340
South Fork Kings	0	6.5	7.7	0	6.5	7.7	0	6.5	7.7
South Kings	0	2.9	1.1	0	2.9	1.1	1.6	2.0	0.4
Tri-County Water Authority	0	16	7.8	0	16	7.8	0	16	7.8
Triangle T Water District	0	0.84	22	0	0.84	22	0	0.84	22
Central Valley Total	20	3800	7000	66	3800	6900	330	4000	6400

Table C 14: Suitable land by subbasin using Darcy's law for well buffers, assuming minimum porosity (note that only areas with water level measurements are included).

GSA	Minimum porosity (0.25)								
	Facilities with disinfected tertiary			Facilities with any recycled water			Any treatment facility		
	Good	Moderate	Poor	Good	Moderate	Poor	Good	Moderate	Poor
Aliso Water District	0	7.6	33	0	7.6	33	0.027	7.8	33
Buena Vista	0	0.062	15	0	0.062	15	0	0.47	14
Central Kings	0	160	66	0	160	66	23	150	50
Chowchilla Water District	0	47	77	0	49	75	2.8	52	69
East Kaweah	0	85	43	0.88	86	42	10	80	39
Eastern Tule	0	55	36	0.32	55	36	4.2	54	33
Gravelly Ford Water District	0	3.5	9.6	0	3.5	9.6	0	3.5	9.6
Greater Kaweah	2.2	74	190	2.9	74	190	3.4	84	180
James Irrigation District	0	0.83	42	0	0.83	42	0	6.7	36
Kern Groundwater Authority	0	300	140	17	290	140	27	280	140

Kings River East	0	140	65	5.9	140	63	19	130	59
Madera County - Chowchilla	0	13	52	0	16	50	0.069	16	49
Madera County - Madera	0.12	38	130	1.4	47	120	4.4	54	110
Madera Irrigation District	0	110	89	0.93	110	84	14	120	63
Madera Irrigation District, City of Madera	0	1.9	2.1	0	1.9	2.1	1.7	2.1	0.15
McMullin	0	73	110	0	73	110	4.5	77	100
Merced County	0	1.7	0.13	0	1.7	0.13	0	1.7	0.13
Merced Subbasin	0.78	52	210	3.3	63	200	8	67	190
Mid Kaweah	0.88	18	98	0.88	18	98	1.4	26	90
Mid Kings River	0	7.3	5.2	0	7.3	5.2	0	7.3	5.2
New Stone Water District	0	0.31	6.2	0	0.31	6.2	0	0.31	6.2
North Fork Kings	0	35	220	0	35	220	1.1	44	210
North Kings	5.9	140	120	5.9	140	120	17	140	110
Northern & Central Delta-Mendota	0	58	170	0	58	170	0.40	68	160
San Joaquin River Exchange Contractors Water Authority	0	23	350	0	23	350	0.16	32	350
South Fork Kings	0	6.6	7.7	0	6.6	7.7	0	6.6	7.7
South Kings	0	2.9	1.1	0	2.9	1.1	1.6	2.0	0.4
Tri-County Water Authority	0	16	7.8	0	16	7.8	0	16	7.8
Triangle T Water District	0	0.85	22	0	0.85	22	0	0.85	22

Central Valley Total	20	3800	7000	66	3800	6900	340	4100	6400

A.9.6 On-farm versus not on-farm recharge

Seven GSAs have plans for recharge on farmland. The land required for these projects is included with all of the other land requirements in the main analysis; however, since on-farm recharge would not require land fallowing while other types would, it may be worthwhile to view them separately. Analysis was conducted considering all available land for all needs except on-farm recharge; this assumes that necessary land will be converted to basins regardless of current use (Figure C 17). A second analysis was conducted considering only agricultural land and only on-farm recharge needs (Figure C 18). While McMullin and Kern GSAs do not have enough suitable land to meet all of their recharge goals with recycled water MAR, they do have enough to meet either their on-farm *or* not on-farm goals. All of the GSAs planning on-farm recharge have enough suitable farmland except for North Fork Kings, but only Greater Kaweah and North Kings can meet their on-farm needs solely with land surrounding treatment facilities currently producing disinfected tertiary water.

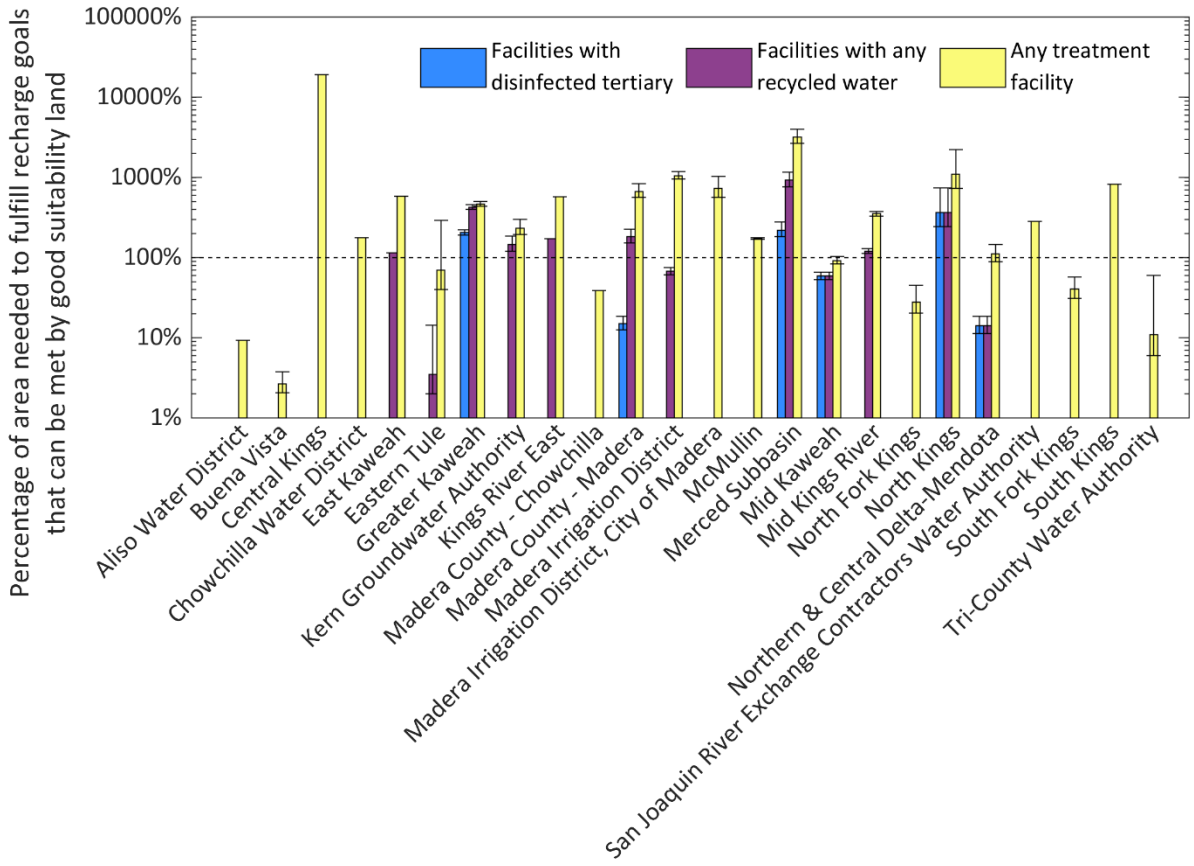

Figure C 18: Land with proximity to facility assessment, excluding on-farm needs. Percentage of area needed by each GSA to fulfill recharge goals for projects not classified as

on-farm that can be met by good suitability land considering proximity to different types of treatment facilities (e.g., facilities with disinfected tertiary, facilities with any recycled water, and facilities with any treated water). Some Plans did not explicitly state land needs; for these Plans, we estimated a mean, min, and max amount of land based on proposed MAR projects. For these GSAs, bar represent the mean land; minimum and maximum estimated land requirements are shown with error bars. GSAs without suitable area not shown. Dashed line indicates 100% of area needed to fulfill recharge goals can be met by good suitability land within proximity to treatment facilities.

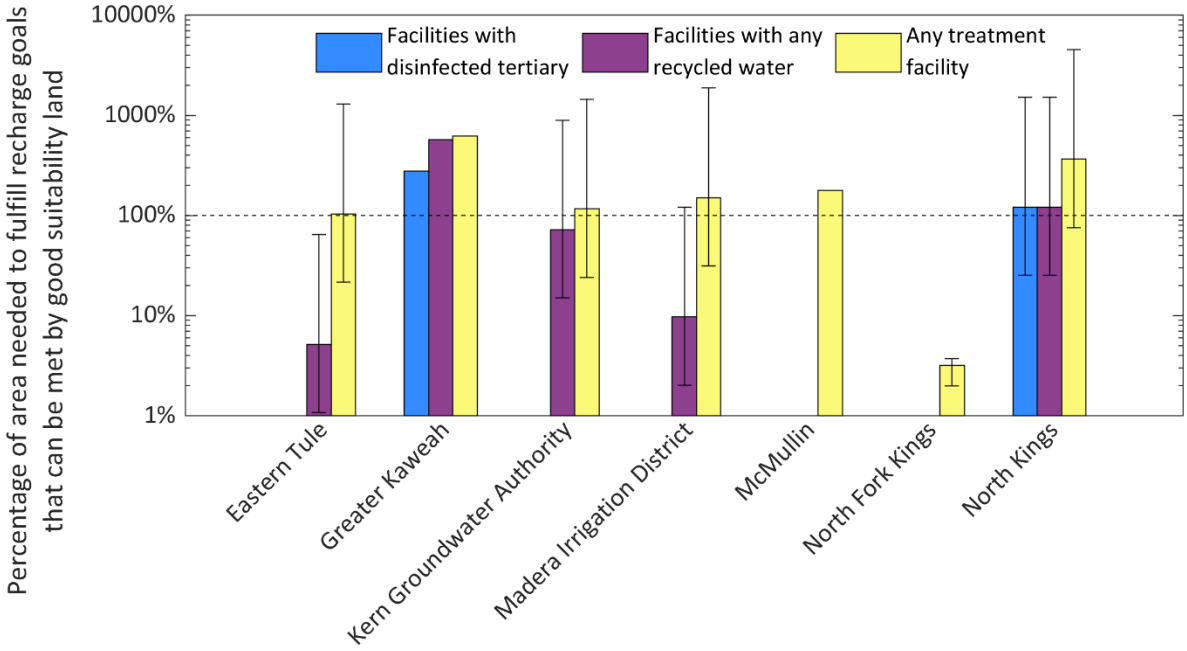

Figure C 19: Land with proximity to facility assessment for on-farm recharge. Percentage of area needed by each GSA to fulfill recharge goals for projects classified as on-farm that can be met by good suitability land considering proximity to different types of treatment facilities (e.g., facilities with disinfected tertiary, facilities with any recycled water, and facilities with any treated water). Some Plans did not explicitly state land needs; for these Plans, we estimated a mean, min, and max amount of land based on proposed MAR projects. For these GSAs, bar represent the mean land; minimum and maximum estimated land requirements are shown with error bars. GSAs without suitable area not shown. Dashed line indicates 100% of area needed to fulfill recharge goals can be met by good suitability land within proximity to treatment facilities.

A.9.7 Differentiating water needs by project

MAR projects described in GSPs were classified as ASR/injection, Banking, Basin, Basin and flood, Creek bed, Dry well, FloodMAR, On-Farm, Physical, Both in-lieu and physical, or No information. Water sources were classified as Central Valley Project, State Water Project, Local surface water, Imported water, Recycled water, Stormwater, or Other.

The main analysis considers water needed for projects classified as anything other than ASR/injection, Dry well, or FloodMAR for consistency with the land needs analysis.

Alternative analyses were conducted considering different types of projects or water sources as a sensitivity analysis. For the first alternative, the same set of projects was considered except that on-farm recharge projects were also excluded, in order to only evaluate projects likely to require land fallowing (Figure C 20). The second alternative considers all water needs except those that the GSPs state will be met by stormwater, since stormwater projects are frequently intended to manage a sudden influx of water that will be problematic if not used, as opposed to competing for treated water for which there are many other possible uses (Figure C 21). The third alternative considers the total water needs for all projects, which is the most conservative evaluation (Figure C 22). All three alternatives give the same results as the main analysis in terms of which GSAs will have sufficient water based on explicitly stated water needs plus average needs assumed for projects that do not give a number (see Section 7 for water needs calculations). There is some variation in how close the GSAs come to meeting 100% of their needs.

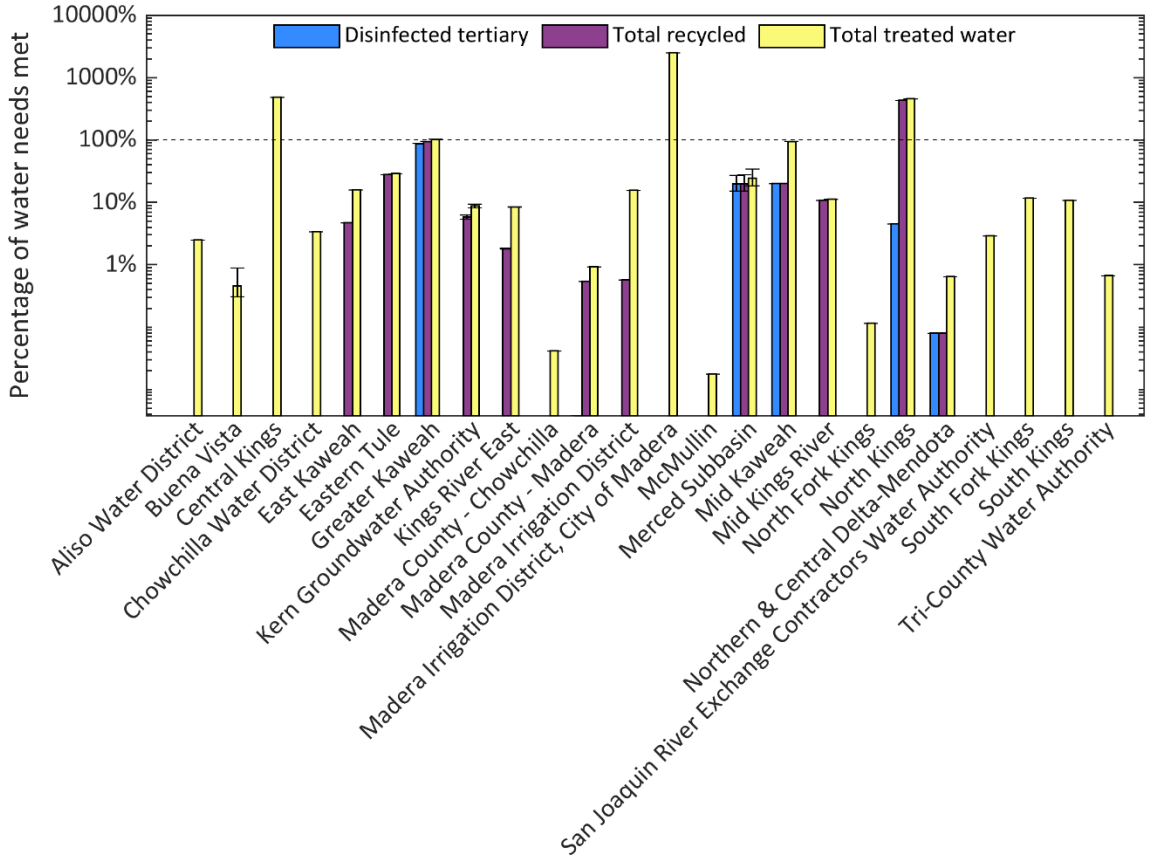

Figure C 20: Percentage of water needs met for surface recharge projects that are not considered on-farm.

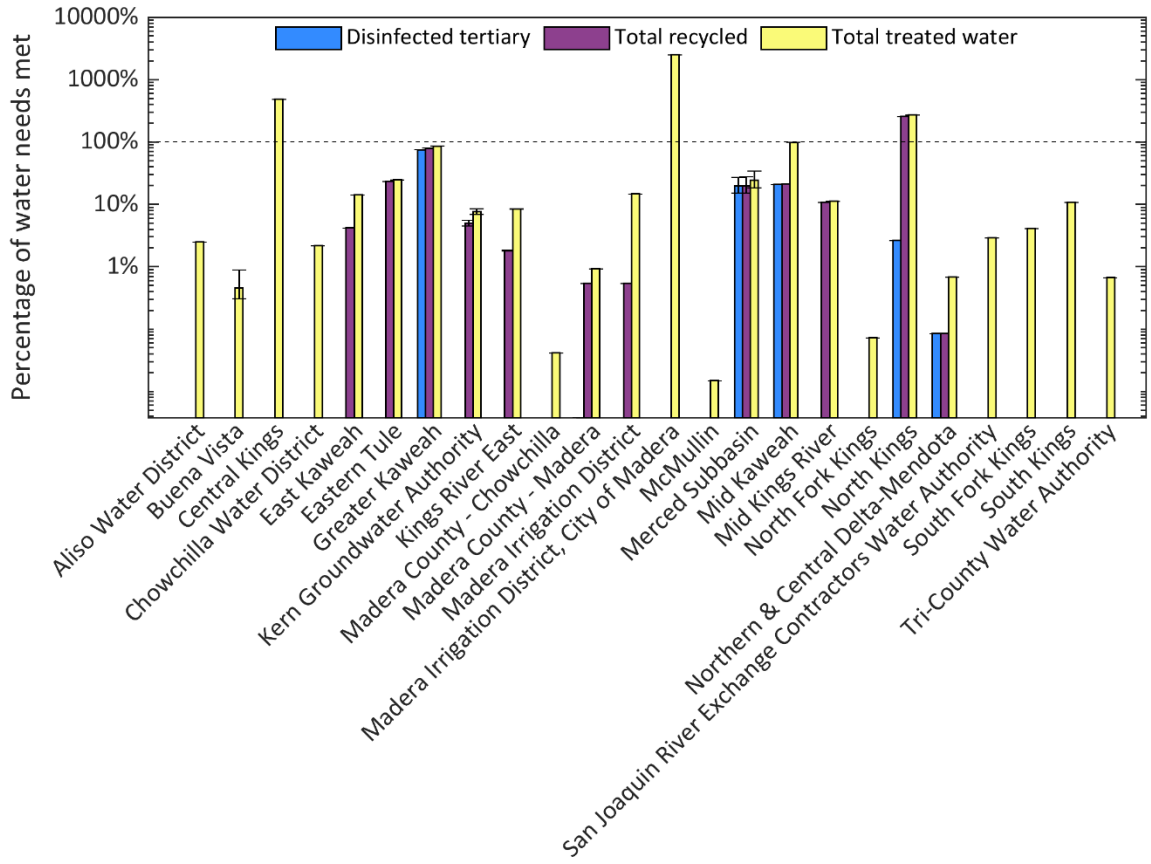

Figure C 21: Percentage of water needs met excluding stormwater needs.

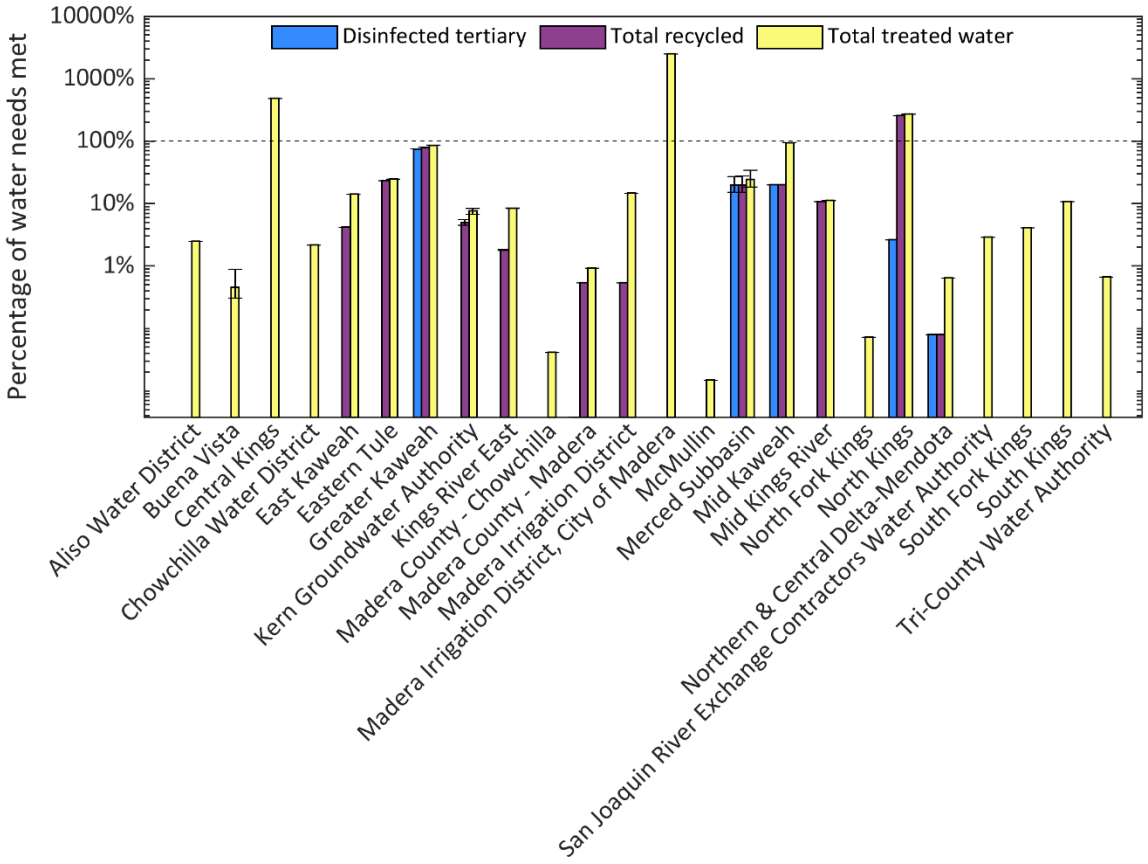

Figure C 22: Percentage of total water needs met.

A.10. References

Ahmadi MM, Mahdavirad H and Bakhtiari B. 2017. Multi-criteria analysis of site selection for groundwater recharge with treated municipal wastewater. Water Sci Technol, 76. doi:10.2166/wst.2017.273.

Al-Otaibi M and Al-Senafy M. 2004. Recharging Aquifers Through Surface Ponds: Hydraulic Behaviour. Emir J Eng Res, 9:21–27.

Anane M, Kallali H, Jellali S et al. 2008. Ranking suitable sites for Soil Aquifer Treatment in Jerba Island (Tunisia) using remote sensing, GIS and AHP-multicriteria decision analysis. Int J Water, 4:121. doi:10.1504/IJW.2008.018151.

Bennani AC, Lary J, Nrhira A et al. 1992. Wastewater Treatment of Greater Agadir (Morocco): An Original Solution for Protecting the Bay of Agadir by Using the Dune Sands. Water Sci Technol, 25:239–245. doi:10.2166/wst.1992.0355.

Bertoldi G, Johnston R and Evenson KD. 1991. *Ground water in the Central Valley, California - a summary report*, U.S. Geological Survey. 55 p.

Bouwer H, Pyne RDG and Brown J. 2008. *Design, Operation, and Maintenance for Sustainable Underground Storage Facilities*, Awwa Research Foundation. 485 p.

Brown CJ. 2005. *Planning Decision Framework for Brackish Water Aquifer, Storage and Recovery (ASR) Projects*. PhD. University of Florida.

Brown CJ, Ward J and Mirecki J. 2016. A Revised Brackish Water Aquifer Storage and Recovery (ASR) Site Selection Index for Water Resources Management. Water Resour Manag, 30:2465–2481. doi:10.1007/s11269-016-1297-7.

Brown CJ, Weiss R, Verrastro R et al. 2005. Development of an aquifer, storage and recovery (ASR) site selection suitability index in support of the Comprehensive Everglades Restoration Project. J Environ Hydrol, 13.

Campbell A. 2020. Recharge Basins - All.

Campbell A and Fan B. 2021. *Chino Basin Recycled Water Groundwater Recharge Program 2020 Annual Report*, Chino, CA: Inland Empire Utilities Agency. 184 p.

[State of California] California Code of Regulations Title 22, Div. 4, Chapt. 3 Water Recycling Criteria. 2018. https://govt.westlaw.com/calregs/Browse/Home/California/CaliforniaCodeofRegulations?guid=IE8ADB4F0D4B911DE8879F88E8B0DAAAEandoriginationContext=documenttocandtransitionType=DefaultandcontextData=(sc.Default).

Chaieb H. 2014. Tunisian Experience in Artificial Recharge using Treated Waste Water.

City of Yelm, WA. Cochrane Memorial Park. https://www.ci.yelm.wa.us/play/parks/cochrane_memorial_park.php [Accessed October 14, 2021].

[CNRA] California Natural Resources Agency. 2021. Well Completion Reports.

[DWR] California Department of Water Resources. i08_GroundwaterElevationSeasonal_Points.

El-Fakharany Z. 2013. Environmental impact assessment of artificial recharge of treated wastewater on groundwater aquifer system. Case study: Abu Rawash, Egypt. J Am Sci, 9.

Gdoura K, Anane M and Jellali S. 2015. Geospatial and AHP-multicriteria analyses to locate and rank suitable sites for groundwater recharge with reclaimed water. Resour Conserv Recycl, 104:19–30. doi:10.1016/j.resconrec.2015.09.003.

Gibson M and Campana M. 2014. *A desktop suitability assessment of aquifer storage and recovery (ASR) in Washington State*, Oregon State University for Washington Department of Ecology. 57 p.

Gibson M, Campana M and Nazy D. 2018. Estimating Aquifer Storage and Recovery (ASR) Regional and Local Suitability: A Case Study in Washington State, USA. Hydrology, 5:7. doi:10.3390/hydrology5010007.

Hatch T, Guobiao H, Guillien A et al. 2020. *C2VSimFG*, DWR.

Hutchinson AS. 2013. *2011-12 Report on Groundwater Recharge in the Orange County Groundwater Basin*, Orange County Water District. 96 p.

Johnson TA. 2009. Ground Water Recharge Using Recycled Municipal Waste Water in Los Angeles County and the California Department of Public Health's Draft Regulations on Aquifer Retention Time. Ground Water, 47:496–499. doi:10.1111/j.1745-6584.2009.00587_3.x.

Kallali H, Anane M, Jellali S et al. 2007. GIS-based multi-criteria analysis for potential wastewater aquifer recharge sites. Desalination, 215:111–119. doi:10.1016/j.desal.2006.11.016.

Kanarek A and Michail M. 1996. Groundwater recharge with municipal effluent: Dan region reclamation project, Israel. Water Sci Technol, 34:227–233.

Kourakos G. 2022. Ichnos. GitHub. https://github.com/giorgk/ichnos [Accessed January 20, 2022].
Land IQ and California Department of Water Resources. 2021. i15 Crop Mapping 2018.
Lau LS, Hardy WR, Gee HK et al. 1989. *Groundwater recharge with Honouliuli wastewater irrigation: Ewa plain, southern Oahu, Hawaii*, Water Resources Center - University of Hawaii at Manoa. 121 p.
Lopes RL and dos Santos AS. 2012. Característica do Solo da Área de Infiltração de Efluentes Domésticos de uma ETE. In: VII CONNEPI Congresso Norte Nordeste de Pesquisa e Inovação. 6 p.
McDermott JA, Avisar D, Johnson TA et al. 2008. Groundwater Travel Times near Spreading Ponds: Inferences from Geochemical and Physical Approaches. J Hydrol Eng, 13:1021–1028. doi:10.1061/(ASCE)1084-0699(2008)13:11(1021).
McFarlane DD. 2019. *Wastewater as a potential source of recycling in the Perth-Peel region*, West Australian Department of Water and Environmental Regulation. 29 p.
McKinney TS. 2012. Predicted nitrate and arsenic concentrations in basin-fill aquifers of the Southwest Principal Aquifers study area.
Murray R, Ravenscroft P, Tredoux G et al. 2010. *Potential Artificial Recharge Schemes: Planning for Implementation*, Republic of South Africa Department of Water Affairs. p 759-768.
Page D, Dillon P, Vanderzalm J et al. 2010. *Managed aquifer recharge case study risk assessments*, CSIRO. 156 p.
Pedrero F, Albuquerque A, Marecos do Monte H et al. 2011. Application of GIS-based multi-criteria analysis for site selection of aquifer recharge with reclaimed water. Resour Conserv Recycl, 56:105–116. doi:10.1016/j.resconrec.2011.08.003.
Pi Y and Wang J. 2006. A field study of advanced municipal wastewater treatment technology for artificial groundwater recharge. J Environ Sci, 18:1056–1060. doi:10.1016/S1001-0742(06)60038-7.
Rahman MA, Rusteberg B, Uddin MS et al. 2013. An integrated study of spatial multicriteria analysis and mathematical modelling for managed aquifer recharge site suitability mapping and site ranking at Northern Gaza coastal aquifer. J Environ Manage, 124:25–39. doi:10.1016/j.jenvman.2013.03.023.
Reed SC and Crites RW. 1984. *Handbook of Land Treatment Systems for Industrial and Municipal Wastes*, Park Ridge, NJ, USA: Noyes Publications. 427 p.
Salt River Project. How SRP manages Phoenix's water supply. srpnet. http://www.srpnet.com/water/resource-management.aspx [Accessed October 14, 2021].
Sendrós A, Urruela A, Himi M et al. 2021. Characterization of a Shallow Coastal Aquifer in the Framework of a Subsurface Storage and Soil Aquifer Treatment Project Using Electrical Resistivity Tomography (Port de la Selva, Spain). Appl Sci, 11:2448. doi:10.3390/app11062448.
Smith WB, Miller GR and Sheng Z. 2017. Assessing aquifer storage and recovery feasibility in the Gulf Coastal Plains of Texas. J Hydrol Reg Stud, 14:92–108. doi:10.1016/j.ejrh.2017.10.007.
Stefan C and Ansems N. 2018. Web-based global inventory of managed aquifer recharge applications. Sustain Water Resour Manag, 4. doi:10.1007/s40899-017-0212-6.

Taylor GL. 1981. Land Treatment Site Evaluation in Southeastern Mountainous Areas. Bull Assoc Eng Geol, 18:261–266.

Towers L and Hugman R. 2021. Cycles of Uncertainty: An Exploration of 40 Years of the Atlantis-Managed Aquifer Recharge Scheme Through a Geoethical Lens. In: Abrunhosa M, Chambel A, Peppoloni S, et al., (eds.). *Advances in Geoethics and Groundwater Management : Theory and Practice for a Sustainable Development*. Advances in Science, Technology and Innovation. Cham: Springer International Publishing, p. 421–424.

Toze S and Bekele E. 2009. *Determining Requirements for Managed Aquifer Recharge in Western Australia*, CSIRO. 59 p.

Tsangaratos P, Kallioras A, Pizpikis Th et al. 2017. Multi-criteria Decision Support System (DSS) for optimal locations of Soil Aquifer Treatment (SAT) facilities. Sci Total Environ, 603–604:472–486. doi:10.1016/j.scitotenv.2017.05.238.

Ulibarri N, Garcia NE, Nelson RL et al. 2021. Assessing the feasibility of managed aquifer recharge in California. Water Resour Res, 57. doi:https://doi.org/10.1029/2020WR029292.

[US EPA] United States Environmental Protection Agency. 2004. *Guidelines for water reuse*, 480 p.

US EPA. 1984. *Process design manual for land treatment of municipal wastewater - Supplement on rapid infiltration and overland flow*, Center for Environmental Research Information, Cincinnati, Ohio. 427 p.

US EPA. 2006. *Process Design Manual: Land Treatment of Municipal Wastewater Effluents*, Cincinnati, OH: Land Remediation and Pollution Control Division National Risk Management Research Laboratory Office of Research and Development. 193 p.

US EPA and [USGS] United States Geological Survey. 2012. National Hydrography Dataset Plus.

USGS. 2021. NLCD 2016 Land Cover Conterminous United States.

Van Houtte E and Verbauwhede J. 2012. Sustainable groundwater management using reclaimed water: the Torreele/St-André case in Flanders, Belgium. J Water Supply Res Technol-Aqua, 61:473–483. doi:10.2166/aqua.2012.057b.

Washington Department of Ecology. 2017. Fact Sheet for Lott Clean Water Alliance Martin Way Reclaimed Water Plant State Reclaimed Water Permit St 6206.

Wieczorek ME, Schwarz GE and Jackson SE. 2018. Select Attributes for NHDPlus Version 2.1 Reach Catchments and Modified Network Routed Upstream Watersheds for the Conterminous United States. doi:10.5066/F7765D7V.

Woody J. 2007. *A Preliminary Assessment of Hydrogeologic Suitability for Aquifer Storage and Recovery (ASR) in Oregon*. Master of Science. Oregon State University.

Appendix B: Derivation of water transfer equations

In samples with SF_6 concentrations exceeding what can be measured by the headspace method (> 23.6 nmol/L), a small quantity of the equilibrated solution in the original container can be transferred to a new container (Fig. B.1). The transferred solution has a lower concentration than what was originally injected to the first container, so when the second container reaches equilibrium, the solution and headspace concentrations are much lower. For instance, if a Vacutainer contains equal volumes of sample and headspace, the ratio of equilibrium to initial concentration of SF_6 in solution will be

$$\frac{C_{Seq}}{C_{Si}} = \frac{1}{H+1} \tag{B.1}$$

Where C_s is the concentration in solution initially (C_{si}) and at equilibrium (C_{Seq}), and H is the Henry's law coefficient.

By starting with the lower, equilibrium concentration of the solution from the first container, the headspace concentration in the second container is more likely to fall within the measurable range. The initial concentration of the original solution can then be calculated from the headspace concentration of the new container as follows:

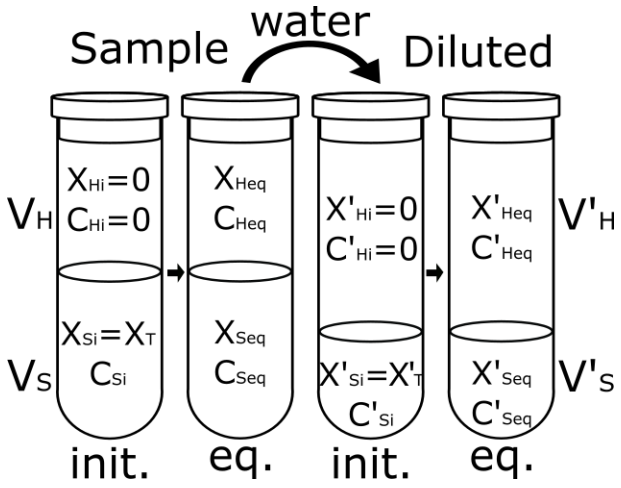

Figure B.1: Illustration of water transfer showing parameters associated with each step.

In each container, the total amount of SF_6 in moles, denoted X, will be divided between the solution and the headspace according to Henry's Law such that:

$$X_T = X_S + X_H \tag{B.2}$$

Because all of the SF_6 starts in the solution:

$$X_T = X_{Si} \tag{B.3}$$

The number of moles in a given phase is equal to its volume V multiplied by concentration C.

$$X_S = V_S C_S \text{ and } X_H = V_H C_H \tag{B.4}$$

According to Henry's Law, the headspace and solution concentrations at equilibrium are related to each other by the Henry's Law coefficient, *H*:

$$H = \frac{C_{Heq}}{C_{Seq}} \tag{B.5}$$

Multiplying both sides by the volume ratio makes them equal to the equilibrium mole ratio.

$$H\frac{V_H}{V_S} = \frac{V_H C_{Heq}}{V_S C_{Seq}} \tag{B.6}$$

Combining equations (B.2), (B.3), (B.4), and (B.6) at equilibrium:

$$H\frac{V_H}{V_S} = \frac{V_H C_{Heq}}{V_s C_{Si} - V_H C_{Heq}} \tag{B.7}$$

Solve for C_{Si}.

$$C_{Si} = \frac{C_{Heq}(HV_H + V_S)}{HV_S} \tag{B.8}$$

When C_{Heq} is measured in a new container after a portion of the original solution has been transferred and allowed to equilibrate, then *H* is *H'*, the equilibrium ratio the when the measurement was taken in the second container, and C_{Si} is C'_{si}, the concentration of the solution when it was transferred. Thus, the equation can be re-written:

$$C'_{Si} = \frac{C'_{Heq}(H'V'_H + V'_S)}{H'V'_S} \tag{B.9}$$

Equation (B.9) provides the initial concentration of the solution in the new container. To calculate the initial concentration in the original container, once again equations (B.2), (B.3), (B.4), and (B.6) are combined and solved for C_{Si} using C_{Seq} instead of C_{Heq}.

$$H\frac{V_H}{V_S} = \frac{V_s C_{Si} - V_S C_{Seq}}{V_S C_{Seq}} \tag{B.10}$$

Solve for C_{Si}.

$$C_{Si} = \frac{C_{Seq}(HV_H + V_S)}{V_S} \tag{B.11}$$

In our case, C_{Seq} is C'_{Si}, and *H* refers to when the solution was equilibrated in the first container and transferred to the new one, so the equation becomes:

$$C_{Si} = \frac{C'_{Si}(HV_H + V_S)}{V_S} \quad \text{(B.12)}$$

Because the dry air mole fraction *x*, not C_H is directly measured, and that the quantity of solution is more accurately measured as mass, equations (B.9) and (B.12) become:

$$C'_{Si} = \frac{x\left(H'_{grav}V'_H\rho_{N2} + m'_S\right)}{H'_{grav}M_{N2}m'_S} \quad \text{(B.13)}$$

and

$$C_{Si} = \frac{C'_{Si}\left(H_{grav}V_H\rho_{N2} + m_S\right)}{m_S} \quad \text{(B.14)}$$

It is important to note that the *H* values used in equations (B.13) and (B.14) are gravimetric, as opposed to the volumetric values used in prior equations. In order to determine *H*, it is helpful to use a parameter that Weiss and Price (1980) define as F, where:

$$F = \frac{C_{Seq}}{x} \quad \text{(B.15)}$$

Using the parameters determined by Bullister et al. (2002), the F for SF_6 in fresh water can be determined as a function of absolute temperature T with the following equation:

$$\ln F = -82.1639\ mol/(kg\ atm) + 120.152\ mol/(kg\ atm)\ (100/T) + 30.6372\ mol/(kg\ atm)\ \ln(T/100) \quad \text{(B.16)}$$

A gravimetric *H* is obtained by substituting equation (B.15) into equation (B.5) where total pressure P is assumed to equal 1 atm and M_{N2} is the molar mass for nitrogen gas (14 mol/g).

$$H_{grav} = 1 / (F\ P * M_{N2}) \quad \text{(B.17)}$$

Combining the water transfer method with the headspace method allows water samples containing SF_6 up to 64 μmol/L to be analyzed. Out of 379 accepted SF_6 concentration data points used in this study, 31 were measured with water transfers.

Variables

C	concentration
C_{Heq}	concentration in headspace at equilibrium
C_{Seq}	concentration in solution at equilibrium
C_{Si}	initial concentration in solution (sample concentration)
F	equilibrium ratio of solution concentration to headspace dry air mole fraction
H	Henry's Law constant
H_{grav}	Henry's Law constant (gravitational)
M_{N2}	molar mass of nitrogen gas (28.0134 g/mol)
m_S	mass of solution
P	total pressure
T	absolute temperature (Kelvin)
V	volume
V_H	headspace volume
V_S	solution volume
X	number of moles
X_H	number of moles in headspace
X_S	number of moles in solution
X_T	total number of moles in container
x	dry air mole fraction of SF_6 in headspace
ρ_{N2}	density of nitrogen gas (1.250 g/L at STP)

An apostrophe following any variable (e.g. V'_H) indicates that it refers to the second container.

References

Bullister, J.L., D.P. Wisegarver, and F.A. Menzia. 2002. “The Solubility of Sulfur Hexafluoride in Water and Seawater.” *Deep-Sea Research Part I: Oceanographic Research Papers* 49 (1): 175–87.

Weiss, R.F., and B.A. Price. 1980. “Nitrous Oxide Solubility in Water and Seawater.” *Marine Chemistry* 8 (4): 347–59.

Appendix C: Separation of double peaked breakthrough curves

The double peak in both tracers observed at MW-5 is assumed to represent two distinct flow paths to that well. In order to separate the signatures of the two paths, the breakthrough curve for each tracer was broken into two curves. Clearly defined breakthrough curves observed in other wells were fitted for linear and first order exponential decline from their peaks, and exponential decay was determined to provide a better representation of the decline in tracer concentrations based on greater R^2 values (Table C.1).

Table C.1: R^2 values for linear and exponential fits of the decline in tracer concentrations following peaks in observed, clearly defined breakthrough curves. Note that MW-5 refers to the measured decline from the second peak.

	Well	Linear R^2	Exponential R^2
Br^-	MW-3a	0.6271	0.9897
	MW-5	0.2821	0.998
	MW-8	0.7131	0.9886
	MW-9	0.6579	0.9801
SF_6	MW-5	0.3573	0.9059
	MW-8	0.4067	0.9628
	MW-9	0.2775	0.8115
	MW-16	0.3858	0.9943
	MW-27	0.6414	0.9913

At MW-5, the first curve was assumed to be identical to the observed breakthrough curve until the first peak. Following the peak, the first curve was assumed to decline by first order exponential decay, like the other breakthrough curves. The second curve was calculated as the difference between the observed breakthrough curve and the estimated curve for peak 1. Thus, the two curves together produce the observed breakthrough curve (Fig. C.1-C.2). A decay constant of -0.15 was determined to produce the most realistic curves for MW-5, such that the decay equation following the first peak of either tracer can be written as

$$C = C_{peak}\, e^{-0.15\,(t - t_{peak})} \qquad (C.1)$$

Peak and center of mass arrival times were then determined for each of the separated curves.

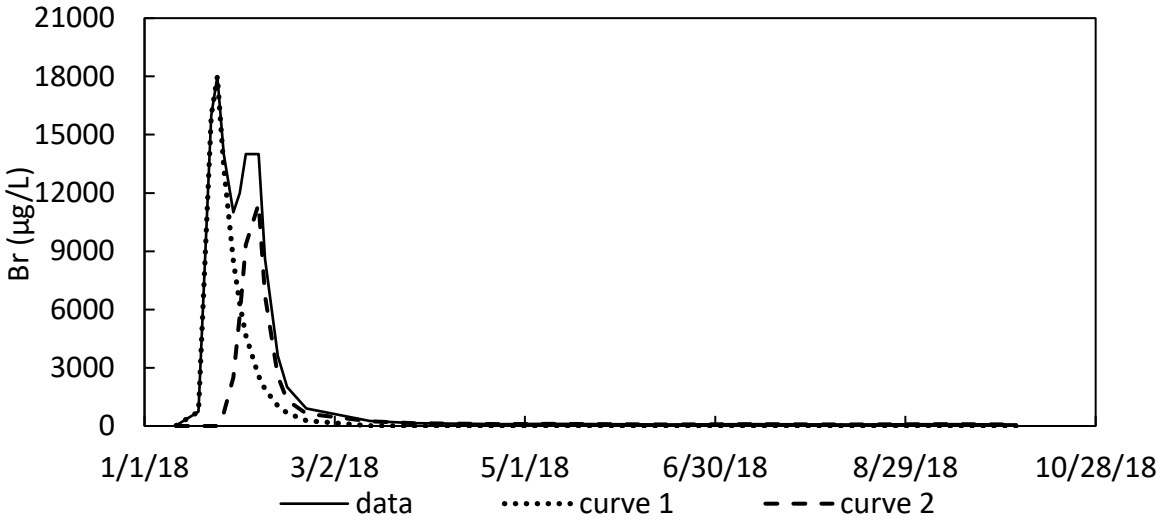

Figure C.1: Br breakthrough curve at MW-5 separated into two single-peak curves.

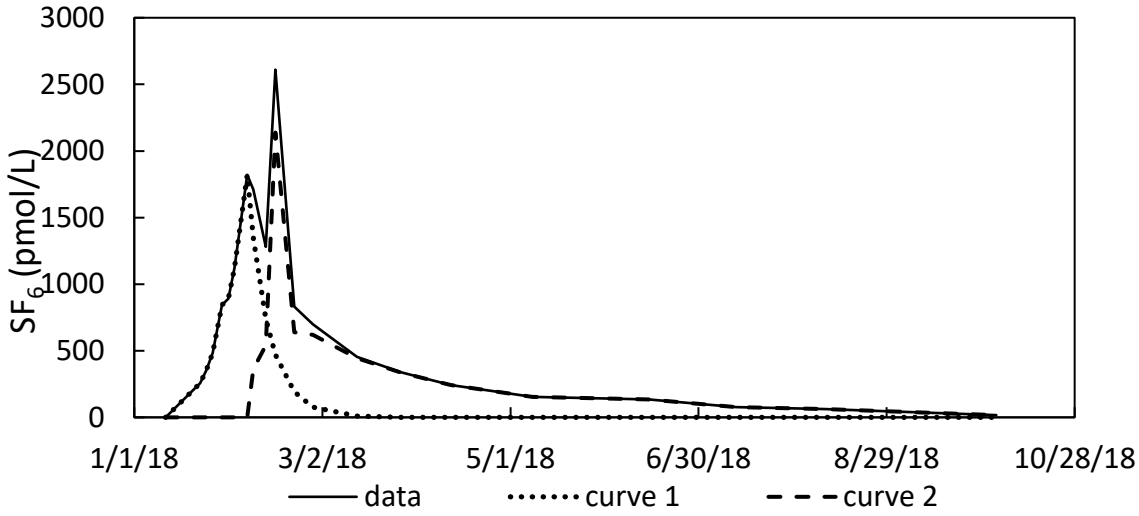

Figure C.2: SF_6 breakthrough curve at MW-5 separated into two single-peak curves.